# RESILIENT MODULUS TESTING FOR PAVEMENT COMPONENTS

STP1437

Editors: Gary N. Durham
W. Allen Marr
Willard L. DeGroff

ASTM INTERNATIONAL
Standards Worldwide

**STP 1437**

# *Resilient Modulus Testing for Pavement Components*

*Gary N. Durham, W. Allen Marr, and*
*Willard L. DeGroff, editors*

ASTM Stock Number: STP1437

ASTM International
100 Barr Harbor Drive
PO Box C700
West Conshohocken, PA 19428-2959

INTERNATIONAL

Printed in the U.S.A.

**Library of Congress Cataloging-in-Publication Data**
**ISBN:** 0-8031-3461-4



**Peer Review Policy**

Each paper published in this volume was evaluated by two peer reviewers and at least one editor. The authors addressed all of the reviewers' comments to the satisfaction of both the technical editor(s) and the ASTM International Committee on Publications.

To make technical information available as quickly as possible, the peer-reviewed papers in this publication were prepared "camera-ready" as submitted by the authors.

The quality of the papers in this publication reflects not only the obvious efforts of the authors and the technical editor(s), but also the work of the peer reviewers. In keeping with long-standing publication practices, ASTM International maintains the anonymity of the peer reviewers. The ASTM International Committee on Publications acknowledges with appreciation their dedication and contribution of time and effort on behalf of ASTM International.

Printed in Ann Arbor, MI
2003

# Foreword

The Symposium on Resilient Modulus Testing for Pavement Components was held in Salt Lake City, Utah on 27–28 June 2002. ASTM International Committee D18 on Soil and Rock and Subcommittee D18.09 on Cyclic and Dynamic Properties of Soils served as sponsors. Symposium chairmen and co-editors of this publication were Gary N. Durham, Durham Geo-Enterprises, Stone Mountain, Georgia; W. Allen Marr, Geocomp Incorporated, Boxborough, Massachusetts; and Willard L. DeGroff, Fugro South, Houston, Texas.

# Contents

Session 4: Equipment, Test Procedures, and Quality Control Issues



Session 5: Modeling Data Reduction and Interpretation

# Overview

Resilient Modulus indicates the stiffness of a soil under controlled confinement conditions and repeated loading. The test is intended to simulate the stress conditions that occur in the base and subgrade of a pavement system. Resilient Modulus has been adopted by the U.S. Federal Highway Administration as the primary performance parameter for pavement design.

The current standards for resilient modulus testing (AASHTO T292-00 and T307-99 for soils and ASTM D 4123 for asphalt) do not yield consistent and reproducible results. Differences in test equipment, instrumentation, sample preparation, end conditions of the specimens, and data processing apparently have considerable effects on the value of resilient modulus obtained from the test. These problems have been the topic of many papers over the past thirty years; however, a consensus has not developed on how to improve the testing standard to overcome them. These conditions prompted ASTM Subcommittee D18 to organize and hold a symposium to examine the benefits and problems with resilient modulus testing. The symposium was held June 27–28, 2002 in Salt Lake City, Utah. It consisted of presentations of their findings by each author, followed by question and answer sessions. The symposium concluded with a roundtable discussion of the current status of the resilient modulus test and ways in which the test can be improved. This ASTM Special Technical Publication presents the papers prepared for that symposium. We were fortunate to receive good quality papers covering a variety of topics from test equipment to use of the results in design.

On the test method, Groeger, Rada, Schmalzer, and Lopez discuss the differences between AASHTO T307-99 and Long Term Pavement Performance Protocol P46 and the reasons for those differences. They recommend ways to improve the T307-99 standard. Boudreau examines the repeatability of the test by testing replicated test specimens under the same conditions. He obtained values with a coefficient of variation of resilient modulus less than 5 % under these very controlled conditions. Groeger, Rada, and Lopez discuss the background of test startup and quality control procedures developed in the FHWA LTPP Protocol P46 to obtain repeatable, reliable, high quality resilient modulus data. Tanyu, Kim, Edil, and Benson compared laboratory tests to measure resilient modulus by AASHTO T294 with large-scale tests in a pit. They measured laboratory values up to ten times higher than the field values and they attribute the differences to disparities in sample size, strain amplitudes, and boundary conditions between the two test types. Rada, Groeger, Schmnalzer, and Lopez review the LTPP test program and summarize what has been learned from the last 14 years of the program with regard to test protocol, laboratory startup, and quality control procedures.

Considering the test equipment, Bejarano, Heath, and Harvey describe the use of off-the-shelf components to build a PID controller for a servo-hyraulic system to perform the resilient modulus test. Boudreau and Wang demonstrate how many details of the test cell can affect the measurement of resilient modulus. Marr, Hankour, and Werden describe a fully automated computer controlled testing system for performing Resilient Modulus tests. They use a PID adaptive controller to improve the quality of the test and reduce the labor required to run the test. They also discuss some of the difficulties and technical details for running a Resilient Modulus test according to current test specifications.

Test results are considered by Li and Qubain who show the effect of water content of the soil specimens on resilient modulus for three subgrade soils. Butalia, Huang, Kim, and Croft examine the effect of water content and pore water pressure buildup on the resilient modulus of unsaturated and saturated cohesive soils. Bandara and Rowe develop resilient modulus relationships for typical subgrade soils used in Florida for use in design. Trindale, Carvalho, Silva, de Lima, and Barbosa examine empirical relationships among CBR, unconfined compressive strength, Young's modulus, and resilient modulus for soils and soil-cement mixtures. Titi, Herath, and Mohammad investigate the use of miniature cone penetration tests to get a correlation with resilient modulus for cohesive soils and describe a method to use the cone penetration results on road rehabilitation projects in Louisiana. Iasbik, de Lima, Carvalho, Silva, Minette, and Barbosa examine the effect of polypropylene fibers on resilient modulus of two soils. Konrad and Robert describe the results of a comprehensive laboratory investigation into the resilient modulus properties of unbound aggregate used in base courses.

The importance of resilient modulus in design is addressed by Nazarian, Abdallah, Meshkani, and Ke, who demonstrate with different pavement design models the importance of the value of resilient modulus on required pavement thickness and show its importance in obtaining a reliable measurement of resilient modulus for mechanistic pavement design. Nazarian, Yan, and Williams examine different pavement analysis algorithms and material models to show the effect of resilient modulus on mechanistic pavement design. They show that inaccuracies in the analysis algorithms and in the testing procedures have an important effect on the design. Boudreau proposes a constitutive model and iterative layered elastic methodology to interpret laboratory test results for resilient modulus as used in the AASHTO Design Guide for Pavement Structures.

The closing panel discussion concluded that the resilient modulus test is a valid and useful test when run properly. More work must be done to standardize the test equipment, the instrumentation, the specimen preparation procedures, and the loading requirements to improve the reproducibility and reliability among laboratories. Further work is also needed to clarify and quantify how to make the test more closely represent actual field conditions.

We thank those who prepared these papers, the reviewers who provided anonymous peer reviews, and those who participated in the symposium. We hope this STP encourages more work to improve the testing standard and the value of the Resilient Modulus test.

*Gary Durham*
Durham Geo-Enterprises

*Willard L. DeGroff*
Fugro South

*W. Allen Marr*
GEOCOMP/GeoTesting Express

# SESSION 1: THEORY AND DESIGN CONSTRAINTS

Soheil Nazarian,[1] Imad Abdallah,[2] Amitis Meshkani,[3] and Liqun Ke[4]

# Use of Resilient Modulus Test Results in Flexible Pavement Design

---

**Reference:** Nazarian, S., Abdallah, I., Meshkani, A., and Ke, L., **"Use of Resilient Modulus Test Results in Flexible Pavement Design,"** *Resilient Modulus Testing for Pavement Components, ASTM STP 1437*, G. N. Durham, W. A. Marr, and W. L. De Groff, Eds., ASTM International, West Conshohocken, PA, 2003.

**Abstract:** The state of practice in designing pavements in the United States is primarily based on empirical or simple mechanistic-empirical procedures. Even though a number of state and federal highway agencies perform resilient modulus tests, only few incorporate the results in the pavement design in a rational manner. A concentrated national effort is on the way to develop and implement mechanistic pavement design in all states. In this paper, recommendations are made in terms of the use of the resilient modulus as a function of the analysis algorithm selected and material models utilized. These recommendations are also influenced by the sensitivity of the critical pavement responses to the material models for typical flexible pavements. The inaccuracies in laboratory and field testing as well as the accuracy of the algorithms should be carefully considered to adopt a balance and reasonable design procedure.

**Keywords:** resilient modulus, pavement design, laboratory testing, base, subgrade, asphalt

An ideal mechanistic pavement design process includes (1) determining pavement-related physical constants, such as types of existing materials and environmental conditions, (2) laboratory and field testing to determine the strength and stiffness parameters and constitutive model of each layer, and (3) estimating the remaining life of the pavement using an appropriate algorithm. Pavement design or evaluation algorithms can be based on one of many layer theory or finite element programs. The materials can be modeled as linear or nonlinear and elastic or viscoelastic. The applied load can be considered as dynamic or static. No matter how sophisticated or simple the process is made, the material properties should be measured in a manner that is compatible with the

---

[1] Professor, [2] Research Engineer, Center for Highway Materials Research, The University of Texas at El Paso, El Paso, TX 79968.

[3] Assistant Engineer, Flexible Pavement Branch, Texas Department of Transportation, 9500 Lake Creek Parkway, Bldg 51, Austin, TX 78717.

[4] Senior Engineer, Nichols Consulting Engineers, Chtd., 1101 Pacific Ave Ste 300, Santa Cruz, CA 95060.

algorithm used. If a balance between the material properties and analytical algorithm is not struck, the results may be unreliable.

The state of practice in the United States is primarily based on empirical or simple mechanistic-empirical pavement design procedures. Under the AASHTO 2002 program, a concentrated national effort is under way to develop and implement mechanistic pavement design in all states. The intention of this paper is not to provide a dialogue on the technical aspects of pavement design since the methodologies described here are by no means new or novel to the academic community. Rather, the paper is written for the practitioners that are interested in evaluating the practical impacts of implementing resilient modulus testing into in their day-to-day operations. In general, the discussions are limited to the base and subgrade layers because of space limitations. However, as reflected in other papers in this manuscript, the visco-elastic and temperature-related variation in the stiffness parameters of the asphalt concrete (AC) layer should be considered.

In this paper, different pavement analysis algorithms and material models are briefly described. The sensitivity of the critical pavement responses to the nonlinear material models for typical pavements is quantified. The tradeoff between the computation time as a function of approximation in the analysis and material models are demonstrated. Theoretically speaking, the more sophisticated the material models and the analysis algorithms are, the closer the calculated response should be to the actual response of the pavement. However, the inaccuracies in laboratory and field testing as well as the inadequacies of the algorithms should be carefully considered to adopt a balanced design system. If the model is not calibrated well, irrespective of its degree of sophistication, the results may be unreliable.

**Material Models**

Brown (1996) discussed a spectrum of analytical and numerical models that can be used in pavement design. With these models, the critical stresses, strains and deformations within a pavement structure and, therefore, the remaining life can be estimated. Many computer programs with different levels of sophistication exist. The focal point of all these models is the moduli and Poisson's ratio of different layers.

The linear elastic model is rather simple since the modulus is considered as a constant value. In the state of practice, the modulus is also assumed to be independent of the state of stress applied to the pavement. As such, the modulus of each layer does not change with the variation in load applied to a pavement. Most current pavement analysis and design algorithms use this type of solution. The advantage of these models is that they can rapidly yield results. Their main limitation is that the results are rather approximate if the loads are large enough for the material to exhibit a nonlinear behavior. In the context of the resilient modulus testing, the relevant information is the representative value to be used in the design. Specifically, the resilient modulus at what confining pressure and deviatoric stress should be used in the design? This will be discussed later.

The nonlinear constitutive model adopted by most agencies and institutions can be generalized as:

$$E = k_1 \sigma_c^{k_2} \sigma_d^{k_3} \tag{1}$$

where σc and σd are the confining pressure and deviatoric stress, respectively and $k_1$, $k_2$ and $k_3$ are coefficients preferably determined from laboratory tests. In Equation 1, the modulus at a given point within the pavement structure is related to the state of stress. The advantage of this type of model is that it is universally applicable to fine-grained and coarse-grained base and subgrade materials. The accuracy and reasonableness of this model are extremely important because they are the keys to successfully combine laboratory and field results. Barksdale et al. (1997) have summarized a number of variations to this equation. Using principles of mechanics, all those relationships can be converted to the other with ease. The so-called two-parameter models advocated by the AASHTO 1993 design guide can be derived from Equation 1 by assigning a value of zero to $k_2$ (for fine-grained materials) or $k_3$ (for coarse-grained materials). As such, considering one specific model does not impact the generality of the conclusions drawn from this paper.

Using conventions from geotechnical engineering, the term $k_1\sigma_c^{k2}$ corresponds to the initial tangent modulus. Since normally parameter $k_2$ is positive, the initial tangent modulus increases as the confining pressure increases. Parameter $k_3$ suggests that the modulus changes as the deviatoric stress changes. Because $k_3$ is usually negative, the modulus increases with a decrease in the deviatoric stress (or strain). The maximum feasible modulus from Equation 1 is equal to $k_1\sigma_c^{k2}$, i.e. the initial tangent modulus.

In all these models, the state of stress is bound between two extremes, when no external loads are applied and under external loads imparted by an actual truck. When no external load is applied the initial confining pressure, $\sigma_{c\_init}$, is

$$\sigma_{c\_init} = \frac{1+2k_0}{3}\sigma_v \tag{2}$$

where $\sigma_v$ is the vertical geostatic stress and $k_o$ is the coefficient of lateral earth pressure at rest. The initial deviatoric stress, $\sigma_{d\_init}$ can be written as

$$\sigma_{d\_init} = \frac{2-2k_0}{3}\sigma_v \tag{3}$$

When the external loads are present, additional stresses, $\sigma_x$, $\sigma_y$ and $\sigma_z$, are induced in two horizontal and one vertical directions under the application of an external load. A multi-layer elastic program can conveniently compute these additional stresses. The ultimate confining pressure, $\sigma_{c\_ult}$ is

$$\sigma_{c\_ult} = \frac{1+2k_0}{3}\sigma_v + \frac{\sigma_x+\sigma_y+\sigma_z}{3} \tag{4}$$

and the ultimate deviatoric stress, $\sigma_{d\_ult}$, is equal to

$$\sigma_{d\_ult} = \frac{2-2k_0}{3}\sigma_v + \frac{2\sigma_z-\sigma_x-\sigma_y}{3} \tag{5}$$

Under actual truckloads, the modulus can become nonlinear depending on the amplitude of confining pressure $\sigma_{c\_ult}$ and deviatoric stress of $\sigma_{d\_ult}$. In that case

$$E = k_1 \sigma_{c\_ult}^{\ k_2} \sigma_{d\_ult}^{\ k_3} \tag{6}$$

**Analysis Options**

The analysis algorithm can be either a multi-layer linear system, or a multi-layer equivalent-linear system, or a finite element code for a comprehensive nonlinear dynamic system. A multi-layer linear system is the simplest simulation of a flexible pavement. In this system, all layers are considered to behave linearly elastic. WESLEA (Van Cauwelaert et al. 1989) and BISAR (De Jong et al. 1973) are two of the popular programs in this category.

The equivalent-linear model is based on the static linear elastic layered theory. Nonlinear constitutive models, such as the one described in Equation 1, can be implemented in them. An iterative process has to be employed to implement this method. Nonlinear layers are divided into several sublayers. One stress point is chosen for each nonlinear sub-layer. An initial modulus is assigned to each stress point. The stresses and strains are calculated for all stress points using a multi-layer elastic computer program. The confining pressure and deviatoric stress can then be calculated for each stress point using Equations 2 through 5. A new modulus can then be obtained from Equation 6. The assumed modulus and the newly calculated modulus at each stress point are compared. If the difference is larger than a pre-assigned tolerance, the process will be repeated using updated assumed moduli. The above procedure is repeated until the modulus difference is within the tolerance and, thus, convergence is reached. Finally, the required stresses and strains are computed using final moduli for all nonlinear sub-layers. This method is relatively rapid; however, the results are approximate. In a layered solution, the lateral variation of modulus within a layer cannot be considered. To compensate to a certain extent for this disadvantage, a set of stress points at different radial distances are considered. Abdallah et al. (2002) describes such an algorithm.

The all-purpose finite element software packages, such as ABAQUS, can be used for nonlinear models. These programs allow a user to model the behavior of a pavement in the most comprehensive manner and to select the most sophisticated constitutive models for each layer of pavement. The dynamic nature of the loading can also be considered. The constitutive model adopted in nonlinear models is the same as that in the equivalent-linear model, as described in Equation 1.

The goal with all these models is of course to calculate the critical stresses and strains and finally the remaining life. We will concentrate on the tensile strain at the bottom of the AC layer and compressive strain on top of the subgrade. These two parameters can be incorporated into a damage model (e.g., the Asphalt Institute models) to estimate the remaining lives due to a number of modes of failure (e.g., rutting and fatigue cracking). These equations are well known and can be found in Huang (1993) among other sources.

**Appropriate Modulus Parameter for Models**

As indicated before, the structural model and the input moduli should be considered together. Different structural models require different input parameters. For the equivalent linear and nonlinear models, all three nonlinear parameters are required. The process of defining these parameters can be categorized as material characterization. For the linear model, a representative linear modulus has to be determined. The process of approximating the modulus is called the design simulation.

One significant point to consider has to do with the differences and similarities between material characterization and design simulation. In material characterization one attempts in a way that is the most theoretically correct to determine the engineering properties of a material (such as modulus or strength). The material properties measured in this way, are fundamental material properties that are not related to a specific modeling scenario. To use these material properties in a certain design methodology, they should be combined with an appropriate analytical or numerical model to obtain the design output. In the design simulation, one tries to experimentally simulate the design condition, and then estimate some material parameter that is relevant to that condition. Both of these approaches have advantages and disadvantages. In general, the first method should yield more accurate results but at the expense of more complexity in calculation and modeling during the design process.

The implication of this matter is best shown through an example. We consider a typical pavement in Texas. The asphalt layer is typically 75 mm thick with a modulus of 3.5 GPa. For simplicity, let us assume that the subgrade is a linear-elastic material with a modulus of 70 MPa. The base is assumed to be nonlinear according to Equation 1 with $k_1$, $k_2$ and $k_3$ values of 50 MPa, 0.4 and -0.1, respectively. The thickness of the base of 200 mm is assumed. This pavement section is subjected to an 80 kN wheel load. In the first exercise, the thickness of the base is varied between 100 mm and 300 mm. The variation in base modulus with depth is shown in Figure 1 in a normalized fashion. In all three cases, the moduli are not constant and decrease with depth within the base. As the thickness of the base increases, the contrast between the top and bottom modulus becomes more evident.

In a similar fashion, the impact of parameters $k_1$, $k_2$ and $k_3$ are also shown in Figure 2. In this case, the moduli are normalized to the modulus determined at mid-height of the base ($E_{avg}$). Once again, these parameters impact the variation in modulus with depth. In some cases, the difference between the moduli of the middle of the layer and the top and the bottom is as much as 20%. Since the design is based on the interface stresses or strains, if one decides that the

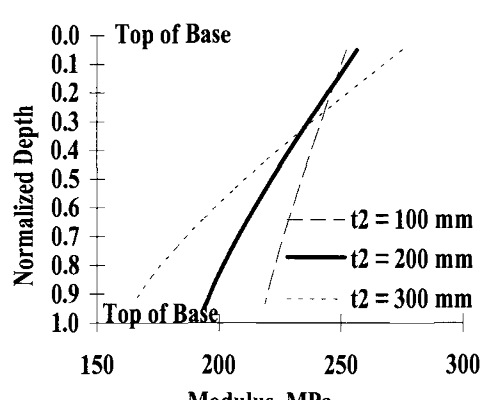


Figure 1 – *Impact of layer thickness on variation in modulus within base layer.*

modulus in the middle of the layer is appropriate for a linear elastic based design, he/she may introduce large errors in the analysis, since in most models the estimated strains have to be raised to a power of about four.

As an example, the responses of the typical pavement described above for different structural and material models are summarized in Table 1. To generate Table 1, the subgrade was also assumed to be nonlinear when applicable. Values of $k_1$, $k_2$ and $k_3$ of 50 MPa, 0.2 and -0.2 were respectively assumed for this layer. These values are representative of materials in east Texas. In the table, the linear static model refers to the state of practice. In the linear dynamic model the dynamic nature of the load is considered in the analysis. In the equivalent-linear model, the nonlinear nature of the base and subgrade is considered in an approximate fashion, but the dynamic nature of the load is ignored. The nonlinear static condition is similar to the equivalent linear solution with the exception that the nonlinear behavior of each material is rigorously modeled. Finally, in the nonlinear dynamic analysis both the dynamic nature of the load and the nonlinear nature of the base and subgrade are considered.

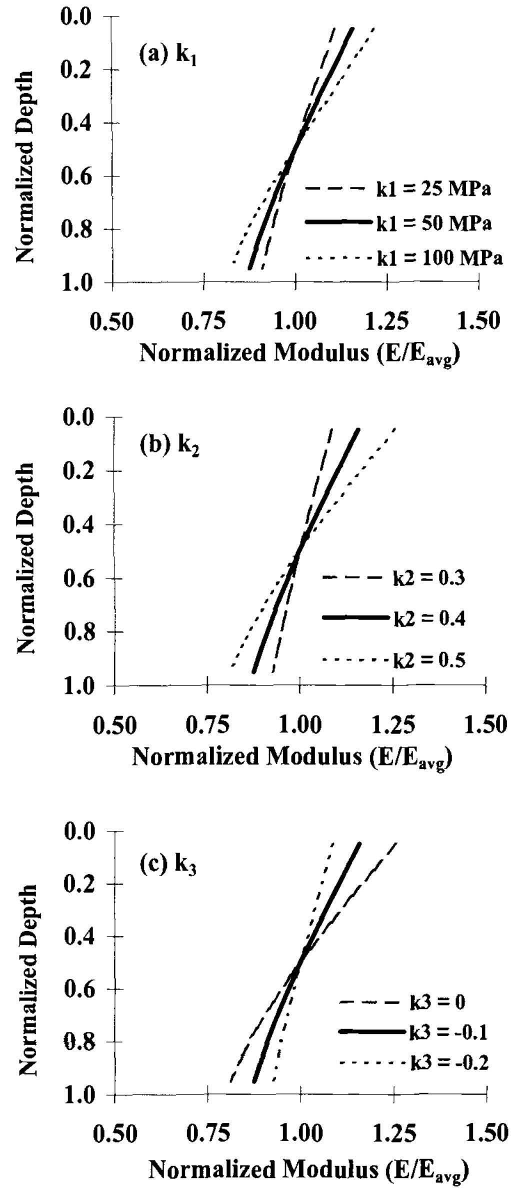


Figure 2 – *Impact of nonlinear parameters on variation in modulus within base layer.*

The surface deflections that would have been measured under a falling weight deflectometer (FWD) at a 40 kN load, and critical strains, and remaining lives of the typical pavement section under an 80 kN dual tandem load are presented in the table. The response under the FWD is demonstrated because AASHTO 1993 allows the use of the surface deflection to backcalculate moduli. The impact of the nonlinear behavior of the base and subgrade

Table 1—*Pavement responses under different models.*

| Material Model (Approximate Computation time)[a] | Surface Deflections (microns) | | | | | | | Critical Strains (micro-strain) | | Remaining Lives[b] ($10^3$ EASLs) | |
|---|---|---|---|---|---|---|---|---|---|---|---|
| | Radial Distance (m) | | | | | | | $\varepsilon_t^c$ | $\varepsilon_c^d$ | Fatigue Cracking | Rutting |
| | 0 | 0.3 | 0.6 | 0.9 | 1.2 | 1.5 | 1.8 | | | | |
| Linear Static (2 sec) | 541 (-15)[e] | 333 (-14) | 213 (-10) | 147 (-8) | 104 (-11) | 76 (-19) | 58 (-29) | 204 (-33) | 587 (-21) | 1505 (271) | 401 (185) |
| Linear Dynamic (600 sec) | 523 (-17) | 328 (-15) | 213 (-10) | 152 (-5) | 114 (-2) | 91 (-3) | 76 (-3) | 203 (-33) | 596 (-20) | 1532 (278) | 373 (165) |
| Equivalent - Linear (120 sec) | 673 -6 | 396 -2 | 226 (-4) | 147 (-7) | 104 (-11) | 76 (-20) | 58 (-27) | 282 (-7) | 844 (14) | 518 (28) | 79 (-44) |
| Nonlinear Static (1500 sec) | 638 -1 | 384 (-1) | 229 (-3) | 150 (-6) | 104 (-11) | 74 (-22) | 56 (-29) | 307 (1) | 702 (-5) | 392 (-3) | 120 (28) |
| Nonlinear Dynamic (2400 sec) | 632 | 386 | 236 | 160 | 117 | 94 | 79 | 304 | 764 | 406 | 141 |

[a] using a 500 MHz PC
[b] estimated from Asphalt Institute Equations
[c] tensile stress at bottom of AC layer
[d] compressive strength on top of subgrade
[e] percent difference between this quantity and quantity from nonlinear dynamic model.

materials on the backcalculated moduli is beyond the scope of this paper. However, from the change in the magnitude of the deflections as a function of model, it is intuitive that it impacts the backcalculated values.

Assuming the results from the nonlinear dynamic model are the most accurate ones, the differences in the results of the other models from those of the nonlinear dynamic model are also given in Table 1. For the linear elastic model using the mid-depth modulus for base, the surface deflections are about 8–30 % less than those from the nonlinear dynamic model. For the first three sensors, most of the differences in deflections can be attributed to material nonlinearity. For the other sensors, on the other hand, the differences can be mainly from the dynamic effects. As a result of ignoring material nonlinearity in the linear static model, the critical tensile strain is about 30 % smaller and the critical compressive strain is about 20 % smaller than those in the nonlinear dynamic model. Correspondingly, the fatigue remaining life and the rutting remaining life are overestimated by 270 % and 185 %, respectively.

Since the material nonlinearity affects the surface deflections near the load application and the dynamic effects mainly affect the surface deflections at the outer sensors, the last four surface deflections are very close to those from the nonlinear dynamic model. However, the first three surface deflections are 10–17 % less than those from the nonlinear dynamic model. As compared with the nonlinear dynamic model, the critical tensile strain is 33 % smaller and the critical compressive strain is 20 % smaller. Correspondingly, the fatigue remaining life and the rutting remaining life are overestimated by 278 % and 165 %, respectively. The computation of the linear dynamic model is also relatively rapid. However, the levels of approximation in the critical strains and remaining lives are similar to those in the linear static model, and the results are not satisfactory.

In the equivalent-linear model, the material nonlinearity is taken into consideration in an approximate fashion, while the dynamic effects are not considered. The largest differences in deflections occur at the three outer sensors, 11–27 % smaller than those from the nonlinear dynamic model. The differences in the surface deflections at the first four sensors are small. The critical tensile strain is 7 % smaller and the critical compressive strain is 14 % larger than the results from the nonlinear dynamic model. Correspondingly, the fatigue remaining life and the rutting remaining life are underestimated by 28 % and 44 %, respectively. The levels of approximation in the critical strains and remaining lives are relatively large but, given the state of practice, perhaps acceptable.

In the nonlinear static model, the material nonlinearity is taken into consideration, but the dynamic effects are not considered. The largest differences in deflections occur at the three outer sensors, where they are 11–29 % smaller than those from the nonlinear dynamic model. These differences are similar in magnitude to those of the equivalent-linear model. The critical tensile strain is 1 % larger and the critical compressive strain is 5 % smaller than the results from the nonlinear dynamic model. Correspondingly, the fatigue remaining life is underestimated by 3 %, and the rutting remaining life is overestimated by 28 %. The results from the nonlinear static model are close to those from the nonlinear dynamic model, in this case, except for the three surface deflections at the outer sensors.

To be practical, the solution should be obtained in a timely manner. Table 1 also contains this information when a 500 MHz personal computer is used. The computation time of the linear static model is very rapid (about 2 sec). However, without considering material nonlinearity and dynamic effects, the results are rather approximate. On the other hand, the rigorous nonlinear dynamic analysis may be too time consuming (about 4 hours).

Based on the example shown for a typical pavement in Texas, the consequences of selecting different models on the accuracy of the estimated strains and remaining lives should be clear. A balance between the acceptable level of model sophistication and the computational time should be struck. The decision on how sophisticated the analysis should be made has to be made based on the importance of the project. As soon as a decision on the model is made, the level of sophistication in the laboratory testing can be determined. This decision is also governed by determining which pavement property will impact the results of a given analysis significantly. To answer this question, Ke et al. (2001) and Meshkani et al. (2002) have conducted an extensive sensitivity analysis to identify the most critical parameters. A brief summary of their conclusions is described below.

The focus of both studies has been on four categories of pavements: Thick AC-Thick Base (e.g., interstate roads), Thick AC-Thin Base (e.g., farm to market roads), Thin AC-Thick Base (e.g., secondary roads) and Thin AC-Thin Base (e.g., street roads). The sensitivities of remaining lives due to fatigue cracking and rutting for different parameters and for the four pavement categories are included in Figures 3 and 4. These graphs can

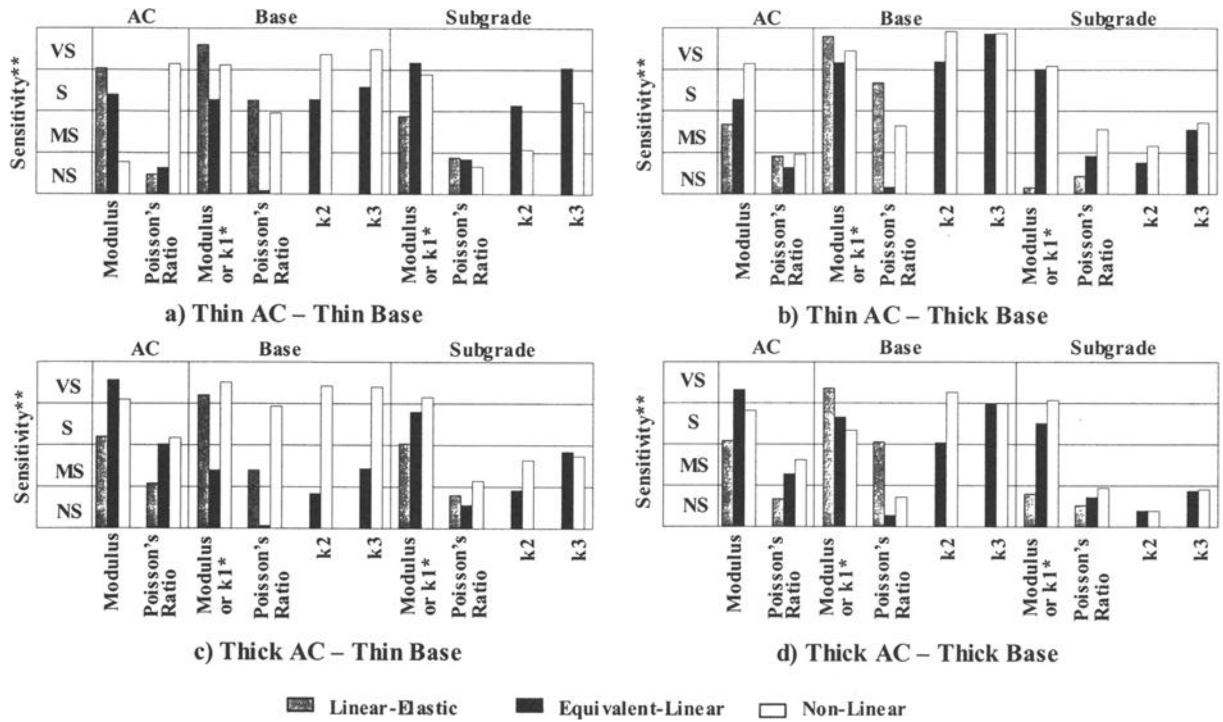


* - elastic modulus was substituted for $k_1$

** - NS = Not Sensitive, MS = Moderately Sensitive, S = Sensitive, VS = Very Sensitive (See Table 2 for definition of these parameters)

Figure 3 – *Sensitivity of remaining life of pavements in fatigue cracking to different pavement layer stiffness parameters*

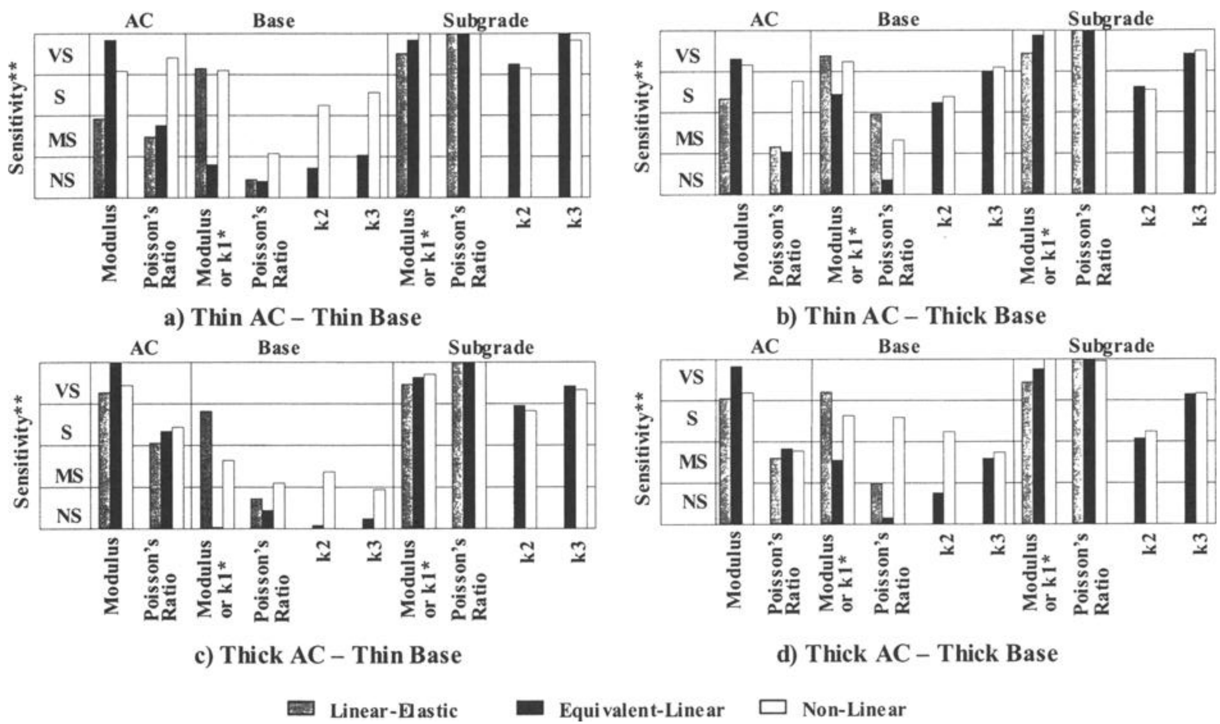


* - elastic modulus was substituted for $k_1$

** - NS = Not Sensitive, MS = Moderately Sensitive, S = Sensitive, VS = Very Sensitive
(See Table 2 for definition of these parameters)

Figure 4 – *Sensitivity of remaining life of pavements in rutting to different pavement layer stiffness parameters*

be used as guidelines during the design, evaluation or construction of pavements. The cases that the dynamic analyses are performed are not considered any further because of a lack of widespread use.

In Figures 3 and 4, the x-axis is the relevant parameters for different models and the y-axis is the sensitivity of the remaining life either due to fatigue cracking or rutting to that parameter. To determine the sensitivity of a given parameter, the particular parameter was allowed to vary by 25 % above and below the assigned value. Based on our experience with pavement analysis and design and laboratory testing, this value seemed reasonable for Texas. Five hundred sets of input data were generated using a Monte Carlo simulation. The values were uniformly distributed within the minimum and maximum values assigned to a parameter. The impact of a parameter on the remaining life was quantified using a parameter termed the sensitivity index. The sensitivity index ($S_i$) is defined as the ratio of the percentage change in the target parameter (one of the two remaining lives) to the percentage change in the perturbed input parameter. Mathematically,

$$S_i = \frac{\text{Percentage Change in Target Parameter}}{\text{Percentage Change in Perturbed Input Parameter}} \tag{7}$$

where

$$\text{Percentage Change} = \frac{|\text{Calculated or Used Quantity} - \text{Original Quantity}|}{\text{Original Quantity}} \times 100 \tag{8}$$

Therefore, the larger the sensitivity index is, the more sensitive the target parameter will be to the varied parameter.

A set of limits was used to define the significance of a given parameter. These levels are defined in Table 2. The interpretation of these levels of sensitivity in terms of their applicability to the laboratory and field measurements is also summarized in Table 2. For example, for a parameter that is labeled not sensitive, its value can be estimated from literature and there is no need to spend effort and funds to measure them accurately. However, when a parameter is very sensitive for a given model, the agency involved in the pavement design either should spend necessary time and effort to measure them

Table 2 – *Levels of sensitivity assigned to each parameter based on sensitivity index.*

| Level of Sensitivity | Sensitivity Index | Significance to Pavement Design |
|---|---|---|
| Not Sensitive (NS) | <0.25 | Can be probably estimated with small error in final results |
| Moderately Sensitive (MS) | ≥0.25 and < 0.5 | Must be measured to limit errors in design |
| Sensitive (S) | ≥0.5 and <1.0 | Must be measured with reasonable accuracy for satisfactory design |
| Very Sensitive (VS) | ≥1.0 | Must be measured very accurately or design may not be considered appropriate |

accurately or should use a simpler structural model. It should be mentioned that the conclusions drawn here are only applicable to the models that are similar to the Asphalt Institute models. Should an agency adopt different failure models or material models, this exercise should be repeated. The comments made here may not be valid for those models. Meshkani et al. (2002) demonstrate one process that can be carried out to establish important parameters.

From the two figures that correspond to typical pavements in East Texas, depending on the thickness of the base and AC layers, the material model used and the mode of failure considered, different parameters become important. For example, for a thin AC and thin base, the nonlinear parameters $k_2$ and $k_3$ impact the response of the pavement significantly. On the other hand, when the base and AC are thick, one should not be concerned about these parameters in the fatigue cracking mode.

For the fatigue cracking mode, the least significant parameter is the Poisson's ratio of the subgrade. On the other hand, for the rutting failure mode, one of the most significant parameters is the Poisson's ratio of subgrade. The other important observation from Figure 3 is that the modulus of the base should be measured more carefully when the linear elastic model is used. For this mode of failure, the nonlinear parameters $k_2$ and $k_3$ should be measured more carefully for the thinner pavements. For an interstate type pavement section, it may not be necessary to conduct any laboratory tests to determine the nonlinear parameters of the subgrade. This statement may be counterintuitive. But considering that thick layers of AC and base has to be placed on top of the subgrade to endure the large number of vehicular loads, the stresses within the subgrade may be too small to induce nonlinear behavior. In this case, according to Figure 3, any misestimating of the nonlinear parameters of the base may significantly impact the estimated remaining life.

For the rutting mode of failure, as shown in Figure 4, the most significant parameters are the modulus (or parameter $k_1$ for the nonlinear material models) and Poisson's ratio of the subgrade[5]. The modulus of the AC layer is also reasonably important. On the other hand, the nonlinear parameters of thin bases are of limited significance. But for thicker bases, these parameters should be considered.

These graphs, and a large number of similar ones presented in Meshkani et al. (2002) clearly demonstrate that one testing program does not fit all projects. During the initial phases of design, based on the structural model adopted by the agency and based on the typical layer materials and thicknesses that the agency is comfortable with, adequate and appropriate laboratory testing should be considered.

This study, and other similar ones in Meshkani et al. (2002), also demonstrates that if the linear elastic layered theory is considered for the analysis, perhaps the resilient modulus tests can be simplified so that the large number of steps necessary under current protocol can be optimized. Tests can be perhaps performed under close to zero confining pressure (corresponding to the unloaded condition) and one other confining pressure that

---

[5] Poisson's ratio becomes important when a value greater than 0.4 is assumed. Since the soils in east Texas are generally saturated, a central value of 0.45 was assumed during the simulation.

is reasonably close to the confining pressure induced in the particular pavement layer under the design vehicular loads. On the other hand, it seems that for saturated or near saturated subgrades, efforts are needed to determine the in-place Poisson's ratio.

## Conclusions

In this paper an attempt has been made to bring to the attention of those who are involved in pavement design the importance of harmonizing the laboratory testing, especially resilient modulus testing, with the design procedure used by the agency. Simplified design procedures may not require as much emphasis on some of the stiffness properties of some layers. A protocol is proposed to identify the significant parameters as a function of pavement structure and structural model and material model used.

## Acknowledgments

This work was supported by the Texas Department of Transportation. The authors would like to express their sincere appreciation to Mark McDaniel, Joe Thompson, and John Rantz for their ever-present support and valuable advice. The contents of this paper reflect the view of the authors, who are responsible for the facts and the accuracy of the data presented herein. The contents do not necessarily reflect the official views or policies of the funding agencies.

## References

Abdallah I., Meshkani A., Yuan D., and Nazarian S., 2002, "An Algorithm for Determining Design Moduli from Seismic Methods," Research Report 1780-4, Center for Highway Materials Research, The University of Texas, El Paso, TX.

Barksdale, R. D., Alba, J., Khosla, P. N., Kim, R., Lambe, P. C. and Rahman, M. S., 1997, "Laboratory Determination of Resilient Modulus for Flexible Pavement Design," NCHRP Web Document 14, Federal Highway Administration, Washington, D.C., 486 p.

Brown, S. F., 1996, "Soil Mechanics in Pavement Engineering," *Geotechnique*, Vol. 46. No. 3, 1996, pp. 383-426.

Huang, Y. H., 1993, *Pavement Analysis and Design,* Prentice Hall, Inc., Englewood Cliffs, NJ, 805 p.

De Jong, D. L., Peatz, M. G. F., and Korswagen, A. R., 1973, "Computer Program Bisar Layered Systems Under Normal and Tangential Loads," Konin Klijke Shell-Labaratorium, External Report AMSR.0006.73, Amsterdam.

Van Cauwelaert, F. J., Alexander, D. R., White, T. D., and Baker, W. R., 1989, "Multilayer Elastic Program for Backcalculating Layer Moduli in Pavement Evaluation," *ASTM STP 1026*, ASTM International, West Conshohocken, PA, 1989, pp. 171-188.

Jonathan L. Groeger,[1] Gonzalo R. Rada,[2] Aramis Lopez[3]

# AASHTO T307 – Background and Discussion

---

**Reference:** Groeger, J. L., Rada, G. R., and Lopez, A., "**AASHTO T307 – Background and Discussion,**" *Resilient Modulus Testing for Pavement Components, ASTM STP 1437,* G. N. Durham, W. A. Marr, and W. L. De Groff, Eds., ASTM International, West Conshohocken, PA, 2003.

**Abstract:** The current AASHTO protocol for determination of resilient modulus of soils and aggregate material (T307-99) is based largely on Long Term Pavement Performance (LTPP) Protocol P46. The LTPP protocol evolved over a number of years and has had numerous contributors (including significant guidance and input from the authors of this paper). To-date, over 3000 samples have been tested with P46 and results of this testing effort will have far-reaching implications in the development of performance models for pavement structures. Many lessons were learned during development of P46 and this history is documented in a companion paper. The present paper provides a background of the reasons and rationale behind some of the major technical aspects of P46, and by direct association, AASHTO T307. The paper also offers suggestions for improvement or modification of T307. It is hoped that this discussion will lead to a deeper understanding of the test procedure and perhaps facilitate a discussion of the direction the T307 procedure should follow in the future.

**Keywords:** resilient modulus, laboratory testing, unbound materials, subgrade, guidelines, LTPP, T307, LTPP Protocol P46

## Introduction

The current AASHTO Standard Method of Test for Determining the Resilient Modulus of Soils and Aggregate Materials, AASHTO Designation (T307-99) is based largely on Long Term Pavement Performance (LTPP) Protocol P46, Resilient Modulus of Unbound Granular Base/Subbase and Subgrade Materials. The LTPP protocol evolved over a number of years and has had numerous contributors (including significant guidance and input from the authors of this paper). To date, over 3000 samples have been tested with P46 and results of this testing effort will have far-reaching implications in the development of performance models for pavement structures.

Many lessons were learned during development of P46 and this history is documented in a companion paper (Rada et al. 2003). The present paper provides a background of the reasons and rationale behind some of the major technical aspects of

---

[1] Vice President, Axiom Decision Systems, Inc., 6420 Dobbin Road, Suite E, Columbia, MD 21045.
[2] Assistant Vice President, LAW PCS, 12104 Indian Creek Court, Suite A, Beltsville, MD 20705.
[3] LTPP Team Leader, Federal Highway Administration, 6300 Georgetown Pike, McLean, VA 22101.

P46, and by direct association, AASHTO T307. The paper also offers suggestions for improvement or modification of T307. It is hoped that this discussion will lead to a deeper understanding of the test procedure and perhaps foster a discussion of the direction the procedure should follow in the future.

The paper will first discuss the similarities and differences between LTPP Protocol P46 and ASSHTO T307. This discussion frames the various technical issues involved with the current procedures. The topics covered include the following:

- Loading system
- Load cell location
- Deformation measurement
- Confining fluid
- Load pulse shape
- Load and cycle duration
- Number and type of LVDTs
- Number of points per cycle
- Specimen size
- Compaction parameters
- Compaction procedures
- Quick shear test

Each topic is covered in detail to give the reader an understanding of *why* the test procedure was developed as it was, and not just *how* it is performed. This discussion is critical to comprehension of the limitations of T307 and is intended to facilitate discussion of possible improvements that can be made in the future. It is intended that this will lead to a more robust test procedure that can be used to generate repeatable, accurate, and consistent resilient modulus data for use in pavement design and evaluation.

**Resilient Modulus – Condensed History**

Pavement thickness design prior to World War II was basically empirical, based on experience, soil classification, and response of a pavement structure to static load, (e.g., a plate load or CBR test). A minimum thickness for a surface course was often selected based on plastic deformation as the only failure criterion. Elastic deformations were not even considered (Vinson 1989).

Shortly thereafter, several investigators used repeated plate load tests on model pavement sections with the number of load repetitions around 10. The primary objective of their investigations was to determine the effect of repetition of load on the deformation and not to determine the resilient modulus. The collective work of these investigators focused on the determination of the deformation characteristics and resilient modulus of compacted subgrades. The investigators came to the conclusion that the behavior of soils under traffic loading could only be obtained from repeated load tests. This conclusion was further supported with data obtained by the California Department of Highways that illustrated a large difference in pavement deflections occurring under standing and slowly moving wheel loads (Vinson 1989).

This work continued in the 1960s and 70s. It was noted that vehicle speed and depth beneath the pavement surface are of great importance in selecting the appropriate axial compressive stress pulse time to use in repeated load testing. Based on the results of a linear elastic finite element representation of a typical pavement structure, relationships concerning the variation of equivalent vertical stress pulse time with vehicle velocity and depth were established (Vinson 1989).

All of this work led to the adoption of AASHTO T274 in 1982. This standard was the first modern procedure used to define the test method for resilient modulus. The concept of resilient modulus was subsequently incorporated into the 1986 AASHTO Guide for Design of Pavement Structures. During this time, the standard had varying degrees of acceptance throughout the materials testing community.

In 1988, a thorough review was conducted of ASTM T274 by the LTPP Materials Expert Task Group (ETG) and the LTPP team. This group identified areas within the standard that were ambiguous or that offered alternatives. Through this process, LTPP Protocol P46, "*Resilient Modulus of Unbound Granular Base/Subbase Materials and Subgrade Soils*," was developed and issued in 1989. Over the years, the protocol was revised and amended and was issued in its final form in 1996. Subsequently, in 1999 P46 was balloted through the AASHTO process and was adopted (with some modification) as AASHTO standard T307-99, "*Determining the Resilient Modulus of Soils and Aggregate Materials*."

Over the past quarter of a century, a great deal of practical research has been undertaken in the pavement design and management community regarding resilient modulus. All of this research cannot be documented herein, however, suffice it to say that the reader can find ample research results in the literature. There is no doubt that the state of the practice of resilient modulus testing will be advanced through the adoption of new technology and testing procedures. The reader is directed to Vinson (1989) for a more detailed treatment of the history of resilient modulus.

## Overview of Resilient Modulus Protocols

### *Protocol P46*

P46 contains many conditions and requirements that apply only to the LTPP program. For example, measurement of deformation outside of the test chamber is a requirement that is very specific to the goals and objectives of the LTPP program. Because of the large numbers of samples to be tested, the ETG that reviewed the protocol decided that this was the most practical and efficient method. However, this method may not apply to all test conditions. In addition, the compaction procedures were specifically chosen for similar reasons.

Protocol P46 covers the following topics:

Scope
Testing Locations
Definitions
Applicable Documents
Unbound Materials Testing Prerequisites
Apparatus
Preparation of Test Specimens
Test Procedures
Calculations
Reporting
Compaction of Test Specimens

The P46 protocol is suitable for use by organizations wishing to perform their tests exactly as they were conducted by LTPP for correlation or other purposes. However, its use as a general test method by other organizations should be considered carefully.

*AASHTO T307*

As mentioned previously, T307 was developed primarily by modifying LTPP Protocol P46. Many features of the standard are similar to P46 while some sections have been modified to facilitate use of the procedure by a broader range of organizations. At the time of the development of this paper, this is the only test standard adopted by AASHTO to determine resilient modulus values from pavement materials.

AASHTO T307 covers the following topics:

Scope
Referenced Documents
Terminology
Summary of Method
Significance and Use
Apparatus
Preparation of Test Specimens
Test Procedures
Reporting
Compaction of Test Specimens

Of particular note, the standard includes the use of either hydraulic or pneumatic test systems and includes additional sections detailing compaction by use of a kneading apparatus.

*P46/T307 Similarities and Differences*

Because T307 is a direct descendant of P46, it stands to reason that they share many similarities. However, they also contain some differences. Table 1 highlights these similarities and differences.

*Other Procedures*

There are several other test procedures developed, or under development, throughout the world. Each procedure has its own strengths and weaknesses. For example, NCHRP 1-28 (Barksdale et al. 1998) has proposed new procedures for testing asphalt and unbound materials. Several other researchers have also put forth revised test procedures. For now, it seems that AASHTO T307, based primarily on LTPP development efforts, is the state of the practice within the United States.

Table 1 – *Comparison of P46 and T307*

| Protocol Specification | P46 | T307 |
|---|---|---|
| Type of Loading System | Hydraulic | Hydraulic/Pneumatic |
| Load Control | Closed Loop | Closed Loop |
| Load Cell Location | External | External |
| Deformation Measurement | External | External |
| Confining Fluid | Air | Air |
| Load Pulse Shape | Haversine | Haversine |
| Load Duration | 0.1 s | 0.1 s |
| Cycle Duration | 1.0 s | 1.0 to 3.0 s |
| Number of LVDTs | 2 | 2 |
| # of pts per cycle | 500 | 200 |
| Specimen L/D Ratio | >= 2:1 | > = 2:1 |
| Type of Compaction | Static/Vibratory | Static/Vibratory/Kneading |

The next portion of this paper will involve a detailed discussion of various technical aspects of the protocol.

## Loading System

LTPP protocol P46 and AASHTO T307 require a haversine loading waveform with varying frequencies and magnitudes. Equipment manufacturers have gone exclusively to fluid power to apply these loads. Mechanical testers employing cams, levers, gear or screw drive, while suitable for static or slow displacement testing, prove too cumbersome for repeated load, especially in a load-controlled mode. Electromagnetic drive systems, while well suited for metal fatigue testing in resonant drive machines at frequencies much higher than 10 Hz are not suitable for resilient modulus testing. The high currents needed to produce repeated loads at 1 Hz and below create a noisy environment to nearby electronic instrumentation. Fluid power options open to the designer include:

- fluid medium: air or hydraulic oil
- control mode: open or closed-loop

A brief discussion of advantages and disadvantages of each follows:

### *Fluid Medium*

Compressed air is a logical choice as a source of load power. It is non-messy, non-toxic, and readily available in most labs. As an additional advantage, the noisy compressor can be placed remote from the test lab. At normal line pressures, however, (100-125 psi) upper load limits are 1000 to 2000 lb for reasonably sized actuators. Also, since air is highly compressible, considerable energy is expended to cycle high loads continuously. Compressibility also places a limit on the quickness of load application (rise time to attain full load).

Hydraulic fluid (oil) is well suited as a means of fluid power. For example, at working pressures of 2500 to 3000 psi, it can be very quick in load rise time, and a 5 kip, 2 in. stroke actuator can be very small. The first cost of hydraulic systems is high, though these systems are more complex than pneumatic systems. Additionally, the pump unit usually resides close to the test apparatus, and may require external cooling as well as noise reducing cabinetry. Oil leakage can potentially be a problem in ill-maintained equipment.

Protocol P46 allows only hydraulic systems. This type of system was chosen as it was believed by the ETG that this type of machine was the best to produce consistent and repeatable resilient modulus values. It was also chosen to reduce a potential source of variability in the testing process. The LTPP program procured three laboratories to conduct soils resilient modulus testing. As such, it was desired that each lab use the same type of equipment. Based upon these rationale, it was decided that each lab should be equipped with a servo-hydraulic testing system.

As mentioned, these systems are rather expensive and some DOT and university laboratories doubtless still employ pneumatic systems since they are a much cheaper alternative to a hydraulic system. Thereby, it is surmised that the AASHTO committee that developed T307 allowed the use of such systems as a comparable solution. This may be a valid rationale. To the author's knowledge there has never been a comparison study conducted to compare the two alternatives to determine their comparability. It is strongly suggested that such a study be implemented prior to re-development of the T307 test procedure as it is expected there will be significant differences in the results obtained from a hydraulic versus pneumatic system. Most systems sold for resilient modulus testing today are of the hydraulic variety.

*Control Systems*

Open loop control systems respond to a command input without regard to current output status of load or displacement of the actuator. A good example is a constant-rate triaxial load frame (older style without servo-motor). The command input is a setting at a constant speed. Once started the platen moves until shutoff. No self-adjusting takes place to maintain speed.

Repeated load machines of the open-loop variety use a source of constant pressure to derive the load pulse. Typically, the actuator cylinder is toggled by a valve between a high pressure source and a low pressure source to gain the desired train of load pulses. The chief advantages are simplicity, reliability and low cost. The valves used are rugged on/off devices which are easy to service or replace, and the actuator can be single acting (unidirectional). Pressure regulators with output gauges can supply the high and low pressure; the gauges give the operator a rough idea of applied loads. *Due to a lack of ongoing control, no modern resilient modulus standard allows use of such a system.*

Closed loop control systems employ a sensor at the actuator output that can monitor the desired variable, either load or displacement. The signal that reports the current output status is called the feedback signal. It is compared to another signal, input command, at a summing point. The difference between the input command and output status is the error and is used to drive the actuator control valve to rapidly minimize the error. The chief advantage of closed loop control is its ability to follow command signal input changes, within the speed and amplitude capabilities of the actuator. Indeed, a large industry has evolved in the field of structural response testing, both destructive and nondestructive, based on the capabilities of closed loop controlled actuators to simulate field phenomena. However, closed loop systems are inherently more complex and expensive than open loop systems. A servo amp drives the servo valve; dynamic response of the complete system with feedback must be "optimized" or tuned for the materials and load frame used. Performance of an improperly adjusted system can range from sluggish to wildly unstable and can potentially be extremely dangerous (Brickman 1989). For these reasons, neither P46 nor T307 allows use of open-loop systems.

**Load Cell Location**

Both P46 and T307 require the use of a load cell mounted outside the triaxial chamber. This is one area of T307 that should undergo scrutiny. For LTPP, there were a large number of samples that needed to be tested. Therefore, after a period of pilot testing and for efficiency concerns, it was decided to mount the load cell and deformation transducers outside the confining chamber. Making this decision means that a great deal of effort must be expended ensuring that there is no friction or extraneous deformations in the system. This topic was a source of great anguish within LTPP due to the very tight tolerances that resulted.

Under normal circumstances, it should be entirely appropriate, and perhaps advised, to mount the load cell within the test chamber. In fact, this is the approach used by several manufacturers. Mounting the load cell within the chamber allows for more precise control and a more accurate reading of exactly the load the specimen is "feeling." The "uplift" adjustment necessary to account for the confining pressure can also be negated. All in all, mounting the load cell within the chamber should be considered as a suitable alternative in T307.

With that being said, however, if the load cell is mounted within the chamber, then the deformation measurement devices must be mounted inside the chamber as well (usually on the specimen). This is necessary because a typical load cell is essentially a device that provides it readings through strain measurements. Thereby the load cell has to deflect to read load. If the deformation devices are mounted outside the chamber, this strain will become part of the specimen strain reading. Obviously, this is not a desired outcome. Thereby, if the load cell is mounted internally, care should be taken to locate the deformation measurement devices in an area that will not "see" this deformation.

**Deformation Measurement**

Similarly, both P46 and T307 require use of deformation devices mounted outside the triaxial chamber. This is another area of T307 that should undergo scrutiny. The same rationale applies here as was discussed for the load cells. For LTPP, it was efficient and reasonable to use transducers mounted only on the outside of the chamber. One overriding reason for this decision was that LVDTs mounted on the specimen may slip during testing. This action may or may not be readily apparent to the operator. If this happens, the test must be halted and the entire procedure repeated. This has the potential to cause a great deal of inefficiency when testing numerous samples.

However, it has been the author's recent experience that mounting the LVDTs directly on the sample has its merits. This approach negates any "slop" in the system that may appear as specimen strain when measuring outside the chamber. It also alleviates concerns with stress concentrations that are evident at the ends of the specimens. However, great care must be used with this approach. The operator must ensure that the deformation measurement devices do not slip during the test. Also, depending on the configuration, they must be removed prior to conduct of any type of shear test.

It is very strongly recommended that this issue be revisited during any proposed revision to T307. Internal deformation measurement can work and under certain circumstances may provide more accurate values than measuring outside the chamber.

Finally, P46 requires the bottom of the triaxial cell be bolted down to the test table while T307 does not contain such a provision. If the configuration shown in T307 is used (deformation measured outside the chamber) it has been demonstrated that it is very important to bolt the chamber down. In this test procedure we are measuring very, very small strains. If the bottom of the plate is allowed to "float," small deformations are picked up by the deformation transducers mounted outside of the chamber. Bolting the system down will help to reduce this problem. This is a very important part of the procedure and should be strictly followed. It is recommended that T307 be revised to accommodate this requirement.

**Confining Fluid**

LTPP Protocol P46 and AASHTO T307 both require the use of air as the confining fluid. Practically, this is the best recommendation. However, to play devil's advocate, under certain circumstances water can be appropriate as a confining medium. In the final analysis, however, practically speaking water can be messy and may compromise the specimen's integrity if a leak or other failure occurs. It is recommended that air remain the only choice in this regard. Pressure transducers that can automatically regulate the air pressure within a chamber are relatively cheap and provide for accurate control of pressure. In any case, the tester should monitor this item very carefully and record the actual pressure in the chamber, not the nominal pressure. Experience has shown that some users only record what the pressure should be, and not what it actually is. This can have dire consequences when analyzing test results.

**Load Pulse Shape**

Both protocols allow only a haversine waveform. This type of waveform has been proven through research to be fairly representative of the effect of a moving wheel load over a pavement section (Vinson 1989). There should be no argument as to the validity of this premise. However, one topic that has been a subject of debate within the LTPP program is - what constitutes a haversine waveform? How close must you be to the theoretical equation to have it be considered correct? Some systems on the market today come with "acceptance bands" and automatic PID settings. But each is different. This can potentially have a significant impact on modulus values due to differences in applied energy.

To answer this question within LTPP, the following acceptance criteria were adopted:

> Plot the load values (readings from the load cell) versus time for a representative cycle(s) at each load. Superimpose an ideal load over this typical load pulse. Compare the actual load pulse with the ideal load pulse. For resilient modulus testing, this criterion is as follows: Construct a theoretical ideal loading pulse for each load sequence from the maximum load and the 0.1 second loading duration specified in the protocol. The peak theoretical load is matched in time with the peak recorded load of a given sequence. An acceptance tolerance band is then created around the theoretical load pulse that is used to flag suspect data falling outside of the band. The development of the minimum and maximum values of the acceptance band is based on the following considerations:
>
> - Acceptance tolerance range. A ± 10 percent variation from the theoretical load is judged to be acceptable. In combination with the other checks, this range is effective at higher load levels and those near the peak. However, at low load levels this range may create an unreasonably tight tolerance.
> - Servo valve response time. A ± 0.006 second time shift in load from the theoretical load pulse is reasonable to allow for the physical limitations on the response time of the servo hydraulic system. This will provide a reasonable tolerance band that will be effective at intermediate loading and unloading portions of the load cycle.
> - Resolution of the electronic load cell. The resolution of the electronic load cell generally used in resilient modulus testing for these materials is ± 4.4 N. Therefore, a range of twice the minimum resolution of the load cell is used; i.e., ± 8.8 N. This range provides acceptable tolerances for testing at low load levels.
> - Logic. The minimum load allowed is 0 N.
>
> For each time step in the load curve, the tolerance range from all of these components is computed. The maximum value of these three components is selected as the upper tolerance limit, while the minimum value is used for the lower limit at each time step. Over the entire range of loading, five points are allowed to be out of tolerance before the load cycle is considered failed (Alavi et al. 1997).

This is but one approach to determining if a waveform is acceptable. In general, it is recommended that acceptance criteria be established in T307 as well. This will work to assist in repeatability and lower variability both within and between laboratories.

**Load and Cycle Duration**

P46 and T307 both allow 0.1 second loading periods. However, P46 only allows a cycle duration of 1.0 second while T307 allows 3.0 seconds. It is believed that the difference in these two specifications is primarily related to the use of hydraulic and pneumatic test systems. Due to the compressibility of air, pneumatic systems generally require more time to "ramp up" for each load cycle. Therefore they require an additional two seconds to perform the cycle. Hydraulic systems are immediately ready to perform the next load cycle. If pneumatic systems are retained within T307, then this requirement should be retained. If, however, the standard is modified to only allow hydraulic systems, it is recommended that the standard contained in P46 be applied. There is some concern on the author's part that use of both pneumatic and hydraulic systems in a materials study or inter-laboratory comparison may yield a great deal of variability although admittedly we have no data to back up this claim. Thereby, this issue should be given consideration at a later time.

**Number and Type of LVDTs**

Both protocols require the use of two spring-loaded LVDTs. In the case of P46, this is required due to efficiency and accuracy considerations. The outputs of the LVDTs were used to determine if the sample was "rocking" (an indication that the sample is incorrectly mounted in the triaxial chamber). There is no real reason however to limit the number to two. There are some testing configurations that utilize three or more LVDTs. It is our recommendation that the specification allow two or more LVDTs. This recommendation goes hand-in-hand with the prior discussion related to inside versus outside LVDT placement.

As far as the type of LVDT is concerned, it is highly recommended that LVDTs other than spring-loaded be allowed in the test procedure. There are many types of LVDTs on the market today and each has its advantages and disadvantages. Also, the technology is always evolving and the use of non-contact deformation transducers is probably not far off. Other types of deformation measurement devices should be allowed in the protocol. The specification should be redeveloped with a performance based scope. The protocol should only specify the accuracy of the device and leave the choice to application engineers who can best determine how to get the job done. This point needs a great deal of attention in the current T307 protocol.

**Number of Points per Cycle**

There has been much discussion concerning the number of data points that must be collected during one cycle of a resilient modulus test. P46 requires 500 points per second while T307 recommends a minimum of 200 points per second. Within the LTPP program, a great deal of effort was dedicated to this issue. From our experience, it was determined that 200 points (assuming a constant sampling rate) was NOT adequate to fully characterize the true shape of the curve. Some systems employ a system whereby 100 points are collected within the first 0.1 second and 100 points are collected in the remaining cycle duration (or some similar logic). While it is agreed that this serves a comparable goal as the LTPP option, it is not implemented consistently among software developers. Thereby the 500 points per second criteria serves to standardize this part of the procedure. Modern data acquisition systems and software data reduction programs should have no problem performing this task. The authors would argue that systems that employ data acquisition systems that cannot perform this requirement should not be used for resilient modulus testing. In any case, these criteria should be formalized and "minimums" should be avoided. Standardization is the key to producing solid resilient modulus results.

**Specimen Size**

Sample size was an important issue for the LTPP program. The sample size chosen was highly dependent on the amount of material that could be obtained from a given layer in the pavement structure. Therefore, the smallest sample sizes possible were selected. However, the sample sizes were determined by using the criteria outlined in T307 which is still very much relevant today. For LTPP procedures, Type 2 (generally cohesive) samples are molded in 2.8 inch diameter molds (to replicate a thinwall tube sample) and type 1 (generally non-cohesive) materials are molded in 6 inch molds. In T307, various specimen sizes are allowed as long as the diameter is greater than five times the nominal aggregate size. Additionally, both protocols require the L/D ratio to be greater than 2:1.

For LTPP, it was necessary to be extremely precise in this regard to ensure repeatability and consistency. The AASHTO approach makes a lot of sense for general testing and it is recommended that it be retained in the procedure in its current form.

**Compaction Parameters**

Each protocol has a similar approach to specifying target density and moisture parameters. For LTPP General Pavement Studies (and thus P46), the first choice was to compact specimens to approximate the in situ wet density and moisture content. This requirement was instituted in an attempt to better correlate laboratory test results and those from the analysis of deflection measurements performed immediately prior to sampling. It is important to recognize that establishing this correlation is an important objective of the LTPP program. Where in situ information was not available, a consistent and repeatable compaction density/moisture was desired. Therefore, after consultation with many experts, it was decided to compact all other specimens, including Specific Pavement Studies (SPS) samples, at optimum moisture and 95 percent maximum dry density. This was done to approximate construction specifications for most materials.

T307 requires a similar approach except that reconstituted specimens that have no field density/moisture data are compacted to parameters selected by the agency.

It should be noted that the compaction parameters selected for P46 were based upon the unique needs of the program. It is suggested that T307 be revised to allow compaction parameters that suit the objective of the testing process. For example, if in situ testing conditions are most important then these compaction parameters should be specified, if standard density and moisture parameters are appropriate, then these should be used. The way in which T307 is currently worded may be able to accommodate this subtlety; however, the verbiage could be improved. For example, their does not need to be a hierarchy in the sample compaction area to duplicate P46. Each set of compaction parameters is appropriate for a given situation. In other words, the range of compaction parameters used is highly dependent on the purpose behind the resilient modulus testing program. It may be unsuitable to use in situ moisture/density parameters for pavement design. A more suitable set of parameters would be related to the moisture and density upon layer placement or improvement. In general, this issue should be revisited if T307 is revised.

### Compaction Procedures

Protocol P46 allows static compaction for type 2 materials (generally cohesive) and vibratory compaction for type 1 materials (generally non-cohesive). AASHTO T307 allows similar requirements with the addition of allowance of kneading compaction for type 2 materials. Once again, the test parameters for P46 were chosen for efficiency, consistency, and repeatability concerns. These procedures are very specific to the program. Therefore, it was very prudent for the committee that adopted T307 to allow use of kneading compaction as this type of compaction has been shown to best represent the configuration of in situ particles in a subgrade. However, great care should be exercised for intra- or inter- laboratory testing comparison programs. It seems obvious, but the same compaction procedures, equipment, and parameters should be used to perform the comparison. The T307 protocol appears to be solid in this area and the author's have no recommendations in this regard.

### Quick Shear Test

Both P46 and T307 require a "Quick Shear Test" to be performed. This part of the procedure was added to P46 very late in the protocol development process because of shortcomings in the overall LTPP materials characterization program (i.e. a soil strength test was needed). It is not a necessary part of the resilient modulus procedure. By specifying the quick shear test, the configuration of the equipment used to perform the test changes dramatically and the resulting sensitivity of the system suffers. In general, the user must use a load cell much larger than would be needed to perform the test in the first place. Therefore, there is a potential loss of accuracy in performance of the procedure.

It is highly recommended that the Quick Shear Test be deleted from AASHTO T307. It is a totally separate procedure that was "tacked on" to P46 and really has no business as a part of the procedure. Its use can actually compromise the accuracy and sensitivity of the equipment used to perform the resilient modulus procedure. If a strength test is desired, consideration should be given to using different equipment and samples to perform the test. Generally speaking, the equipment used to perform resilient modulus testing should not be used for performing strength tests.

## Summary and Conclusions

The current AASHTO protocol for determination of resilient modulus of soils and aggregate material (T307-99) is based largely on Long Term Pavement Performance (LTPP) Protocol P46. This paper has provided a background of the reasons and rationale behind some of the major technical aspects of P46, and by direct association, AASHTO T307. The paper also offered suggestions for improvement or modification of T307. It is hoped that this discussion will lead to a deeper understanding of the test procedure and perhaps foster a discussion of the direction the procedure should follow in the future.

It is hoped that the reader has developed an understanding of *why* the test procedure was developed as it was, and not just *how* it is performed. This discussion is critical to comprehension of the limitations of T307 and was presented to foster a discussion of possible improvements that can be made in the future. It is intended that an open discussion of the strengths and weaknesses of T307 will lead to a more robust test procedure that can be used to generate repeatable, accurate, and consistent resilient modulus data for use in pavement design and evaluation.

## References


Alavi, S., Merport, T., Wilson, T., Groeger, J., Lopez, A., January 1997, "LTPP Materials Characterization Program: Resilient Modulus of Unbound Materials (LTPP Protocol P46) Laboratory Startup and Quality Control Procedure," Report No. FHWA-RD-96-176, U.S. Department of Transportation, Federal Highway Administration, McLean, Virginia.

Barksdale, R. D., Alba, J., Khosla, N. P., Kim, R. K., Lambe, P. C., and Rahman, M. S., 1998, "*NCHRP Web Document 14 Laboratory Determination of Resilient Modulus for Flexible Pavement Design*," Project 1-28 Final Report, National Cooperative Highway Research Program, Transportation Research Board, National Research Council, Washington, D.C.

Brickman, A., 1989, "An Overview of Resilient Modulus Test Systems," *Proceedings of the Workshop on Resilient Modulus Testing*, Oregon State University, Corvallis, Oregon.

LAW PCS, a Division of Law Engineering & Environmental Services, Inc., and Axiom Decision Systems, Inc, 2002, "Guide for Determining Design Resilient Modulus Values for Unbound Materials," *LTPP CD-ROM Product*, LTPP Team, Federal Highway Administration, McLean, Virginia.

Rada, G. R., Groeger, J. L., Schmalzer, P. N., and Lopez, A., 2003, "Resilient Modulus Testing of Unbound Materials: LTPP's Learning Experience," *Resilient Modulus Testing for Pavement Components, ASTM STP 1437*, G.N. Durham, A.W. Marr, and W.L. De Groff, Eds., American Society for Testing and Materials, West Conshohocken, PA.

Vinson, T. S., 1989, "Fundamentals of Resilient Modulus Testing", *Proceedings of the Workshop on Resilient Modulus Testing*, Oregon State University, Corvallis, Oregon.

Richard L. Boudreau[1]

**Repeatability of the Resilient Modulus Test Procedure**

---

**Reference:** Boudreau, R. L., "**Repeatability of the Resilient Modulus Test Procedure,**" *ASTM STP 1437, Resilient Modulus Testing for Pavement Components,* G. N. Durham, W. A. Marr, and W. L. De Groff, Eds., ASTM International, West Conshohocken, PA, 2003.

**Abstract:** Through the work of the Strategic Highway Research Program (SHRP, 1987-1992) and the Federal Highway Administration (FHWA, 1992-present), the government has provided financial and technical assistance to develop and improve a laboratory test method to determine the resilient modulus properties of unbound materials. Although the work – part of the Long Term Pavement Performance (LTPP) study – has led towards the adoption of test procedure T307-99 in the current release of the American Association of State Highway and Transportation Officials (AASHTO) Tests, many skeptics insist that the method does not lend itself towards repeatable, reproducible test results.

This paper acknowledges that the work conducted by SHRP and FHWA focused primarily upon developing a test method that would be relatively simple and highly productive with less variability inherent in the previous, existing test procedure. Variables not investigated included compaction methodology, instrumentation location and sensitivities to other influencing factors such as precision of confining pressure, waveform control, membrane thickness and porous stone properties. Additionally, the testing program did not successfully establish a precision and bias statement for the test method utilized.

The repeatability of the test is examined by utilizing eight replicated test specimen sub sampled from a homogenous Alabama soil and nineteen replicated test specimen sub sampled from a homogenous Georgia soil. Each test specimen was prepared using the five-lift static compaction method. All specimens were tested within the range of ±1 pound per cubic foot density and ±0.4 percent moisture content, thus minimizing variations of results due to material variation. Averages, standard deviations, and coefficients of variation (c.v.) were determined for resilient modulus values calculated at each load sequence, resulting in c.v.s of below 4.5%. The resilient modulus values were calculated using the constitutive model: $M_r = K1(S_c)^{K2}(S_3)^{K5}$ in order to normalize the data for comparative purposes.

The test method can promote repeatable test results, although much more testing is recommended to produce precision and bias statements within and between laboratories.

**Keywords:** resilient modulus, soil stiffness, subgrade

[1]President, Boudreau Engineering, Inc., 5392 Blue Iris Court, Norcross, GA 30092.

## Introduction

Resilient modulus testing of cohesive and cohesionless unbound materials began to gain momentum in the highway materials characterization discipline in the mid-1970s. By 1982, the American Association of State Highway and Transportation Officials (AASHTO) adopted test method T-274. In 1986, AASHTO adopted a pavement structure thickness design manual that required resilient modulus as the primary response input for subgrade support.

Since its inception, the test procedure has evolved, mainly through the activity of the Strategic Highway Research Program (SHRP). The first test protocol of SHRP for resilient modulus testing of unbound base/subbase materials and subgrade soils, Protocol P46, was intended to provide a simplified version of T-274 that would lead to improved repeatability and reliability. Many factors were believed to have contributed to the non-repeatability of the test, such as moisture content, density, compaction methodology, waveform control and numerous others. Skeptics have long claimed that the test appears to be extremely user-sensitive, and variation seems too excessive for the test to be practical or useable.

While all these concerns have been credible and warranted throughout the years, the work done under the Long Term Pavement Performance (LTPP) study together with the tremendous technological advances in instrumentation as digital has replaced analog controls and acquisition, have led to both better equipment and more knowledgeable individuals to perform the testing.

Even so, several round-robin proficiency test programs have been initiated recently, and results have been so widespread that potential pavement design professionals remain skeptical that the procedure and laboratories performing the tests cannot provide reliable test data to base a structural pavement design.

Von Quintus and Killingsworth (1998) describe a recommended field sampling and laboratory test program to provide sufficient data for subgrade strength characterization intended for use in selecting a design subgrade resilient modulus. Their report suggests variations as high as 25% at any given stress level are possible, and recommends that perhaps three replicated specimens for each material encountered may be necessary to accurately characterize the material.

The present paper addresses the concerns raised about the test not being able to reproduce similar results. This study is intended to demonstrate that results obtained from testing replicated specimens can be repeated; however, further evaluation is recommended as this work only includes a single test operator and single test system.

## Experimentation

This repeatability study commenced accidentally in the summer of 2000, and has proceeded with intention until March 2002. The study has included two soils, each replicated numerous times to tight tolerances of density (± 1 lb/cu.ft.) and moisture content (± 0.5%). This density tolerance is tighter than the requirement stipulated by AASHTO T307-99 (± 3% of target, which translates to ± 3 lb/cu.ft for a 100 lb/cu.ft target density). The following sections describe the testing process and control.

*Soils*

Both Soil A, sampled from Alabama, and Soil B, sampled from Georgia, are described as sandy silts (AASHTO) or clayey sands (Unified Soil Classification). A summary of properties for each soil is provided in Table 1.

Table 1 – *Summary of Soil Properties*

| Physical Property | Soil A | Soil B |
|---|---|---|
| Liquid Limit, LL | 21 | 36 |
| Plastic Limit, PL | 16 | 27 |
| Plasticity Index, PI | 5 | 9 |
| $P_4$ (%) | 94 | 100 |
| $P_{10}$ (%) | 92 | 96 |
| $P_{200}$ (%) | 47 | 48 |
| Maximum Dry Density, $\gamma_{max}$ (pcf) | 119.8 | 113.3 |
| Optimum Moisture Content, $\omega_{opt}$ (%) | 12.0 | 15.0 |
| AASHTO Classification | A-4 | A-4 |
| Unified Soil Classification | SC | SC |

Maximum dry density and optimum moisture content as determined by AASHTO T-99 (standard Proctor).

Approximately 1500 grams of soil was sub sampled from each soil sample in order to prepare/compact each test specimen replicate.

*Compaction Methodology*

Based on work done under the initial SHRP contract, a double-plunge compaction method of was first used for remolding purposes, similar to ASTM Test Method for Making and Curing Soil-Cement Compression and Flexural Test Specimens in the Laboratory (ASTM D1632). This method yielded specimens visibly uncompacted in the center height while exhibiting relatively dense ends. A three-lift system was evaluated, which improved the condition of the single lift system, but did not provide enough confidence that a uniform condition existed. This led to a five-lift static compaction methodology, which is currently contained in AASHTO T-307 as Annex A3. This method provides for uniform compacted heights using the same mass of soil for each lift.

A five-lift static compaction methodology was used for each specimen tested. The compaction device utilized, similar to that shown in Figure 1, was a 50 000-lb frame constructed on a tripod steel-frame base with a 30-inch total stroke, bottom-mounted ram energized by a 115V single-phase pump. This dual-use unit integrates a convenient, easy ring assembly to guarantee very little risk of over compacting specimen lifts, while allowing the operator to quickly transform the unit for extrusion purposes. Nominal 2.8-inch diameter by 5.6-inch tall cylindrical test specimens were prepared for this study.

Density gradient verification is not required for the five-lift static compaction methodology per AASHTO requirements, and density gradients were not measured for any of the specimens prepared for this study.

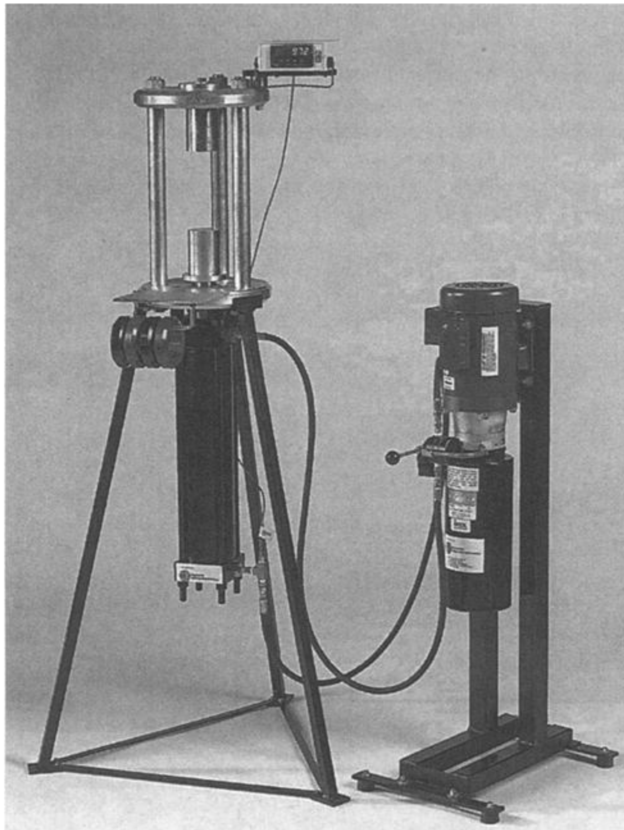

Figure 1 – *Static Compactor (photograph compliments of Durham Geo-Enterprises)*

*Test System*

Resilient modulus testing was performed on an Instron Model 8502 test frame, utilizing Instron's 8800-Series digital controller. The 50 000-lb capacity test frame houses a crosshead-mounted 10-inch stroke servo-hydraulic actuator, operating with a 5 gallon per minute water-cooled hydraulic pump. Although a 50 000-lb capacity machine is certainly not required to perform repeated load testing of soil specimens, in the author's experience a 50 000-lb capacity machine convincingly outperforms 5 000-lb and 20 000-lb capacity servo-hydraulic machines with respect to waveform control.

Calibrated components include two 0.2-inch stroke spring linear variable displacement transducers (LVDTs, Solartron Model AG2.5), a 1000-lb dynamic load cell (Instron Dynacell Model 2527-103) and a 120 psig automated electronic pressure controller (Testcom Model ER3000). The load cell is instrumented with an internally mounted accelerometer which is used in compensation mode to negate the effects of inertial forces resulting from rapid directional changes of the load cell mass. This control is better capable of keeping the load feedback signal within the tolerances prescribed by AASHTO T307.

The instrumentation configuration consisted of externally mounted load cell (attached to the top crosshead actuator) and externally mounted LVDTs. This typical configuration is shown in the photograph below (Figure 2).

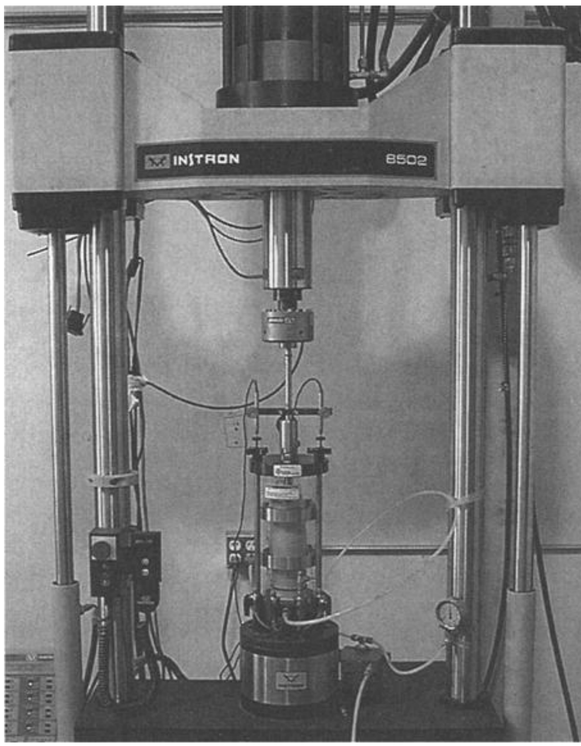


Figure 2 – *Resilient Modulus Test System*

This system possesses automated pressure control for applying, adjusting and measuring confining pressure throughout the duration of a test through software control. This transducer capability is helpful but not required. The system operator must ensure that appropriate pressures are provided and maintained for each load sequence if manual pressure control is utilized.

The test system was self-evaluated using procedures described in the Federal Highway Administration's Startup Procedures (Alavi et al. 1997). The evaluation was limited to only the physical testing requirements of the Report, and was conducted using a 2,000-lb Morehouse proving ring. The evaluation concluded that the test system performs at an acceptable level of accuracy and precision.

*Remolding Requirements*

Values of 95% of the maximum dry standard density at optimum moisture conditions were targeted. Hygroscopic moisture contents were determined for each sample on day one. On day two, each independently measured bulk sample was moisture-conditioned, placed in a plastic bag and allowed to absorb the mixed water over night. A moisture content was taken from each mixed sample at the conclusion of day two. Specimens were compacted on day three, after a moisture content tolerance check was determined. Immediately after compaction, the specimens were extruded, measured for dimensions (utilizing a Mitutoyo 8-inch digital caliper) and mass, placed in a latex membrane with paper disks and porous stones, and tested. Following the test, the entire sample was measured for moisture content.

*Testing*

All testing was conducted in a high-bay warehouse near Atlanta, Georgia. This space did not have temperature controls to moderate temperatures during the extreme hot and cold seasons chosen for the second phase of the work. Tests were conducted for the eight Soil A specimens between August 1 and 9, 2000. Based on the promising repeatability achieved on this small group of replicated specimens, a second testing phase was initiated to measure the repeatability over a long period of time, in order to evaluate the effects of ambient laboratory conditions. Thus, tests for Soil B were conducted over a period of eight months, from August 2001 to March 2002. Temperatures in the test facility ranged from 95°F in the late summer to 50°F in the winter.

**Results**

In order to evaluate the repeatability of the test results, it is important to measure the physical repeatability of the specimens used for testing and evaluation. No attempts were made to measure the sensitivity of the test to significant variations of density or moisture content. Thus reasonable tolerances of density and moisture were controlled. The following table (Table 2) illustrates the density and moisture control achieved for both sample groups.

Table 2 – *Remolded Test Specimen Summary*

| Measurement | Soil A | Soil B |
|---|---|---|
| Dry Density | | |
| Average (pcf) | 113.5 | 107.1 |
| Standard Deviation (pcf) | 0.3 | 0.3 |
| Coefficient of Variation (%) | 0.3 | 0.2 |
| Minimum Value (pcf) | 113.0 | 106.5 |
| Maximum Value (pcf) | 114.1 | 107.5 |
| Moisture Content | | |
| Average (%) | 12.2 | 15.0 |
| Standard Deviation (%) | 0.1 | 0.2 |
| Coefficient of Variation (%) | 0.4 | 1.2 |
| Minimum Value (%) | 12.1 | 14.7 |
| Maximum Value (%) | 12.2 | 15.4 |
| No. of Test Specimens | 8 | 19 |

As can be readily observed, the specimens used for this study are well replicated. The densities obtained are well within the study goal tolerances of ± 1 lb/cu.ft. and ± 0.5% moisture content. This demonstrates the repeatability in which samples can be prepared using the procedures of AASHTO T307-99, Annex A3. The average dry density deviated from the target value of 95 percent of the standard Proctor maximum dry density by 0.3 pcf for Soil A and 0.5 pcf for Soil B. Similarly, the average moisture content deviated from the target optimum moisture content by 0.2 percent for Soil A and 0.01 percent for Soil B. Although density gradients were not measured to assure negligible variation of density and moisture throughout each test specimen, there are reasonable assurances that resilient modulus test variations measured should be mainly attributed to test variations, not material variability.

The stress level targets presented in Table 1 of AASHTO T307 are nominal levels suggested to achieve. This table consists of 15 different combinations of cyclic axial stress and confining pressure, each combination referred to as a sequence. It would be hard to believe that these targets could be exactly matched between command and feedback signals. Because of the difficulty in achieving precise feedback, a constitutive model is necessary in order to compare results of tests. The constitutive model used in this study is that which was first introduced by SHRP in the early 1990's:

$$M_r = K1 S_C^{K2} S_3^{K5} \tag{1}$$

where
$M_r$ = resilient modulus, psi
$S_C$ = cyclic stress, psi
$S_3$ = confining pressure, psi
K1, K2 and K5 = nonlinear elastic regression coefficient/exponents

Results of the testing following the regression of data from each specimen to fit the constitutive model are provided in Table 3. In order to compute the regression constant and coefficients, the dependent variable, $M_r$ and independent variables $S_C$ and $S_3$ must first be transformed to a $Log_{10}$ base. This allows a linear regression to be performed. Once completed, the y-intercept is used as a 10-base exponential to derive the K1 constant, while the K2 and K5 coefficients are used as exponentials in Equation 1.

Table 3 – *Nonlinear Elastic Coefficient/Exponents*

| | Regression Coefficients | | | |
|---|---|---|---|---|
| Sample No. | K1 | K2 | K5 | $R^2$ |
| A-1 | 9 838 | -0.13196 | 0.22194 | 0.99 |
| A-2 | 9 873 | -0.14194 | 0.21102 | 0.99 |
| A-3 | 10 121 | -0.14167 | 0.21493 | 0.99 |
| A-4 | 9 335 | -0.12725 | 0.23100 | 0.98 |
| A-5 | 10 387 | -0.15483 | 0.23229 | 0.98 |
| A-6 | 9 463 | -0.11857 | 0.20279 | 0.98 |
| A-7 | 10 294 | -0.10049 | 0.17310 | 0.98 |
| A-8 | 8 780 | -0.07114 | 0.21455 | 0.97 |

| | | | | |
|---|---|---|---|---|
| B-1 | 7 515 | -0.17220 | 0.21615 | 0.98 |
| B-2 | 7 922 | -0.18555 | 0.22319 | 0.98 |
| B-3 | 7 762 | -0.18606 | 0.21680 | 0.98 |
| B-4 | 7 898 | -0.19693 | 0.24964 | 0.99 |
| B-5 | 7 859 | -0.18428 | 0.25522 | 0.99 |
| B-6 | 8 321 | -0.19894 | 0.23261 | 0.99 |
| B-7 | 7 905 | -0.20854 | 0.25953 | 0.99 |
| B-8 | 7 872 | -0.22103 | 0.26367 | 0.98 |
| B-9 | 8 178 | -0.19842 | 0.25590 | 0.99 |
| B-10 | 7 938 | -0.21171 | 0.23770 | 0.99 |
| B-11 | 6 956 | -0.21025 | 0.30340 | 0.99 |
| B-12 | 7 775 | -0.20790 | 0.25843 | 0.99 |
| B-13 | 8 484 | -0.21230 | 0.23373 | 0.99 |
| B-14 | 8 118 | -0.20199 | 0.23251 | 0.98 |
| B-15 | 7 592 | -0.20140 | 0.25691 | 0.98 |
| B-16 | 7 911 | -0.22068 | 0.25496 | 0.99 |
| B-17 | 7 904 | -0.20062 | 0.27061 | 0.99 |
| B-18 | 7 597 | -0.21391 | 0.26113 | 0.99 |
| B-19 | 7 468 | -0.21679 | 0.26751 | 0.99 |

The constitutive model selected provides an excellent fit for the data, as can be observed by the multiple-correlation coefficient, $R^2$. Although the regression constant, K1, and the coefficients, K2 and K5, seem to be quite variable for supposedly replicated specimens, there is no conclusive evidence of precision and bias that would indicate how much variability is acceptable.

Once satisfied that the constitutive model (Equation 1) was reasonable based on the good $R^2$, the results for each test specimen were calculated or predicted for resilient modulus at the exact stresses for each of the 15 sequences tested. This is done for the purpose of examining the differences in resilient modulus values from sample to sample or collectively as a group of replicated specimens.

As an illustration of importance, a test performed on a specimen targeted for a cyclic stress of 6 psi at a confining pressure of 4 psi (sequence number 8 of 15) may have achieved a cyclic stress of 5.75 psi, whereas another sample tested at the same targets may have achieved only a 5.4 psi value. If the material is sensitive to stress (stress dependent), comparing the raw resilient modulus values will not be ideal, or appropriate.

Tables 4 and 5 present the calculated resilient modulus values of each specimen tested for both soils at each of the 15 sequences. Summary information consisting of average, standard deviation, coefficient of variation and number of tests or observations are provided for each of the 15 sequences (table columns).

Table 4 - *Estimated Resilient Modulus Data (Soil A)*

| Sample | Resilient Modulus (predicted by Constitutive Model at each test loading sequence), psi | | | | | | | | | | | | | | |
|---|---|---|---|---|---|---|---|---|---|---|---|---|---|---|---|
| No. | 1 | 2 | 3 | 4 | 5 | 6 | 7 | 8 | 9 | 10 | 11 | 12 | 13 | 14 | 15 |
| A-1 | 13,362 | 12,194 | 11,559 | 11,129 | 10,806 | 12,212 | 11,145 | 10,564 | 10,171 | 9,876 | 10,471 | 9,556 | 9,058 | 8,721 | 8,468 |
| A-2 | 13,059 | 11,836 | 11,174 | 10,727 | 10,392 | 11,989 | 10,865 | 10,258 | 9,847 | 9,540 | 10,357 | 9,387 | 8,862 | 8,507 | 8,242 |
| A-3 | 13,484 | 12,223 | 11,541 | 11,080 | 10,735 | 12,359 | 11,203 | 10,578 | 10,155 | 9,839 | 10,648 | 9,652 | 9,113 | 8,749 | 8,477 |
| A-4 | 12,929 | 11,837 | 11,242 | 10,838 | 10,535 | 11,773 | 10,779 | 10,237 | 9,869 | 9,593 | 10,031 | 9,184 | 8,722 | 8,409 | 8,173 |
| A-5 | 14,146 | 12,707 | 11,933 | 11,414 | 11,026 | 12,875 | 11,564 | 10,861 | 10,388 | 10,035 | 10,960 | 9,845 | 9,246 | 8,843 | 8,543 |
| A-6 | 12,535 | 11,546 | 11,004 | 10,635 | 10,358 | 11,546 | 10,635 | 10,136 | 9,796 | 9,540 | 10,032 | 9,240 | 8,807 | 8,511 | 8,289 |
| A-7 | 13,093 | 12,212 | 11,724 | 11,390 | 11,138 | 12,205 | 11,384 | 10,930 | 10,618 | 10,383 | 10,825 | 10,097 | 9,694 | 9,418 | 9,209 |
| A-8 | 12,275 | 11,685 | 11,352 | 11,122 | 10,947 | 11,253 | 10,711 | 10,407 | 10,196 | 10,035 | 9,698 | 9,231 | 8,969 | 8,787 | 8,648 |
| avg. | 13,111 | 12,030 | 11,441 | 11 042 | 10,742 | 12,026 | 11,036 | 10,496 | 10,130 | 9,855 | 10,378 | 9,524 | 9,059 | 8,743 | 8,506 |
| s.dev. | 578 | 375 | 306 | 288 | 292 | 506 | 338 | 291 | 286 | 295 | 435 | 327 | 308 | 314 | 326 |
| c.v. | 4.41% | 3.12% | 2.68% | 2.61% | 2.72% | 4.21% | 3.07% | 2.78% | 2.82% | 3.00% | 4.19% | 3.43% | 3.40% | 3.59% | 3.84% |
| obs. | 8 | 8 | 8 | 8 | 8 | 8 | 8 | 8 | 8 | 8 | 8 | 8 | 8 | 8 | 8 |

Table 5 - *Estimated Resilient Modulus Data (Soil B)*

| Sample | Resilient Modulus (predicted by Constitutive Model at each test loading sequence), psi | | | | | | | | | | | | | | |
|---|---|---|---|---|---|---|---|---|---|---|---|---|---|---|---|
| No. | 1 | 2 | 3 | 4 | 5 | 6 | 7 | 8 | 9 | 10 | 11 | 12 | 13 | 14 | 15 |
| B-1 | 9,824 | 8,719 | 8,131 | 7,738 | 7,446 | 9,000 | 7,987 | 7,448 | 7,088 | 6,821 | 7,747 | 6,876 | 6,412 | 6,102 | 5,872 |
| B-2 | 10,391 | 9,137 | 8,475 | 8,034 | 7,708 | 9,492 | 8,346 | 7,741 | 7,339 | 7,041 | 8,131 | 7,150 | 6,632 | 6,287 | 6,032 |
| B-3 | 10,062 | 8,844 | 8,202 | 7,774 | 7,458 | 9,215 | 8,100 | 7,511 | 7,120 | 6,830 | 7,929 | 6,970 | 6,463 | 6,126 | 5,877 |
| B-4 | 10,777 | 9,402 | 8,680 | 8,202 | 7,850 | 9,739 | 8,497 | 7,845 | 7,413 | 7,094 | 8,192 | 7,147 | 6,598 | 6,235 | 5,967 |
| B-5 | 10,927 | 9,617 | 8,924 | 8,463 | 8,122 | 9,853 | 8,671 | 8,047 | 7,631 | 7,324 | 8,255 | 7,265 | 6,742 | 6,394 | 6,136 |
| B-6 | 10,998 | 9,581 | 8,838 | 8,347 | 7,984 | 10,008 | 8,719 | 8,043 | 7,596 | 7,266 | 8,517 | 7,420 | 6,845 | 6,465 | 6,184 |
| B-7 | 10,891 | 9,425 | 8,661 | 8,157 | 7,786 | 9,803 | 8,484 | 7,796 | 7,342 | 7,008 | 8,189 | 7,087 | 6,513 | 6,133 | 5,854 |
| B-8 | 10,832 | 9,294 | 8,497 | 7,974 | 7,590 | 9,734 | 8,351 | 7,635 | 7,165 | 6,820 | 8,108 | 6,956 | 6,360 | 5,968 | 5,681 |
| B-9 | 11,273 | 9,825 | 9,065 | 8,562 | 8,191 | 10,162 | 8,856 | 8,172 | 7,718 | 7,384 | 8,510 | 7,417 | 6,844 | 6,464 | 6,184 |
| B-10 | 10,494 | 9,062 | 8,316 | 7,825 | 7,464 | 9,530 | 8,229 | 7,552 | 7,106 | 6,778 | 8,082 | 6,979 | 6,405 | 6,027 | 5,749 |
| B-11 | 10,355 | 8,951 | 8,219 | 7,737 | 7,382 | 9,157 | 7,915 | 7,268 | 6,841 | 6,528 | 7,420 | 6,414 | 5,890 | 5,544 | 5,290 |
| B-12 | 10,696 | 9,260 | 8,512 | 8,018 | 7,654 | 9,632 | 8,339 | 7,665 | 7,220 | 6,893 | 8,052 | 6,972 | 6,408 | 6,036 | 5,762 |
| B-13 | 11,132 | 9,609 | 8,816 | 8,294 | 7,910 | 10,125 | 8,740 | 8,019 | 7,544 | 7,195 | 8,611 | 7,433 | 6,820 | 6,416 | 6,119 |
| B-14 | 10,705 | 9,306 | 8,574 | 8,090 | 7,734 | 9,742 | 8,469 | 7,803 | 7,362 | 7,038 | 8,292 | 7,208 | 6,641 | 6,267 | 5,990 |
| B-15 | 10,463 | 9,099 | 8,386 | 7,914 | 7,566 | 9,428 | 8,199 | 7,556 | 7,131 | 6,818 | 7,890 | 6,862 | 6,324 | 5,968 | 5,706 |
| B-16 | 10,720 | 9,200 | 8,412 | 7,895 | 7,515 | 9,667 | 8,296 | 7,586 | 7,119 | 6,777 | 8,101 | 6,952 | 6,357 | 5,966 | 5,679 |
| B-17 | 11,169 | 9,719 | 8,960 | 8,458 | 8,087 | 10,009 | 8,709 | 8,029 | 7,579 | 7,247 | 8,297 | 7,220 | 6,656 | 6,282 | 6,007 |
| B-18 | 10,458 | 9,017 | 8,268 | 7,774 | 7,412 | 9,407 | 8,111 | 7,437 | 6,993 | 6,667 | 7,850 | 6,768 | 6,206 | 5,835 | 5,563 |

| | | | | | | | | | | | | | | | |
|---|---|---|---|---|---|---|---|---|---|---|---|---|---|---|---|
| B-19 | 10,378 | 8,930 | 8,178 | 7,684 | 7,321 | 9,311 | 8,012 | 7,338 | 6,894 | 6,569 | 7,735 | 6,656 | 6,096 | 5,727 | 5,457 |
| avg. | 10,660 | 9,263 | 8,532 | 8,049 | 7,694 | 9,632 | 8,370 | 7,710 | 7,274 | 6,953 | 8,101 | 7,040 | 6,485 | 6,118 | 5,848 |
| s.dev. | 376.8 | 311.4 | 287.3 | 275.4 | 268.5 | 328.8 | 280.7 | 264.3 | 256.7 | 252.5 | 296.2 | 266.5 | 256.6 | 251.8 | 249.1 |
| c.v. | 3.5% | 3.4% | 3.4% | 3.4% | 3.5% | 3.4% | 3.4% | 3.4% | 3.5% | 3.6% | 3.7% | 3.8% | 4.0% | 4.1% | 4.3% |
| obs. | 19 | 19 | 19 | 19 | 19 | 19 | 19 | 19 | 19 | 19 | 19 | 19 | 19 | 19 | 19 |

## Observations

The data can be analyzed fairly easily by observing the c.v. term summarized at the bottom of each of the tables above. The c.v. term derived for any sequence is below 4.5%. These small c.v.s indicate very good repeatability. This marginally low spread of data refutes the argument that 3 specimens may be required to properly characterize a particular soil type, as suggested by Von Quintus and Killingsworth (1998) based on anticipated c.v.s of up to 25%.

## Conclusions and Recommendations

The following conclusions can be made from this limited study:

1. The 5-lift static compaction methodology can readily produce specimen properties within tight tolerances. The ability to remold specimen consistently is best served by well-crafted and maintained equipment and normal laboratory standard of care practices. A well-designed data worksheet to prepare specimens is required.
2. The test system must be properly and precisely calibrated. This not only includes component calibrations, but also should consist of a system evaluation similar to that documented in FHWA-RD-96-176.
3. If precautions are taken to eliminate concerns regarding specimen variability and equipment variability, the test procedure is capable of producing results that are repeatable.
4. Only one specimen (not 3) is required to adequately characterize the resilient behavior of a given soil.

The study conclusions are limited to the fact that only A-4 soils were evaluated, prepared by only one remolding method, by only one test operator performing tests in a single triaxial chamber on one test system. Experience has shown that any variation of these mentioned factors can lead to variations of results, even if specimens are measured to within the same tolerances of density and moisture content.

It is recommended that a program be developed and administered to evaluate a precision and bias statement that would include materials covering a wider range of expected resilient properties. These should include A-4, A-5, A-6 and A-7 soils, as a minimum. Once selected, several laboratories that can demonstrate conformance (by on-sight evaluation) to the precise requirements of the test procedure should test a minimum of six replicates from each material combination to develop both within-laboratory (repeatability) and between-laboratory (reproducibility) variation. It would be advantageous to evaluate the effects of compaction methodology during this recommended program as well as effects of moisture and density variations. This additional evaluation is recommended as a second phase, following the development of an accurate and acceptable precision and bias of the test procedure.

## References

Alavi, S., Merport, T., Wilson, T., Groeger, J., and Lopez, A., 1997, "LTPP Materials Characterization Program: Resilient Modulus of Unbound Materials (LTPP Protocol P46) Laboratory Startup and Quality Control Procedures," *Federal Highway Administration Report No. FHWA-RD-96-176.*

Von Quintus, H. and Killingsworth, B., 1998, "Analyses Relating to Pavement Material Characterizations and Their Effects on Pavement Performance," *Federal Highway Administration Publication No. FHWA-RD-97-085.*

Jonathan L. Groeger,[1] Anders Bro,[2] Gonzalo Rada,[3] Aramis Lopez[4]

# Implementation of Startup Procedures in the Laboratory

---

**Reference:** Groeger, J. L., Bro, A., Rada, G., Lopez, A., **"Implementation of Startup Procedures in the Laboratory,"** *ASTM STP 1437, Resilient Modulus Testing for Pavement Components,* G. N. Durham, W. A. Marr, and W. L. De Groff, Eds., ASTM International, West Conshohocken, PA, 2003.

**Abstract:** As part of the Federal Highway Administration's (FHWA) Long-Term Pavement Performance Program (LTPP) Materials Characterization effort, a quality control/quality assurance (QC/QA) procedure was developed to verify the proficiency of laboratory equipment and personnel in performing resilient modulus testing. This effort is documented in report FHWA RD-96-176, "*Resilient Modulus of Unbound Materials (LTPP Protocol P46) Laboratory Startup and Quality Control Procedure*" (Alavi, et al. 1997). Since issuance of that report, a great deal of experience has been gathered in using the procedure. This present paper provides an outline of the procedure, the rationale behind the procedure, and documents recent changes that have been developed by the authors. The paper also discusses issues to look for when implementing the startup procedure. Finally, a brief list of issues that have been found by using the procedure is presented.

**Keywords:** resilient modulus, laboratory testing, unbound materials, quality control and quality assurance, guidelines, LTPP

## Introduction

The Long-Term Pavement Performance (LTPP) resilient modulus test protocols were developed to ascertain stiffness of pavement surface (asphalt concrete), base, subbase, and subgrade materials. The resilient modulus testing process, generally regarded as a research-type procedure, has historically been performed in a university setting and on a

---

[1] Vice President, Axiom Decision Systems, Inc., 6420 Dobbin Road, Suite E, Columbia, MD 21045.
[2] Principal, Geo Test Unlimited, Inc., 27069 N. Bloomfield Rd., Nevada City, CA 95959.
[3] Assistant Vice President, LAW PCS, 12104 Indian Creek Court, Suite A, Beltsville, MD 20705.
[4] LTPP Team Leader, Federal Highway Administration, 6300 Georgetown Pike, McLean, VA 22101.

relatively small number of specimens. Because the modulus value derived from this testing process is a key parameter for pavement design, the test is being performed for the LTPP program in a production testing environment in what may be the largest single resilient modulus testing program ever undertaken.

It is of paramount importance to provide LTPP researchers with the highest quality data possible. As such, a quality control/quality assurance (QC/QA) procedure was developed to verify the ability of laboratory equipment and personnel to perform resilient modulus testing for LTPP. The original procedure, documented in FHWA-RD-96-176, *LTPP Materials Characterization Program: Resilient Modulus of Unbound Materials (LTPP Protocol P46) Laboratory Startup and Quality Control Procedure* was developed primarily for the verification of base, subbase, and subgrade resilient modulus procedure. Since issuance of that report, many lessons have been learned and processes have been added in an ongoing process improvement cycle. An updated and revised version of this procedure is proposed to be issued in 2002.

The purpose of this paper is not to repeat a description of the procedure presented in the above reference. Rather the paper provides a more detailed background of the procedure in order to foster a deeper understanding of the process. Its content represents more of a discussion of the procedure rather than a statement of procedural facts. It is recommended that readers of this document have a copy of the startup procedure handy as this paper can be considered a companion document.

**Procedure Overview**

The startup and quality control procedure was developed to ensure accuracy and reliability of raw measurements produced while testing materials using closed-loop servo-hydraulic systems. It is based on the premise that any engineering analysis requires reliable raw data, and the prerequisite for reliable raw data is properly configured equipment. The procedure is designed to verify the operating accuracy of all essential system components in a logical manner. Each part of the system is verified individually and then the entire system is checked to make sure all parts work together properly.

The procedure is divided into three distinct components:

1. Electronics system performance verification procedure.
2. Calibration check and overall system performance verification procedure.
3. Proficiency procedure.

As part of the electronics system verification procedure, signal conditioning channels, data acquisition processes, and transducers are checked for proper operation. Following the electronics system verification procedure, the calibration check and overall system performance verification procedure is performed. Load and displacement measuring devices; (i.e., load cells, linear variable deformation transducers-LVDTs) are checked for linearity and proper calibration. The ability of software to control and acquire data is also assessed. When the process of verifying individual system components is complete, the overall capability of the machine to conduct a specific experiment is assessed through specially designed static and cyclic experiments on materials with known properties. Once the system has been evaluated, the proficiency phase of the procedure addresses competence of laboratory personnel to prepare and test specimens. Through use of this procedure, all components necessary to obtain repeatable, accurate test results are verified.

The procedure enables laboratories to verify their testing systems prior to the start of production testing by using a comprehensive and logical process. It can also be used to perform ongoing quality control checks of equipment and testing processes being used by the laboratory during the production testing process.

It should be noted that the two primary goals of this process are (1) to ensure that the test system and technicians are capable of performing a test procedure, and (2) to develop a benchmark performance standard against which the laboratory can be evaluated on an on-going basis. This is a very important part of any quality control/quality assurance system.

The procedure should be used prior to starting a testing program, every year during production testing, and after periods of system inactivity (i.e., six weeks of down-time). It can also be used when equipment is replaced, moved, or whenever a suspected overload or malfunction occurs. Another important use of the procedure is to verify operation of new machines being delivered by a manufacturer. Conversely, the procedure can be used to verify the ability of older machines to perform new applications.

There are several obvious benefits of using concepts detailed herein. The first is that the procedure provides guidelines for standardization of an entire test process. It also provides a benchmark performance standard for equipment. If implemented correctly, it can minimize equipment and operator variability and thus provide greater confidence in test results and their application in research or design.

## Electronics Systems Performance Verification Procedure

The *electronics system performance verification procedure* characterizes frequency response of signal conditioners and the data acquisition system. This procedure is generally used prior to initiation of a resilient modulus testing program. As long as all electronic parts of the test system remain the same, this procedure does not necessarily need to be repeated on a continuing basis. However, it may be conducted yearly to verify equipment meets acceptance criteria or when any part of the electronics is replaced or modified. Also, the procedure can be performed when other circumstances suggest that electronics are suspect. Generally, an electronics technician well-versed in data acquisition systems is needed to perform these experiments.

Based upon experience of multiple system evaluations, it has been found that the electronics verification procedure is by far the most complex and difficult portion of the evaluation procedure.

When performing a test, it is generally accepted that test transducers be calibrated. This is a procedure in which output of the transducer is compared to a known test value (e.g., a load, pressure, or displacement), and a relationship (usually linear) is developed between transducer output and known applied test values. The resulting curve is the transducer calibration. This calibration procedure is a required element if the user is to know test values being applied to a specimen under test. But this calibration is by no means the only factor which influences test readings. The calibration procedure may not account for system electronics, and it certainly does not account for time varying test conditions. If test system electronics are improperly configured, test readings may be quite wrong, even if transducers are calibrated.

The purpose of the electronics verification procedure is to assess cyclic system performance of the data acquisition system (DAS) so that the user is confident that values measured by the computer are in fact loads, displacements and pressures being applied to the specimen. To perform this verification test on the data acquisition system, known signals (known in time and magnitude) are applied to each conditioned channel in succession, and response of each channel is compared to a known applied signal. These verification tests are performed "in-system" to as great an extent as possible so that the entire transducer/conditioning/acquisition system is incorporated in the verification test.

An additional benefit of performing these verification tests is that the test system is exercised and operators become more familiar with both software and hardware of the system. If an open mind is used to analyze sources of error and aberrations which are exhibited during these tests, then other interrelated shortcomings of the system can often be deduced and rectified, resulting in a more robust and properly operating system. Therefore, the procedure should not be used in a cookbook manner. Instead the objective of each task and response of the system should also be understood, rather than applying a "go/no-go" mentality.

The procedure has been developed to evaluate filter settings of signal conditioners. When a signal passes through a filter (in most cases this is a low-pass filter), the signal is delayed by a constant amount (the delay of which is for the most part independent of frequencies used in these tests). In addition, the signal is attenuated as the signal frequency increases past the filter cutoff frequency. If the input to the conditioner is compared to the output signal over a range of frequencies, the user can identify the type of filter and filter cutoff frequency. More importantly, the user can evaluate whether the conditioned signal closely duplicates (both in magnitude and in time) the physical processes being monitored.

The procedure used to evaluate filter settings was initially developed using a wholly electrical approach in which transducers were electrically simulated. This approach works well for DC type signal conditioners, but has serious drawbacks for transducers which rely on AC excitation (e.g., LVDTs). For these AC excited transducers, a new simulation interface circuit has to be designed, built, and tested for each type of AC signal conditioner. The new construction and testing of the test circuit is in itself a task which is quite labor intensive and the final test circuit could potentially introduce noise. In addition, any errors introduced by the circuit need to be quantified. Another issue with this approach is that the new circuit needs to be tested in the system before it is deemed acceptable. This approach is very time-consuming.

To work around these shortcomings, a mechanical approach was developed to actuate system LVDTs and test the AC conditioning system by comparing movement of a reference LVDT to displacement of the system LVDT being tested. (This mechanical LVDT actuator could be further modified to include a strain gauged member which would be mechanically flexed and result in a Wheatstone bridge output which could be used to simulate a load cell. Thus, with this mechanical actuator, no electrical simulations would be required to perform the verification tests.)

An alternative procedure to electrical simulation has been developed for evaluating load cell channels. In this approach the load cell is physically actuated using the hydraulic loading system. The hydraulic loading ram applies a sinusoidal load at frequencies up to 50 Hz. Generally most systems encountered to date seem to be limited to a frequency of 20 Hz or so (although this may be software limited rather than being limited by hardware). Due to this inability to reach 50 Hz, DC conditioners will have to be electrically simulated unless this limitation can be overcome.

A note concerning filter settings is warranted in this discussion. Low pass filters are an integral part of most signal conditioning systems. They are used to smooth out desired signals and to block high frequency noise which may be superimposed on the desired signal. In the case of AC conditioning systems, they also filter out any residual noise due to the carrier frequency. With such benefits to be gained from filters, it is tempting to add as much filtering as possible. The problem with this approach is that filters also introduce a time delay and tend to attenuate the desired signal as the frequency of the designed signal starts to approach the filter cut-off frequency. It is best to set these low pass filters as high as possible and yet still obtain a smooth signal. These filter settings should be recorded and tests performed with these filter settings.

Before settling on these filter settings, the user should operate the test system under various conditions to ascertain the settings when a variety of operating environments are encountered. Starting and stopping of large inductive motors create a particularly large amount of electrical interference. To account for these potential sources of electrical noise, air conditioners, compressors, hydraulic pumps, and other large motors should be started and stopped when taking data in an attempt to identify sources of noise which might impact the system. Filter cut-off frequencies should be set to reduce this noise to a tolerable level. If reducing filter settings does not reduce noise sufficiently, the test system should be isolated from the source of electrical noise.

Typically a test system will use filters of the same type on each of its channels. In this instance, it might be a good policy to set cut-off frequencies of the filters to the same values. Thus, even though filters might introduce a delay to each channel, relative delay between channels would be nearly zero, and would still result in a satisfactory channel-to-channel delay (as long as there is no appreciable attenuation).

Filters can be set using software or by physically changing components in the filter section of the signal conditioner. Usually filters are not physically modified due to a natural hesitation on the part of a technician to physically enter into the computer or signal conditioning system and modify the system. Since it requires a knowledgeable effort to modify a filter, once physical filters are set they are not usually modified (although they may be unintentionally changed when a signal conditioning module is changed). On the other hand, software filters may be easily modified, whether intentionally or not, simply with a few keystrokes. Diligence is therefore required on the part of the test operator to be aware of what filter settings are, how to change them, and what they should be for each test. Test procedures should be performed using filter settings for which it is anticipated the test will be normally run. Any filters set with different cutoff frequencies than used in the verification procedure would possibly invalidate any test performed with these filter settings.

Often questions arise regarding choice of frequencies used in this verification procedure. A tester's focus is generally the test being performed. But concern with this portion of the verification procedure is not performance of the ultimate test being performed, but characterization of the electronics system. To this end, users need to measure response of the electrical system. The user performs verification at low frequencies to evaluate system low frequency response. Unless signal conditioners are improperly configured, this low frequency test will measure unattenuated signal throughput. The highest frequency of 50 Hz is used to measure signal delay through signal conditioning/filtering modules. The filtering section introduces a constant time delay which is fairly independent of frequency. This small time delay is observed with better resolution if a high frequency is used. Therefore a verification test at 50 Hz is used to accurately characterize signal delay due to the filtering/conditioning module. The tests at intermediate frequencies of 10 and 20 Hz are performed to more thoroughly characterize frequency/attenuation of the channel being tested.

As documented in the procedure, the following criteria must be met in order to pass the test.

- All channels should have matched input-to-output delays. Delays derived from digital data should indicate matched input-to-output delays within ± 0.000400 s at 50 Hz.
- The maximum deviation in amplitude (signal attenuation) from 2 Hz to 10 Hz for a single channel should be less than 0.5 percent as determined from digitized data.

If above criteria are not met, problems such as inadequate filters (or unmatched filters) or inadequacies in data acquisition hardware/software should be investigated and tests should be repeated. Filter characteristics should not cause excessive amplitude or phase errors in the signals. Filter settings should remain unchanged after the electronics system has passed the acceptance criteria.

There are no easy rules to use in choosing the best verification test configuration. The electronic simulation of LVDTs can be difficult to understand, whereas mechanical actuation is quite easy to comprehend. So more than anything else, user's choice of configuration depends on equipment which is available and design of the data acquisition system, as well as the approach with which the investigator feels comfortable.

If there is noticeable signal attenuation, then filter cut-off settings are generally set too low and need to be modified. It is very instructive for the person performing the test to experiment with filter settings and set them to sequentially lower and lower values. The output signal will be seen to get smaller and smaller even though input signals remain the same. This exercise demonstrates the importance of proper filter settings, and how improper filter setting can result in useless data.

## Calibration Check and Overall System Performance Verification Procedure

Cyclic testing procedures require a system made up of many different pieces of equipment: load frame, load cells, hydraulic system, deformation devices, triaxial pressure chamber, temperature chambers, computer, etc. For the *calibration check and overall system performance verification procedure*, individual elements of test equipment are checked first followed by overall test setup. This verifies that the test system is producing expected responses. By first checking individual components of the test system, it is expected that many problems that would be encountered during actual cyclic testing can be identified and eliminated prior to checking the overall system. This procedure is generally used prior to initiation of a testing program and subsequently on a continuing basis (i.e. monthly) to verify system response.

The following section is broken down into eight components as follows:

1. Deformation measurement device
2. Load cell zero
3. Load cell calibration
4. Verification of load cell calibration (static)
5. Load versus deformation response check (cyclic)
6. System cyclic response check
7. Triaxial pressure chamber
8. Environmental chamber

*Deformation Measurement Devices*

One of the most critical aspects of a cyclic materials testing system is the strain, or deformation transducer, used to measure movement of the specimen. These can consist of Linear Variable Differential Transducers (LVDTs), extensometers, strain gauges, and other types of devices. The purpose of this experiment is to verify that the deformation measurement device is properly calibrated and performing in an acceptable manner. The procedure was developed for LVDTs or extensometers; however a similar approach can be used for other types of deformation measurement equipment.

The deformation measurement device must be matched to the application. For a more detailed explanation of the types of deformation measurement devices and their application, the reader is referred to the cyclic test system manufacturer or various deformation measurement device manufacturers. Much of this information can be obtained from the manufacturer's web site.

As documented in the procedure, the following criteria must be met in order to pass the test.

- The best fit curve shall have a zero intercept (±0.0254 mm), and a $R^2$ value of at least 0.99.
- The maximum difference in readings between micrometer and deformation device cannot exceed one percent of device full scale travel. For example, for a deformation device with a full scale range of 2.54 mm, the micrometer versus deformation device readings should be within ±0.0254 mm
- The deformation device shall be free of visual defects and should operate in an acceptable manner (no visible damage and no sticking of device, etc.).

In a production testing mode, it is recommended that LVDTs be verified every two weeks or after every 50 resilient modulus tests, whichever comes first. In addition, it is highly recommended that the micrometer used to check calibration be NIST calibrated or calibrated using NIST traceable gauge blocks.

*Load Cell Zero*

It is not uncommon in a laboratory to overload a load cell. Overloading can occur due to accidentally exceeding the rated capacity of the load cell, or by dropping it. In addition, if a cell is loaded to near its rated capacity, and the specimen fails brittley, then the cyclic stress wave which passes through the device can also overstress the cell. Such overloading needs to be evaluated periodically. It is often erroneously thought that the cell need only be recalibrated in event of an overload. In some cases of mild overloading, this approach may be acceptable, but often the only recourse is to dispose of the load cell.

An overloaded load cell can acquire some very undesirable characteristics. First of all, the load cell zero will usually shift due to overloading. This is the most obvious sign of an overloaded cell. Again, it is commonly believed that one can just re-zero the cell and continue testing. Unfortunately, by overloading the cell, a portion of the sensing membrane in the cell has gone into plasticity. This permanent deformation changes the elastic behavior of the cell sensing member. In addition to zero offset, the cell may now have a different calibration factor, and more importantly, it may well exhibit hysteresis and creep. Thus the loading curve (of load cell voltage vs. known load) will not follow the unloading curve. Creep behavior is manifested by not returning to zero after being unloaded, and then gradually settling down to a zero reading. Or after applying a large load, the cell will slowly drift to a steady reading. These traits are unacceptable for any transducer, and such an overloaded cell should be repaired or replaced.

When a load cell is fabricated and set up at the factory, the wheatstone bridge is balanced, either using laser trimmed strain gauges or additional resistors, to read a near zero volts when the bridge is excited. When the cell is overloaded, this balance is destroyed.

As documented in the procedure, the following criteria must be met in order to pass the test.

- Load cell zero reading should be within 1.5 percent of its full-scale factory indicated sensitivity.

If load cell zero reading exceeds 1.5 percent of its full-scale factory indicated sensitivity, then it should be returned to the manufacturer for evaluation. If the load cell meets specifications using manufacturer's test equipment then the load cell is considered suitable for use. If it does not meet manufacturer's specifications, then it should be repaired or replaced. It is recommended that the load cell zero check be conducted on all load cells at least yearly or whenever a suspected overload has occurred.

*Load Cell Calibration*

Load cell calibration is equally important as the load cell zero check. As part of any standard laboratory quality control plan, load cells should be evaluated at least yearly either in-house, by trained staff and NIST traceable standards, or using a calibration service with a National Institute of Standards and Technology (NIST) traceable cell. In either case, the calibration should be conducted using the latest version of Standard Practices for Force Verification of Testing Machines (ASTM E4). The calibration should be performed for the entire load cell operating range. The loading device should be verified annually and/or immediately after any repair or any relocation of the testing machine regardless of time interval since the last verification.

During this portion of the procedure, load cell calibration certificates are simply reviewed to determine if this calibration has occurred within one year.

As documented in the procedure, the following criteria must be met in order to pass the test.

- The load cell must have been calibrated within one year of inspection. A missing certificate is cause for rejection of load cell for testing until the necessary calibration has taken place.

*Verification of Load Cell Calibration (Static)*

The verification of the load cell static calibration is conducted with the system fully assembled as if a production test was about to be performed. In this experiment, a proving ring (specimen with known properties), or other suitable device, is used. This procedure does not take the place of the NIST traceable calibration mentioned previously. It is simply a check of the entire system versus a specimen of known properties.

Verification of load cell calibration is conducted for two reasons: (1) to ensure that load cell is performing as expected in the system, and (2) to check for unwanted system deformations.

Two methods may be used to perform this procedure depending on the user's test requirements. If verification of static calibration is all that is required, then a proving ring or external load cell can be used. As, in LTPP Protocol P46 (AASHTO T-307), deformation transducers are mounted outside the test chamber, thus the user would want to measure the difference between deformation measured inside the system versus that measured outside to determine if there is unwanted friction or deformations in the system. In this case, a proving ring with an internally mounted dial gauge or digital readout is preferred so as to make deformation comparisons.

There are many proving rings on the market today. If the user is going to perform an inside deformation versus outside deformation check using a proving ring, it is recommended that the user obtain a high-quality proving ring that consists of one solid piece of metal rather than the type that has separate units for top boss, ring, and bottom boss. Past experience has shown that these multi-piece rings are unsuitable for this application as they contain many metal-to-metal interfaces that can add to measured outside deformation, thus making results difficult to interpret. The single piece rings do not have these extra interfaces and therefore errors due to extraneous deformations of rings are minimized. If load verification is all that is desired, a multi-piece proving ring is adequate for the application. Equipment used to accomplish this procedure depends entirely on user goals.

In order to perform this procedure, the proving ring or other load measurement device must be matched to the application. Many proving rings are only guaranteed to be linear from 10 to 100 percent of their rated capacity. Therefore, if the test procedure contemplated results in loads up to 4.5 kN, the proving ring should be matched to this requirement. The user should verify the load cell calibration for all loads anticipated for a particular test application.

As documented in the procedure, the following criteria must be met in order to pass the test.

- The test system load must be within ±5 percent of proving ring load.
- The test system deformation must be within ±5 percent of proving ring deformation.

If, using the acceptance criteria, the system fails this check, the procedure is repeated. If the system fails second replicate, the system fails. If the system passes the second test, then a third replicate should be run to determine acceptance or failure. The apparatus should be disassembled and re-assembled in-between each replicate. If the system fails this check, the load cell should be recalibrated, or a new load cell should be installed on the test system and the process repeated. If the system does not pass the deformation criteria, check system for friction in triaxial piston, misalignment, loose triaxial cell, loose deformation devices, etc.

*Load versus Deformation Response Check (Cyclic)*

In order to properly evaluate suitability of a particular test system to a given application, it is essential that the machine be compared against a specimen of known properties. This comparison will allow users to assess performance of equipment in near-test conditions without repeatability and accuracy limitations imposed by testing a real specimen. Thereby, the purpose of this experiment is to simulate an actual test as closely as possible and ensure system performance meets anticipated user needs. This experiment is designed to provide a benchmark performance standard that can be repeated in the future to ensure the system is performing in a consistent manner.

In order to perform this procedure, a proving ring with an internally mounted deformation device is required. Alternatively, if measuring deformation outside a triaxial cell (for a soils resilient modulus test), deformation can be monitored using external deformation devices (assuming the system has passed external versus internal deformation test presented previously). Similar requirements regarding proving rings as presented earlier apply to this test. It is assumed herein that the proving rings used for this test procedure have capacity to perform testing in a similar manner as the test procedure requires. Never overload proving rings or load cells when performing this procedure.

As documented in the procedure, the following criteria must be met in order to pass the test.

- Generated haversine waveform is close to ideal haversine waveform.
- Load and deformation consist of 500 points per cycle.
- Generated deformation output is within 10 percent of ideal haversine waveform.
- Time lag between load peak and deformation peak is less than 0.008-s.
- Deformation is occurring after load.
- Maximum and cyclic loads within 5 percent of target.
- Contact load is within 10 percent of target.

- Deformation devices measuring within 10 percent of each other.
- Mean deformation values versus mean applied load within ±5 percent lines.
- $R^2$ of best fit line should be greater than 0.99.

If, using acceptance criteria the system fails this check, the procedure is repeated. If the system fails the second replicate, the system fails the check. If the system passes the second test, then a third replicate should be run to determine acceptance or failure. The apparatus is disassembled and re-assembled in-between each replicate.

If the system fails the loading or deformation check, operators should adjust machine settings to obtain a better waveform. If this does not correct the problem, the manufacturer should be contacted to assist in problem resolution.

If the system fails time lag check, system electronics and software should be evaluated to determine the cause of time delays. Also, check the system for friction in triaxial piston, misalignment, loose connections, loose deformation devices, etc.

*System Cyclic Response Check*

To investigate system cyclic response and investigate the possibility of excessive frictional forces, triaxial fixture misalignment, and machine induced time lag between load and displacement, a series of frequency sweep sinusoidal cyclic loading experiments is conducted. To perform this test, cyclic load and deformation readings are acquired from the data acquisition system using the load cell and the deformation device mounted on the proving ring. The deformation can also be obtained from deformation devices located elsewhere on the system such as on top of the triaxial cell.

The purpose of this test is to ascertain the time delay between load and deformation device channel(s) and to check for attenuation of load and deformation values over a range of loading frequencies. This check not only re-verifies the electronics checks, but it also identifies friction in the system, misalignment and overall system function. This experiment can not take the place of electronics checks as it does not fully characterize the electronics system. It can however be used as a rough check of system electronics. Caution is advised if this process is used to check electronics of the system as other casual factors such as friction and misalignment can cause the results to fail this check. Therefore, a more in-depth evaluation would have to be undertaken to determine the cause of failure than if the electronics procedure and system cyclic response check were run independently.

As documented in the procedure, the following criteria must be met in order to pass the test.

- The phase angle measurement should remain consistent for all five periods at a given frequency (within ±0.5 degree).
- Phase angle measurement less than 2.8 degrees.

If, using the acceptance criteria, the system fails this check, repeat the procedure. If the system fails the second replicate, the system fails the check. If the system passes the second test, then a third replicate should be run to determine acceptance or failure. The apparatus should be disassembled and re-assembled in-between each replicate.

If the system fails this check, the system electronics and software are evaluated to determine the cause of time delay. Also, the system should be checked for friction in triaxial piston, misalignment, loose connections, loose deformation devices, etc.

*Triaxial Pressure Chamber*

Each triaxial pressure chamber to be used for testing should be able to maintain pressure in accordance with testing parameters. It is also very important that test results report actual pressure used for the test. In several instances, it has been found that users report nominal pressure, or pressure that was programmed for the test. For some test systems, pressure used for the test may vary from that specified. In this case, use of nominal pressure can cause errors in test results when compared with other test results.

In order to perform this test procedure, a separate NIST traceable pressure gauge or transducer is necessary. This gauge is used to perform an independent system check. Also, it is very important that the cell pressure is zero before applying the system command to pressurize the chamber.

The pressures used for this experiment are similar to those used for the actual test procedure. This experiment can be conducted during proficiency testing as well if that is deemed more efficient than running the experiment independently.

As documented in the procedure, the following criteria must be met in order to pass the test.

- All system pressure readings should be within ±2.5 percent of the target.
- All NIST gauge pressure readings should be within ±2.5 percent of the target.
- All system and gauge readings should be within ±2.5 percent of each other.
- The target pressure must be achieved within 30 seconds.

Like other portions of a servo-hydraulic system, system pressure system is extremely important. If a pressure transducer is used, it is very important that the transducer is matched to the test system as closely as possible. It may not be advisable to use a 1034 kPa pressure transducer to perform soils and aggregate testing unless it can be scaled to a suitable range without loss of accuracy. Contact the system manufacturer for assistance in selecting a suitable pressure transducer for use in a particular test procedure.

If, using the acceptance criteria, the system fails this check, repeat the procedure. If the system fails the second replicate, the system fails the check. If the system passes the second test, then a third replicate should be run to determine acceptance or failure. The apparatus should be disassembled and re-assembled in-between each replicate.

If problems are found with system pressure, the manufacturer should be contacted to assist in determination of probable causes and efficient solutions.

**Proficiency Procedure**

The ability of laboratory personnel to conduct cyclic testing is evaluated in the *proficiency procedure*. While this procedure has been developed primarily for resilient modulus testing, the concepts can be applied to many test programs. This procedure is generally used prior to initiation of a testing program and subsequently on a continuing basis (i.e., quarterly) to verify operator's ability to conduct resilient modulus testing. The procedure requires approximately 2 days to complete.

In order to perform a complete analysis of the laboratory's ability to perform a particular test, all facets of the test process must be reviewed. To perform this procedure, a person with adequate experience in performance of the test must be enlisted to perform this review. The proficiency procedure brings together all of experiments mentioned previously to ensure accurate, repeatable test values are determined.

The proficiency procedure should not be conducted until all of mechanical and electrical system evaluation processes have been completed to the satisfaction of the evaluation team. In order to perform this procedure, a well-written comprehensive test procedure must be available to document test processes.

Several fundamental procedures should be evaluated during a proficiency testing review as follows:

- Material preparation
- Test performance
- Calculations
- Data reporting
- Data reasonableness

The entire test procedure is observed by personnel that are very familiar with the testing process. This should commence with specimen preparation through to data analysis and reporting. It should be noted that some of the acceptance criteria noted herein are subjective - thus the necessity for a knowledgeable individual to perform this procedure.

For this experiment, the user is looking for the following criteria:

- Generated haversine waveform is within tolerance.
- Load consists of 500 points per cycle.
- Generated deformation output is within tolerance.
- Deformation consists of 500 points per cycle.
- Maximum deformation is occurring after maximum load
- All manually calculated values should be within 5 percent of automated calculated values.
- All test parameters should be within 5 percent of test requirements.
- Vertical deformation readings from each sequence shall be checked to ensure that deformation devices are recording values with averages that (for collected cycles) have a coefficient of variation less than 2.5 percent.
- Deformation values within 30 percent of each other should be observed for all test sequences.
- All final test results should be reasonable as determined by the review team.

If, using the acceptance criteria, the system fails this check, the procedure is repeated. If the system fails the second replicate, the system fails the check. If the system passes the second test, then a third replicate should be run to determine acceptance or failure. The apparatus should be disassembled and re-assembled in-between each replicate.

A laboratory performing resilient modulus testing should give consideration to participation in an interlaboratory testing program to verify calibration of equipment and procedures with respect to other laboratories. Also, it may be desirable to manufacture or procure a standard specimen to test on a continuing basis to detect gross changes in performance of the system over time.

**What Can Go Wrong?**

The procedure discussed herein has been developed to verify operation of closed-loop, servo-hydraulic systems for specific application to the resilient modulus process. It is emphasized that users should implement this procedure with an open-mind and not in a cookbook approach.

From use of the procedure, many potential sources of error have been identified and rectified prior to starting a testing program, thus potentially saving a large amount of effort and resources. From the authors' experience in a number of laboratories, the following problems have been identified through implementation of this procedure:

*Electronics*

- Over-ranged load cells
- Inadequate filters (amplitude attenuation)
- Unmatched filters (excessive time delay between channels)

*Software*

- Inadequate software control of load
- Inadequate sampling rates
- Raw data without units
- Lack of gain control adjustment during testing
- Improper raw data format, command values were saved rather than feedback values

*Mechanical*

- System not fast enough to apply proper haversine loads
- Oversized servo-valve
- Friction in servo-valve piston
- Friction in triaxial cell seals
- Misalignment caused by improperly designed triaxial cell
- Excessive deformation, up to 76% of deformation due to bending of triaxial cell base plate
- Excessive deformation due to unrestrained fixture
- Slippage of LVDT holders
- Lack of control of pressure transducer
- Air pressure regulator malfunction

These examples are not meant to produce fear or anxiety in potential users. Rather they are illustrative of types of problems a user can face when implementing a resilient modulus testing program. Use of the verification procedure can alert users to problems with the system and laboratory processes quickly and efficiently.

**Summary and Conclusions**

The LTPP Resilient Modulus Startup and Quality Control Procedure was developed to ensure high quality, repeatable testing for LTPP researchers. Use of this procedure has yielded significant gains in achieving this goal. The procedure has also been implemented in many DOT, university, and commercial laboratories.

From experience gained within the LTPP program and from the authors' experience implementing this procedure throughout the country, we found it is critical that users implement each phase of the procedure in a systematic and logical manner. In addition, persons skilled in electronics as they apply to these test systems are necessary to fully implement this procedure. Please use care with the procedure and do not implement the processes in a "cook book" manner. The purpose of this paper is to provide a deeper understanding of the procedure in order to promote its use in a way so as to assure success with implementation of the Startup and Quality Control procedure. The reader is referred to the latest version of the procedures for more information in this regard.

**References**

Alavi, S., Merport, T., Wilson, T., Groeger, J., Lopez, A., January 1997, "LTPP Materials Characterization Program: Resilient Modulus of Unbound Materials (LTPP Protocol P46) Laboratory Startup and Quality Control Procedure," Report No. FHWA-RD-96-176, U.S. Department of Transportation, Federal Highway Administration, McLean, Virginia.

# SESSION 2: TESTING CONSTRAINTS AND VARIABLES

Jianchao Li[1] and Bashar S. Qubain[2]

**Resilient Modulus Variations with Water Content**

---

**Reference:** Li, J., and Qubain, B. S., "**Resilient Modulus Variations with Water Content**," *Resilient Modulus Testing for Pavement Components, ASTM STP 1437*, G. N. Durham, W. A. Marr, and W. L. De Groff, ASTM International, West Conshohocken, PA, 2003.

**Abstract:** Resilient modulus ($M_R$) variations with water content were carefully examined for three subgrade soils—lean clay, clayey sand, and clayey gravel. For each soil type, four $M_R$ tests were performed at the following water contents: 2 to 3% dry of optimum, at optimum; 2 to 3% wet of optimum; and at full backpressure saturation. The backpressure-saturated samples were molded at optimum and gained up to 6% moisture during saturation. The $M_R$ testing of the non-saturated specimens was conducted according to ASSHTO T307-99 and specific testing adjustments were developed for the backpressure-saturated ones. After achieving saturation, the specimens were consolidated at a confining pressure equivalent to the stress level of pavement surcharge and then subjected to five levels of deviator stresses under undrained conditions. The test results were utilized together with in situ stresses to develop design curves for resilient modulus versus water content.

**Keywords:** Resilient modulus, seasonal moisture variations, backpressure saturation, subgrade stresses, pavement design

## Introduction

The mechanistic-empirical model in the latest Guide for Design of Pavement Structures (AASHTO 1993) utilizes the resilient modulus ($M_R$) of the subgrade soil as the fundamental material property for pavement design. It follows that an accurate determination of this important parameter is essential. Resilient modulus has long been recognized to be stress and moisture dependent (Thompson and Robnett 1976, Fredlund et al. 1977, Elliott and Thornton 1988, Pezo et al. 1992). Typically, $M_R$ is determined from either field or laboratory tests, both of which incorporate the influence of stresses. Field measurements of pavement deflection using the falling weight deflectometer (FWD) indicate that the subgrade resilient modulus varies with load or stress level (Noureldin 1994). Laboratory tests also show that $M_R$ varies with both deviator and confining stresses, and various constitutive models have been proposed to relate the

---

[1]Associate, GeoStructures, Inc., 985 Old Eagle School Road, Wayne, PA 19087. E-mail: jcli@geostructures.net.
[2]President, GeoStructures, Inc., 985 Old Eagle School Road, Wayne, PA 19087. E-mail: bqubain@geostructures.net.

resilient modulus to the state of stress (Fredlund et al. 1977, Uzan 1985, Houston et al. 1993, Santha 1994).

The influence of water content, on the other hand, is not as easily addressed. For example, field tests such as FWD measure the pavement deflection and back calculate the resilient modulus at the time of the test without accounting for moisture variations. Laboratory resilient modulus tests are also usually performed at optimum water content which may not be representative of the in situ moisture throughout the year.

To overcome these shortcomings, the 1993 AASHTO Guide proposed a procedure for adjusting $M_R$ based on seasonal moisture variations. Although a step in the right direction, the suggested procedure treats all soil types in the same manner and does not offer a rational evaluation approach. Fredlund et al. (1977) recognized the relationship between water content and resilient modulus but they did not perform tests under full saturation—a condition which would result in a high water content and a low $M_R$. Muhanna et al. (1999) utilized a soaking apparatus to simulate full saturation but the setup only achieved about 90% saturation and took two weeks to reach that level.

This paper presents a laboratory testing program to evaluate resilient modulus variations with water content for three subgrade soils along the Pennsylvania Turnpike. As a result, modifications to existing test methods are proposed to enable the determination of $M_R$ at full saturation. The following questions are also addressed herein: What are the upper and lower limits of $M_R$? What are the upper and lower limits of water content? Is soaking adequate to simulate worst-case moisture conditions?

## Testing Program

Resilient modulus tests are conducted on lean clay (CL), clayey sand (SC), and clayey gravel (GC) subgrade soils as part of two pavement design projects along the Pennsylvania Turnpike—one in the Philadelphia area and the other in Somerset County in the western part of the state. To examine the effects of moisture variations, each soil type is tested at the following water contents: 2 to 3% dry of optimum, at optimum; 2 to 3% wet of optimum; and at full backpressure saturation. Water is added and thoroughly mixed with the various soils and a split mold (71 mm diameter and 142 mm height) is used to prepare remolded specimens at the targeted water contents. The soil is placed in five lifts, each compacted with a steel rod to achieve 100% of the standard Proctor. Resilient modulus testing for non-saturated specimens is conducted according to ASSHTO Method for Determining the Resilient Modulus of Soils and Aggregate Materials (T307-99). Specific testing details, however, are developed for the saturated specimens that are remolded at optimum water content as described later in this paper.

The resilient modulus testing setup used for this work is an electro-hydraulic servo-control system. The cyclic loading is applied through an actuator powered by a closed-loop hydraulic system. The confining air pressure in the triaxial chamber is measured by a pressure transducer and controlled through a regulator. Deformations are measured by two externally mounted LVDTs on the actuator. For saturation, water is introduced to the specimen by backpressure through a pressure control panel and a data acquisition unit (ADU). Pore pressure is measured through a pressure transducer connected to the lower drainage line of the specimen. Both back and pore pressures are continuously measured and monitored on a computer screen through the ADU.

*Standard Resilient Modulus Test Methods*

Currently, there are two primary standards for resilient modulus testing in the context of pavement design: T307 and AASHTO Method for Resilient Modulus of Subgrade Soils and Untreated Base/Subbase Materials (T292-96). The procedure of T307 is applicable to both fine-grained and coarse-grained subgrade soils. It includes a preconditioning sequence (1000 cycles) and 15 loading sequences (100 cycles per sequence) with a combination of 3 levels of confining pressures (41.4, 27.6, and 13.8 kPa) and 5 levels of deviator stresses (12.4, 24.8, 37.3, 49.7, and 62.0 kPa). The drainage lines are kept open to the atmospheric pressure during application of cyclic loading. This method recognizes the influence of confining pressure on $M_R$ for fine-grained as well as coarse-grained soils but does not include any provisions for saturation.

Unlike the previous test method, T292 has different treatments for fine-grained (cohesive) and coarse-grained (granular) subgrade soils and its cyclic loading is applied under undrained conditions with all the drainage lines closed. This method maintains, "the small range of confining pressure expected within subgrades has only a minimal effect on $M_R$ values obtained from cohesive specimens." Accordingly, cohesive soils are tested at a single confining pressure of 21 kPa but the specimen is consolidated under that same pressure prior to loading. A preconditioning sequence and 5 levels of deviator stresses are included similar to T307, except with different deviator stresses (21, 34, 48, 69, and 103 kPa). A saturation procedure is also included for cohesive soils. It is similar to that utilized in standard triaxial testing but requires full saturation without specifying a minimum value for the pore pressure parameter *B*.

*Implemented Procedure for Saturation and $M_R$ Testing*

Saturation for this work is performed through backpressure increments. Prior to applying air pressure, the triaxial cell is filled with water up to 15 mm off its top. Cell pressure is applied through air above the water surface. During the increments of backpressure application, pore pressure is recorded in order to calculate *B* parameter. Saturation is considered achieved when a *B* value of 0.90 or greater is reached. Full saturation (*B* greater than 0.95 as in conventional triaxial testing) is not targeted herein for two reasons: (1) for *B* equal to 0.9 or greater, the degree of saturation is 98% or more (Black and Lee 1973) and the subgrade is not likely to be saturated to such a high degree; and (2) the testing setup limits the backpressure to about 310 kPa and full saturation for remolded specimens would require much higher values.

After saturation is completed, the specimen is consolidated to a confining pressure of 17 kPa, which corresponds to the estimated stress level of a 580 mm pavement section. After consolidation is completed, all drainage valves are closed and the specimen is subjected to 500 cycles of preconditioning at a deviator stress of 25 kPa. The specimen is then tested in the standard manner—100 cycles at 5 levels of deviator stresses—as specified in T307. The final water content is measured upon completing the test.

## Results and Analyses

Figure 1 shows a typical plot of $M_R$ versus deviator and confining stresses for a lean clay specimen remolded at 2% wet of optimum and Figure 2 depicts a typical plot

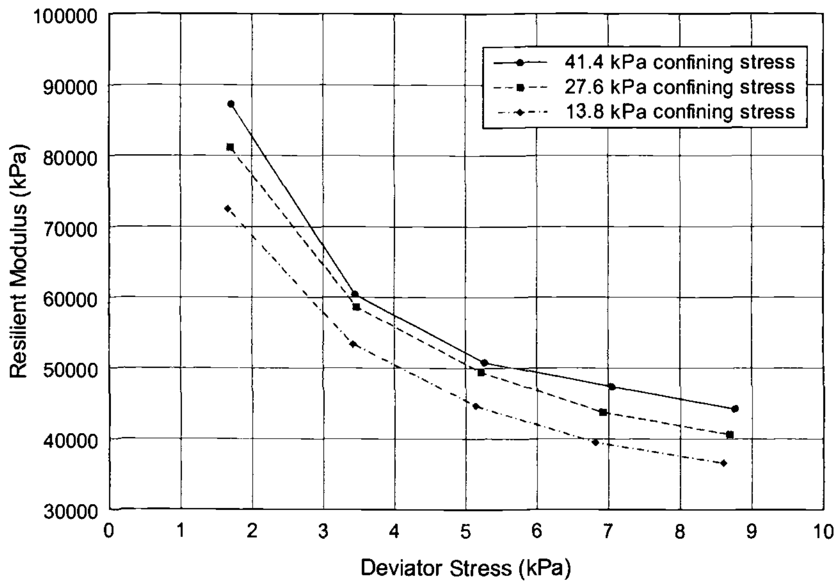


Figure 1 – *Typical Plot of Resilient Modulus vs. Deviator and Confining Stresses for Lean Clay*

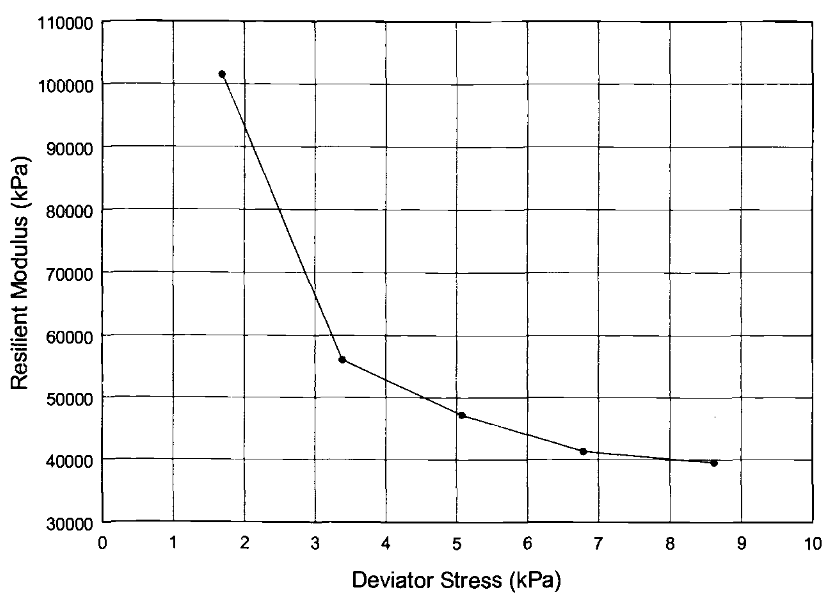


Figure 2 – *Resilient Modulus vs. Deviator Stress for Saturated Clayey Gravel at $\sigma_c$ = 17 kPa*

for a saturated clayey gravel specimen. Both of these figures illustrate that $M_R$ decreases with the increase in deviator stress $\sigma_d$. The decrease is more pronounced at lower values of $\sigma_d$ and levels off at values greater than 35 kPa. Figure 1 also shows that $M_R$ increases with the increase in confining stress $\sigma_c$ for lean clay, which is in agreement with T307 but contrary to the position maintained by T292. The $M_R$ testing results are summarized in Table 1 for the Pennsylvania Turnpike project in the Philadelphia area and in Table 2 for the Somerset project.

Table 1 – *Summary of Resilient Modulus Testing Results for Philadelphia Area Project*

| Soil Type/ Specimen | Remolded Dry Density ($g/cm^3$) | Remolded Moisture (%) | Compaction Level (%) | Moisture Variation | Degree of Saturation (%) | Moisture at Test (%) | Design $M_R$ (kPa) |
|---|---|---|---|---|---|---|---|
| CL-Dry of optimum | 1.94 | 8.5 | 99 | 3.0% dry | 57 | 8.3 | 110,649 |
| CL-Optimum | 1.96 | 11.8 | 100 | Optimum | 85 | 11.8 | 83,534 |
| CL-Wet of optimum | 1.90 | 13.4 | 97 | 1.9% wet | 85 | 13.2 | 59,241 |
| CL-Saturated | 1.96 | 11.8 | 100 | 6.3% wet | 100 | 17.6 | 38,080 |
| SC-Dry of optimum | 2.04 | 8.2 | 101 | 1.6% dry | 68 | 8.2 | 110,411 |
| SC-Optimum | 2.03 | 11.1 | 101 | Optimum | 91 | 11.1 | 125,391 |
| SC-Wet of optimum | 1.97 | 14.2 | 97 | 3.0% wet | 95 | 14.2 | 56,298 |
| SC-Saturated | 2.03 | 11.1 | 101 | 1.9% wet | 100 | 13.1 | 87,976 |
| GC-Dry of optimum | 2.16 | 7.1 | 101 | 1.3% dry | 84 | 7.7 | 103,831 |
| GC-Optimum | 2.15 | 9.4 | 100 | Optimum | 90 | 9.4 | 69,771 |
| GC-Wet of optimum | 2.05 | 11.6 | 96 | 1.6% wet | 90 | 10.6 | 52,737 |
| GC-Saturated | 2.15 | 9.4 | 100 | 2.1% wet | 100 | 11.1 | 62,465 |

Table 2 – *Summary of Resilient Modulus Testing Results for Somerset County Project*

| Soil Type | Remolded Dry Density ($g/cm^3$) | Remolded Moisture (%) | Compaction Level (%) | Moisture Variation | Degree of Saturation (%) | Moisture at Test (%) | Design $M_R$ (kPa) |
|---|---|---|---|---|---|---|---|
| Clayey sand | 1.87 | 12.8 | 99 | Optimum | 78 | 12.8 | 108,330 |
| | | | | Saturation | 100 | 16.4 | 50,370 |
| Sandy lean clay | 1.92 | 12.2 | 102 | Optimum | 81 | 12.2 | 96,600 |
| | | | | Saturation | 100 | 15.5 | 71,070 |
| Sandy lean clay with gravel | 1.93 | 13.6 | 99 | Optimum | 92 | 13.6 | 90,390 |
| | | | | Saturation | 100 | 15.2 | 54,510 |
| Sandy lean clay | 1.96 | 11.3 | 100 | Optimum | 82 | 11.3 | 137,310 |
| | | | | Saturation | 100 | 14.2 | 57,960 |
| Clayey sand with gravel | 1.87 | 12.0 | 100 | Optimum | 67 | 12.0 | 132,480 |
| | | | | Saturation | 100 | 17.5 | 41,400 |
| Clayey sand with gravel | 1.91 | 12.4 | 98 | Optimum | 81 | 12.4 | 91,080 |
| | | | | Saturation | 100 | 15.0 | 53,820 |

The backpressure-saturated specimens were molded at optimum and gained up to 6% moisture for the lean clay soil during saturation as shown in Table 1. The resulting water contents for the different specimens varied from 8% to 18% with the saturated specimens generally representing the upper bound of water content. The basis for remolding the saturated specimens at optimum is that subgrade soils are usually compacted close to optimum and absorb moisture upon prolonged exposure to rain to the limit of their effective consolidation stresses. In contrast, a remolded laboratory specimen at moisture close to full saturation would not likely achieve proper compaction and therefore would not realistically simulate the subgrade soil. Evidently, the density of the remolded specimen at high water content would be much lower than that of the subgrade.

*Design $M_R$*

As shown in Figure 1, the laboratory tests produce a set of curves that relate $M_R$ to deviator and confining stresses. However, pavement design according to the AASHTO Guide requires a single input value for the resilient modulus. This is called the effective roadbed resilient modulus and it is determined by three processes: (1) selecting a design $M_R$ value based on the in situ stress state; (2) determining the upper and lower limits of resilient modulus and water content variations; and (3) adjusting the design $M_R$ to reflect the seasonal moisture variations throughout the year.

In situ stresses are calculated using *KENLAYER* computer program (Huang 1993), which is based on a multi-layer elastic model. Traffic loads including various 80 kN axle load combinations together with surcharge from the pavement section are utilized. For a 580 mm pavement section, the analysis results in deviator and confining stresses in the range of 14 to 21 kPa, and a bulk stress on the order of 60 kPa. These in situ stresses are directly used in a constitutive relation between $M_R$ versus deviator and bulk stresses to establish the design $M_R$. This relationship is developed through a nonlinear regression analysis of the laboratory resilient modulus data to fit the constitutive model proposed by Uzan (1985) and discussed by Santha (1994). The regression analysis (not included herein) is similar to that illustrated by Von Quintus and Killingsworth (1997).

On the basis of the estimated in situ stress state, a design $M_R$ is determined for each specimen as shown in Table 1 for the Pennsylvania Turnpike project in the Philadelphia area and Table 2 for the Somerset project. These design $M_R$ values correspond to the specific water contents at the time of testing and only represent the first process. The upper and lower limits of resilient modulus and water content variations are determined as follows.

*Resilient Modulus and Water Content Variations*

The $M_R$ values in Table 1 are plotted against the corresponding moisture contents for each subgrade soil as shown in Figures 3 through 5. The curves clearly suggest a general trend or relationship that applies to all tested soil types. The lean clay and clayey gravel $M_R$ test results produced good fit to the suggested trend with multiple correlation coefficients $R^2$ = 0.97, and 0.85, respectively. The clayey sand test results were not as

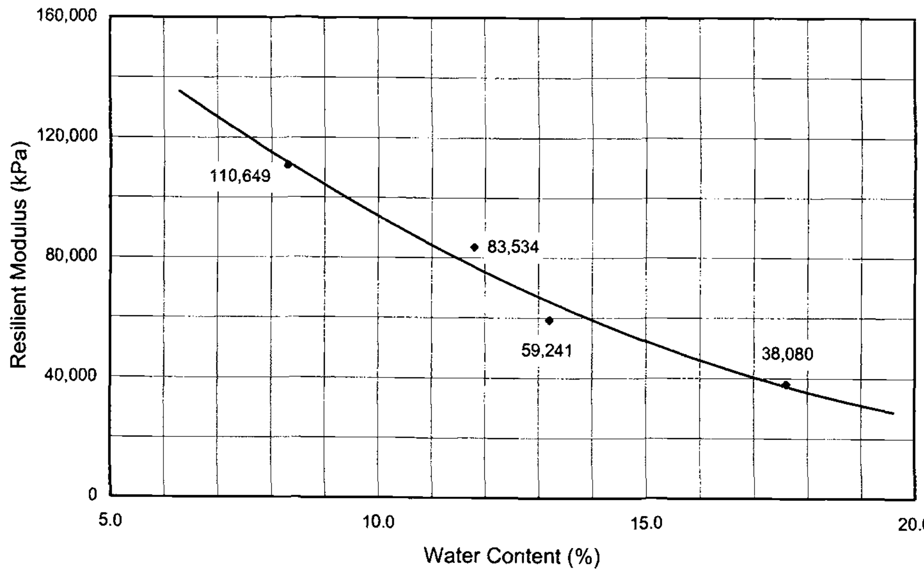


Figure 3 – *Resilient Modulus vs. Water Content for Lean Clay*

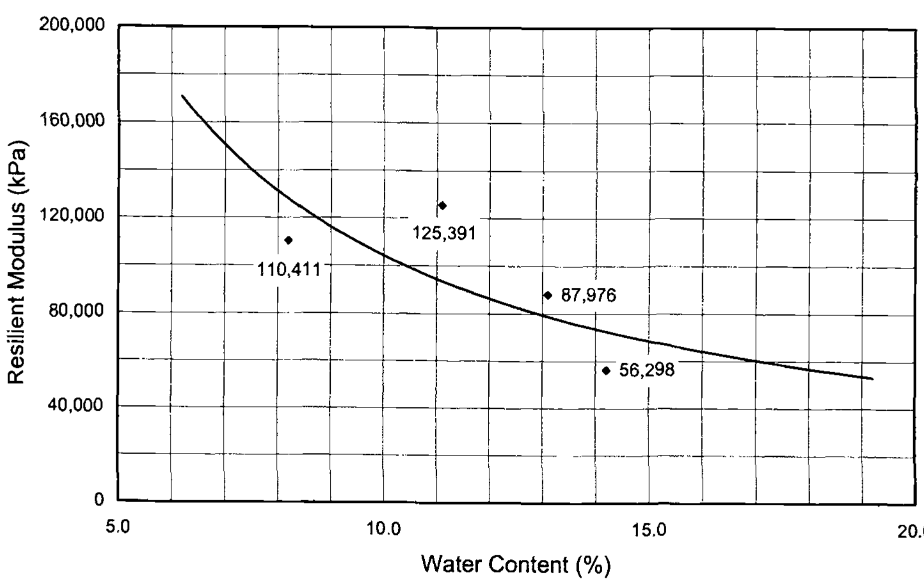


Figure 4 – *Resilient Modulus vs. Water Content for Clayey Sand*

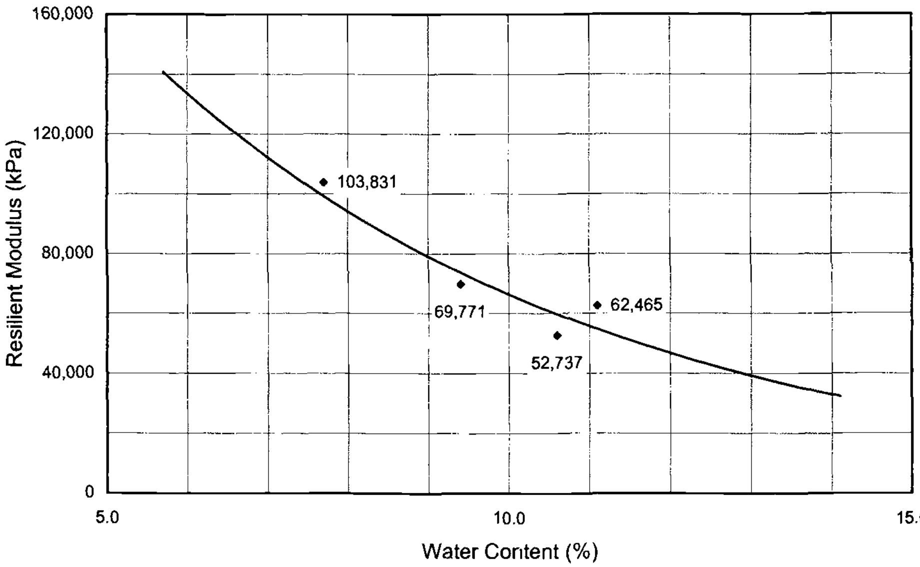


Figure 5 – *Resilient Modulus vs. Water Content for Clayey Gravel*

well conforming as indicated by their correlation coefficient of 0.51. It is also noted that the saturated clayey sand specimen did not provide the upper limit of water content as experienced by the other specimens. This may explain the lack of conformity of the clayey sand data.

A close examination of Table 1 shows that the backpressure-saturated specimens generally resulted in the lowest resilient modulus values. Also, all saturated specimens achieved a degree of saturation equal to 100%. Saturated $M_R$ values, on average, represent 50% of the optimum resilient modulus values for the lean clay soils. In comparison, the soaking apparatus proposed by Muhanna et al. (1999) resulted in 15 to 25% reduction in the resilient modulus values. The test results in Table 2 for the Somerset project also indicate that for all but the second sample of the sandy lean clay or clayey sand subgrade, $M_R$ values at saturation are about 50% of those at optimum. The data in Table 2 are plotted in Figure 6, which shows that it conforms to the general relationship indicated by the other subgrade soils presented in Table 1 and Figures 3 to 5. The multiple correlation coefficient for the curve in Figure 6 is 0.88.

It is noted that the saturated clayey sand and clayey gravel resilient moduli are only 30% and 10% lower than the $M_R$ values at optimum. This is explained by the less dependence of these slightly granular soils on water content variations. The clayey sand and sandy lean clay of the Somerset project, however, behaved in a manner close to that of the lean clay due to their borderline classification.

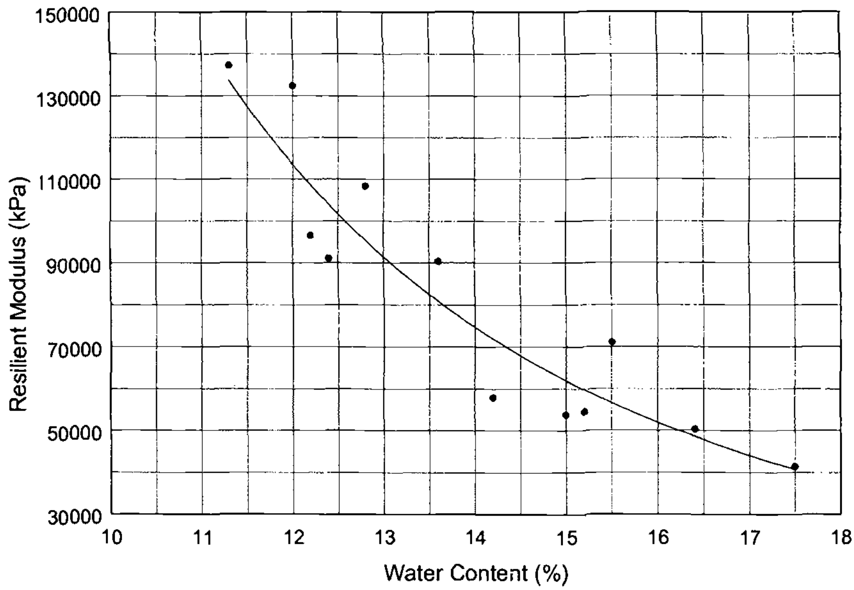


Figure 6 – *Resilient Modulus vs. Moisture Content for Sandy Lean Clay/Clayey Sand*

## Conclusions

Perhaps the most important outcome of the resilient modulus testing results presented herein is the insight gained concerning the influence of water content on $M_R$ values. As previously explained, three processes are necessary to ultimately determine the effective roadbed resilient modulus. This paper presented a detailed treatment of the first and second ones. The third process requires seasonal collection of subgrade moisture data.

Figures 3 through 6 depict the variation of the subgrade resilient modulus with water content. As clearly shown, the data suggest a general trend or relationship between the resilient modulus and water content. Moisture variations may be determined by direct measurement of the subgrade moisture, from historical data, if available, or based on local experience. Regardless of how moisture variations are determined, such a relationship can always be used to determine the effective roadbed resilient modulus.

The testing results indicate that the backpressure-saturated specimens produced the highest possible water contents and the lowest resilient moduli likely to be experienced in pavement subgrades. Saturated $M_R$ values are approximately 50% of the optimum resilient modulus values for the tested lean clay soils. The clayey sand and clayey gravel soils, however, exhibited less reduction in the resilient modulus values at full saturation. Although freeze and thaw effects are not considered here, the typical reduction due to saturation for the tested soils appears to be similar to that suggested for freeze and thaw conditions.

**Acknowledgment**

The laboratory tests presented in this paper were performed at Valley Forge Laboratories, Inc. Kenneth M. Heirendt of the Pennsylvania Turnpike Commission is acknowledged for his technical suggestions and enthusiasm towards improving pavement subgrade evaluation practices.

**References**

AASHTO, *Guide for Design of Pavement Structures*, Washington, D.C., 1993.

Black, D. K., and Lee, K. I., 1973, "Saturating Laboratory Samples by Back Pressure," *Journal of Soil Mechanics and Foundation Division*, ASCE. Vol. 99, No. SM1, pp. 75-93.

Elliott, R. P., and Thornton, S. I., 1988, "Simplification of Subgrade Resilient Modulus Testing," *Transportation Research Record 1192*, TRB, National Research Council, Washington, D.C.

Fredlund, D. G., Bergan, A. T., and Wong, P. K., 1977, "Relation between Resilient Modulus and Stress Conditions for Cohesive Subgrade Soils," *Transportation Research Record 642*, TRB, National Research Council, Washington, D.C.

Houston, W. N., Houston, S. L., and Anderson, T. W., 1993, "Stress State Considerations for Resilient Modulus Testing of Pavement Subgrade," *Transportation Research Record 1406*, TRB, National Research Council, Washington, D.C.

Huang, Y. H., 1993, *Pavement Analysis and Design*, Prentice Hall, Englewood, NJ.

Muhanna, A. S., Rahman, M. S., and Lambe, P. C., 1999, "Resilient Modulus Measurement of Fine-Grained Subgrade Soils," *Transportation Research Record 1687*, TRB, National Research Council, Washington, D.C.

Noureldin, A. S., 1994, "Influence of Stress Levels and Seasonal Variations on In Situ Pavement Layer Properties," *Transportation Research Record 1448*, TRB, National Research Council, Washington, D.C.

Pezo, R. F., Carlos, G., Hudson, W. R., and Stokoe, II, K. H., 1992, *Development of a Reliable Resilient Modulus Test for Subgrade and Non-Granular Subbase Materials for Use in Routine Pavement Design*, Report II 77-4F, Center for Transportation Research, University of Texas at Austin.

Santha, B. L., 1994, "Resilient Modulus of Subgrade Soils: Comparison of Two Constitutive Equations," *Transportation Research Record 1462*, TRB, National Research Council, Washington, D.C.

Thompson, M. R., and Robnett, Q. L., 1976, *Resilient Properties of Subgrade Soils, Final Report – Data Summary*, Transportation Engineering Series No. 14, Illinois Cooperative Highway Research and Transportation Program Series No. 160. University of Illinois at Urbana-Champaign.

Uzan, J., 1985, "Characterization of Granular Materials," *Transportation Research Record 1022*, TRB, National Research Council, Washington, D.C.

Von Quintus, H. and Killingsworth, B, 1997, Design *Pamphlet for the Determination of Design Subgrade in Support of the 1993 AASHTO Guide for the Design of Pavement Structures*, FHWA-RD-97-083, Federal Highway Administration, Washington, D.C.

Tarunjit S. Butalia,[1] Jun Huang,[2] Dong-Gyou Kim, [3] and Frank Croft [4]

# Effect of Moisture Content and Pore Water Pressure Buildup on Resilient Modulus of Cohesive Soils in Ohio

**Reference:** Butalia, T. S., Huang, J., Kim, D.-G., and Croft, F., **"Effect of Moisture Content and Pore Water Pressure Buildup on Resilient Modulus of Cohesive Soils,"** *Resilient Modulus Testing for Pavement Components, ASTM STP 1437,* G. N. Durham, W. A. Marr, and W. L. De Groff, Eds., ASTM International, West Conshohocken, PA, 2003.

**Abstract:** High positive pore pressures in subgrade soils can be expected to contribute to reduction in soil strength and stiffness. Measurement of elevated pore water pressures in the subgrades of instrumented sections of Specific Pavement Studies conducted in Ohio over the past several years have raised concerns about the long-term stability of these test sections. The objective of this study was to identify the effects of moisture content and pore water pressure on the resilient modulus ($M_r$) of unsaturated and saturated cohesive soils. Test results conducted on unsaturated cohesive soils at three different moisture contents (optimum, 2 to 4% dry of optimum, and 1 ½ to 3% wet of optimum) showed that the resilient modulus and the effect of confining stress decreased with increasing moisture content. Laboratory tests on fully saturated cohesive soils showed that the resilient modulus of saturated soils decreased to less than half that of soil specimens tested at optimum moisture content. Residual pore water pressure increased with an increase in the deviator stress, and a decrease in the loading period. The time to dissipate residual pore water pressure, which was large in comparison to the load rate, increased with increasing deviator stress. The resilient modulus of fully saturated cohesive soil was much less under faster (1 second per cycle) cyclic loading than slower (8 seconds per cycle) cyclic loading.

**Keywords:** cohesive soil, loading period, moisture content, pore water pressure, resilient modulus, residual, saturated, subgrade, unsaturated

[1] Research Scientist, Department of Civil and Environmental Engineering and Geodetic Science, The Ohio State University, 2070 Neil Avenue, Columbus, OH 43210.

[2] Geotechnical Engineer, Fugro-McClelland Marine Geosciences, Inc., 6100 Hillcroft, Houston, TX 77081.

[3] Graduate Research Associate, Department of Civil and Environmental Engineering and Geodetic Science, The Ohio State University, 2070 Neil Avenue, Columbus, OH 43210.

[4] Associate Professor, Department of Civil and Environmental Engineering and Geodetic Science, The Ohio State University, 2070 Neil Avenue, Columbus, OH 43210.

## Introduction

A mechanistic analysis method, requiring an accurate determination of the resilient modulus of subgrade soils, has been adopted by the American Association of State Highway and Transportation Officials (AASHTO) for designing roadway pavement systems. This method of pavement design is based on the original work by Seed et al. (1962) who suggested that some flexible pavement failures, such as the cracking of the pavement surface, may be caused by elastic or recoverable strain of the subgrade soils. For over 40 years, many researchers have studied and documented the characteristics of resilient response of various cohesive soils used as subgrade. These research efforts have shown that the resilient modulus of cohesive soils decreases with increasing deviator stress (e.g., Brodsky 1989, Drumm et al. 1990, Fredlund et al. 1977, Huang 2001, Kim 1999, Mohammad et al. 1994, Seed et al. 1962, Woolstrum 1990), increases with increasing confining stress (e.g., Brodsky 1989, Kim 1999), and decreases with increasing moisture content (e.g., Burczyk et al. 1994, Drumm et al. 1997, Fredlund et al. 1977, Huang 2001, Kim 1999, Lee et al. 1997, Mohammad et al. 1996, Seed et al. 1962, Woolstrum 1990). Mohammad et al. 1996 attributed this reduction in the resilient modulus to an increase in positive pore pressures with an increase in moisture content associated with greater levels of saturation.

As part of an overall program to modernize highway design, the Federal Highway Administration (FHWA) developed the Strategic Highway Research Program (SHRP) in 1993. As part of its support for SHRP, the Ohio Department of Transportation (ODOT), with FHWA, constructed a comprehensive test road consisting of four experiments (40 sections) on U.S. Route 23 near Delaware, Ohio. In this project, important pavement response parameters were measured. The purpose of this project was to evaluate the performance of specific pavement designs under traffic loading. At a limited number of sections, the field monitoring included measuring the pore water pressure. At each of these locations, pore water pressures observed under traffic loading were higher than expected and took a long time to dissipate. This pore water pressure buildup in the soils would reduce the effective confining stress, leading to a decrease in the resilient modulus. Therefore, the current method of calculating resilient modulus of subgrade soil may not be adequate without consideration of the effects of pore water pressure buildup in subgrade soils (Huang 2001, Kim 1999).

If partially saturated cohesive soils constructed at optimum moisture content become saturated, the pore water pressure will buildup under traffic loading due to the low permeability of cohesive soils. This can result in a reduction in effective confining stress and possibly the resilient modulus. Some researchers have observed that pore water pressure buildup in a cohesive soil is related to the deviator stress levels and the number of loading cycles under dynamic loading (Ansal and Erken 1989, Mendoza and Hernandez 1994, Ogawa et al. 1977). Cyclic loading of different frequencies created different levels of pore water pressure buildup in saturated soil samples in the first few loading cycles (Ansal et al. 1989).

## Objectives and Scope

The objectives of this study are to evaluate the effect of moisture content on the resilient modulus of unsaturated cohesive soils, and to investigate the effect of pore water pressure on the resilient modulus of saturated cohesive soils. To achieve these objectives, six cohesive soils, representing major soil subgrade types in Ohio, were collected from road construction sites in five counties in Ohio by the Ohio Department of Transportation. In addition, one cohesive soil sample was selected from the Specified Pavement Studies test program on U.S. Route 23. A total of seven soil samples were investigated in this study.

## Soil Properties and Specimen Preparation

### *Properties of Ohio Subgrade Soils*

The seven soil samples came from Washington, Athens, Shelby, Crawford, and Delaware Counties. All soil samples were placed in an oven, which was maintained at 60°C for 24 hours, and then were air-dried in the laboratory over a two-week period. Atterberg limits, Sieve Analysis, Hydrometer, Standard Proctor Compaction, and Specific Gravity tests were conducted to determine the engineering indices of the selected soil samples.

Table 1 shows the sample name, soil type and basic engineering indices for the predominantly glacial soil samples. The liquid limit for the sample set ranged from 25% to 60%, and plasticity index ranged between 9% and 31%. The samples were primarily silt (45-81%) with lesser amounts of sand (0-17%) and clay (7-39%). The samples were classified as either A-4, A-6 or A-7-6. There were two samples in the A-4 group, three samples in the A-6 group, and two samples in the A-7-6 group. According to USCS soil classification, six of the soil samples were classified as CL (low plasticity clay). One sample from Athens County was classified as CH (high plasticity clay).

Table 1 - *Soil Classification and Engineering Indices*

| Sample | Soil Classification | | Liquid Limit | Plasticity Index | Percent of Sand | Percent of Silt | Percent of Clay |
|---|---|---|---|---|---|---|---|
| | AASHTO | USCS | | | | | |
| WAS-7 | A-4 | CL | 29 | 10 | 3 | 56 | 7 |
| SHE-47 | A-4 | CL | 26 | 9 | 17 | 66 | 14 |
| WAS-821 | A-6 | CL | 32 | 11 | 13 | 56 | 21 |
| ATH-50-Cool | A-6 | CL | 33 | 13 | 8 | 45 | 39 |
| DEL-23 | A-6 | CL | 38 | 17 | 14 | 70 | 13 |
| CRAW-Beal | A-7-6 | CL | 41 | 21 | 7 | 81 | 12 |
| ATH-7 | A-7-6 | CH | 59 | 31 | 0 | 66 | 34 |

### *Specimen Preparation*

Table 2 shows the moisture content and dry density obtained for each soil sample as a result of Standard Proctor Compaction test (ASTM D698). The optimum moisture contents ranged from 14 to 25% while the maximum dry density varied from 1500 to 2000 $kg/m^3$.

Six samples were each tested at three different moisture contents, dry of optimum moisture content (DRY), optimum moisture content (OMC), and wet of optimum moisture content (WET), to evaluate the effect of moisture content on resilient modulus of unsaturated soils. The range of moisture contents were chosen to correspond to typical moisture contents during field compaction. The DRY samples were 2 to 4% below the optimum condition, and WET samples were compacted at 1½ to 3% above optimum. The natural moisture contents for the soils at the time of sample collection were generally higher than the optimum moisture contents.

The samples for resilient modulus testing were prepared using a constant mass of soil material that was thoroughly mixed with distilled water to obtain the desired moisture content and dry density. The mixed soil material was placed in a glass bowl with plastic cover, and stored in a humid box for twenty-four hours. This ensured a uniformly distributed moisture in the soil material. After twenty-four hours, the material was compacted in the mold in five layers of approximately equal mass. Each layer of the specimen was compacted using a manual rammer in a Harvard Miniature Compaction apparatus. The compactive effort applied per unit volume for the Harvard Miniature Compaction Test was the same as that for the Standard Proctor Compaction Test. After the sample was compacted in five layers, each specimen was carefully extruded from the compaction mold, and its diameter and height were measured.

Table 2 - *Summary of Soil Specimen Properties*

| Sample | Dry of Optimum (DRY) | | Optimum (OMC) | | Wet of Optimum (WET) | | Saturation (SAT) | |
|---|---|---|---|---|---|---|---|---|
| | Moisture Content (%) | Dry Density (kg/m³) | Moisture Content (%) | Dry Density (kg/m³) | Moisture Content (%) | Dry Density (kg/m³) | Moisture Content (%) | Dry Density (kg/m³) |
| WAS-7 | 11.0 | 1906 | 14.0 | 1937 | 16.0 | 1896 | - | - |
| SHE-47 | 12.5 | 1814 | 14.5 | 1864 | 16.0 | 1828 | - | - |
| WAS-821 | 10.8 | 1860 | 14.8 | 1897 | 17.8 | 1850 | - | - |
| ATH-50-Cool | 14.0 | 1840 | 16.0 | 1879 | 18.0 | 1840 | - | - |
| DEL-23 | - | - | 16.6 | 1813 | - | - | 18.8 | 1,813 |
| CRAW-Beal | 15.7 | 1684 | 17.7 | 1720 | 19.7 | 1686 | - | - |
| ATH-7 | 21.2 | 1513 | 24.2 | 1541 | 27.2 | 1508 | - | - |

DEL-23 samples were tested at two different moisture contents, optimum moisture content (OMC), and 100% of saturation (SAT) to evaluate the effect of pore water pressure on resilient modulus. DEL-23 sample for SAT condition was first compacted at maximum dry density and optimum moisture content, and then was fully saturated in a triaxial test chamber. Saturation was achieved by applying a backpressure of 227 kPa. The cell pressure was 248 kPa, for an effective confining pressure of 21 kPa, which was almost the same effective pressure as that of subgrade soil at a depth of 0.6 m below the pavement.

## Equipment and Test Procedure

The major components for the resilient modulus tests as performed in the Soil Mechanics Laboratory at The Ohio State University are shown Figures 1 and 2. The specified load was applied by an axial-torsion loading system manufactured by MTS Systems Corporation. An IBM compatible personal computer including an internal Data

Acquisition Board (DAQ) and LabVIEW software, a triaxial chamber, a loadcell, a Linear Variable Differential Transformer (LVDT), and a pore water pressure transducer were used in the test set up. The system used in this study was developed for measuring resilient modulus of subgrade soils according to AASHTO Method of Test for Resilient Modulus of Unbound Granular Base/Subbase Materials and Subgrade Soils-SHRP Protocol P46 (T294-94).

*Loading System and Data Acquisition*

All the resilient modulus tests in this study were conducted using an axial-torsion loading system developed by MTS Systems Corporation. This system comprised of a servohydraulic control system and a load frame with an actuator as shown in Figure 1. The force capacity of the load frame was 250 kN. The internal interface DAQ and the graphic language program software, LabVIEW, were used to control the system and to collect all data from the loadcell, LVDT, and pore water pressure transducer. The applied load was controlled by the servohydraulic control system. The applied load generally consisted of a haversine with a load duration of 0.1 sec and cycle duration of 1.0 sec (as per AASHTO T294-94), except for the modified testing sequences. This wave was generated and sent to the servohydraulic control system by a program coded using LabVIEW. Signals were recorded and generated at a rate of 100 points per second.

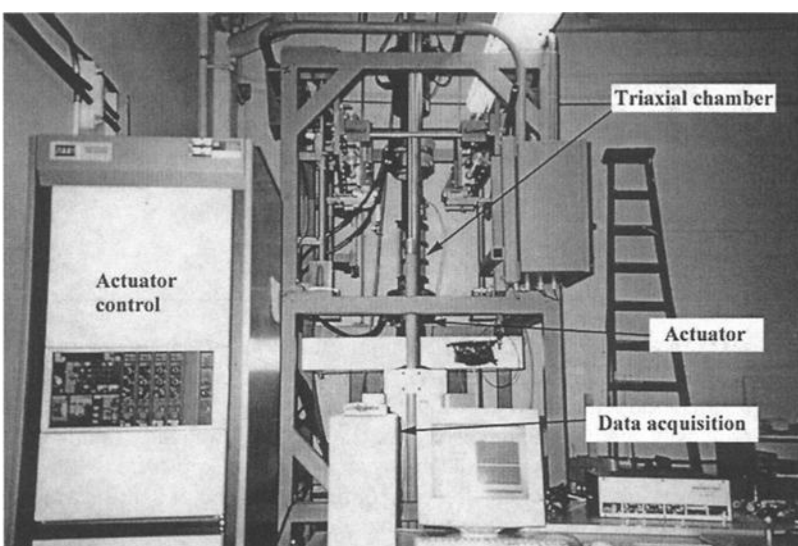


Figure 1 - *Resilient Modulus Testing System*

*Triaxial Apparatus and Measurement Systems*

The triaxial pressure chamber was modified to include the loadcell and the LVDT to facilitate the determination of the resilient modulus. Figure 2 shows a modified triaxial pressure chamber mounted in the load frame. The loadcell was mounted inside the triaxial pressure chamber between the steel piston and the top platen on the soil specimen. The capacity of the load cell was 441 N. The LVDT was mounted on the external steel rod in the top cover of the triaxial pressure chamber as shown Figure 2. This external LVDT was a DC-DC miniature LVDT with a range of +/- 5.08 mm. The pore water pressure transducer was mounted on the bottom drainage valve. The capacity of the pore water pressure transducer was 345 kPa. It was only used to measure the pore water pressure in the saturated DEL-23 samples.

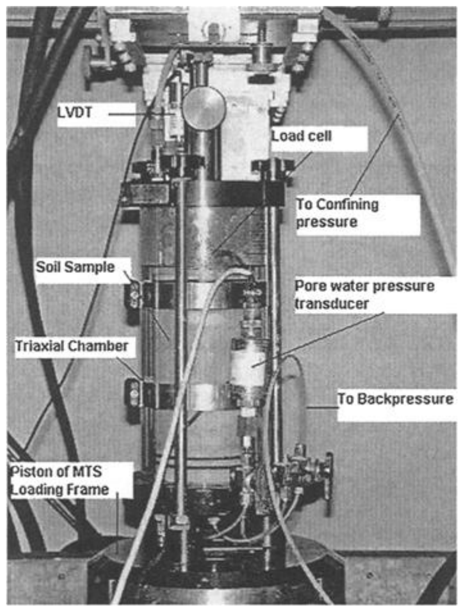


Figure 2 - *Triaxial Cell for Resilient Modulus Test*

*Testing Procedure*

In this study, two procedures were used to measure resilient modulus for the soil samples. The first was the testing sequence for Material Type 2 in AASHTO T294-94 testing procedure. The resilient modulus of unsaturated soil samples was obtained using this testing sequence. During this test, the two bottom drainage valves were open and no pore pressures were measured. The other was the modified testing sequence for fully saturated soil sample as shown in Table 3. This test consisted of two different types of testing procedures. Modified Testing I was to measure resilient modulus of fully saturated specimen at 21 kPa effective confining stress, and Modified Testing II was developed to investigate the buildup and dissipation of pore water pressure at four different load rates. In the Modified Testing II procedure, the number of loading cycles was reduced to 30. The loading period was varied to check the effect of length of unload time on the pore pressure buildup and degradation of resilient modulus. In these tests, the actual load time was kept constant as 0.1 sec, but the unload time was varied as the loading period changed. Four load cycles (1, 4, 6, and 8 sec) were employed in the

Modified Testing II program. A loading period of 1 sec consisted of 0.1 sec of loading time and 0.9 sec of unloading time. A loading period of 4 sec consisted of 0.1 sec of loading time and 3.9 sec of unloading time. During the Modified Testing I and II procedures, the two bottom drainage valves were closed to ensure undrained conditions. After the resilient modulus test on unsaturated and saturated soil samples, the length of each specimen was measured. The specimen was then weighed to determine the moisture content.

Table 3 - *Modified Testing Sequences for Saturated Samples*

| Testing Procedure | Sequence | Confining Pressure, kPa | Number of Loading Cycles | Loading Periods, s | Deviator Stress, kPa |
|---|---|---|---|---|---|
| Modified Testing I, Saturated Soil (drainage valve closed) | 1 | 21 | 1000 | 1 | 14 |
| | 2 | 21 | 100 | 1 | 14 |
| | 3 | 21 | 100 | 1 | 28 |
| | 4 | 21 | 100 | 1 | 41 |
| | 5 | 21 | 100 | 1 | 55 |
| | 6 | 21 | 100 | 1 | 69 |
| Modified Testing II, Saturated Soil (drainage valve closed) | 1 | 21 | 1000 | 1 | 21 |
| | 2 | 21 | 30 | 1 | 14 |
| | 3 | 21 | 30 | 1 | 41 |
| | 4 | 21 | 30 | 1 | 55 |
| | 5 | 21 | 30 | 1 | 69 |
| | 6 | 21 | 30 | 4 | 41 |
| | 7 | 21 | 30 | 4 | 55 |
| | 8 | 21 | 30 | 4 | 69 |
| | 9 | 21 | 30 | 6 | 41 |
| | 10 | 21 | 30 | 6 | 55 |
| | 11 | 21 | 30 | 6 | 69 |
| | 12 | 21 | 30 | 8 | 41 |
| | 13 | 21 | 30 | 8 | 55 |
| | 14 | 21 | 30 | 8 | 69 |

## Test Results and Discussion

### *Test Results*

Figures 3 and 4 show typical results of resilient modulus tests on samples WAS-7, WAS-821, CRAW-Beal and ATH-50-Cool. The results illustrate the effects of varying deviator stresses, confining stresses, and moisture contents. Figure 3 was developed using a linear scale for both axes and Figure 4 presents the resilient modulus test data using a log scale for both axes in accordance with the AASHTO T294-94. Figure 4 shows the coefficient of determination, $R^2$, and regression coefficients, $k_1$ and $k_2$, as per the simple linear regression model for Type 2 Material recommended in AASHTO T294-94 for three different moisture contents of ATH-50-Cool. Table 4 also shows the coefficient of determination, $R^2$, and regression coefficients, $k_1$ and $k_2$ determined from the resilient modulus test results for six of the soil samples. $k_1$, $k_2$, and $R^2$ were determined for each case from 15 data points using simple linear regression model for Type 2 Material as recommended in AASHTO T294-94.

*Deviator Stress, Confining Stress and Moisture Content*

Resilient moduli measured in the six soil samples with three different moisture contents were analyzed on the basis of deviator stresses, confining stresses and moisture content. As shown in Figure 3, resilient modulus of the cohesive soils gradually decreased with an increase in deviator stress. In many cases, the decreasing rate at the low deviator stress was more pronounced than that at the high deviator stress. Resilient modulus for each of the six soil samples in this study increased slightly with an increase in confining stress. As shown in Figure 4 and Table 4, this behavior is easily explained by evaluating the results of a linear regression analysis of the data points measured during the resilient modulus test on each specimen. The coefficient of determination from resilient modulus for the six soil samples had a range between 0.0018 and 0.6646. Only four specimens, two at optimum moisture content and wet of optimum moisture content in WAS-821, and one specimen each with wet of optimum moisture content in ATH-50-Cool and ATH-7 had a coefficient of determination greater than 0.5. The average of the coefficient of determination for samples with dry of optimum moisture content, optimum moisture, and wet of optimum moisture content were 0.113, 0.258, and 0.45, respectively. This result may be an effect of gradually decreasing effective confining stress with an increase in the moisture content. Although the range of the coefficients of determination in each moisture content was slightly high, it can be considered that the confining stress may influence resilient modulus for cohesive subgrade soils.

As mentioned previously, it is noted that resilient modulus for cohesive soils is closely related to the moisture content in subgrade soils. As shown in Figure 3, the resilient modulus of the soil samples decreased with an increase in moisture contents. Figure 5 shows the relationship between three moisture contents and values of resilient modulus, measured at a deviator stress of 41 kPa and a confining stress of 21 kPa, for the six unsaturated samples. Resilient modulus of samples dry of optimum moisture content are 10 to 76% greater than that of samples at optimum moisture content, and the resilient modulus of samples wet of optimum moisture content are 20 to 70% lower than that of samples compacted at optimum moisture content. The results of this study clearly show that an increase in moisture content causes significant degradation of resilient modulus of cohesive soils.

Figure 6 shows the resilient moduli of the sample with optimum moisture content and fully saturated soil sample for DEL-23. The resilient modulus of the saturated soil sample is less than half that measured at optimum for each corresponding deviator stress level. In the resilient modulus testing performed in this study on saturated soil samples, pore water pressure increases were observed. Therefore, it is possible that the reduction in resilient modulus, resulting from pore water pressure buildup, can be measured.

*Pore Pressure Buildup*

The first group of tests was carried out after the pore water pressure that was built up in the conditioning process had dissipated. The loading period was varied from 1 to 8 sec

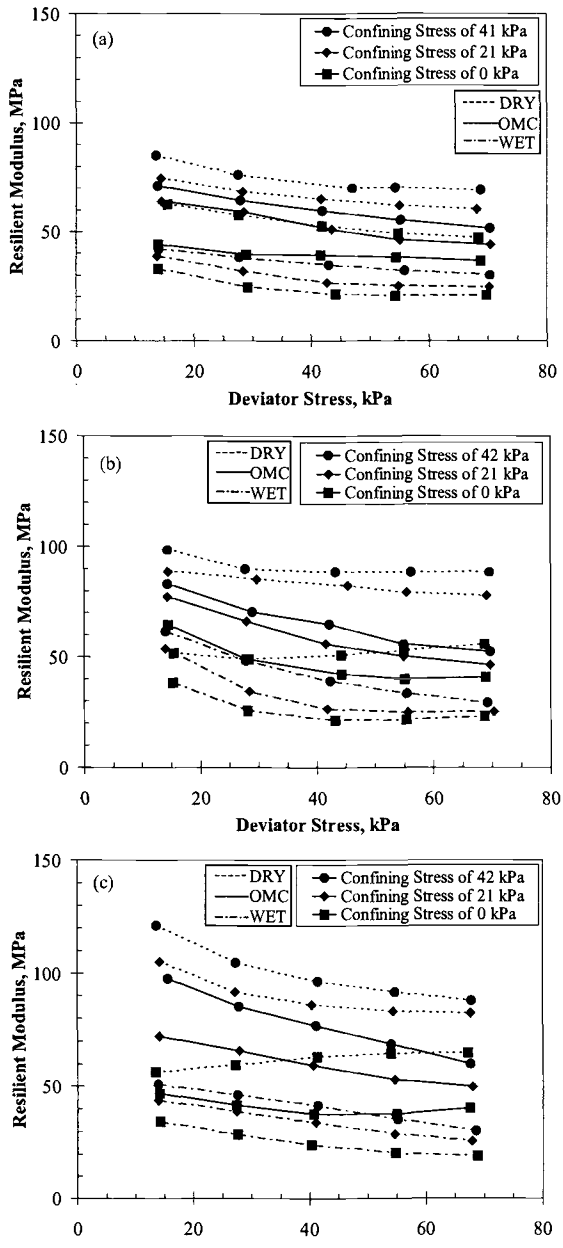


Figure 3 - *Resilient Modulus Test Result for (a) WAS-7(A-4), (b) WAS-821(A-6), (c) CRAW-Beal(A-7-6)*

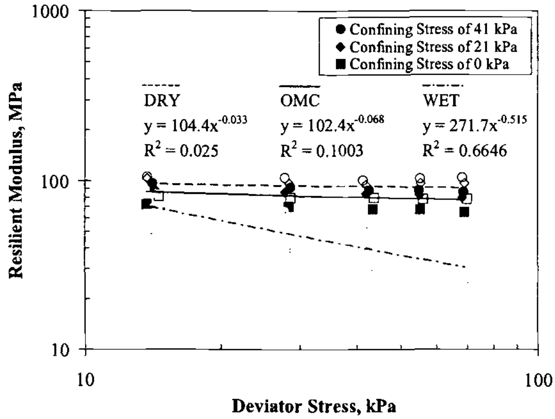


Figure 4 - *Resilient Modulus Test Result for ATH-50-Cool(A-6), Log Scale*

Table 4 - *Regression Constants*

| Sample | DRY | | | OMC | | | WET | | |
|---|---|---|---|---|---|---|---|---|---|
| | $k_1$ | $k_2$ | $R^2$ | $k_1$ | $k_2$ | $R^2$ | $k_1$ | $k_2$ | $R^2$ |
| WAS-7 | 111.09 | -0.153 | 0.285 | 96.35 | -0.183 | 0.249 | 76.46 | -0.270 | 0.459 |
| SHE-47 | 144.77 | -0.207 | 0.272 | 90.2 | -0.256 | 0.426 | 13.43 | -0.044 | 0.01 |
| WAS-821 | 84.26 | -0.04 | 0.008 | 171.84 | -0.312 | 0.61 | 160.71 | -0.448 | 0.595 |
| ATH-50-Cool | 104.36 | -0.033 | 0.025 | 102.38 | -0.068 | 0.1 | 271.7 | -0.515 | 0.665 |
| CRAW-Beal | 111.43 | -0.087 | 0.047 | 122.53 | -0.214 | 0.158 | 108.96 | -0.341 | 0.458 |
| ATH-7 | 109.41 | -0.064 | 0.043 | 79.18 | -0.01 | 0.002 | 129.42 | -0.222 | 0.511 |

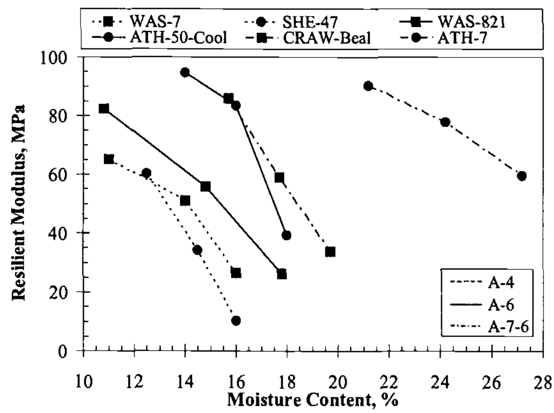


*Figure 5 - Resilient Modulus versus Moisture Content (deviator stress of 41 kPa and confining stress of 21 kPa)*

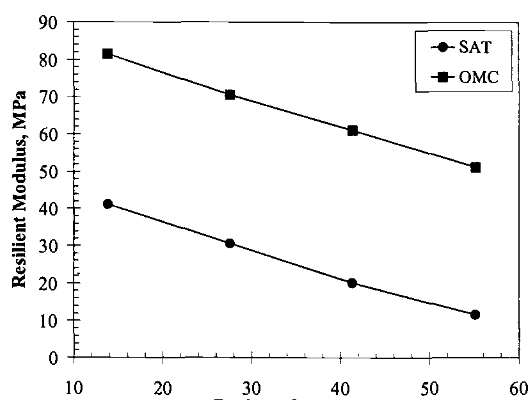


Figure 6 - *Resilient Modulus for DEL-23 with Optimum Moisture Content and Saturation*

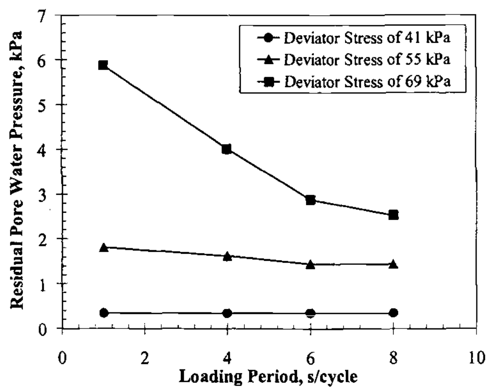


Figure 7 - *Residual Pore Pressure, Loading Period and Deviator Stresses for Saturated DEL-23*

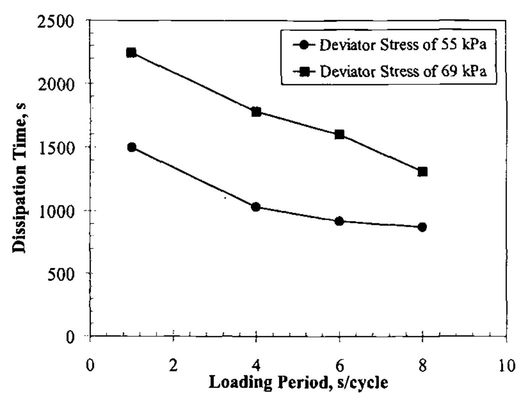


Figure 8 - *Dissipation Time, Loading Period and Deviator Stress for Saturated DEL-23*

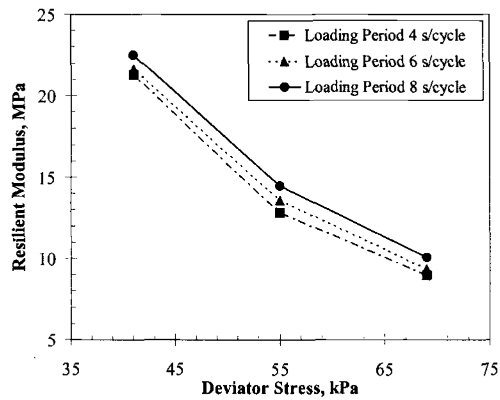


Figure 9 - *Resilient Modulus versus Loading Period for Saturated DEL-23*

and the number of loading cycles was chosen to be 30. Four sequences of testing were carried out at different deviator stress levels, 14, 41, 55, and 69 kPa. Each testing sequence was carried out after the pore water pressure created by the previous testing sequence dissipated. Residual pore water pressure built up after several cycles of loading and it took some time to dissipate completely. Residual pore water pressure herein is defined as the pore water pressure measured just after the loading cycle is imposed. In general, higher deviator stress created higher dynamic pore water pressure buildup.

Figure 7 shows the influence of loading period and deviator stress on the buildup of the residual pore water pressure. The residual pore water pressure increased as the period of loading decreased. Larger deviator stresses tended to create higher residual pore water pressures. Figure 8 shows how the dissipation time is related to loading period and deviator stress level. The required dissipation time decreased as the loading period increased at each deviator stress level, and increased as the deviator stress level increased at each loading period. Shorter loading periods created higher pore water pressure buildups and required longer dissipation time.

Figure 9 shows the degradation of resilient modulus due to the pore water pressure buildup at different loading periods and deviator stress levels. The resilient modulus of the saturated soil was higher at longer loading period at each deviator stress level.

## Conclusions

Based on the resilient modulus testing of the seven cohesive soil samples, it can be concluded that:

1. Resilient modulus for unsaturated and fully saturated cohesive soils decreases with an increase in the deviator stress.
2. The confining stress affects resilient modulus for unsaturated cohesive soils, and the soil samples exhibit an increase in the resilient modulus with an increase in the confining stress.

3. The resilient modulus for cohesive soils is considerably affected by the moisture content in the cohesive soil material. An increase in moisture content resulted in a significant degradation in the resilient modulus.
4. The resilient modulus of the saturated soil reduced to less than half that of the soil specimen at optimum moisture content. Some reduction would possibly be caused by the buildup of pore water pressure, which is shown by the modified resilient modulus testing under laboratory cyclic loading.
5. The pore water pressure buildup in saturated cohesive soils depends on the unload time between two spikes of loading cycles. Shorter loading period tend to create higher residual pore water pressure. Larger deviator stresses tend to create higher residual pore water pressure. Thus, it takes longer time for the residual pore water pressure to dissipate at shorter loading period and higher deviator stresses. The resilient modulus of fully saturated cohesive soil was much less under faster (1 second per cycle) cyclic loading than slower (8 seconds per cycle) cyclic loading.
6. The effect of confining stress seems to gradually decrease with an increase in the moisture content. This aspect needs to be investigated further.

*Acknowledgments*

This research was partially supported by the Ohio Department of Transportation and the Federal Highway Administration. The guidance and review comments provided by Professor William E. Wolfe of The Ohio State University are greatly appreciated.

**References**

AASHTO Guide for Design of Pavement Structures, 1993, *American Association of State Highway and Transportation Officials,* Washington, D. C.

Ansal, A. M., Erken, A., 1989, "Undrained Behavior of Clay under Cyclic Shear Stresses," *Journal of Geotechnical Engineering,* Vol. 115, No. 7, pp. 968-983.

Brodsky, N. S., 1989, "Resilient Modulus Measurements on Cohesive Soils as a Function of Deviator Stress and Confining Pressure," *Resilient Moduli of Soils: Laboratory Conditions*, edited by David J. Elton and Richard P. Ray, New York, N.Y., American Society of Civil Engineers, pp. 15-30.

Burczyk, J. M., Ksaibati, K., Anderson-Sprecher, R., and Farrer, M.J., 1994, "Factors Influencing Determination of a Subgrade Resilient Modulus Value," *Transportation Research Record No. 1462,* Transportation Research Board, National Research Council, pp. 72-78.

Drumm, E. C., Boateng-Poku, Y. and Pierce, T. J., 1990, "Estimation of Subgrade resilient Modulus fromStandard Tests," *Journal of Geotechnical Engineering*, Vol. 116, No. 5, pp. 774-789.

Drumm, E. C., Reeves, J. S., Madgett, M. R., and Trolinger, W. D., 1997, "Subgrade

Resilient Modulus Correction for Saturation Effects," *Journal of Geotechnical and Geoenvironmental Engineering*, Vol. 123, No. 7, pp. 663-670.

Fredlund, D. G., Bergan, A. T. and Wong, P. K., 1977, "Relation Between Resilient Modulus and Stress Research Conditions for Cohesive Subgrade Soils," *Transportation Record No. 642,* Transportation Research Board, National Research Council, pp. 73-81.

Huang, J., 2001, *Degradation of Resilient Modulus of Saturated Clay Due to Pore Water Pressure Bulidup under Cyclic Loading, Master Thesis*, Department of Civil and Environmental Engineering and Geodetic Science, The Ohio State University.

Kim, D. G., 1999, *Engineering Properties Affecting The Resilient Modulus of Fine-Grained Soils as Subgrade, Master Thesis,* Department of Civil and Environmental Engineering and Geodetic Science The Ohio State University.

Lee, W., Bohra, N. C., Altschaeffl, A. G., and White, T. D., 1997, "Resilient modulus of cohesive soils," *Journal of Geotechnical and Geoenvironmental Engineering*, Vol. 123, No. 2, pp. 131-136.

Mendoza, M. J., Hernandez, V. M., 1994, "Pore-pressure Build-up under Cyclic Loading in Mexico City Clay," *XIII ICSMFE, Proceedings, 13$^{th}$ International Conference on Soil Mechanics and Foundation Engineering,* New Delhi, India, Vol. 1, pp. 181-186.

Mohammad, L. N. Puppala, A. J. and Alavilli, P., 1994, "Influence of Testing Procedure and LVDT Location on Resilient Modulus of Soils," *Transportation Research Record No. 1462,* Transportation Research Board, National Research Council, pp. 91-101.

Mohammad, L. N. Puppala, A. J. and Alavilli, P., 1996, "Resilient Properties of Laboratory Compacted Subgrade Soils," *Transportation Research Record No. 1504,* Transportation Research Board, National Research Council, pp. 87-102.

Ogawa, S., Shibayama, T., and Yamaguchi, H., 1977, "Dynamic Strength of Saturated Cohesive Soil," XIII ICSMFE, *Proceedings, 9th International Conference on Soil Mechanics and Foundation Engineering*, Vol. 2, pp. 317-320.

Seed, H. B., Chan, C. K., and Lee, C. E., 1962, "Resilience Characteristics of Subgrade Soils and Their Relation to Fatigue Failure in Asphalt Pavement," *Proceedings, International Conference on Structural Design of Asphalt Pavement*, University of Michigan, Ann Arbor, pp. 611-636.

Woolstrum, G. 1990, "Dynamic Testing of Nebraska Soils and Aggregates," *Transportation Research Record No. 1278,* Transportation Research Board, National Research Council, pp. 27-34.

Nishantha Bandara[1] and Geoffrey M. Rowe[2]

**Design Subgrade Resilient Modulus for Florida Subgrade Soils**

---

**Reference:** Bandara, N. and Rowe, G. M., "**Design Subgrade Resilient Modulus for Florida Subgrade Soils,**" *Resilient Modulus Testing for Pavement Components, ASTM STP 1437*, G. N. Durham, W. A. Marr, and W. L. De Groff, Eds., ASTM International, West Conshohocken, PA, 2003.

**Abstract:** Many agencies still use empirical correlations developed to determine design subgrade resilient modulus based on California Bearing Ratio (CBR), R-Value or Soil Support Value (SSV) for pavement design projects. These relationships do not consider the stress dependency of the laboratory determined resilient modulus value. Backcalculated subgrade modulus values from Falling Weight Deflectometer (FWD) tests are also used for this purpose. This study was conducted to determine the relationships between laboratory determined subgrade resilient modulus and the results of Lime Rock Bearing Ratio (LBR) and FWD tests for certain Florida subgrade soils. Laboratory resilient modulus values were determined using subgrade soil samples collected from nine pavement sections. The resilient modulus values were computed by considering stress levels under a standard dual wheel in three typical pavement sections. The roadway sections were selected from various locations in Polk County, Florida. FWD tests were conducted along the selected roadways and LBR tests were conducted on bulk subgrade soil samples. Preliminary relationships to determine design subgrade resilient modulus equivalent to AASHTO Road Test subgrade from FWD and LBR tests were developed for considered typical pavement sections.

**Keywords:** resilient modulus, california bearing ratio, backcalculation

## Introduction

The resilient modulus of subgrade ($M_r$) is used to characterize the roadbed soil for pavement design in the 1993 AASHTO flexible pavement guide as a direct input parameter and indirectly in the rigid pavement as the coefficient of subgrade reaction (k). The elastic modulus based on the recoverable strain under repeated loads is characterized by the resilient modulus ($M_r$) as given below (Huang 1993).

$$M_r = \frac{\sigma_d}{\varepsilon_r} \tag{1}$$

---

[1] Pavement Engineer, Dynatest Consulting Inc., Route 5, Box 1510, Starke, FL 32091.
[2] President, Abatech, Inc. 73, Old Dublin Pike, #312, Doylestown, PA 18901.

In the above equation, $\sigma_d$ is the deviator stress and $\varepsilon_r$ is the recoverable strain under repeated loading. Although the laboratory method of determining of resilient modulus is described in the AASHTO Test Method T 307-99, many agencies still use empirical correlations to determine resilient modulus based on California Bearing Ratio (CBR) or Limerock Bearing Ratio (LBR), R-Value, Soil Support Value (SSV). The following relationships are generally used in Florida to determine the design subgrade modulus (in lbs per square inch) for roadway construction or rehabilitation projects.

$$SSV = 4.596 \times LOG_{10}(LBR) - 0.576 \tag{2}$$

$$M_r = 10^{\left(\frac{SSV+18.72}{6.24}\right)} \tag{3}$$

In addition to the above relationships, other correlations between $M_r$, CBR and R-Value are also available.

$$M_r = 1500(CBR) \tag{4}$$

$$M_r = 1155 + 555R \tag{5}$$

In the relationship given in the Equation 4, the coefficient 1500 may vary from 750 to 3000, and is more suitable for fine grained soils than granular material. Generally, the Equation 4 is suitable for fine grained soils with CBR of less than 25 and Equation 5 is suitable for materials with R-Value of less than 60 (Huang 1993). According to the above discussion, it can be seen that a vast variation exists in estimating resilient modulus using conventional soil properties.

The project involved determination of laboratory resilient modulus for nine road sections scattered around Polk County, Florida and was aimed at developing relationships for subgrade modulus for Florida subgrade soils. Selected pavement sections were constructed with open-graded asphalt course on a compacted subgrade. A clayey sand sub-base was encountered below the open-graded asphalt course at a few roadway sections. Laboratory resilient moduli values were determined for the roadway sections using bulk soil samples obtained from representative subgrade materials. LBR tests for the subgrade soils to determine the subgrade soils to determine the subgrade soil modulus using empirical relationships and FWD tests on the pavement sections to determine backcalculated soil modulus were also performed to establish relationships with laboratory resilient modulus, LBR tests and FWD results.

## Description of Sites

Twenty-five roadway sections were visually evaluated. Pavement coring, soil borings and hand penetrometer testing were performed to determine the representative sites for laboratory resilient modulus and LBR tests. Soil borings performed on the selected roadway sections identified clean fine sands (A-3) and clean to slightly silty fine sands (A-2-4) underneath the pavement sections. These soil types are typical subgrade soils in

Florida. Based on the soil boring results, nine roadway sections were selected to obtain bulk soil samples for LBR and resilient modulus testing.

**Laboratory Test for the Resilient Modulus of Subgrade Soils**

The resilient modulus test for granular material and fine grained soils is specified in the AASHTO "T307-99 Resilient Modulus of Soils and Aggregate Materials". The resilient modulus is determined by the repeated load triaxial compression test on the test specimen. Resilient modulus ($M_r$) is the ratio of the amplitude of the repeated axial stress to the amplitude of the resultant recoverable axial strain.

Standard "Proctor" compaction tests were performed on the each subgrade soil sample to determine the optimum moisture content and maximum dry density values. These soil properties were used to prepare a remolded sample with a diameter of 73.6 mm (2.9 inches) and a height of 144.8 mm (5.7 inches). A remolding target value of 95% of the maximum dry density was used for the sample preparation. The resilient modulus testing for each sample uses a series of deviator stresses, confining pressures and loading cycles as given in Table 1. A repeated axial cyclic stress of fixed magnitude, load duration of 0.1 seconds was applied to the remolded cylindrical sample. One hundred repetitions of the corresponding cyclic axial stress using a haversine-shaped load pulse were applied. Average recovered deformation for each deformation measuring device for the last five cycles were separately recorded. These values were used to calculate the average resilient modulus at each sequence. After completion of the resilient modulus test, a quick shear test using a confining pressure of 27.6 (4 psi) was performed for each sample. A typical resilient modulus verses cyclic-stress plot in English units is illustrated in Figure 1.

TABLE 1—*Testing Sequence for Resilient Modulus Test.*

| Sequence No. | Confining Pressure (kPa) | Deviator Stress (kPa) | Number of Load Applications |
|---|---|---|---|
| 0 (conditioning step) | 41.4 (6 psi) | 27.6 (4 psi) | 500-1000 |
| 1 | 41.4 (6 psi) | 13.8 (2 psi) | 100 |
| 2 | 41.4 (6 psi) | 27.6 (4 psi) | 100 |
| 3 | 41.4 (6 psi) | 41.4 (6 psi) | 100 |
| 4 | 41.4 (6 psi) | 55.2 (8 psi) | 100 |
| 5 | 41.4 (6 psi) | 68.9 (10 psi) | 100 |
| 6 | 27.6 (4 psi) | 13.8 (2 psi) | 100 |
| 7 | 27.6 (4 psi) | 27.6 (4 psi) | 100 |
| 8 | 27.6 (4 psi) | 41.4 (6 psi) | 100 |
| 9 | 27.6 (4 psi) | 55.2 (8 psi) | 100 |
| 10 | 27.6 (4 psi) | 68.9 (10 psi) | 100 |
| 11 | 13.8 (2 psi) | 13.8 (2 psi) | 100 |
| 12 | 13.8 (2 psi) | 27.6 (4 psi) | 100 |
| 13 | 13.8 (2 psi) | 41.4 (6 psi) | 100 |
| 14 | 13.8 (2 psi) | 55.2 (8 psi) | 100 |
| 15 | 13.8 (2 psi) | 68.9 (10 psi) | 100 |

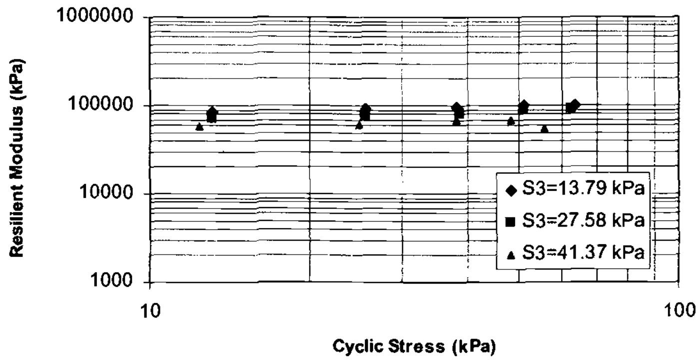


Figure 1—*A Typical Resilient Modulus Vs. Cyclic Stress plot.*

Based on similar plots developed for each site, following constitutive relationship for resilient modulus (*$M_r$*) in lbs per square inch (psi) with cyclic stress and confining stress was obtained using regression techniques.

$$M_r = K1(S_c)^{K2}(S3)^{K5} \tag{6}$$

where $S_c$ = cyclic stress, psi
$S3$ = confining pressure, psi
$M_r$ = resilient modulus, psi

The correlation coefficient $R^2$ for each soil sample is presented in Table 2 along with the values for *K1*, *K2* and *K5*.

TABLE 2—*Resilient Modulus Coefficients for Each Site.*

| Site No. | K1 | K2 | K5 | $R^2$ |
|---|---|---|---|---|
| 1 | 6053 | 0.13149 | 0.33581 | 0.98 |
| 2 | 5997 | 0.11818 | 0.33144 | 0.98 |
| 3 | 5108 | 0.11113 | 0.40061 | 0.98 |
| 4 | 6462 | 0.12326 | 0.31182 | 0.97 |
| 5 | 6034 | 0.10263 | 0.35482 | 0.98 |
| 6 | 6155 | 0.10347 | 0.36572 | 0.98 |
| 7 | 4925 | 0.06727 | 0.37802 | 0.92 |
| 8 | 5895 | 0.10716 | 0.36371 | 0.98 |
| 9 | 5836 | 0.06397 | 0.36352 | 0.98 |

**Laboratory Test for the Limerock Bearing Ratio (LBR)**

LBR tests and modified Proctor tests were performed in accordance with the Florida Department of Transportation Standard FM 5-525. The LBR test is a measure of the bearing capacity of soil as relating to pavement design. The test consists of measuring the load required to cause a standard circular plunger (with an area of 1 935 $mm^2$) to penetrate a specimen at a specified rate. The LBR is the load required to force the plunger into the soil 2.54 mm (0.1 inches) expressed as a percentage of the load required to force the same plunger the same depth into a standard sample of crushed limerock. The average penetration load for a typical crushed limerock found in Florida has been standardized to 5 516 kPa (800 psi). Based on the above LBR values and employing Equations 2 and 3, the subgrade modulus value for each selected roadway section was estimated. The test results and estimated subgrade modulus values for each roadway section are presented in Table 3.

TABLE 3—*Limerock Bearing Ratio (LBR) Values.*

| Site No. | LBR | Estimated Subgrade Modulus (MPa) |
|---|---|---|
| 1 | 23 | 56.1 |
| 2 | 37 | 79.7 |
| 3 | 49 | 98.0 |
| 4 | 32 | 71.6 |
| 5 | 32 | 71.6 |
| 6 | 40 | 84.4 |
| 7 | 75 | 134.0 |
| 8 | 35 | 76.5 |
| 9 | 35 | 76.5 |

## Falling Weight Deflectometer (FWD) Testing

FWD tests were performed on the selected roadways to evaluate the in-situ subgrade moduli values at each site. These tests were performed using Dynatest 8082 equipment at an approximate spacing of 304.8 meters (1 000 feet). In the roadway sections shorter than 304.8 meters, minimum of three locations were tested. Three tests were conducted at each location at load levels of 26.7, 40.05, 66.75 kN (6 000, 9 000, 15 000 lbs) (which corresponds to stress levels of approximately 378, 567 and 945 kPa over a 300 mm diameter loading platen) to check for linearity of the pavement structure. Deflections were measured using seven geophones located at 0, 200, 300, 600, 900, 1200, 1500 mm from the center of the loading plate.

## Backcalculation of FWD Data

Deflection Analysis of Pavement Structures (DAPS™) was used for backcalculation of subgrade modulus values from the FWD data. Three soil models rigid half-space and subgrade thickness (RHSST), known half-space stiffness (KHSS) and non-linear A,B subgrade (A,B Sg) are included with DAPS™ backcalculation algorithm. In the RHSST model, a rigid base beneath the subgrade (bedrock) is assumed. This allows for known effects of non-linearity within the subgrade soil. In the KHSS model, a rigid base beneath the subgrade is not assumed and is suitable for unusual situations with very soft underlying materials etc. The non-linear soil model for the subgrade modulus ($E_{sub}$) uses following relationship for the analysis.

$$E_{sub} = A\left(\frac{p}{q}\right)^{B} \tag{7}$$

where $p$ = mean normal effective stress due to self weight of the pavement structure
$q$ = deviator stress due to wheel loading
$A,B$ = soil constants

The user can select the best suitable soil model for the analysis considering the geology and soil properties in the area. A least-square solution process is applied, employing all measured deflections as parameters characterizing the deflection bowl.

Seed values for the asphalt concrete (AC) and subgrade stiffness were obtained from empirical correlations and are used to generate trail values for the parameters characterizing the bowl. A set of simultaneous equations was setup and solutions to these simultaneous equations were obtained by an iterative process. The RHSST model and non-linear A,B subgrade model were considered for the analysis as follows.

For the RHSST model a two-layer elastic system with a half-space stiffness of 2 000 MPa was considered for the analysis. The non-linear subgrade (A,B Sg) was modeled by four layers with thicknesses of 0.6 m, 0.9 m, 1.2 m, and 1.8 m on a compressible half-space. The subgrade stiffness was calculated at a depth of 0.3 m below the underside of the asphalt layer using the $A$ and $B$ parameters determined by the analysis. Further, a least-square solution process with a root mean square error value of less than 4% was employed to evaluate the quality of the backcalculated results.

In addition to the above backcalculation process, the subgrade modulus was backcalculated by using the following equation given in the 1993 AASHTO guide.

$$M_r = \frac{0.24P}{d_r r} \tag{8}$$

where $P$ = applied load in lbs
$d_r$ = measured deflection at radial distance r, inches
$r$ = radial distance at which the deflection is measured, inches

A minimum distance for $d_r$, to perform the backcalculation using Equation 8 is recommended in the AASHTO design guide as given in the following relationship.

$$r \geq 0.7a_e \tag{9}$$

where, $a_e$ $= \sqrt{\left[a^2\left(D\sqrt[3]{\frac{E_p}{M_r}}\right)^2\right]}$

$a$ = FWD load plate radius, inches
$D$ = total thickness of pavement layers above the subgrade, inches

$E_p$ = effective modulus of all pavement layers above the subgrade, psi

The effective modulus of all pavement layers can be backcalculated from the following relationship.

$$d_0 = 1.5pa\left\{\frac{1}{M_r\sqrt{1+\left(\frac{D}{a}\sqrt[3]{\frac{E_p}{M_r}}\right)^2}} + \frac{\left[1-\frac{1}{\sqrt{1+\left(\frac{D}{a}\right)^2}}\right]}{E_p}\right\} \tag{10}$$

where, $d_0$ = deflection measured at the center of the load plate, inches
$p$ = FWD load plate pressure, psi

The backcalculated subgrade modulus values were averaged to determine a representative value for each roadway section. The average backcalculated subgrade modulus values from the above analysis methods and other related statistics are presented in Table 4.

TABLE 4—*Backcalculated Subgrade Modulus Values.*

| Site No. | AASHTO Equation (MPa) | | | DAPS™-RHSST Model (MPa) | | | DAPS™-A,B Sg Model (MPa) | | |
|---|---|---|---|---|---|---|---|---|---|
| | Mean | Min. | Max. | Mean | Min. | Max. | Mean | Min. | Max. |
| 1 | 128 | 76 | 181 | 154 | 104 | 207 | 169 | 98 | 212 |
| 2 | 171 | 122 | 231 | 184 | 133 | 242 | 183 | 129 | 252 |
| 3 | 149 | 89 | 258 | 163 | 97 | 258 | 172 | 94 | 280 |
| 4 | 136 | 134 | 139 | 162 | 160 | 165 | 213 | 164 | 214 |
| 5 | 138 | 119 | 165 | 164 | 152 | 180 | 186 | 164 | 203 |
| 6 | 148 | 131 | 165 | 170 | 159 | 183 | 153 | 135 | 170 |
| 7 | 145 | 122 | 176 | 180 | 157 | 208 | 171 | 143 | 202 |
| 8 | 151 | 91 | 200 | 167 | 102 | 229 | 167 | 96 | 244 |
| 9 | 120 | 86 | 192 | 131 | 59 | 193 | 144 | 42 | 189 |

**Interpretation of Results**

As shown in Equation 6, the constitute model for the laboratory resilient modulus is a function of the deviator stress and the confining pressure. To compare the subgrade modulus obtained using FWD tests and LBR tests with the laboratory determined values, the resilient modulus from the constitute model should be determined for the equivalent field stresses. Elastic Layered System Software (ELSYS™) was used to calculate the stresses on the subgrade due to standard dual wheel. This program calculates the stresses and strains, at any requested point due to a given loading, by inputting layer thicknesses, densities and Poisson's ratios of each layer.

Three typical pavement sections were considered for the analysis. These sections included three different asphaltic layer thicknesses consisting of 50 mm (2 inches), 75 mm (3 inches) and 100 mm (4 inches) and 228.6 mm (9 inches) of granular base. These layer thicknesses are considered as the minimum thicknesses required for typical major roadway as recommended by the Florida Department of Transportation. An elastic moduli value of 3 125 MPa at 20°C for asphaltic materials and 100 MPa for granular materials were assumed for the stress calculations.

The vertical stress ($\sigma_Z$) on the subgrade layer was assumed to be equal to the deviator stress of the laboratory model. The confining stress was assumed to be equal to the normal octahedral stress in the subgrade layer (Nazarian et al. 1998). The normal octahedral stress can be calculated as follows.

$$\sigma_C = \sigma_{OCT} = (\sigma_X + \sigma_Y + \sigma_Z)/3$$

Initially, deviator and confining stresses of 13.8 kPa (2 psi) were used to compute the corresponding resilient modulus using the constitutive equation given in Equation 6. The calculated resilient modulus values were then employed in ELSYS to calculate corresponding subgrade stress values. These calculated stress values were used in the constitutive model to calculate resulting subgrade resilient modulus values. This procedure was repeated until two successive calculation steps produced equal pavement stress values. Using the above discussed procedure, the following laboratory resilient modulus values for each asphalt layer thickness were computed as presented in Table5

TABLE 5—*Computed Resilient Modulus Based on Laboratory Results.*

| Site No. | Laboratory Resilient Modulus (MPa) | | |
|---|---|---|---|
| | 50 mm AC | 75 mm AC | 100 mm AC |
| 1 | 96.3 | 85.0 | 75.3 |
| 2 | 91.1 | 80.8 | 71.7 |
| 3 | 83.7 | 72.6 | 62.9 |
| 4 | 97.2 | 86.7 | 77.4 |
| 5 | 91.4 | 80.9 | 71.5 |
| 6 | 95.5 | 84.2 | 74.4 |
| 7 | 68.4 | 60.3 | 53.2 |
| 8 | 90.5 | 80.6 | 71.1 |
| 9 | 80.4 | 71.4 | 63.6 |

## Comparison of Results

A typical comparison of laboratory resilient modulus with FWD estimated modulus using the RHSST model and LBR estimated modulus are illustrated in Figure 2 and Figure 3, respectively.

According to Tables 4 and 5, the average value of the backcalculated subgrade modulus, using the considered three analysis models was always higher than the laboratory resilient modulus. The AASHTO (1993) design guide recommends modifying the backcalculated modulus using a correction factor to obtain design subgrade resilient modulus value equivalent to AASHTO road test subgrade. The AASHTO design guide recommends a correction factor of no more than 0.33 to modify the backcalculated subgrade modulus values. However, AASHTO road test data show that the resilient modulus of the AASHTO road test soil is stress sensitive and consists of mainly fine-grained soils. The AASHTO design guide also suggests the granular subgrades would not require a correction factor as great as that required for fine-grained cohesive subgrades. According to the soil boring data, the subgrades of the sites considered for this study mainly consists of non-cohesive sandy materials and a correction factor as great as 0.33 may not be required to adjust the backcalculated subgrade modulus values appropriate for use in design with the AASHTO model.

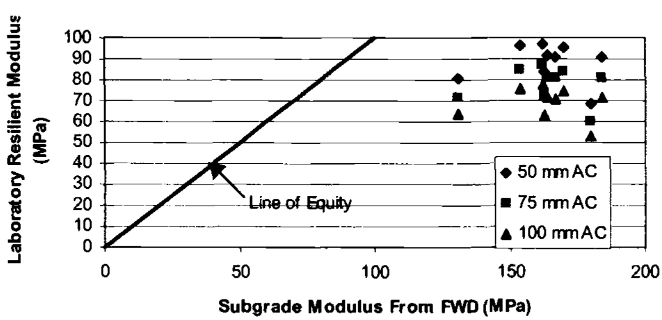


FIG. 2—*Comparison of Laboratory Resilient Modulus with Average Subgrade Modulus Estimated from FWD Data Using RHSST Model.*

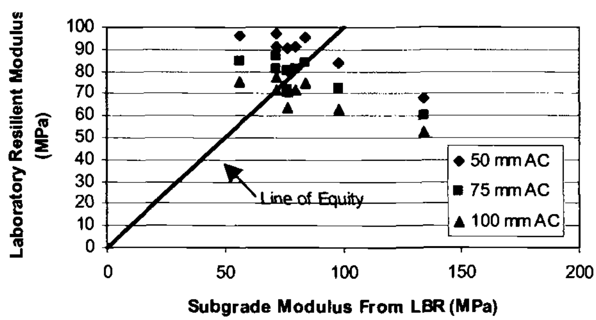


FIG. 3—*Comparison of Laboratory Resilient Modulus with Average Subgrade Modulus Estimated from LBR Results.*

Similarly, laboratory resilient modulus values were compared with subgrade modulus calculated from LBR results and reasonable correlations were observed as illustrated in Figure 3.

TABLE 6—*Average Ratios Between Laboratory and Field Subgrade Modulus Values.*

| AC Layer Thickness (mm) | Correction Factor for FWD Backcalculated Subgrade Modulus | | | | | | Correction Factor for Estimated Subgrade Modulus from LBR | |
|---|---|---|---|---|---|---|---|---|
| | RHSST Model | | Non-linear A,B Sg. Model | | AASHTO Equation | | | |
| | Avg. | Std. Dev. | Avg. | Std. Dev. | Avg. | Std. Dev. | Avg. | Std. Dev. |
| 50 | 0.54 | 0.07 | 0.51 | 0.07 | 0.62 | 0.09 | 1.14 | 0.33 |
| 75 | 0.48 | 0.07 | 0.45 | 0.06 | 0.55 | 0.08 | 1.00 | 0.3 |
| 100 | 0.42 | 0.06 | 0.40 | 0.05 | 0.48 | 0.07 | 0.89 | 0.26 |

As illustrated in Table 6, the ratio for FWD backcalculated subgrade modulus varied from 0.62 to 0.40 based on the considered models for the considered pavement structures. The LBR estimated subgrade modulus is matched with the laboratory resilient modulus for 75 mm (3-inch) asphalt layer thickness.

The relationships were developed to obtain the ratios between laboratory and field subgrade modulus from backcalculated subgrade modulus and LBR estimated subgrade modulus as follows:

$$\text{Ratio for FWD backcalculated subgrade modulus} = A \times e^{B(AC-thickness)} \qquad (12)$$

$$\text{Ratio for LBR estimated subgrade modulus} = C \times e^{D(AC-thickness)} \qquad (13)$$

where,

A,B,C,D are model constants

AC-thickness = Asphalt concrete surface thickness in mm

The A,B parameters obtained for different models used for FWD backcalculation and C,D parameters obtained for LBR estimated subgrade modulus are given in Table 7.

TABLE 7—*Model Parameters to Estimate Correction Factors.*

| Model Parameter | FWD Backcalculated Subgrade Modulus | | | LBR Backcalculated Subgrade Modulus |
|---|---|---|---|---|
| | RHSST Model | A,B Subgrade Model | AASHTO Equation | |
| A | 0.6961 | 0.6495 | 0.803 | - |
| B | -0.005 | -0.0049 | -0.0051 | - |
| C | - | - | - | 1.4567 |
| D | - | - | - | -0.005 |

These relationships should be considered preliminary as more research is needed to obtain generalized relationships. The differences can be due to several reasons including sampling disturbance, non-representative specimens, etc. The above analyses are based on hypothetical pavement sections consisting of 50 mm, 75 mm and 100 mm of asphalt layers with 229 mm of granular base. These asphalt layer thicknesses are approximately related to minimum structural course for limited access, Equivalent Single Axle Loads (ESALs) of greater than 3 500 000 and ESALs between 300 000 to 3 500 000 roadways.

## Conclusions

CBR or LBR and FWD tests are widely used to obtain subgrade soil properties for pavement design as an alternative to the determination of subgrade resilient modulus using laboratory resilient modulus testing. As a standard practice, empirical correlations are used to obtain design resilient modulus using CBR or LBR test results. In AASHTO (1993) pavement design guide, a correction factor of 0.33 is defined as a correction factor for FWD backcalculated subgrade modulus values for fine-grained subgrade soils.

The primary objective of this study was to obtain relationships for design resilient modulus based on FWD and LBR tests. Since the laboratory-determined resilient modulus is stress dependent, a pavement layer stress analysis was conducted to quantify the stress dependency for the empirical correlations to estimate design subgrade resilient modulus using FWD and LBR tests.

The laboratory-determined subgrade modulus values were generally less than the FWD backcalculated subgrade modulus values. The backcalculated modulus values with DAPS using different soil models generally produced similar results for selected pavement thicknesses. The ratios between laboratory and FWD backcalculated modulus varied from 0.40 to 0.62. The standard deviation varied from 0.05 to 0.09. These differences can be due to several reasons, including sampling disturbance, non-representative specimens etc. More research is needed to obtain generalized relationships with laboratory and field subgrade modulus values.

The ratios between laboratory and LBR estimated subgrade modulus varied from-0.89 to 1.14. The standard deviation varied from 0.26 to 0.33. The LBR estimated resilient modulus matched with the laboratory determined resilient modulus for a pavement section with 75 mm of asphalt layer. This pavement section can be considered as the minimum pavement section required for a typical arterial roadway section. Therefore, the empirical relationship to determine the design subgrade modulus based on LBR tests can be considered as valid for typical subgrade soils in Florida. However, modifications for the estimated values are necessary for thinner of thicker pavement sections.

### *Acknowledgments*

The authors would like to offer their sincere appreciation to Rees Nickerson with Professional Service Industries, Tampa, Florida for providing the data for this study.

**References**

Abatech, Inc., 2001, "Deflection Analysis of Pavement Structures (DAPS™) Software User Manual," Doylestown, PA.

Abatech, Inc., 2001, "Elastic Layered System Software (ELSYS™) Software User Manual," Doylestown, PA.

AASHTO, 1993, "Guide for the Design of Pavement Structures," American Association of State Highway and Transportation Officials, Washington, D.C.

Florida Department of Transportation (FDOT), 2000, "Flexible Pavement Design Manual," Tallahassee, FL.

Huang, Y. H., 1993, *Pavement Analysis and Design*, Prentice Hall, Inc., Englewood Cliffs, NJ.

Nazarian, S., Rojas, J., Pezo, R., Yuan, D., Abdullah, I., and Scullion, T., 1998, "Relating Laboratory and Field Moduli of Texas Base Materials," Preprint CD-ROM, 77th Annual Meeting, Transportation Research Board, Washington, D.C.

Tam, W. S. and Brown, S. F., 1998, "Back-analyzed Elastic Stiffness: Comparison Between Different Evaluation Procedures," First International Symposium on Nondestructive Testing of Pavements and Backcalculation of Moduli, Baltimore, MD.

Thompson, M. R., 1989, "Illi-pave Based NDT Analysis Procedures," *Nondestructive Testing of Pavements and Backcalculation of Moduli*, ASTM STP 1026, A.J. Bush III and G.Y. Baladi, Eds., American Society for Testing and Materials, Philadelphia, PA.

Von Quintus, H. L., Killingsworth, B. M., 1998, "Comparison of Laboratory and Insitu Determined Elastic Layer Moduli," Preprint CD-ROM, 77th Annual Meeting, Transportation Research Board, Washington, D.C.

# SESSION 3: ASPHALT AND ADMIXTURES

Tiago P. Trindade,[1] Carlos A. B. Carvalho,[2] Cláudio H. C. Silva,[3] Dario C. de Lima,[4] and Paulo S. A. Barbosa[5]

# Resilient Modulus of Soils and Soil-Cement Mixtures

**Reference:** Trindade, T. P., Carvalho, C. A. B., Silva, C. H. C., Lima, D. C., and Barbosa, P. S. A., **"Resilient Modulus of Soils and Soil-Cement Mixtures,"** *ASTM STP 1437, Resilient Modulus Testing for Pavement Components,* G. N. Durham, W. A. Marr, and W. L. DeGroff, Eds., ASTM International, West Conshohocken, PA, 2003.

**Abstract:** Knowledge of the resilient modulus ($M_R$) of the sub-grade soils and materials that compose the layers of road pavements is mandatory for an efficient analysis of their structural behavior as a whole. However, laboratory determination of $M_R$ requires employment of relatively sophisticated loading systems and data acquisition, besides demanding considerable testing time. Therefore, it is desirable to look for standard test methods that can be used to estimate this engineering parameter. This paper presents geotechnical engineering parameters of two soils and their soil-cement mixtures, and provides empirical correlations between CBR, unconfined compression strength determined at 1 % of axial strain, Young's tangent modulus, and measured values of $M_R$ of these soils and mixtures.

**Keywords:** resilient modulus, repeated-loading triaxial test, CBR, unconfined compression test, soils and soil-cement mixtures

[1] M.Sc. Student, Department of Civil Engineering, Federal University of Viçosa, 36571-000 Viçosa, MG, Brazil.
[2] Associate Professor, Department of Civil Engineering, Federal University of Viçosa, 36571-000 Viçosa, MG, Brazil.
[3] Associate Professor, Department of Civil Engineering, Federal University of Viçosa, 36571-000 Viçosa, MG, Brazil.
[4] Professor, Department of Civil Engineering, Federal University of Viçosa, 36571-000 Viçosa, MG, Brazil.
[5] Assistant Professor, Department of Civil Engineering, Federal University of Viçosa, 36571-000 Viçosa, MG, Brazil.

**Nomenclature**

| | |
|---|---|
| AASHTO | American Association of State Highway and Transportation Officials DNER Brazilian National Highway Officials |
| HRB | Highway Research Board |
| MCT | Miniature, Compacted and Tropical |
| TRB | Transportation Research Board |
| USC | Unified Soil Classification |
| a, b | Constants for determination of Young's tangent modulus |
| CBR | California Bearing Ratio |
| $E_T$ | Initial or Young's tangent modulus |
| $K_1, K_2$ | Constants determined experimentally for each material |
| LL | Liquid limit |
| LVDT | Linear variable differential transformer |
| PI | Plasticity index |
| PL | Plastic limit |
| $M_R$ | Resilient modulus |
| $S_u$ | Unconfined compression strength at failure |
| $S_{u1.0\%}$ | Unconfined compression strength at 1 % of strain |
| $W_i$ | Water content |
| $W_{opt}$ | Optimum water content |
| $\varepsilon_a$ | Axial strain |
| $\gamma_d$ | Dry unit weight |
| $\gamma_{dmáx}$ | Maximum dry unit weight |
| $\sigma_a$ | Axial stress |
| $\sigma_d$ | Deviator stress |
| $\sigma_1$ | Major principal stress |
| $\sigma_2$ | Intermediate principal stress |
| $\sigma_3$ | Minor principal stress, or confining pressure |
| $\theta$ | Bulk stress |

**Introduction**

Regarding the Brazilian highway system, it is mandatory to analyze the resilient behavior of the sub-grade soils, especially when considering the need for performing pavement reinforcement of the paved road net. Data from 1999 disclosed that the Brazilian paved road system amounted for approximately 160 000 km (nearly 8 % of the total Brazilian road system). Research reported by Felipe (1999), and based on sampling involving nearly 43 000 km of this net, states that at least 77.5 % were in poor or deficient conditions, and require pavement maintenance and, mainly, reinforcement. An elucidative information on the importance of this system to the Brazilian economy is that this net is responsible for 65 % of all transported load and 95 % of all transported people in the country, corresponding to, approximately, 70 % of the Brazilian Gross Domestic Product (Reis, 2002).

It is well known that the structural degradation of bituminous pavements, and even of the cemented base layers, is strongly associated with the resilient response of the subgrade soils. Generally, determination of the resilient modulus ($M_R$) of highway engineering materials is based on laboratory repeated-loading triaxial testing.

Concerning the resilient response of soils, it is known that granular materials show an increase in $M_R$ with an increase in the confining pressure; on the other hand, this parameter is less influenced by the applied axial deviator stress, for stress levels below those corresponding to failure (Fossberg, 1969). For cohesive soils, this author refers that the confining pressure less influences the resilient modulus, and conversely, the axial deviator stress plays a remarkable role in the resilient soil response.

In Brazil, research works directed to the determination of $M_R$ for pavement design begun in 1978, with the agreement between the Brazilian Institute for Highway Research (IPR) and the Post Graduation Program in Engineering at the Federal University of Rio de Janeiro (COPPE-RJ), as reported by Motta and Macêdo (1998). The first procedure for laboratory determination of $M_R$ was published by the Brazilian National Highway Office-DNER, in 1986, under the designation DNER-ME 131/86 "Standard Method for Determining the Resilient Modulus of Soils," and later revised by this Office in 1994 under the designation DNER-ME 131/94.

Historically, determination of $M_R$ for highway design purpose requires equipment with relatively high degree of complexity that has been restricted to a few technical institutions. This fact has led researchers to propose empirical correlations between $M_R$ and other soil parameters more easily determined in laboratory, as internationally reported by Jones and Witczak (1977), Drumm et al. (1990), Cardoso and Witczak (1991), and more recently by Lee et al. (1997). Development of correlations obtained from Brazilian soils database are reported by Medina and Preuslller (1980), Motta et al. (1985), Franzoi (1990), Nogami and Villibor (1995), Bernucci (1995), and Parreira et al. (1998).

Considering the importance of developing engineering correlations on a regional basis, this paper focuses on two soils of the County of Viçosa, Minas Gerais State, Brazil, and presents correlations developed between $M_R$ and some geotechnical engineering parameters of these soils (CBR and unconfined compression strength), and using specimens prepared from plain soils and soil cement mixtures.

## Methodology

The two soil samples used in this study represent typical gneissic residual soils from the County of Viçosa, located in the Southeast of Minas Gerais State, Brazil. In terms of pedology, the first one is a mature sandy-silty-clayey soil classified as yellow and reddish latosol, predominantly found in smooth slopes, and constituted basically of 1:1 clay minerals, iron and aluminum oxides. The second one is a young clayey-silty-sandy soil, classified as a saprolite, gray colored, constituted mainly by quartz with presence of mica. Table 1 presents information regarding soil type, sample horizon and sampling depth; Tables 2 and 3 show soils geotechnical engineering index parameters, and Table 4 depicts soils classification according to HRB (Highway Research Board) and USC (Unified Soil Classification) systems, and according to the MCT (Miniature, Compacted and Tropical) methodology (Nogami and Villibor, 1995).

TABLE 1—*Soil samples description.*

| Soil Designation | Pedological Formation | Soil Horizon | Sampling Depth (m) |
|---|---|---|---|
| 01 | Yellow Reddish Latosol | B | 6.00 |
| 02 | Saprolite | C | 11.20 |

TABLE 2—*Grain size distribution.*

| Soil Designation | Clay (% < 0.005 mm) | Silt (0.074 < % ≤ 0.005 mm) | Sand (2 < % ≤ 0.074 mm) |
|---|---|---|---|
| 01 | 54 | 24 | 22 |
| 02 | 7 | 18 | 75 |

TABLE 3—*Atterberg limits.*

| Soil Designation | LL (%) | PL (%) | PI (%) |
|---|---|---|---|
| 01 | 68 | 35 | 33 |
| 02 | 30 | 19 | 11 |

TABLE 4—*Soil classification systems: HRB, USC, and MCT (Nogami and Villibor, 1995).*

| Soil Designation | Soil Classification Systems | | |
|---|---|---|---|
| | HRB | USC | MCT |
| 01 | A-7-5 (20) | MH | LG' |
| 02 | A-2-4 (0) | SM-SC | NA' |

Compacted soil specimens prepared from soils and soil-cement mixtures were used throughout this study. The cement used in the mixtures was the Brazilian Portland CPII-E-32 type. Optimum cement contents referred to soil dry weight determined according to the Brazilian standards released by DNER (Ferraz, 1994) were added to the soils, as follows: 11 % to soil 01, and 5 % to soil 02. Specimen preparation and testing procedures were carried out as follows:

- CBR tests: Compaction of specimens at the AASHTO Intermediate compaction effort, and determination of CBR and Expansion$_{CBR}$ curves. Specimen acceptance criteria were: water content of (Wi ± 0.3 %), and compaction degree of (100 ± 0.3 %);
- Unconfined compression and repeated-loading triaxial tests:
    - Compaction of specimens 10 cm high and 5 cm in diameter at the AASTHO Intermediate compaction effort, at water contents of $W_{opt}$ −2 %, $W_{opt}$ and $W_{opt}$ + 2 %. Specimens acceptance criteria were: sample height of 10 ± 0.05 cm, sample diameter of 5 cm, water content of Wi ± 0.3 %, and degree of compaction of 100 ± 0.3 %;
    - After molding, the specimens were involved in plastic bags, in order to maintain their water content, and properly stored in wet chamber until beginning of tests;

- Unconfined compression tests of soils and soil-cement mixtures were performed at the strain rate of 1 mm/min. Soil specimens were tested right after being molded, while soil-cement mixtures were tested after a 7 days curing period. Unconfined compression strengths ($S_u$) are referred to 1% strains and failure stresses, following methodology proposed by Lee et al. (1997). For each specimen water content, three specimens were tested and the final value of $S_u$ was adopted as the average;
- Repeated-loading triaxial tests were performed according to the following sequence: (1) placement of the specimen involved by a latex membrane in the triaxial chamber; (2) installation of displacement transducers (LVDT's); (3) final setup adjustments and recording of initial readings regarding specimen position; (4) performing of tests according to DNER-ME 131/94, as presented in Table 5.

TABLE 5—*Repeated-loading triaxial test steps according to the Brazilian Standard DNER-ME 131/94.*

| Type of soils | Steps | | | |
|---|---|---|---|---|
| | Sample conditioning | | Strain registration | |
| | $\sigma_3$ (kPa) | $\sigma_d$ (kPa) | $\sigma_3$ (kPa) | $\sigma_d$ (kPa) |
| Clayey and silty soils | 21 | 70 | 21 | 21 |
| | | | 21 | 35 |
| | | | 21 | 52.5 |
| | | | 21 | 70 |
| | | | 21 | 105 |
| | | | 21 | 140 |
| | | | 21 | 210 |
| Sandy and gravelly soils | 70<br>70<br>105 | 70<br>210<br>315 | 21 | 21 |
| | | | 21 | 42 |
| | | | 21 | 63 |
| | | | 35 | 35 |
| | | | 35 | 70 |
| | | | 35 | 105 |
| | | | 52.5 | 52.5 |
| | | | 52.5 | 105 |
| | | | 52.5 | 157.5 |
| | | | 70 | 70 |
| | | | 70 | 140 |
| | | | 70 | 210 |
| | | | 105 | 105 |
| | | | 105 | 210 |
| | | | 105 | 315 |
| | | | 140 | 140 |
| | | | 140 | 280 |
| | | | 140 | 420 |

The Brazilian Standard DNER-ME 131/94 is based on the AASHTO "Standard Method of Test for Resilient Modulus of Subgrade Soils (AASHTO T 274-82)." However, it uses twenty cycles and loading time of 0,1 s for each loading sequence. The soil specimen is conditioned by applying two hundred repetitions of the specified deviator stress at a certain confining pressure. After conditioning, the soil specimen is subjected to different deviator stress sequences at the same confining pressure as informed in Table 5. Figure 1 depicts the Federal University of Viçosa (UFV)'s repeated-loading triaxial testing apparatus, which was funded by the Minas Gerais State Research Funding Agency, Brazil, through the grant TEC 2431/97.

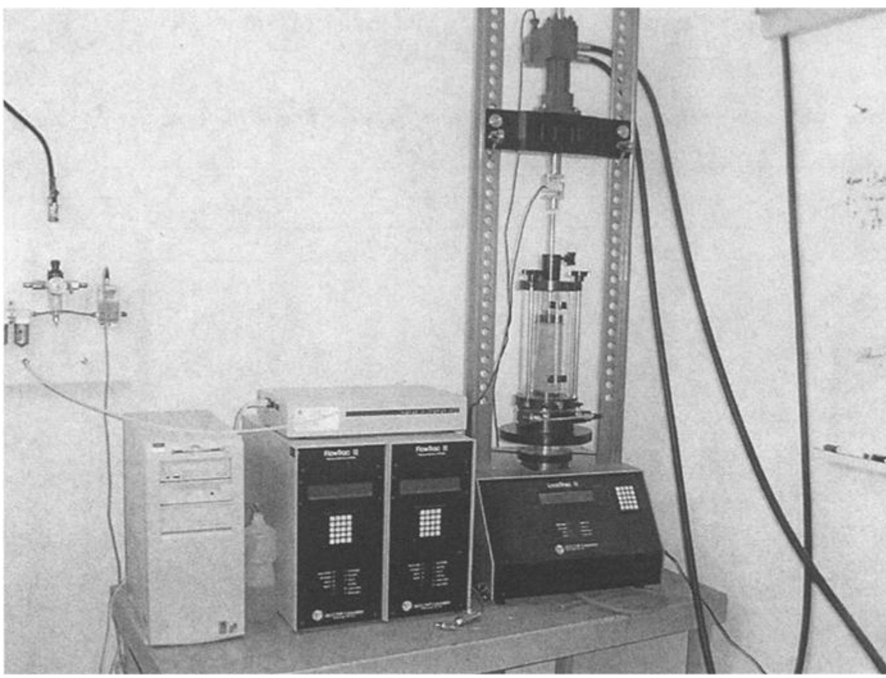

FIG. 1—*UFV's Repeated-loading triaxial test apparatus.*

**Data Analysis**

Tables 6 and 7 present soils and soil-cement mixtures testing data regarding the following parameters: maximum dry unit weight ($\gamma_{dmáx}$), optimum water content ($W_{opt}$), CBR and expansion determined in the CBR tests. Individual testing data analyses are as follows:

*Compaction and CBR Testing Data*

Testing data presented in this work show that addition of cement promotes a slight increase in $W_{opt}$, and a small decrease in $\gamma_{dmáx}$, as depicted in Tables 6 and 7. It is also noticeable significant increases in CBR of the tested soil-cement mixtures compared to the soils up to 730 % and 530 % respectively for soils 01 and 02.

*Unconfined Compression Testing Data*

Many conventional devices used in common geotechnical laboratory testing practice are neither able nor precise enough to measure very low strains and the respective loads in order to assess the initial tangent modulus. Therefore, to overcome or minimize this drawback the method described by Duncan and Chang (1970) was used in this study, assuming a hyperbolic relationship between axial strains and stresses, as follows:

$$\frac{\varepsilon_a}{\sigma_a} = a + b \cdot \varepsilon_a \qquad (1)$$

The initial tangent modulus can be approximated by:

$$E_0 = \frac{1}{a} \qquad (2)$$

Figure 2 shows the results of unconfined compression tests, from which it can be observed that soils stabilized with cement present substantial increases in theirs $S_u$ measured at failure and at 1 % of axial strain ($S_{u1.0\%}$), as well as in theirs initial tangent modulus compared to the corresponding values determined for plain soils. Textural soil composition has revealed to be an important parameter to characterize the mechanical response of soils and soil-cement mixtures. Figure 2 shows that soil 01 and its soil-cement mixtures present maximum values of stress at failure, at 1 % of strain and initial tangent modulus at the optimum water content, while soil 02 and its soil-cement mixtures exhibit maximum values at the dry side of the compaction curve.

*Repeated-Loading Triaxial Testing Data*

$M_R$ of soils can vary widely mainly according to loading conditions, stress state and soil type (Parreira et al., 1998). Models have been proposed to represent variation of $M_R$ according to the variation of the state of stress. Such models, in their great majority, were derived taking into account the soil type. For instance, there are specific models for describing the behavior of sand and clay soils. In these models the most significant variables are, respectively, the confining pressure and the deviator stress.

TABLE 6—*Compaction and CBR testing data; AASHTO Intermediate compaction effort (Soil 01)*

| Soil and mixture parameters | Soil and soil-cement mixture | |
|---|---|---|
| | Soil 01 | Soil 01 stabilized with 11 % of cement |
| Plots | 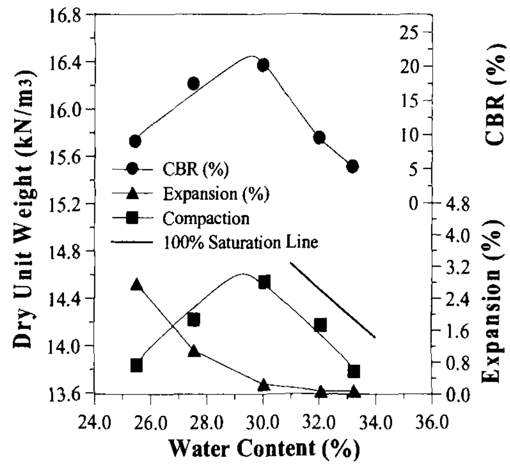  | 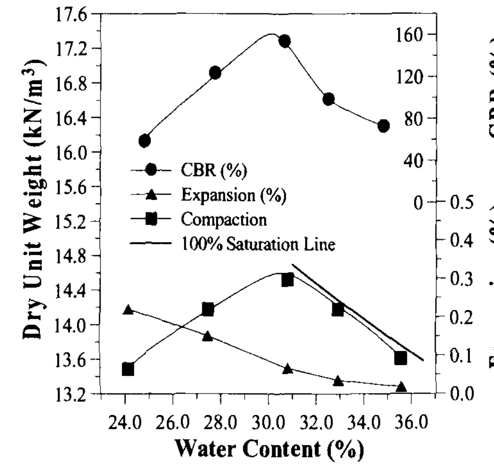  |
| $\gamma_{dmáx}$ (kN/m$^3$) | 14.6 | 14.5 |
| $W_{opt}$ (%) | 29.3 | 30.5 |
| CBR (%) | 21 | 166 |
| Expansion (%) | 0.5 | 0.1 |

TABLE 7—*Compaction and CBR testing data; AASHTO Intermediate compaction effort (Soil 02).*

| Soil and mixture parameters | Soil and soil-cement mixture | |
|---|---|---|
| | Soil 02 | Soil 02 stabilized with 5 % of cement |
| Plots | 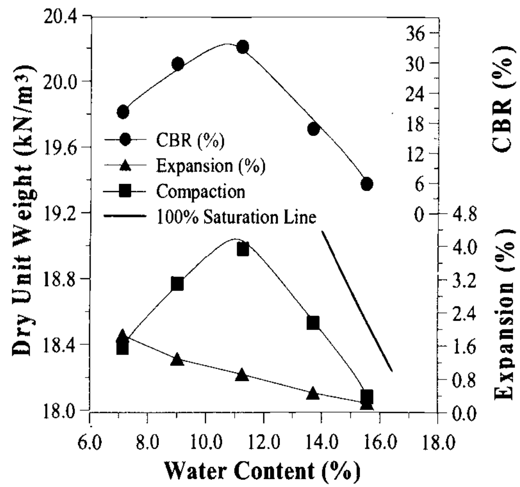  | 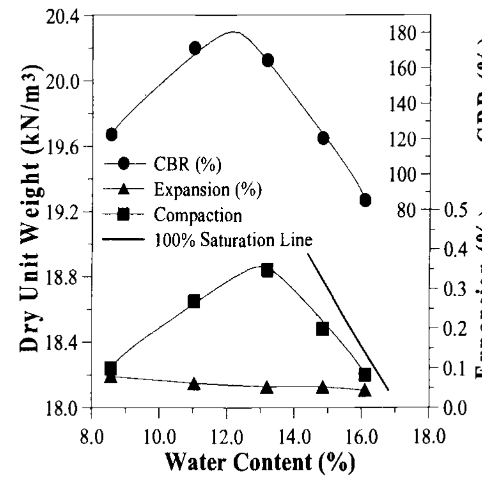  |
| $\gamma_{dmáx}$ (kN/m$^3$) | 19.0 | 18.8 |
| $W_{opt}$ (%) | 11.0 | 13.1 |
| CBR (%) | 33 | 173 |
| Expansion (%) | 0.9 | 0.1 |

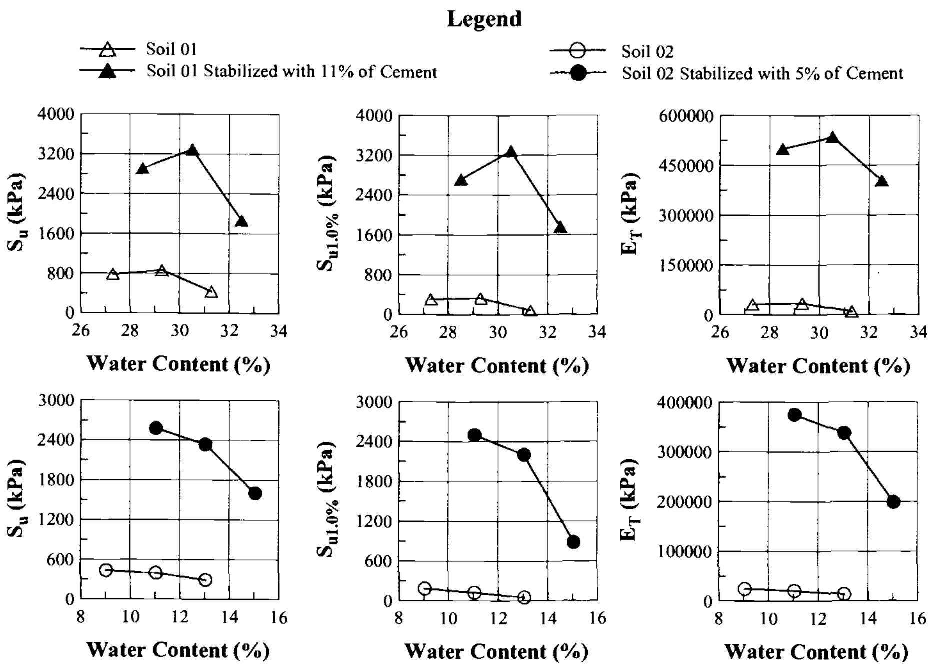


FIG. 2—*Unconfined compression testing data of soils and soil-cement mixtures: Stress at failure, at axial strain of 1 %, and initial tangent modulus*

The following models were used in this study to represent variation of $M_R$ of soils and soil-cement mixtures:

- Model referred by the method DNER-ME 131/94, and here represented by equation 3, is directed to clayey soil and mixtures, while equation 4 is directed to sandy soil and mixtures.

$$M_R = K_1 \cdot \sigma_d^{K_2} \quad (3)$$

$$M_R = K_1 \cdot \sigma_3^{K_2} \quad (4)$$

where:

$M_R$ = resilient modulus (kPa),
$\sigma_d$ = deviator stress (kPa),
$\sigma_3$ = confining stress (kPa), and
$K_1$ and $K_2$ = constants determined experimentally for each material.

Figures 3 and 4 show repeated-loading triaxial testing data of soils and soil-cement mixtures tested at water contents of $W_{opt} - 2$ %, $W_{opt}$ and $W_{opt} + 2$ % with the constants

$K_1$ and $K_2$ that fits experimental data for equations 3 and 4. It is observed relatively high coefficients of determination ($R^2$) in almost all of the tested soils and mixtures, representing also the good quality of testing data. Molding water content of soils and mixtures specimens affects $M_R$, especially at the wet side of the compaction curve, noticing a decrease in this parameter with corresponding increase in specimen water content.

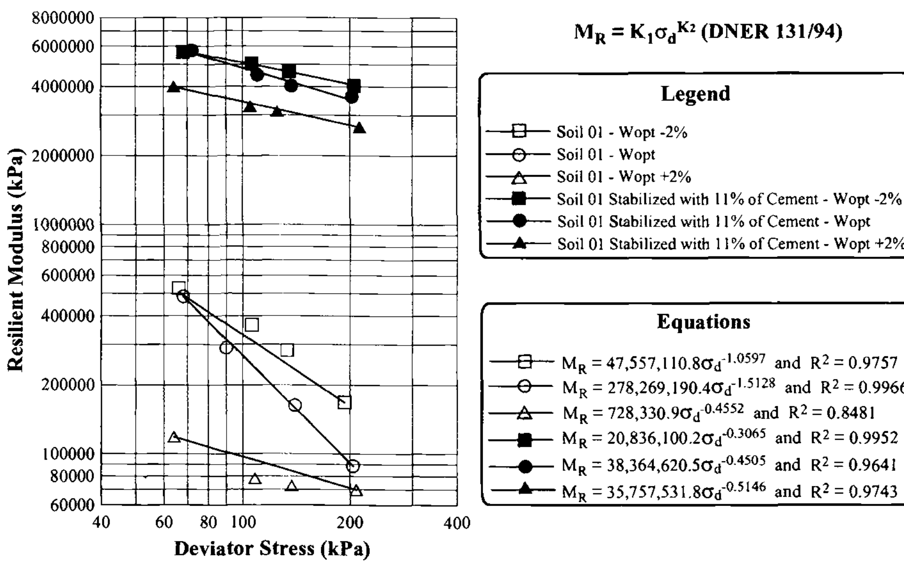


FIG. 3—*Resilient modulus versus deviator stress of soils and mixtures.*

- Model described by Cardoso and Witczak (1991), and here presented in equation 5.

$$M_R = \frac{761.79 \cdot (\mathrm{CBR})^{1.0877} \cdot (\theta)^{1.4383}}{(\sigma_1)^{1.1860}} \tag{5}$$

where

$M_R$ = resilient modulus (kPa),
CBR = California bearing ratio (%),
$\theta = \sigma_1 + \sigma_2 + \sigma_3$ = bulk stress (kPa), and
$\sigma_1$ = major principal stress (kPa).

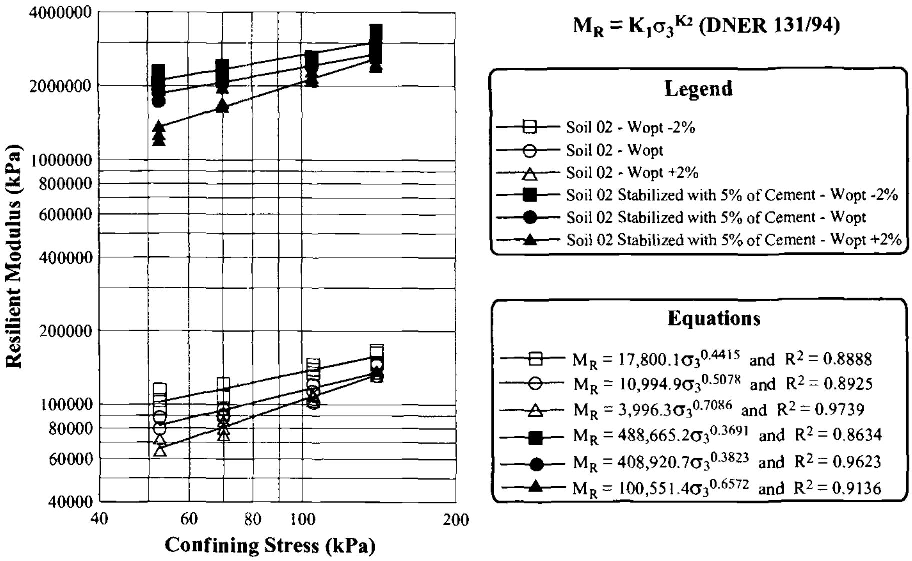


FIG. 4—*Resilient modulus versus confining stress of soils and mixtures.*

- Model proposed by Lee et al. (1997), and here represented by equation 6.

$$M_R = 645.40(S_{u1.0\%}) - 0.86(S_{u1.0\%})^2 \tag{6}$$

where

$M_R$ = resilient modulus (kPa), for a given deviator stress, and
$S_{u1.0\%}$ = stress (kPa) causing 1 % of strain during the conventional unconfined compression test.

- Model proposed by Parreira et al. (1998), and here represented by equations 7 and 8.

$$M_R = \frac{4{,}523.12 \cdot (E_T)^{0.3158} \cdot (\theta)^{0.4393}}{(\sigma_d)^{0.3436}} \tag{7}$$

$$M_R = 848.15 \cdot (E_T)^{0.4559} + 1{,}147.24 \cdot (\theta)^{0.8630} \tag{8}$$

where

$M_R$ = resilient modulus (kPa),
$E_T$ = Young's tangent modulus (kPa),
$\theta$ = bulk stress (kPa), and
$\sigma_d$ = deviator stress (kPa).

In the present work, a statistical analysis was carried out to study the performance of the above-mentioned models when applied to soils and mixtures experimental data. Correlations between $M_R$ and CBR, stress determined at 1 % axial strain, initial tangent modulus, deviator stress, first stress invariant and combinations of these variables were considered in the study, as presented in Table 8. Analysis of the data presented in this table shows that the variables considered in the analysis correlate well with the resilient modulus, $M_R$, of soils and mixtures. The coefficient of determination ranged from 0.8504 to 0.9567.

TABLE 8—*Application of models for estimating the $M_R$ of soils and mixtures.*

| Samples | | Representative model | Coefficient of Determination ($R^2$) and Standard Error |
|---|---|---|---|
| Soil 01 natural and stabilized with 11 % of cement | $M_R = F(\theta, S_{u1.0\%})$ | $M_R = \dfrac{53{,}038.92 \cdot (S_{u1.0\%})^{1.1837}}{(\theta)^{0.9902}}$ | $R^2 = 0.9235$ Error = 0.1464 |
| | $M_R = F(\theta, E_T)$ | $M_R = \dfrac{1{,}031{,}965.89 \cdot (E_T)^{1.0109}}{(\theta)^{0.9779}}$ | $R^2 = 0.9567$ Error = 0.1137 |
| | $M_R = F(\theta, CBR)$ | $M_R = \dfrac{412{,}233.75 \cdot (CBR)^{1.5045}}{(\theta)^{1.2396}}$ | $R^2 = 0.9099$ Error = 0.1760 |
| Soil 02 natural and stabilized with 5 % of cement | $M_R = F(\theta, \sigma_d, S_{u1.0\%})$ | $M_R = \dfrac{48.78 \cdot (\theta)^{0.9204} \cdot (S_{u1.0\%})^{0.9772}}{(\sigma_d)^{0.4125}}$ | $R^2 = 0.8504$ Error = 0.1858 |
| | $M_R = F(\theta, \sigma_d, E_T)$ | $M_R = \dfrac{103.28 \cdot (\theta)^{0.9110} \cdot (E_T)^{1.0754}}{(\sigma_d)^{0.4044}}$ | $R^2 = 0.9338$ Error = 0.0839 |
| | $M_R = F(\theta, \sigma_d, CBR)$ | $M_R = \dfrac{12.47 \cdot (\theta)^{0.9109} \cdot (CBR)^{1.7476}}{(\sigma_d)^{0.4055}}$ | $R^2 = 0.9249$ Error = 0.1013 |

**Note:** $M_R$ = Resilient modulus (kPa), $S_{u1.0\%}$ = stress at 1 % of strain during the conventional unconfined compression test (kPa), $E_T$ = Young's tangent modulus (kPa), CBR = California bearing ratio (%), $\theta$ = bulk stress (kPa), and $\sigma_d$ = deviator stress (kPa).

## Conclusions

It could be premature to make final conclusions based on data presented in this study, mainly considering that it was carried out over only two soil types. However, on a preliminary basis, analysis of the laboratory testing program data suggests that:

- Higher values of CBR, unconfined compression strength, initial tangent modulus and resilient modulus are related to soil and mixtures specimens compacted at the optimum or at the dry side of the compaction curve;

- Figures 3 and 4 show that resilient modulus decreases with the increase in water content for the soils tested;

- Applying DNER-ME 131/94 models, it can be seen that $M_R$ decreases with the increase of deviator stress and increases with the increase of confining stress. Also, $M_R$ always decreases with the increase in water content; and

- Acceptable statistical correlations were developed between $M_R$ and the following variables: stress at 1 % of axial strain, initial tangent modulus, CBR, bulk stress, and deviator stress.

### *Acknowledgment*

The authors wish to express their gratitude to FAPEMIG, through the grant TEC 2431/97, UFV and CNPq that contributed with scholarships, materials, laboratory testing devices and the required financial support to develop this study.

### References

Bernucci L. L. B., 1995, *Considerations about Pavement Design Using Lateritic Soils Applied to Low-Traffic Volume Roads*, Thesis (Ph.D.), Politécnica School, University of São Paulo, São Paulo, Brazil, 237p. (In Portuguese).

Cardoso, S. H., and Witczak, M. W., 1991, "Permanent Deformation for Flexible Airfield Pavement Design," *Transportation Research Record*, Washington, DC, No.1307, pp. 111-121.

Drumm, E. C., Boateng-Poku, Y., and Pierce, T. J., 1990, "Estimation of Subgrade Resilient Modulus from Standard Tests," *Journal of Geotechnical Engineering*, ASCE, No. 116, Vol. 5, pp. 774-789.

Duncan, J. M., and Chang, C. Y., 1970, "Nonlinear Analysis of Stress and Strain in Soils," *Journal of the Soil Mechanics and Foundation Division*, ASCE, Vol. 96, No SM5, pp. 1629-1653.

Felipe, T., 1999, "A Real Portrait of Brazilian Roads," *Transportes*, Jornal do Brasil Special Publication, November 28, p. 37.

Ferraz, R. L., 1994, *Contribution to Soil Stabilization Applied to Road Engineering and Housing*, Thesis (M.Sc.), Federal University of Viçosa, University Press, Viçosa, Brazil, 174p. (In Portuguese).

Fossberg, P. E., 1969, "Some Deformations Characteristics of a Lime Stabilized Clay," *Highway Research Record*, Vol. 1192, pp. 1-7.

Franzoi, S., 1990, *Some Resilient Peculiarities of Lateritic Soils and Saprolites*, Thesis (M.Sc.), Politécnica School, University of São Paulo, São Paulo, Brazil. (In Portuguese).

Jones, M. P., and Witczak, M. W., 1977, "Subgrade Modulus on the San Diego Test Road," *Transportation Research Record*, No. 641, pp. 1-6.

Lee, W., Bohra, N. C., Altschaeffl, A. G., and White, T. D., 1997, "Resilient Modulus of Cohesive Soils," ASCE, *Journal of Geotechnical and Geoenvironmental Engineering*, No. 123, Vol. 2, pp. 131-136.

Medina, J., and Preussler, E. S., 1980, "Resilient Characteristics of Soils in Pavement Studies," *Solos e Rochas (Brazilian Geotecnical Journal)*, Vol. 3, pp. 3-26. (In Portuguese).

Motta, L. M. G., Aranovich, L. A., and Ceratti, J. A. P. (1985) "Resilient Behavior of Soils Used in Low-Cost Pavements," *Solos e Rochas (Brazilian Geotechnical Journal)*, Vol. 8, pp. 15-42. (In Portuguese).

Motta, L. M. G., and Macêdo, J. A. G., 1998, "Dynamic Triaxial Test for Pavements - New Tendencies," *XI Brazilian Soil Mechanics and Foundation Engineering Congress*, Brasília, November 5-10, Vol. 1, pp. 623-628. (In Portuguese)

Nogami, J. S., and Villibor, D. F., 1995, *Low-Cost Pavement Using Lateritic Soils*, Villibor, São Paulo-SP, Brazil, 213 p. (In Portuguese).

Parreira, A. B., Cunto, F. J. C., Carmo, C. T., and Rodrigues, J. K. G., 1998, "The Resilient Modulus of Some Pavement Materials and Its Estimative from Unconfined Compression Testing Data," *XI Brazilian Congress of Soil Mechanics and Geotechnical Engineering*, Brasília-Brazil, November 5-10, V. 1, pp. 149-155. (In Portuguese).

Reis, R. M. M., 2002, *Asphalt Mix Type SMA for Heavy Traffic Load High-Performance Pavements*, Thesis (M.Sc.), Politécnica School, University of São Paulo, São Paulo, Brazil, 111 p. (In Portuguese).

Israel Iasbik,[1] Dario C. de Lima,[2] Carlos A. B. Carvalho,[3] Cláudio H. C. Silva,[4] Enivaldo Minette,[5] and Paulo S. A. Barbosa[6]

# Geotechnical Characterization of a Clayey Soil Stabilized with Polypropylene Fiber Using Unconfined Compression and Resilient Modulus Testing Data

---

**Reference:** Iasbik, I., Lima, D. C., Carvalho, C. A. B., Silva, C. H. C., Minette, E., and Barbosa, P.S.A., **"Geotechnical Characterization of a Clayey Soil Stabilized with Polypropylene Fiber Using Unconfined Compression and Resilient Modulus Testing Data,"** *Resilient Modulus Testing for Pavement Components, ASTM STP 1437,* G. N. Durham, W. A. Marr, and W. DeGroff, Eds., ASTM International, West Conshohocken, PA, 2003.

**Abstract:** This paper focuses on the geotechnical characterization of a clayey soil and its mixture with polypropylene fiber. The laboratory testing program was directed to: (i) analysis of the influence of fiber content and fiber length on the unconfined compression strength of a clayey soil in order to determine optimum parameters to be used in repeated-loading triaxial tests, and (ii) analysis of the influence of fiber on the resilient modulus of the clayey soil, according to the Brazilian Standard DNER-ME 131/94. The laboratory testing data support that: (i) the mechanical response of the composite is fiber content and fiber length dependent; (ii) addition of fiber to the soil improves substantially its unconfined compression strength; and (iii) addition of fiber to the soil is also responsible for substantial decrease in its $M_R$ values, and produces a composite that can be useful in road engineering practice.

[1] M. Sc., Department of Civil Engineering, Federal University of Viçosa, 36571-000 Viçosa, MG, Brazil.
[2] Professor, Department of Civil Engineering, Federal University of Viçosa, 36571-000 Viçosa, MG, Brazil.
[3] Associate Professor, Department of Civil Engineering, Federal University of Viçosa, 36571-000 Viçosa, MG, Brazil.
[4] Associate Professor, Department of Civil Engineering, Federal University of Viçosa, 36571-000 Viçosa, MG, Brazil.
[5] Associate Professor, Department of Civil Engineering, Federal University of Viçosa, 36571-000 Viçosa, MG, Brazil.
[6] Assistant Professor, Department of Civil Engineering, Federal University of Viçosa, 36571-000 Viçosa, MG, Brazil.

**Keywords:** resilient modulus, repeated-loading triaxial test, soil-polypropylene fiber mixtures, soil reinforcement

## Nomenclature

| | |
|---|---|
| AASHTO | American Association of State Highway and Transportation Officials |
| DNER | Brazilian National Highway Officials |
| HRB | Highway Research Board |
| MCT | Miniature, Compacted and Tropical |
| USC | Unified Soil Classification |
| LVDT | Linear variable differential transformer |
| CBR | California Bearing Ratio |
| PI | Plasticity index |
| LL | Liquid limit |
| PL | Plastic limit |
| $M_R$ | Resilient modulus |
| $S_u$ | Failure stress obtained in the unconfined compression test |
| $W_i$ | Water content |
| $W_{opt}$ | Optimum water content |
| $\varepsilon_r$ | Elastic axial strain |
| $\gamma_s$ | Solid unit weight |
| $\gamma_{dmáx}$ | Maximum dry unit weight |
| $\sigma_d$ | Deviator stress |
| $\sigma_1$ | Major principal stress |
| $\sigma_2$ | Intermediate principal stress |
| $\sigma_3$ | Minor principal stress, or confining pressure |

## Introduction

In the past two decades, data from laboratory research directed to the geotechnical characterization of soil-fiber mixtures have emphasized their great potential to improve soil shear strength, compressibility and permeability from a civil engineering perspective. Typical applications encompass shallow foundations, steep slope embankments, and pavement layers, among others.

This paper is directed to the geotechnical evaluation of soil-fiber mixtures considering highway-engineering applications. A mature gneissic residual soil, pedologically classified as a yellow and reddish latosol from the North Forest of Minas Gerais State, Brazil, was used throughout the study. Soil and soil mixtures were tested under repeated-loading triaxial tests following the Brazilian Standard Method for Determining the Resilient Modulus of Soils (DNER-ME 131/94).

## Literature Review

### *Introduction*

Reinforcement of soils by addition of fibers creates an attractive composite to be used in geotechnical and road engineering. As in others soil reinforcement techniques, composite design requires determining in laboratory the optimum fiber content for each specific application. It demands soil type and fiber type and geometry considerations. Parameters that affect fiber soil design are as follows: soil type, fiber type and geometry, compaction effort, water content, and fiber aspect ratio.

Regarding soil and loading types, the majority of papers on this topic are directed to the analysis of engineering behavior of sands tested under static loads. Few of these papers deals with reinforced clayey soils, and mainly with these soils tested under repeated-loading. Researches on clayey soils tested under static loads are reported by Andersland and Khattak (1979), Maher and Ho (1994), Teixeira et al. (1994), Silva et al. (1995), Lima et al. (1996) and Lima et al. (1999), and under repeated-loading by Ho (1992), and Buzzelli (1995).

### *Highway Engineering Resilient Modulus*

After Seed et al. (1962), mostly of the researches directed to the analysis of the behavior of highway engineering materials has been based on laboratory repeated-loading testing data in order to determine their resilient modulus ($M_R$). In Brazil, these studies were first performed in 1978, as reported by Motta and Macêdo (1998). $M_R$ is defined as the ratio between the applied repeated axial deviator stress ($\sigma_d = \sigma_1 - \sigma_3$) and the elastic axial strain. Therefore, this parameter is understood as:

$$M_R = \frac{\sigma_d}{\varepsilon_r} \tag{01}$$

where

$M_R$ = Resilient modulus (kPa or Kgf/cm$^2$),
$\sigma_d$ = Axial repeated deviator stress ($\sigma_d = \sigma_1 - \sigma_3$, kPa),
$\sigma_1$ = Major principal stress,
$\sigma_3$ = Minor principal stress, and
$\varepsilon_r$ = Elastic axial strain.

Historically, it is known that the axial deviator stress plays a significant role in the soil resilient response ($M_R$) of fine-grained soils. On the other hand, in these soils this parameter is less influenced by the applied confining stress (Fossberg, 1969).

## Methodology

### *Materials*

The tested soil sample is a gneissic residual soil from the County of Viçosa, located in the North Region of Minas Gerais State, Brazil. It is a sandy-silty clay with clay fraction constituted by 1:1 clay minerals, iron and aluminum oxides.

Randomly distributed polypropylene staple fibers with lengths of 10, 15, 20 and 30 mm, 1.2 mm wide, 0.016 mm thick (linear mass of 0.1168 g/m), and fiber contents of 0.25, 0.50 and 0,75 % referenced to soil dry unit weight were used throughout the study.

### *Testing Procedures*

The laboratory-testing program included specimen compaction, and unconfined compression and repeated-loading triaxial tests, as follows:

- Specimen compaction acceptance criteria: Height of 100 ± 0.5 mm, diameter of 50 mm, water content of ($W_i$ ± 0.3 %), and degree of compaction of (100 ± 0.3 %);
- Unconfined compression tests:
    - Specimen compaction:
        - AASHTO Intermediate compaction effort;
        - Fiber lengths: 10, 15, 20 and 30 mm;
        - Fiber contents: 0, 0.25, 0.50 and 0.75 %;
        - Water content: $W_{opt}$ (optimum water content), ($W_{opt}$ - 2 %), and ($W_{opt}$ + 2 %); and
        - After molding, the specimens were involved in plastic bags in order to maintain their water content, and then properly stored in the wet chamber until beginning of tests.
    - Tests performed at the strain rate of 1mm/min (Head, 1982);
    - Unconfined compression strengths at failure ($S_u$) are referred to the average of three tested specimens; and
    - Optimum fiber content and optimum fiber length: defined as the parameters associated to the composite higher unconfined compression strength.
- Repeated-loading triaxial tests:
    - Specimen compaction:
        - AASHTO Intermediate compaction effort;
        - Water content: $W_{opt}$ (optimum water content);
        - Fiber length: 20 mm, i.e., optimum fiber length defined from unconfined compression testing data;

    - Fiber content: 0.25 %, i.e., optimum fiber content obtained from the unconfined compression testing data; and
    - After molding, the specimens were involved in plastic bags in order to maintain their water content, and then properly stored in chamber until beginning of tests.
- Placement of two linear variable differential transducers (LVDTs) in the middle half length of the specimen inside the triaxial chamber;
- Testing procedures conducted at confining pressures and deviator stresses shown in Table 1, following the Brazilian Standard DNER-ME 131/94; and
- $M_R$ values are referred to one tested specimen.

Figure 1 depicts the repeated-loading triaxial testing apparatus used throughout this study.

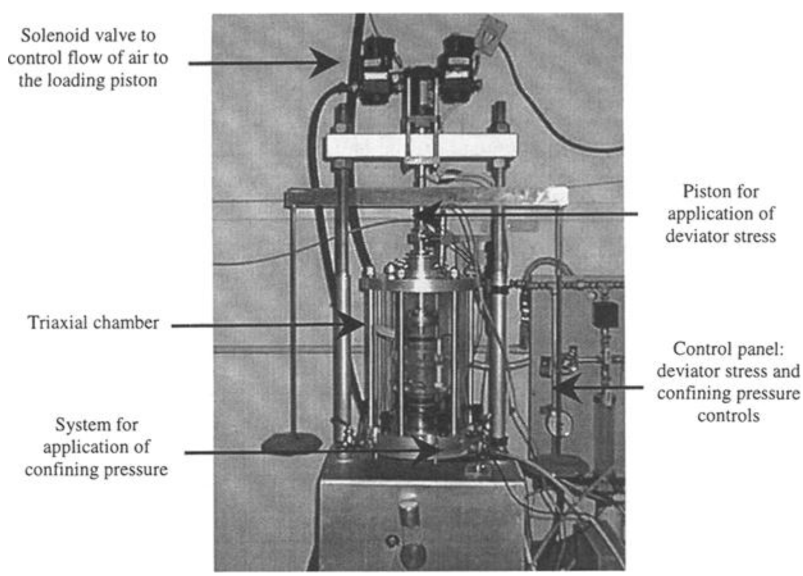


Figure 1 – *Repeated-loading triaxial test apparatus*

The Brazilian Standard DNER-ME 131/94 is based on the AASHTO "Standard Method of Test for Resilient Modulus of Subgrade Soils (AASHTO T 274-82)." However, it uses twenty cycles and loading time of 0,1 s for each loading sequence. The soil specimen is conditioned by applying two hundred repetitions of the specified deviator stress at a certain confining pressure. After conditioning, the soil specimen is subjected to different deviator stress sequences at the same confining pressure as informed in Table 1.

Table 1 – *Repeated-loading triaxial test procedures applied to clayey and silty soils according to DNER-ME 131/94*

| Soil type | Testing sequence | | | |
|---|---|---|---|---|
| | Sample conditioning | | Strain measurement | |
| | $\sigma_3$ (kPa) | $\sigma_d$ (kPa) | $\sigma_3$ (kPa) | $\sigma_d$ (kPa) |
| Clayey and silty soils | 21 | 70 | 21 | 21 |
| | | | 21 | 35 |
| | | | 21 | 52.5 |
| | | | 21 | 70 |
| | | | 21 | 105 |
| | | | 21 | 140 |
| | | | 21 | 210 |

## Data Analysis

The optimum combination of fiber length, fiber content and compaction parameters which led to the highest unconfined compression strength of the composite was determined, and repeated-loading triaxial tests were performed at this ideal combination.

### *Soil and Composite Laboratory Testing Data: Compaction and Unconfined Compression Tests*

Table 2 and Figure 2 present geotechnical soil laboratory testing data. The soil is classified as A-7-5 (20), MH, and LG' following, respectivelly, the Highway Research Board (HRB) Classification System, the Unified Soil Classification (USC) System, and the Miniature, Compacted and Tropical (MCT) Methodology developed by Nogami and Villibor (1995).

Regarding the range of fiber content used in this research, compaction testing data support that addition of fiber to soil lead to insignificant changes in its $W_{opt}$ in accordance with previous study developed by Bueno et al (1997). Working with the same clayey soil and same range of polypropylene fiber content, these authors report variations in $W_{opt}$ of soil and composite smaller than 1 %. Therefore, for practical purpose same $W_{opt}$ was adopted in this research for soil and composite.

Table 2 – *Soil characterization testing data*

| Soil Parameter | Value |
|---|---|
| LL (%) | 65 |
| PL (%) | 33 |
| PI (%) | 32 |
| $\gamma_S$ (kN/m$^3$) | 27.25 |
| $W_{opt}$ (%, AASHTO Standard compaction effort) | 31.40 |
| $\gamma_{dmax}$ (kN/m$^3$, AASHTO Standard compaction effort) | 14.06 |
| $S_u$ (kPa, AASHTO Standard compaction effort) | 293 |
| CBR (%, AASHTO Standard compaction effort) | 10 |
| Expansion$_{CBR}$ (%, AASHTO Standard compaction effort) | 0.1 |

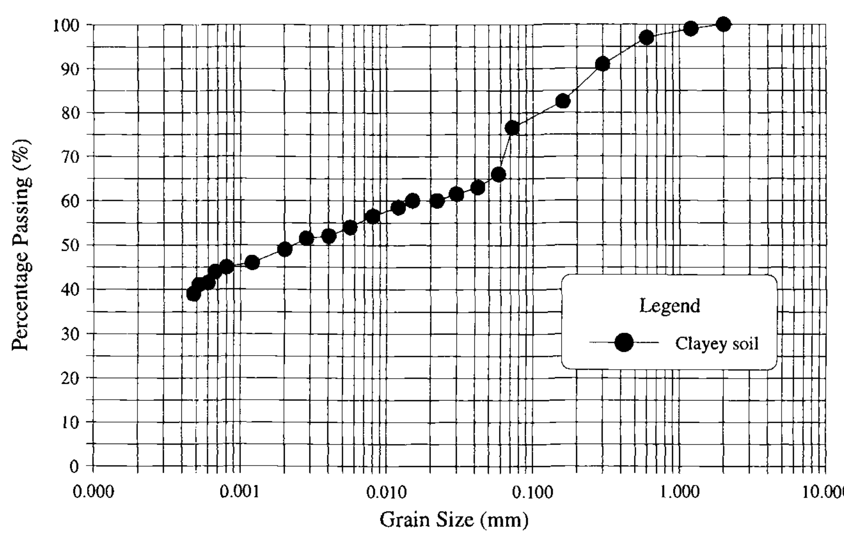


Figure 2 – *Grain size distribution of the clayey soil*

Figure 3 presents soil and composite variations of $S_u$ versus fiber content for all tested fiber lengths. Data support that both parameters are major factors in the mechanical response of the composite, and that maximum $S_u$ is associated to fiber content of 0.25 % and fiber length of 20 mm.

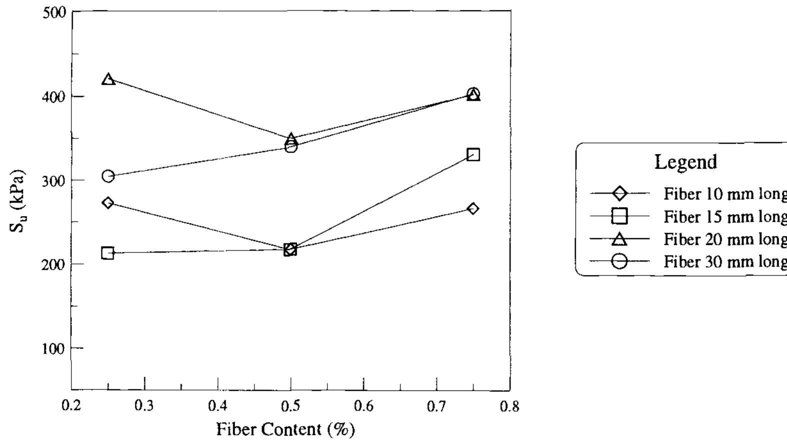


Figure 3 – *Unconfined compression strength (Su) versus fiber content at different fiber lengths*

Figure 4 displays variations of Su with water content of soil and composite. Maximum values of Su can be associated to the dry side ($W_{opt}$ – 2%) and to the optimum water content ($W_{opt}$) of the compaction curves of soil and composite, respectively.

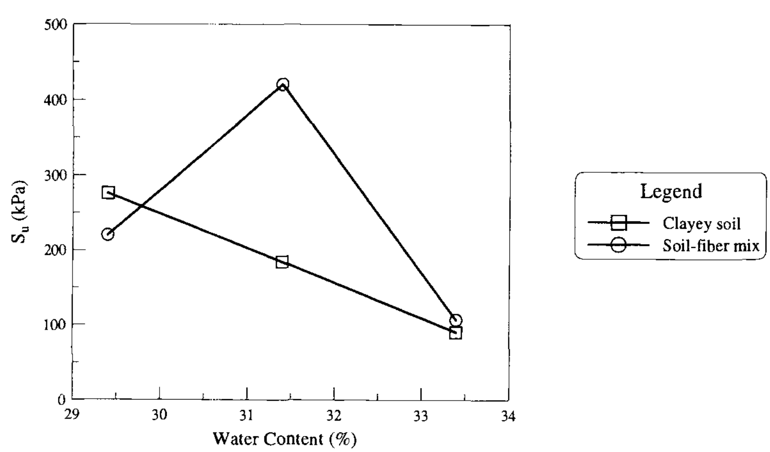


Figure 3 – *Unconfined compression strength (Su) versus water content of soil and composite at fiber content of 0.25 % and fiber length of 20 mm*

*Repeated-Loading Testing Data*

Figure 4 introduces trend of $M_R$ versus deviator stress.

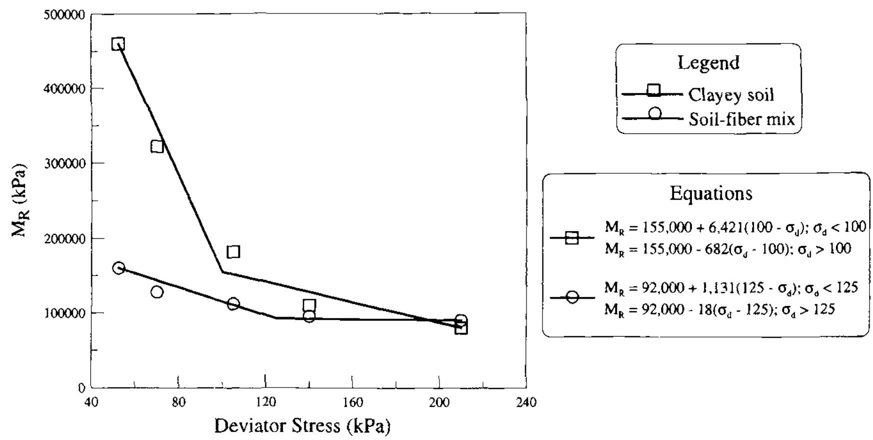


Figure 4 - *$M_R$ versus deviator stress of soil and mixtures of soil and fiber at fiber content of 0.25 % and fiber length of 20 mm*

Figure 4 illustrates that $M_R$ values of soil and composite follow a bilinear trend that decreases with increases in the deviator stress, as expected and reported by Duncan et al. (1968) for clayey soils. Data presented in this figure support that:

- $M_R$ values of the soil ranges from 460 000 to 80 000 kPa, reaching a decrease of 67% between its maximum and minimum values in the first part of the bilinear model;
- $M_R$ of the composite ranges from 160 000 to 90 000 kPa;
- The bilinear models of soil and composite are characterized by deviator stresses of 100 and 130 kPa, respectively; and
- Influence of the deviator stress on the $M_R$ of the composite is less significant than on the $M_R$ of the soil, suggesting that addition of fiber is responsible for shifting the behavior of the clayey soil in the direction of sandy soils.

Further comments on this topic are as follows:

- It can be inferred that at high deviator stresses contribution of fiber is more evident in absolute terms. Therefore, the observed $M_R$ reduction is more significant in the composite than in the soil;

- However, at low strain values it can be estimated that the dynamic modulus of the lightweight composite will be less than the soil because fiber is lighter than soil; and
- Addition of fiber to the soil makes it behave as a more resistant and more flexible material. From an engineering perspective, and under specific design requirements, the mechanical response of the composite under repeated loading can be technically useful. Certainly, a pavement layer more tolerant to settlements and more resistant to cracking will minimize influence of loading repetition on the long-term behavior of pavement layers.

## Conclusions

The laboratory-testing program was directed to the geotechnical characterization of a clayey soil stabilized with polypropylene fiber using unconfined compression testing and resilient modulus data. Repeated loading triaxial tests following the Brazilian Standard DNER-ME 131/94 were performed at the optimum fiber content and fiber length, respectively, of 0.25 % and 20 mm.

Although the scope of the testing program is somewhat limited, and the conclusions drawn are not conclusive, the laboratory testing data suggest that:

- The mechanical response of the composite is fiber content and fiber length dependent;
- Addition of fiber to the soil improves substantially its unconfined compression strength; and
- $M_R$ values of soil and composite present typical bilinear trend of cohesive soils; $M_R$ values of the composite are generally smaller than those of the soil, and major decreases in $M_R$ values of the composite are observed at deviator stresses up to 100 kPa.

## Acknowledgement

The authors would like to express their gratitude to FAPEMIG, FIEMG, CAPES and the Federal University of Viçosa, who supported this research.

## References

Andersland, O. B., and Khattak, A. S., 1979, "Shear Strength of Kaolinite/Fiber Soil Mixtures," *International Conference on Soil Reinforcement, I*, Paris, France, pp. 11-16.

Bueno, B. S.; Lima, D. C.; Teixeira, S. H., and Minette, E., 1997, *"The Mechanical Response of Reinforced Soils Using Short Randomly Distributed Plastic Strips,"* Recent Development in Soil and Pavement Mechanics, Edited by Marcio Almeida, Balkema, Rotterdam, pp. 401-408.

Buzzelli, P., 1995, *"Dynamic Triaxial Testing of Unreinforced and Reinforced Soil,"* New York, Thesis (M.S.), The Cooper Union Albert Nerken School of Engineering, 220 p.

Duncan, J. M., and Chang, C. Y., 1970, "Nonlinear Analysis of Stress and Strain in Soils," *Journal of the Soil Mechanics and Foundation Division*, ASCE, Vol. 96, No. SM5, pp. 1629-1653.

Fossberg, P. E., 1969, "Some Deformations Characteristics of a Lime Stabilized Clay," *Highway Research Record*, Vol. 1192, pp. 1-7.

Head, K. H., 1982, *Manual of Soil Laboratory Testing - Volume 2 - Permeability, Shear Strength and Compressibility Tests*, New York, John Wiley & Sons, 418 p.

Ho, Y. C., 1992, *Behavior of Fiber-Reinforced, Cemented Soils Under Static and Cyclic Loads*, New Jersey, Thesis (Ph.D.), The State University of New Jersey, 152 p.

Lima, D. C., Bueno, B. S., Marques, E. T., and Minette, E., 1999, "Influence of Addition of Polypropylene Fibers and Compaction Effort on the Mechanical Response of Soil-Lime Mixtures," *First South American Symposium on Geosynthetics*, Rio de Janeiro, October 19-22, pp. 177-182. (In Portuguese).

Lima, D. C., Bueno, B. S., and Thomasi, L., 1996, "The Mechanical Response of Soil-Lime Mixtures Reinforced with Short Synthetic Fibers," *Third International Symposium on Environmental Geotechnology*, June 10-12, San Diego, California, pp. 868-877.

Maher, M. H., and Ho, Y. C., 1994, "Mechanical Properties of Kaolinite/Fiber Soil Composite," *Journal of Geotechnical Engineering*, Vol. 120, No. 8, pp. 1381-1393.

Motta, L. M. G., and Macêdo, J. A. G., 1998, "Dynamic Triaxial Test for Pavements – New Tendencies," *XI Brazilian Soil Mechanics and Foundation Engineering Congress*, Brasília, November 5 – 10, Vol. 1, pp. 623-628. (In Portuguese).

Nogami, J. S., and Villibor, D. F., 1995, *Low-Cost Pavement Using Lateritic Soils*, Villibor, São Paulo-SP, Brazil, 213 p. (In Portuguese).

Seed, H. B., Chan, C. K., and Lee, C. E., 1962, "Resilience Characteristics of Sub grade Soil and their Relation to Fatigue Failures in Asphalt Pavements," *International Conference on the Structural Design of Asphalt Pavement*, University of Michigan.

Silva, W. R., 1998, *Behavior of Cold-Mixed Dense-Graded Asphalt Mix Reinforced with Randomly Distributed Synthetic Fiber*, Viçosa-Brazil, Thesis (M.S.), Federal University of Viçosa, University Press, 91 p. (In Portuguese).

Silva, M. A., Bueno, B. S., and Lima, D. C., 1995, "Soil Stabilization Using Short Fibers," *Geosynthetics 95 - Brazilian Congress on Geosynthetics*, São Paulo, Brazil, Vol. 1, pp. 327-335. (In Portuguese).

Teixeira, S. H., Bueno, B. S., and Lima, D. C., 1994, "Analysis of the Behavior of Soils Reinforced with Fibers," *First Civil Engineering Congress*, Federal University of Juiz de Fora, August, pp. 54-64. (In Portuguese).

# SESSION 4: EQUIPMENT, TEST PROCEDURES, AND QUALITY CONTROL ISSUES

Manuel O. Bejarano,[1] Andrew C. Heath,[1] and John T. Harvey[2]

# A Low-Cost High-Performance Alternative for Controlling a Servo-Hydraulic System for Triaxial Resilient Modulus Apparatus

---

**Reference:** Bejarano, M. O., Heath, A. C., and Harvey, J. T., "**A Low-Cost High-Performance Alternative for Controlling a Servo-Hydraulic System for Triaxial Resilient Modulus Apparatus,**" *Resilient Modulus Testing for Pavement Components, ASTM STP 1437*, G. N. Durham, W. A. Marr, and W. L. De Groff, Eds., ASTM International, West Conshohocken, PA, 2003.

**Abstract:** A triaxial test apparatus for the characterization of pavement materials was designed and built at the Pavement Research Center (PRC) at the University of California, Berkeley (UCB). The system was designed for high quality testing of unbound, stabilized, and asphaltic materials. The design process included the design of the hardware and the servo-controlling systems. An important step in the design of the system was the design of the controller for the servo-hydraulic system. Alternatives for controllers of servo-hydraulic systems for waveform generation included the use of the data acquisition system along with proportional, integral, and derivative (PID) algorithms for setting the minimum and maximum loads/displacement. Software programming for these solutions was very complex with limited satisfactory consistency. Commercial ready-to-use controllers are expensive and limited to the specifications of the manufacturer. Therefore, a commercially available programmable motion controller PIC card was implemented for controlling the servo-hydraulic system. The motion controller required only one PID controller to generate repeated waveforms or monotonic loading. An available commercial test solution software compatible with the motion controller card was used to program the motion controller and data acquisition system. This capability was preferable to provide flexibility in modifying the system based on research needs. Software programming was simple. In addition, the cost of the new system was reduced by about 80 percent with respect to the ready-to-use motion controllers.

The paper describes the implementation of the motion controller, the philosophy of the software program, and the success obtained with the new system. The system meets all the quality control provision of the LTTP Protocol P-46. Currently the triaxial apparatus is being use to investigate the resilient response and permanent deformation performance of typical California aggregate base and subbases.

**Keywords:** resilient modulus, triaxial testing, servo-hydraulic system, motion controller, testing equipment

---

[1]Assistant Research Engineer and Graduate Student Researcher, respectively, Pavement Research Center, University of California, 1353 S. 46th St., Richmond, CA 94804.
[2]Associate Professor, University of California, Davis, CA 95616.

## Introduction

The California Department of Transportation (Caltrans) uses the resistance "R" value obtained from the Hveem stabilometer test for the characterization of untreated and treated unbound materials (California Test 301 2000). The R-value gives an indication of performance of pavement bases, subbases, and the subgrades subjected to traffic loading. The current Caltrans design procedure is a semi-theoretical method that uses the R-value along with material equivalency factors to design the pavement structure (Hveem and Carmany 1948).

Material equivalency factors were developed for standard California materials based on correlations of field performance with the material properties obtained with the stabilometer test. Extrapolations from the empirical equivalency factors and pavement structures to accommodate new and innovative pavement materials (such as recycled materials) may result in questionable designs.

Because of these and other limitations with empirical methods, Caltrans has put considerable attention on the development of mechanistic-based approaches for the design and evaluation of pavements in recent years. Most mechanistic-based design methods use the resilient modulus of each layer in the design process. The resilient modulus of pavement materials is usually obtained using repeated load triaxial tests and has been shown to be a function of both confining and deviatoric stress (Hicks and Monismith 1970; Uzan 1985).

The triaxial equipment described in this paper was developed during the year 2000 in order to provide a test apparatus to study the mechanical properties of pavement materials. The test apparatus has been used to determine the resilient modulus, static shear and permanent deformation characteristics of California bases, subbases, and subgrades. The equipment has been slightly modified from its initial configuration to include a temperature control system in the confining cell to determine viscoelastic properties of asphalt bound materials. Figure 1 shows the test system without the temperature control system installed.

## Test Apparatus and Loading System

The components of the triaxial testing system include the frame, the hydraulic actuator, the triaxial cell, and electronic equipment (Figure 1). The frame and hydraulic actuator were obtained from outdated testing equipment. The triaxial cell was designed and constructed in-house. The cell top and bottom plates were constructed using aluminum and the cell is a 25.4 mm (1 inch) thick plexiglass cylinder. Aluminum was chosen for the top and bottom plates as stainless steel would have been too heavy.

A 150 mm diameter, 300 mm high cylindrical specimen is covered with a latex membrane and placed in the triaxial cell which is pressurized using air. The axial loading system has a capability of 44.4 kN (10 000 lbf). Cell pressures are applied in the range of 0 to 700 kPa (0 to 100 psi). A pressure transducer is used to control the pressure in the triaxial cell.

Two load cells are provided, one inside the test cell and the other outside the cell. The internal load cell is not affected by loading rod friction or confining pressure changes, while the external load cell will give higher readings as confining stress and friction increase. During load-controlled testing, the loads are applied using the internal load cell readings, which are considered more accurate.

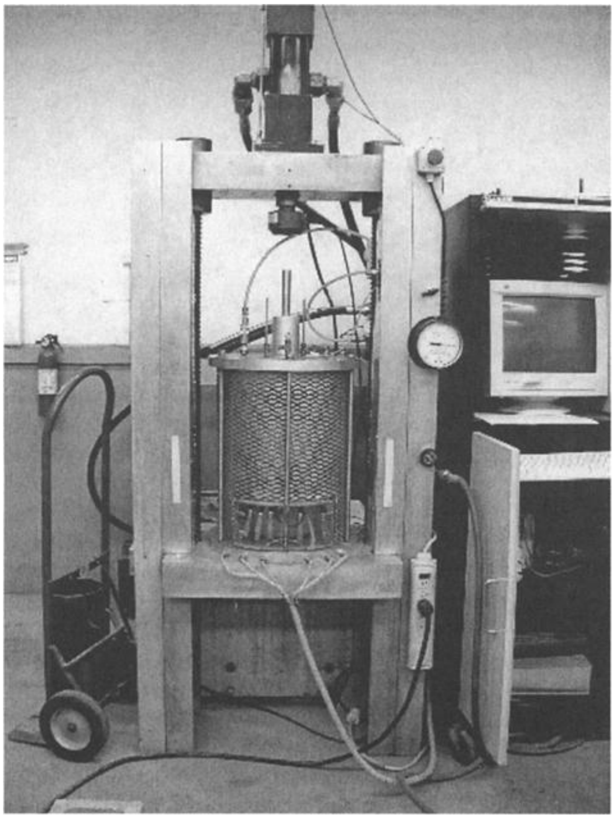

Figure 1 - *UCB Triaxial Testing System for Pavement Materials*

Two LVDTs are mounted on the specimen and two more on top of sample. Radial displacements are monitored using a chain device. Poor signal to noise ratios for the radial chain suggest the use of non-contact proximeters to measure radial displacements. The on-sample instrumentation is illustrated in Figure 2. Data from the instrumentation are collected by means of signal conditioning and data acquisition systems.

**Servo Controller System Description**

The axial load is applied to the specimen using a hydraulic actuator and is monitored with a displacement transducer inside the actuator, or with the internal load cell. During repeated loading, the feedback signal is compared with target value and adjustments made in the controller to minimize the error between the feedback signal and the target value. Figure 3 shows a diagram of the four components of the electronic system of the triaxial apparatus. A description of each component follows.

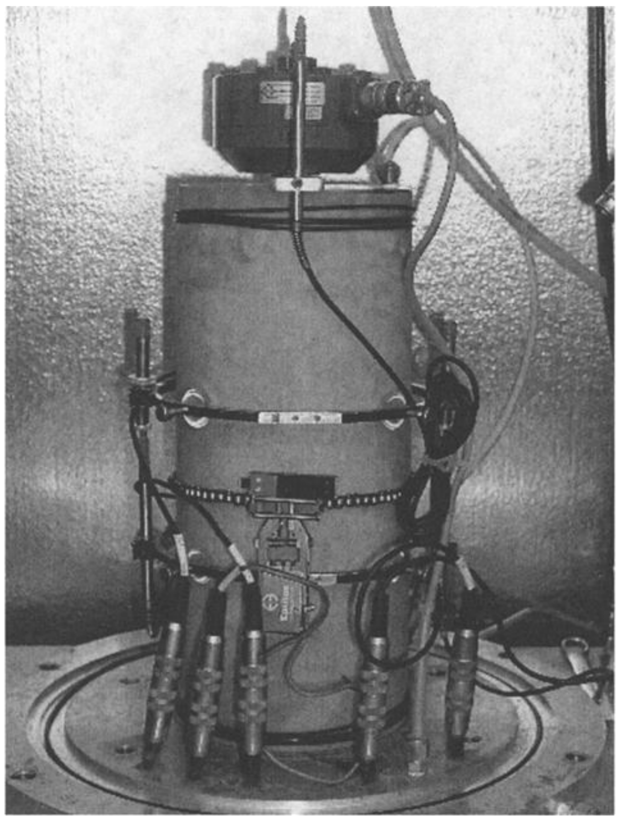

Figure 2 - *On-Sample Instrumentation*

*Signal Subsystem*

The signal subsystem is currently composed of two feedback signals, and one is selected depending on whether the test is run under displacement or load control. Displacement control is accomplished using a signal from the LVDT mounted inside the actuator piston. Load control is carried out using a signal from the load cell mounted on top of the sample, inside the triaxial cell. Non-feedback signals are those obtained from the externally mounted load cell and from the internally mounted radial and LVDT transducers. Currently, these non-feedback signals can be used as feedback signals if required.

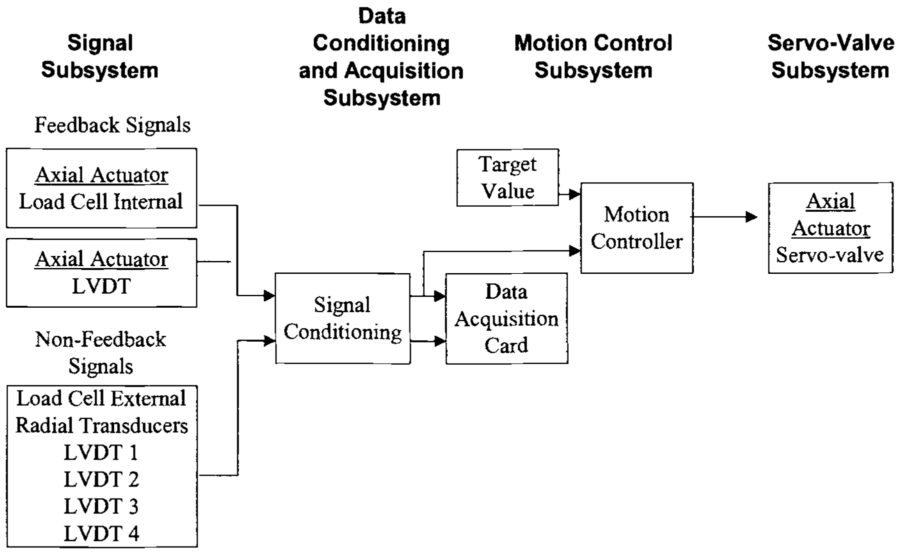


Figure 3 - *Components of the Electronic System*

*Signal Conditioning and Data Acquisition (SCDA) Subsystem*

Signal conditioning is provided by a programmable multi-channel chassis-based system. The system consists of two modules that amplify, filter, isolate, and multiplex the load/pressure and LVDTs signals. The data acquisition is provided by a high performance data acquisition card with 16-single ended analog inputs capable of a sampling rate of up to 100 thousand samples per second and a 16-bit resolution. The data acquisition card also included two16-bit analog outputs and eight input/output digital lines (National Instruments 2002). Digital lines were used to control switches that open and close the hydraulic lines and change the test mode from/to displacement control to/from load control.

*Motion Control Subsystem*

During the early development of the system several alternatives were tested in order to control the system for waveform and monotonic loading testing. The alternatives included 1) using the analog inputs and outputs of the data acquisition card, 2) using a commercially available ready-to-use servo-controller typically used in this type of applications, or 3) using a commercially available motion controller card that requires programming to develop the application.

Alternative 1 required proportional, integral, derivative (PID) algorithms to control the system. The alternative was acceptable for monotonic loading because the target or set values were easy to follow. A single point generation approach was used. However, waveforms with frequencies higher than 0.03 Hz could not be generated because the loop used in the software to control each point of the waveform was too slow for the application. The fastest PID loop rate was of 55 milliseconds per sample. A real-time data acquisition card showed no significant improvement. Other solutions using the data acquisition card included a buffered analog input/output solution. However, the results were not satisfactory because it required several PID algorithms to set the maximum, minimum, and shape of the waveforms. Based on the results of the data acquisition card option, a viable alternative was to purchase a ready-to-use motion controller (alternative 2). Technically, the ready-to-use motion controller would provide excellent control of a single servo-hydraulic channel. The cost of a single unit was above \$10 000 dollars which was over the budget allocated for developing the system in-house. In addition, another motion controller would have to be purchased if other channels needed to be controlled (e.g., confining pressure, shear actuator, etc).

Because of budget constraints and higher capabilities expected from the motion controller it was decided to purchase a motion controller card with programable compatibilities with the software used for data acquisition. Among the many features in the motion controller, the most significant for the triaxial applications were a four channel controller PCI card (rather than one channel with alternative 2), $62 \times 10^{-9}$ seconds PID loop update rate (rather than $55 \times 10^{-3}$ seconds with alternative 1), contouring, and on-board programming. The contouring feature of the motion controller allows the user to specify any type of complex waveform and have the motion controller create a smooth path through them. The on-board programming was also desirable, as the waveform motion can be program in the processor of the motion controller instead of the host computer (National Instruments 2002). Running the on-board programs offers reliability and predictability of the tests such as a repeated loading test with no rest periods at frequencies above 10 Hz. Many other features are available for the programmable motion controllers which are properly described in the manufactures technical fact sheets.

*Servo-Valve Subsystem*

A high performance servo-valve that covers a range of rated flows from 0.063 to 0.946 l/s (1 to 15 gpm) at 6.89 MPa (1000 psi) is used in the hydraulic system. Input signals are in the range of ± 15 mA. Since the output signal of the motion controller card are in the range of ±10 V, a buffer amplifier was obtained to bridge this difference.

*Temperature Control Subsystem*

The temperature control subsystem is only used for testing asphaltic materials and is independent of the other control systems. The air entering the cell is heated with a 400W in-line air heater, capable of heating air at pressures of up to 700 kPa (100 psi). An air bleed valve slowly removes air from the cell, and the replacement air is heated before entering the cell. Two small fans circulate the air inside the cell to ensure uniform temperature distribution. The temperature is controlled using a separate, commercially available electronic temperature controller that can control the air temperature to within 0.55 C (1 F).

Because the heat transfer through the aluminum top and bottom caps was high, it was necessary to install a temperature control box around the apparatus and heat the air around the cell using a small fan heater and a thermostat. This ensures that temperatures of over 40 C can be maintained inside the cell. The test system with temperature control box is illustrated in Figure 5.

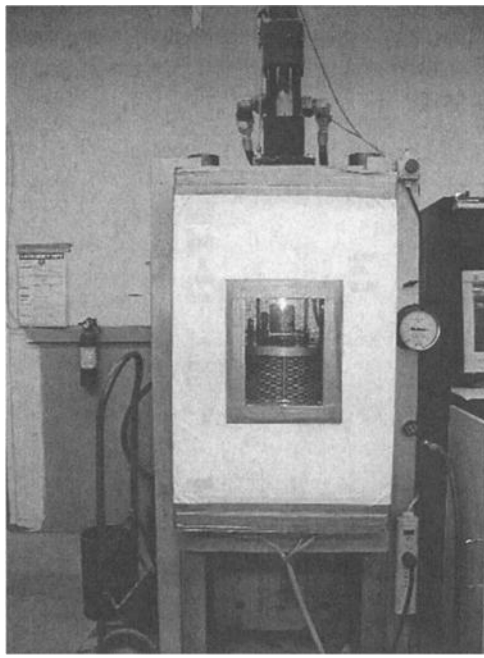

Figure 4 - *Triaxial System with Temperature Control Box Installed*

**Performance of Hydraulic System**

Currently the performance of the system is excellent and it has been used not only to conduct laboratory testing under the P-46 test protocols (Federal Highway Administration 1997) for granular materials but also other laboratory tests. Results of these test procedures have been used to calibrate a bounding surface plasticity constitutive model for unsaturated granular pavement materials. The system is being used to calibrate a constitutive model for asphalt concrete materials. The need for altering the software and the hardware based on research needs was a feature that was required for the development of the system.

The system allows very accurate control of loads during dynamic testing. The system was checked against the P-46 laboratory startup procedures (Federal Highway Administration 1997) and fell within the allowable range for phase shift and all other required specifications. Applied stresses and measured strains during two typical test blocks during a P-46 test are illustrated in Figures 6 and 7. The applied waves are intended to be 0.1 second haversine pulses with a 0.9 second rest period between pulses (not shown). Both figures show three waves superimposed on each other, and the data is unfiltered.

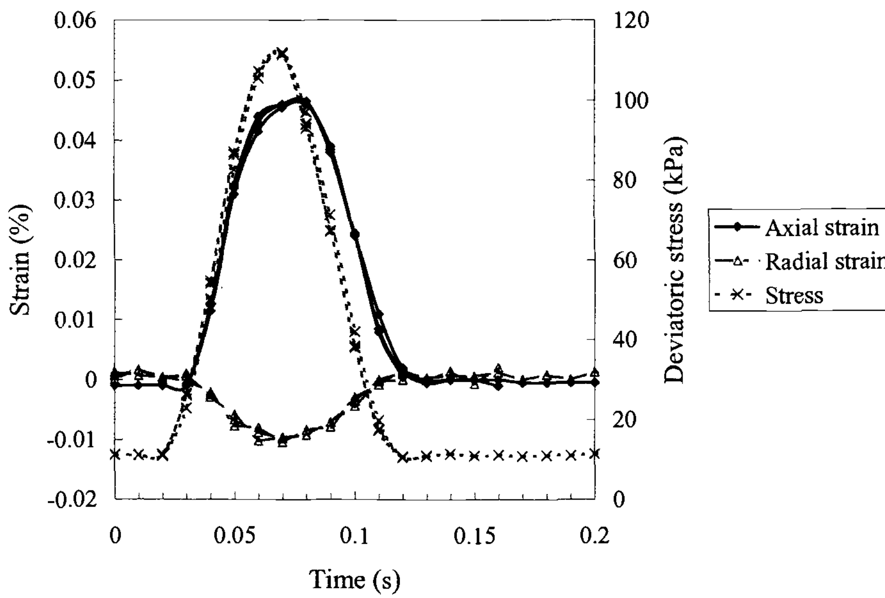


Figure 5 - *Stresses and Strains with Time for a High Deviatoric Stress*

As shown, the repeatability of the waves is excellent, and the control system and hydraulic actuator control the waves well, with very little deviation from a true haversine shape. The deviatoric stress is calculated using the internal load cell, the axial strain is calculated using the on-sample LVDTs, and the radial strain is calculated using the radial chain.

**Performance of the Instrumentation and Data Acquisition System**

As shown in Figures 5 and 6, the load cell and LVDTs have excellent repeatability and little noise, while the noise from the radial transducer is easily noticeable, especially at low stress levels. For this reason, it is anticipated that the radial transducer will be replaced with proximity sensors.

There is a slight time lag between the load and displacement curves in Figures 5 and 6, but this is attributed to non-linear, time dependent material behavior rather than to the data acquisition system. The radial transducer is connected to the same data acquisition module as the load cell, while the LVDTs are connected to another module. Fourier analysis of the haversine waves indicated an average phase lag of 9.2 ms between the LVDTs and load cell, and 7.4 ms between the radial transducer and load cell. The wavelength was also different, indicating time dependent material behavior. The average wavelength for the load pulse was 11.1 ms (target = 10 ms), while it was 12.1 and 12.5 ms for the LVDTs and radial transducer respectively.

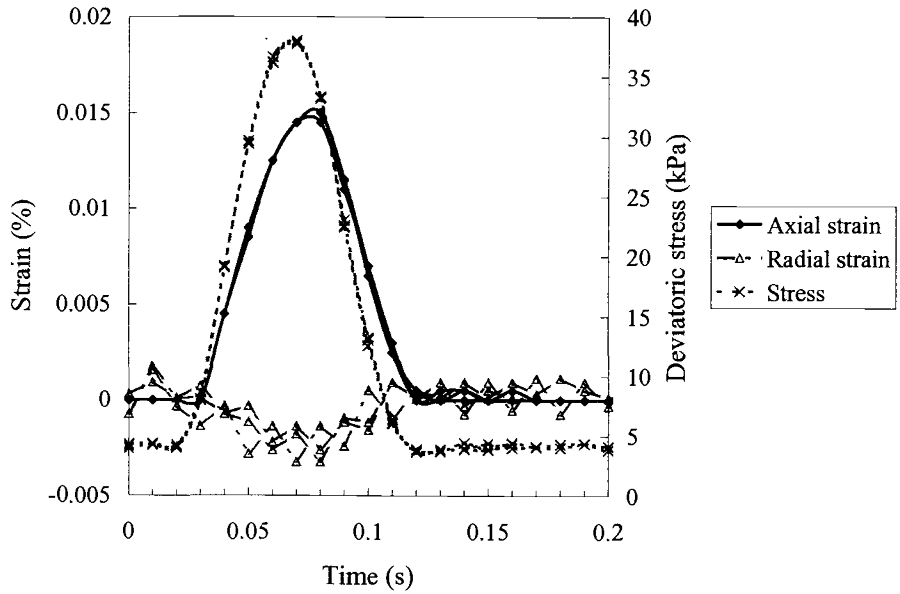


Figure 6 - *Stresses and Strains with Time for a Low Deviatoric Stress*

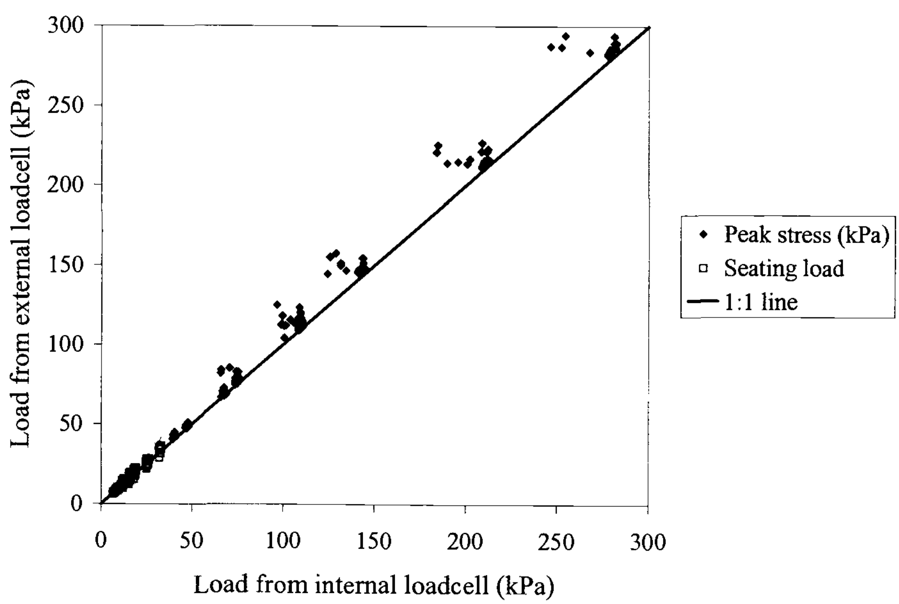


Figure 7 - *Comparison of Internal and External Load Cell Readings*

The reading from the internal and external load cell were compared to assess the effect of load road friction and confining stress on measured loads. The results from P-46 testing on four different Caltrans class 2 aggregate base materials (California Department of Transportation 1999) are illustrated in Figure 7.

As shown, the external load cell readings are generally higher than for the internal load cell, because of load road friction and uplift pressure on the load rod. While this difference is usually small, this is not always the case, particularly at higher loads where the external load cell can read over 15 percent higher. The load rod friction was minimized as much as practically possible by using a low friction linear bearing system in the top cap, and a single o-ring. O-ring grease was applied before testing to further minimize friction. This indicates that while many triaxial test apparatus use only an external load cell, this may not yield acceptable results. There does not appear to be a constant relationship between internal and external load cell reading, and it is likely that this is affected by sample stiffness, confining stress and test system compliance.

The measured resilient modulus ($M_r$) calculated using the on-sample, top cap and actuator LVDTs is compared in Figure 8. The data are from the same four aggregates used to determine the difference between internal and external load cell readings.

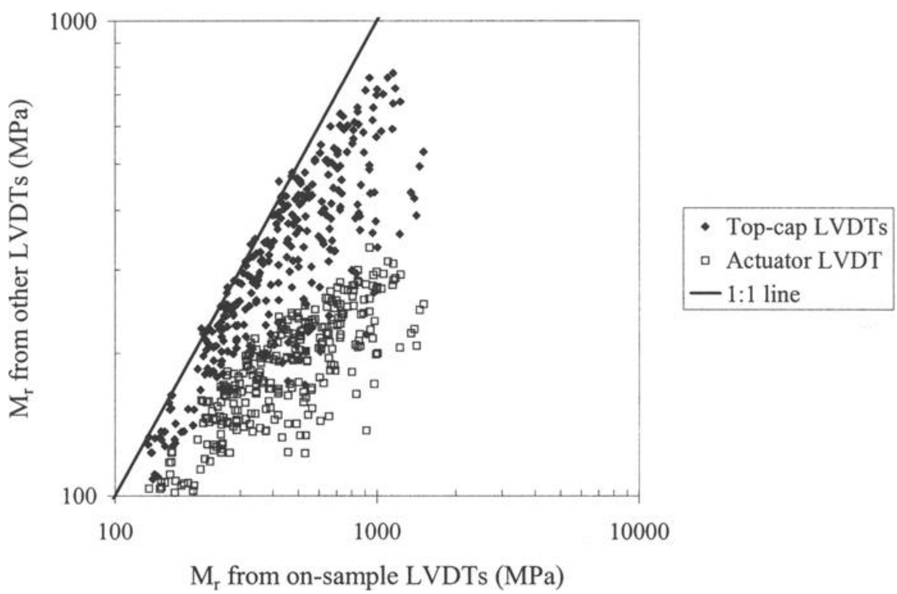


Figure 8 - *Comparison of Measured Resilient Modulus from Different LVDTs*

As shown, the resilient modulus measured using the on-sample LVDTs is consistently higher than for the other LVDTs. This is because the top-cap LVDTs are influenced by sample end effects. The actuator LVDT is influenced by sample end effects and compliance in the load cells, actuator and frame. For these reasons, the resilient modulus measured using the on-sample LVDTs is expected to be highest, while that measured using the actuator LVDT is expected to be lowest. The difference increases with increasing sample stiffness as the compliance will have a greater effect relative to the true sample deformations.

This is also an aspect that is often not considered in resilient modulus testing of pavement materials, although some laboratories apply an empirical correction factor to account for compliance. As shown in Figure 8, there is no consistent relationship between the measurements from the different LVDTs as sample end effects are specific to the actual sample. The use of an empirical correction factor is therefore unlikely to yield accurate results.

**Other Tests**

An important aspect of the triaxial system development was to include flexibility to allow the development of new tests for bound and unbound pavement materials. In addition to resilient modulus tests, load control static shear tests, volumetric strain tests and permanent deformation tests were required on unbound materials.

The volumetric strain tests enable the time independent volumetric elastic and hysteretic behavior to be measured. This behavior is currently being implemented into a bounding surface plasticity model for unsaturated granular pavement materials. The on-sample instrumentation enables accurate measurement of small volumetric strains with changes in confining stresses. This behavior was traditionally difficult to measure, and as a result many researchers assumed little or no volumetric hysteresis for granular materials. The behavior is measured by slowly cycling the confining stress to different stress levels. An example of the test results is illustrated in Figure 9.

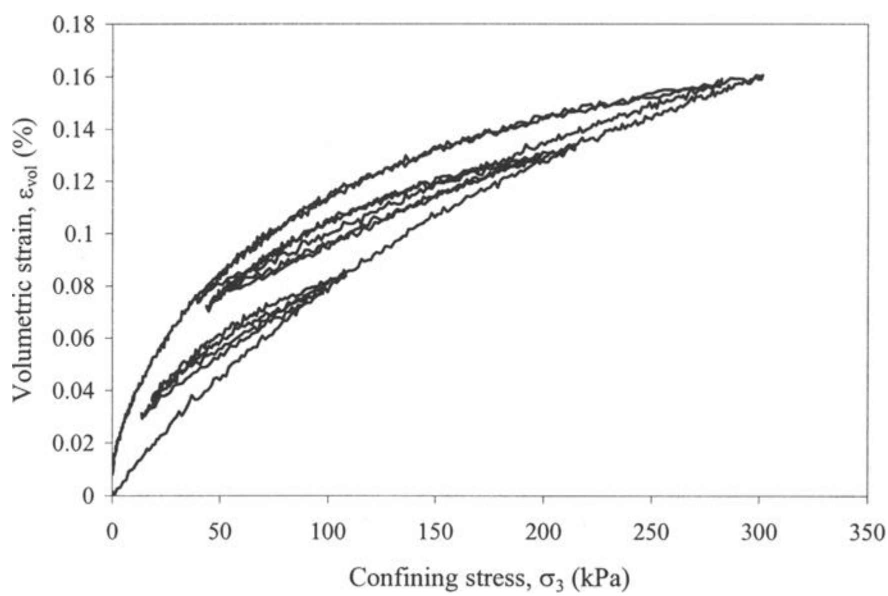


Figure 9 - *Typical Volumetric Test Result*

Because the volumetric tests are run by changing only the confining stress and only a very small constant deviatoric stress is applied to hold the sample upright, the bulk behavior can be separated from the shear behavior which is important for determining model parameters for advanced constitutive models.

## Conclusions

A triaxial test apparatus was designed and built at the Pavement Research Center at the University of California, Berkeley for the characterization of untreated and treated granular materials and other materials. The system conforms to the P46 quality requirements. A programmable motion controller PCI card controls the servo-hydraulic system. The motion controller was integrated with the data acquisition to have a complete easy to program system with the flexibility to allow system modifications, based on research needs.

The performance of the test apparatus is considered excellent, providing quality data for investigating different aspects regarding resilient modulus testing, material characterization, and constitutive model verification. The system is currently being used to characterize various California pavement materials and to verify constitutive models for both granular and asphaltic materials.

## References

California Department of Transportation, July 1999, "Standard Specifications."

California Test 301, March 2002, "Resistance "R" Value of Treated and Untreated Bases, Subbases, and Basement Soils (Stabilometer)."

Federal Highway Administration, January 1997, "LTPP Materials Characterization Program: Resilient Modulus of Unbound Materials (LTPP Protocol P46) Laboratory Start-Up and Quality Control Procedure," Publication No. FHWA-RD-96-176, U.S. Department of Transportation, Federal Highway Administration. Research and Development, McLean, VA.

Hicks, R. G. and Monismith C. L., 1971, "Factors Influencing the Resilient Properties of Granular Materials," *Highway Research Record* 345, 15–31.

Hveem, F.N., and Carmany R. M., 1948, "The Factors Underlying the Rational Design of Pavements, " *Proceedings Highway Research Board* Vol. 28.

National Instruments, 2002, "The Measurement and Automation Catalog."

Uzan, J., 1985, "Characterization of Granular Material," *Transportation Research Record* 1022, 52-59.

W. A. Marr,[1] R. Hankour,[2] and S. K. Werden[3]

# A Fully Automated Computer Controlled Resilient Modulus Testing System

**Reference:** Marr, W. A., Hankour, R., and Werden, S. K., "**A Fully Automated Computer Controlled Resilient Modulus Testing System,**" *Resilient Modulus Testing for Pavement Components, ASTM STP 1437*, G. N. Durham, W. A. Marr, and W. L. DeGroff, Eds., ASTM International, West Conshohocken, PA, 2003.

**Abstract:** This paper describes a fully automated computer controlled testing system for performing resilient modulus tests. It describes the use of a PID adaptive controller to improve the quality of the test and reduce the labor required to run the test. It also addresses some of the difficulties and technical details for running a resilient modulus test according to current test specifications.

**Keywords**: resilient modulus testing, PID control, test automation

## Introduction

A resilient modulus test is a complicated cyclic test in which the stiffness of the sample changes with loading. These changes are caused by the nonlinear stiffness behavior of tested materials for different stress levels and the change of stiffness of tested material during cyclic stressing with the same load. Since the control parameters of a cyclic loading system depend on the stiffness of the sample, most systems fail to apply the correct load throughout the test. A system adjusted to give the specified load at the beginning of the test may be off at the end of the test. Some people make manual adjustments to the equipment throughout the test to maintain the correct load. Others ignore this problem, which produces results that do not conform to the test specifications. Incorrect settings of the load control equipment can produce load overshoot, load undershoot, or slow load response so that the applied load deviates far from that defined by the test standards.

The system presented in this paper uses real-time adjustment of a PID controller to change the system control parameters as the stiffness of the specimen changes. PID stands for Proportional-Integral-Derivative. This is a feedback controller whose output, a control variable, is based on the error between some user-defined set point and some measured process variable. This feature permits the application of an accurate load from the beginning to the end of the test without manual adjustment. Therefore, this system meets the rigid AASHTO T-294/T-307, and LTPP Protocol P46 specifications for

[1] CEO, GEOCOMP Corporation, 1145 Massachusetts Ave, Boxborough, MA 01719.
[2] Geotechnical Engineer, GEOCOMP Corporation.
[3] Senior Systems Engineer, GEOCOMP Corporation.

precision on loading through all stages of the test without requiring manual adjustment during the test. As illustrated in Figure 1, this test protocol requires the load to be applied and removed in 0.1 sec according to a haversine shape, followed by a 0.9 second rest period for hydraulic loading systems.

Pneumatic systems do not come close to applying a haversine waveform that meets the AASHTO standards requirements (T-307 Section 4.1 and T-294 Section 6.2.2). As a result the current AASHTO standard T307-99 Section 6.2 is more forgiving for pneumatic systems. The rest period can stretch from 0.9 to 3.0 seconds.

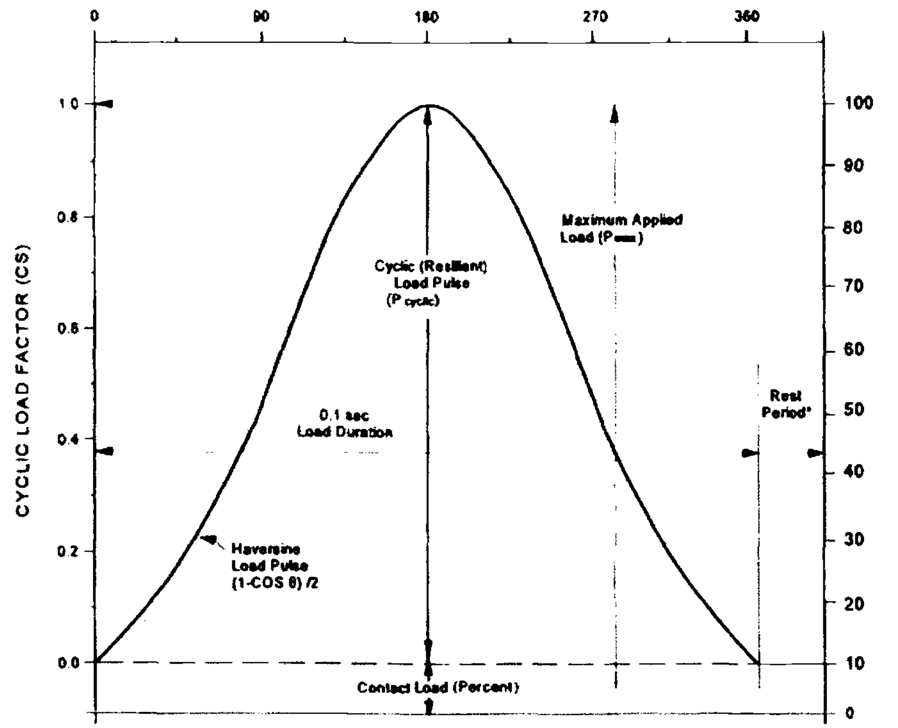


***The rest period will be 0.9s for hydraulic loading devices and 0.9 to 3.0 s for pneumatic loading devices.**

FIG. 1—*Load Shape from AASHTO T-307.*

The system described in this paper fully automates the conduct of a resilient modulus test according to AASHTO T292/T 307, and LTPP Protocol P46. Once a material specimen is in place and the test conditions selected, the system will run the entire test from start to finish without manual intervention. Test data will be stored in a file for subsequent reduction and plotting by the system software. At the end of the test, the system generates the test data in a variety of output formats so users can get the most use out of the data. Options include a complete final test report with all appropriate calculations on the data, text file of raw data and a text file of data in engineering units, either of which can be imported into a spreadsheet for further data analysis.

Coefficients for the resilient modulus constitutive relationships defined in FHWA Design Pamphlet (FHWA-RD-97-083) are automatically computed in the report options.

**Fully Automated Resilient Modulus Hardware**

Figure 2 shows the new system described in this paper. It consists of a load frame, a hydraulic pump, and a servo-valve with a hydraulic cylinder, an external signal-conditioning unit, and a computer with a network card and an A/D card for data

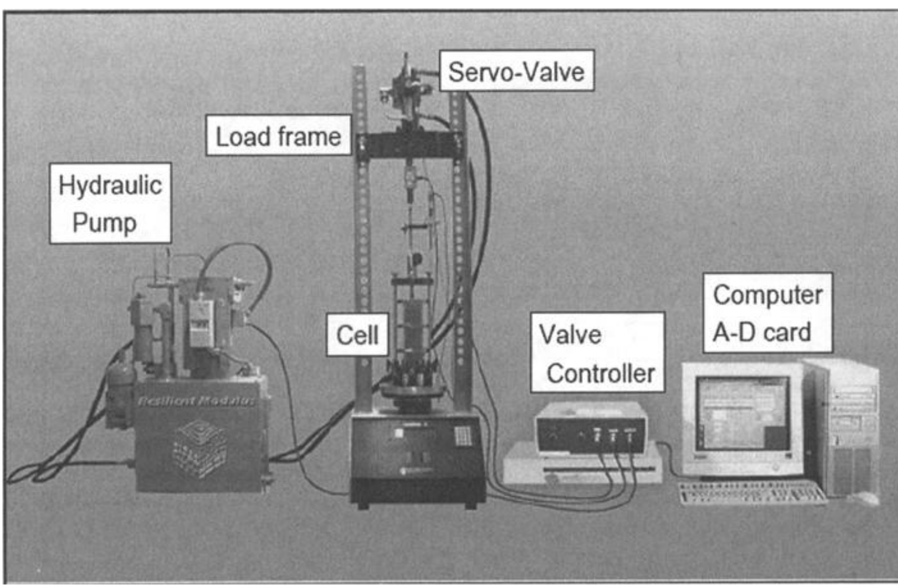


FIG. 2—*Automated resilient modulus system.*

The hydraulic components consist of a cylinder, coupled with a servo-control valve and a hydraulic actuator driven by a 2.5 gpm at 3000 psi (10 L/min at 21 MPa) air-cooled hydraulic pump for applying the cyclic load. The hydraulic actuator provides the cyclic component of vertical force. The system works as a closed-loop electro-hydraulic system for applying repeated axial deviator stress of fixed magnitude, load duration (0.1 second), and cycle duration (1 second). These cyclic load parameters can be changed through the software program to provide flexibility in cyclic loading pulse and rest durations.

An electro-pneumatic cell pressure regulator applies and adjusts the specified cell pressure automatically from one step to the other. Pressure is continually monitored and maintained at the required value throughout the test. The electro-pneumatic pressure controller is a proportional regulator with built-in feedback. The input signal is 0-5VDC voltage provided by the A/D card through software control. Pressure is controlled to within 0.1 psi (0.7 kPa).

The equipment is controlled with a personal computer running the Windows™ operating system. A 16-bit analog-to-digital card placed inside the computer collects data from the sensors and sends control signals to the servo-valve controller.

**Fully Automated Resilient Modulus Software**

The system software consists of a single program that runs the test, collects data for the test and stores the data in a file. It also performs the necessary calculations and prepares the final tables and graphs of the test results. This program will run on any PC using the Windows™ NT, XP or 2000 operating systems. The configuration for any previous test can be used to establish the initial conditions of a subsequent test by loading the existing test file. This capability allows an operator to set up and start a test within a very short time.

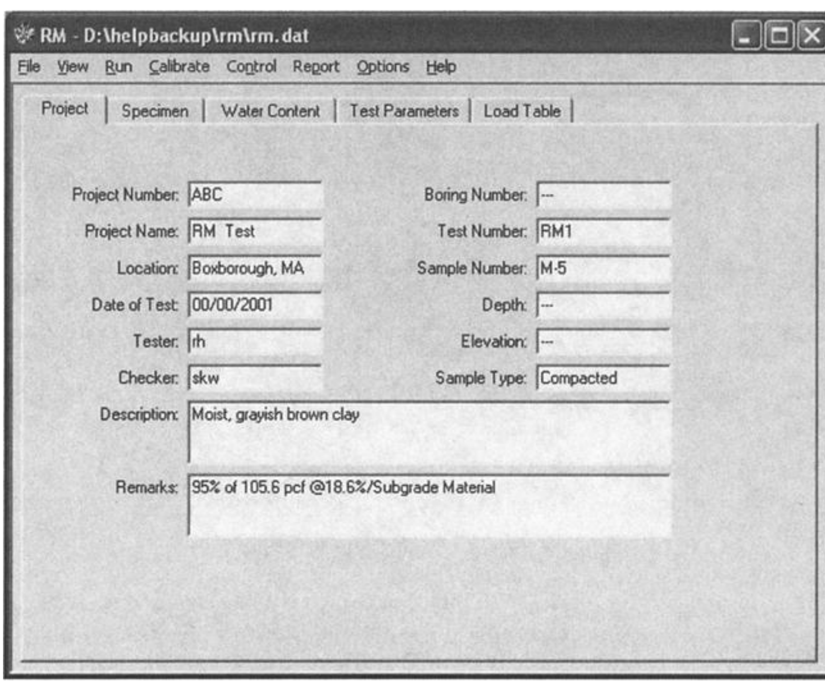


FIG. 3—*Main window for system software.*

The software allows the user to define the conditions for controlling the equipment and running the test. Figure 3 illustrates the main window. Specimen specific information can be entered for inclusion on the tabulated and graphed results. This window is composed of a menu bar at the top and a property sheet with five tabs. Each of the menus (File, View, Run, etc.) can be selected in the standard way of clicking on the menu word or using short-cut keys. Each tab on the property sheet (Project, Specimen, Water Content, etc.) specifies a property page, which can be displayed by clicking on the tab. Information for a test is typed into the entry fields on each property page after clicking on the field where information is to be entered. Once a test has been defined, the test can be started with a single mouse click. During the test, real time data and status information are displayed on the monitor in numeric form or graphical form by accessing menu options.

**PID Control of Load**

Resilient modulus testing requires precise control of the applied load, which must change rapidly. The applied load value is part of a measurable process that uses a feedback controller designed to generate an output that causes some corrective effort to be applied so that the target load is obtained accurately. Control of the load is accomplished by using a closed loop controller. At equally spaced time intervals, called the control loop period, the controller compares the applied load measured with a load cell to the target load. The load error is the difference between the two. The controller uses this error to compute and send a signal to the servo valve to reduce the load error in the next loop period.

The signal to the servo valve controls the valve's spool position. Assuming constant pressure drop across the valve, flow to the hydraulic cylinder is proportional to the spool position, which in turn is also proportional to the signal. The constant flow to the cylinder produces a constant displacement rate of the actuator. The resulting loading rate will be proportional to the stiffness of the test specimen. Table 1 summarizes the key relationships that define a PID controller.

TABLE 1—*PID Controller.*

| | |
|---|---|
| 1 Load Error | = Target Load – Actual Load |
| 2 Displacement Rate | = Signal * Valve Constant |
| 3 Load Rate | = Specimen Stiffness * Displacement Rate |
| | = Specimen Stiffness * Signal * Valve Constant |
| 4 Signal | = Load Rate / Specimen Stiffness / Valve Constant |
| 5 Load Error Rate | = Load Error / Control Loop Period |
| 6 Signal | = Load Error / Control Loop Period / Specimen Stiffness / Valve Constant |
| 7 Proportional Gain (GP) | = 1 / Control Loop Period / Specimen Stiffness / Valve Constant |
| 8 Signal (P) | = Load Error * Proportional Gain |
| 9 Signal (I) | = Sum (Load Errors) * Integral Gain |
| 10 Signal (D) | = Change Load Error * Derivative Gain |
| 11 Signal | = Signal (P) + Signal(I) + Signal(D) |

These equations contain two physical unknowns, the valve constant and the specimen stiffness, and three system unknowns, the proportional, integral and derivative gains. The valve constant is constant only if the pressure drop across the valve is constant. The pressure drop depends on the ability of the hydraulic pump to maintain the supply pressure for a given flow. It also depends on the load applied to the specimen.

The specimen stiffness is obviously unknown; otherwise we would not be running the test. An estimate of the stiffness is not enough to run the test accurately from start to finish. As the loading progresses, the stiffness of the specimen changes.

The variable servo constant and variable specimen stiffness requires that the proportional gain must be changed throughout the test to maintain the target load. Changing the gain setting during the test to improve performance is called "adaptive control." The controller computes and uses new values of gain as the test runs to adjust to the changing stiffness of the system. Simple PID controllers consider only the error in the load to control the valve. These are proportional controllers. More refinement in the control can be obtained by considering the behavior of the load error over time. If the sum of the previous load errors is increasing, we might want to adjust the signal to the valve. This is called "integral gain." If the load error is increasing, we might want to adjust the signal to the valve. This is called "derivative gain." A controller that uses all three measures of error is referred to as a PID controller.

As it turns out, a system with PID adaptive control can adjust for changes in the valve constant throughout the test as well. Therefore, a system with adaptive control capability only needs initial estimates of the proportional, integral and derivative gains to start the test. The adaptive controller will converge to the correct gain settings in the first few cycles of the test and continue to adjust those settings throughout the test to match the actual load to the target load as closely as possible. Figure 4 illustrates the typical adjustments to proportional gain during one load sequence of a resilient modulus test.

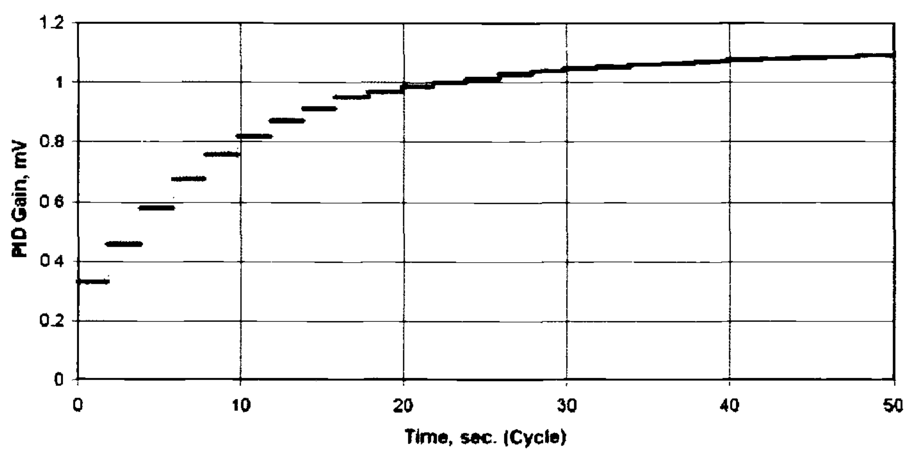


FIG. 4—*Proportional gain with time.*

## Typical Test Results

The software program menu has option to produce a report of the cyclic phase results in graphical form or in tabular form and to choose the settings for the graphs included in the graphical report. It also provides an option for editing the data, which will be used in the report. Figure 5 shows a typical set of results for a Type 1 per AASHTO T-307. Figure 6 shows a typical set of results for Type 2 per AASHTO T-307 loading. These single page test reports are produced automatically by the system using data reduction techniques dictated by the test standard. The tabulated data show that the adaptive controller is controlling the applied deviator stress to within a variation < 1.0 % when comparing the nominal maximum deviator stress (column No. 2) to the actual mean deviator stress (column No. 3).

TABLE 2—*Nominal versus applied deviator stresses.*

| Nominal Max.[1] Deviator Stress (kPa) | Mean Deviator Stress (kPa) | Variation (%) |
|---|---|---|
| 13.8 (2psi) | 13.7 (1.997 psi) | -0.15 |
| 27.6 (4psi) | 27.6 (4.002 psi) | 0.05 |
| 41.4 (6psi) | 41.1 (5.962 psi) | -0.63 |
| 55.2 (8 psi) | 54.8 (7.943 psi) | -0.71 |
| 68.9 (10 psi) | 68.6 (9.946 psi) | -0.54 |
| 13.8 (2psi) | 13.7 (1.997 psi) | -0.15 |
| 27.6 (4psi) | 27.6 (3.982 psi) | -0.45 |
| 41.4 (6psi) | 41.1 (5.961 psi) | -0.65 |
| 55.2 (8 psi) | 54.8 (7.940 psi) | -0.75 |
| 68.9 (10 psi) | 68.4 (9.921 psi) | -0.79 |
| 13.8 (2psi) | 13.8 (1.998 psi) | -0.10 |
| 27.6 (4psi) | 27.5 (3.982 psi) | -0.45 |
| 41.4 (6psi) | 41.2 (5.971 psi) | -0.48 |

[1] Data from Test on Type 1 Soil from Figure 5

This is excellent control compared to other variables in the resilient modulus test. A system like the one described greatly reduces the labor required to run a resilient modulus test to primarily that required to prepare and set up the test specimen. The automated system requires much less manual trial and error to find the right settings for controlling the load. Adaptive control gives much improved load control over the complete duration of the test. These factors reduce the technician time required to run the test and improve the test quality.

**RESILIENT MODULUS TEST DATA**

SUMMARY REPORT

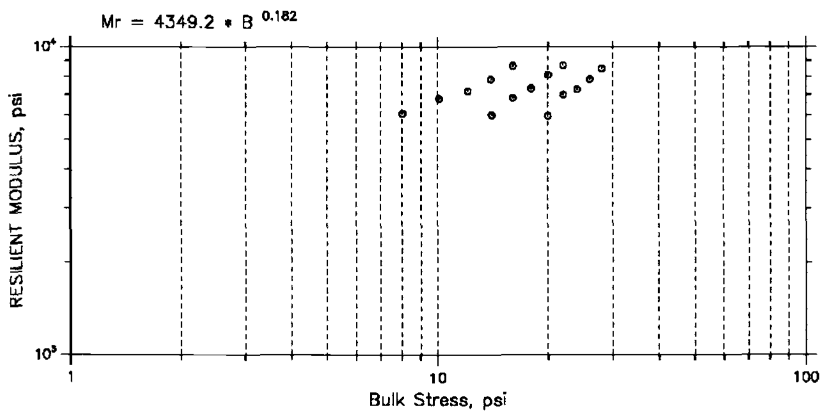


| Confining Stress S3 (psi) | Nom. Max. Deviator Stress (psi) | Mean Deviator Stress (psi) | Std. Dev. Deviator Stress (psi) | Mean Bulk Stress (psi) | Mean Resilient Strain (%) | Std. Dev. Resilient Strain (%) | Mean Resilient Modulus (psi) | Std. Dev. Resilient Modulus (psi) |
|---|---|---|---|---|---|---|---|---|
| 5.999 | 2 | 1.997 | 0.0029 | 19.99 | 0.03 | 0.00 | 5968.8 | 98.819 |
| 5.997 | 4 | 4.002 | 0.0025 | 21.99 | 0.05 | 0.00 | 6994.6 | 45.819 |
| 6.001 | 6 | 5.962 | 0.0066 | 23.97 | 0.07 | 0.00 | 7284.5 | 52.545 |
| 6.006 | 8 | 7.943 | 0.0078 | 25.96 | 0.09 | 0.00 | 7858.1 | 49.527 |
| 5.995 | 10 | 9.946 | 0.0074 | 27.93 | 0.11 | 0.00 | 8503.7 | 52.607 |
| 4.015 | 2 | 1.997 | 0.0030 | 14.04 | 0.03 | 0.00 | 6016.6 | 87.94 |
| 4.014 | 4 | 3.982 | 0.0052 | 16.02 | 0.05 | 0.00 | 6829.9 | 73.116 |
| 4.007 | 6 | 5.961 | 0.0021 | 17.98 | 0.07 | 0.00 | 7332.1 | 73.199 |
| 4.025 | 8 | 7.94 | 0.0030 | 20.01 | 0.09 | 0.00 | 8120.8 | 61.505 |
| 4.015 | 10 | 9.921 | 0.0103 | 21.96 | 0.10 | 0.00 | 8713.1 | 44.754 |
| 2.012 | 2 | 1.998 | 0.0027 | 8.032 | 0.03 | 0.00 | 6080 | 68.904 |
| 2.037 | 4 | 3.982 | 0.0029 | 10.09 | 0.05 | 0.00 | 6793.5 | 32.914 |
| 2.041 | 6 | 5.971 | 0.0029 | 12.1 | 0.08 | 0.00 | 7194.5 | 56.886 |
| 2.006 | 8 | 7.943 | 0.0024 | 13.96 | 0.09 | 0.00 | 7854.8 | 48.071 |
| 2.029 | 10 | 9.936 | 0.0057 | 16.02 | 0.10 | 0.00 | 8669.7 | 45.941 |
| | | | | | | | | |

| | | |
|---|---|---|
| Project: Road Improvements | Location: Boxborough, MA | Project No.: GTX-ABC |
| Boring No.: --- | Tested By: rh | Checked By: akw |
| Sample No.: M-3 | Test Date: 06/27/2001 | Depth: |
| Test No.: RM6 | Sample Type: Compacted | Elevation: |
| Description: Moist, reddish brown silty sand with gravel | | |
| Remarks: 95% of 123.6 pcf @ 8.8% /Subgrade Material | | |
| File: D:\helpbackup\rm\3479-rm6.dat | | |

FIG. 5—*Test report for RM test (subgrade soil, type 1) per AASHTO T307-9.*

**RESILIENT MODULUS TEST DATA**

SUMMARY REPORT

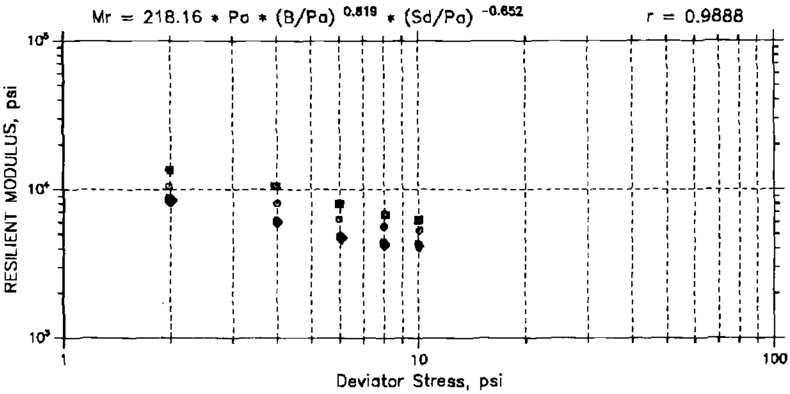


| Confining Stress S3 (psi) | Nom. Max. Deviator Stress (psi) | Mean Deviator Stress (psi) | Std. Dev. Deviator Stress (psi) | Mean Bulk Stress (psi) | Mean Resilient Strain (%) | Std. Dev. Resilient Strain (%) | Mean Resilient Modulus (psi) | Std. Dev. Resilient Modulus (psi) |
|---|---|---|---|---|---|---|---|---|
| 5.99 | 2 | 1.988 | 0.0091 | 19.96 | 0.01 | 0.00 | 13550 | 891.32 |
| 6 | 4 | 3.976 | 0.0072 | 21.98 | 0.03 | 0.00 | 10602 | 237.34 |
| 6.001 | 6 | 5.983 | 0.0102 | 23.99 | 0.06 | 0.00 | 8117.7 | 58.455 |
| 6.008 | 8 | 7.992 | 0.0065 | 26.02 | 0.10 | 0.00 | 6863.9 | 37.358 |
| 6.052 | 10 | 10 | 0.0130 | 28.16 | 0.14 | 0.00 | 6291.6 | 55.211 |
| 4.009 | 2 | 1.992 | 0.0117 | 14.02 | 0.02 | 0.00 | 10473 | 244.97 |
| 4.014 | 4 | 3.993 | 0.0123 | 16.03 | 0.04 | 0.00 | 8042.4 | 318.75 |
| 4.044 | 6 | 5.975 | 0.0095 | 18.11 | 0.08 | 0.00 | 6332.4 | 65.654 |
| 4 | 8 | 7.983 | 0.0119 | 19.98 | 0.12 | 0.00 | 5627.4 | 47.19 |
| 4.029 | 10 | 10.06 | 0.0284 | 22.15 | 0.17 | 0.00 | 5306.9 | 13.28 |
| 2.041 | 2 | 1.987 | 0.0213 | 8.108 | 0.02 | 0.00 | 8838 | 341.81 |
| 2.06 | 4 | 3.988 | 0.0126 | 10.17 | 0.06 | 0.00 | 6210.6 | 21.787 |
| 2.035 | 6 | 6.032 | 0.0149 | 12.14 | 0.11 | 0.00 | 4897.1 | 19.822 |
| 2.048 | 8 | 7.976 | 0.0087 | 14.12 | 0.16 | 0.00 | 4445.6 | 28.136 |
| 2.047 | 10 | 9.964 | 0.0113 | 16.1 | 0.20 | 0.00 | 4326.9 | 15.654 |
| | | | | | | | | |

| | | |
|---|---|---|
| Project: Road Improvements | Location: Boxborough, MA | Project No.: GTX-ABC |
| Boring No.: --- | Tested By: rh | Checked By: skw |
| Sample No.: M-5 | Test Date: 06/27/2001 | Depth: --- |
| Test No.: RM1 | Sample Type: Compacted | Elevation: --- |
| Description: Moist, grayish brown clay | | |
| Remarks: 95% of 105.6 pcf @ 18.6%/ Subgrade Material | | |
| File: D:\helpbackup\rm\3479-rm1a.dat | | |

FIG. 6—*Test report for RM test (subgrade soil, type 2) per AASHTO T307-99.*

**Issues With Current Test Standards**

The requirement of the AASHTO test standards to apply and remove the deviator load in 0.1 sec is difficult and expensive to achieve. It requires high performance servo-valve and fast electronics with little noise. From our own testing experience dynamic effects may become significant for 12 inch (300 mm) high specimens with a stiffness less than 20,000 psi (140 MPa) and for 6 inch (150 mm) high specimens with a stiffness less than 10,000 psi (70 MPa). While the rapid loading rate is used to model moving vehicles on a pavement system, it is not clear that this fast loading rate is necessary to obtain a meaningful stiffness of a soil specimen. The test would be a lot simpler to run and the equipment less expensive if the loading period could be increased to 0.5 seconds.

An accurate measurement of the axial deformation of the specimen is key to obtaining reliable resilient modulus results. When the first AASHTO standard (T 292-91) came out, the vertical deformation was measured with two LVDTs mounted internally and 180° diametrically opposed about the specimen's axis by means of clamps. This method made it extremely difficult to set-up a test specimen. Later on, the two LVDTs were clamped to the piston rod inside the chamber. Because of the potential for the top cap to rock, it made sense to use the average value of the two LVDTs. Even with this change, it was still difficult to setup a test specimen especially if it is a soft sample. The most current AASHTO standards (T 307-99 and T292-94) uses two LVDTs externally mounted to the piston rod. The two LVDTs now rest on a rigid surface. Therefore, there is no need to use two LVDTs. One transducer would be more convenient and sufficient to determine the axial deformation.

AASHTO standard (T 307-99) specifies load cell capacities for different sample sizes as summarized in Table 3. The specified capacity is two to four times the required capacity. This reduces the sensitivity of the load cell and makes it more difficult to achieve precise control of the load during the test. The standard should be changed to specify the required accuracy in the load measuring system as a percent of the maximum applied load.

TABLE 3—*AASHTO T 307-99 load cell capacities.*

| Specimen Diameter mm | Load Cell Capacity kN | Required Maximum Load kN |
|---|---|---|
| 71 | 2.2 | 1.1 |
| 100 | 8.0 | 2.2 |
| 152 | 22.2 | 5.0 |

ASTM D 4123 provides a standard to measure the resilient modulus of asphalt specimens with the indirect tension test. The test is used to study the effects of temperature, loading rate, rest periods and specimen orientation on resilient modulus of bituminous mixtures. The standard requires deformations to be measured to 0.00001 inch (0.4 micrometers). The standard states that cores should have relatively smooth and parallel surfaces. It is not clear what relatively smooth and parallel means. We know from work in rock mechanics used for ASTM standards D2938, D2216 and D4553 that the strength and stiffness of rock is sensitive to the uniformity of the test specimens. These standards require the ends of the test specimen and the loading platens to be flat and parallel to within 0.001 inch

(40 micrometers) to minimize the effects of asperities on the test results. It seems reasonable that a similar requirement should be used for bituminous specimens, especially if one is examining the effects of temperature, specimen orientation, loading rate, and rest periods on resilient modulus.

## Summary and Conclusions

Historically there have been three main deterrents to running the resilient modulus test: the complexity of the test, the high cost of the equipment, and the variability of test results. The automated system described in this paper makes the test easier to run, costs less than other servo-hydraulic systems, and provides consistent test results because of the use of adaptive control. These improvements have resulted from the use of recent advances in electronics, computers and software together with the application of system control theory to run the test.

Automation of the test has reduced the man time required to run the test. Automatic reporting of the test results removes another labor-intensive task. Detailed data are saved for each load cycle, which permits subsequent examination of any suspect or questionable test results. Adaptive control improves the quality and consistency of the test.

Testing errors can still occur. Specimen preparation remains a challenge to obtain a specimen at conditions representative of field conditions. This requires careful consideration of compaction method, density and moisture content to obtain a laboratory specimen that reflects field conditions. Care must be taken to minimize deflections, which can occur outside the specimen but are included in the deflection measurement, especially for specimens with high resilient modulus. This requires rigid connections and flat, parallel specimen ends to the degree possible.

Resilient modulus testing requires a knowledgeable technician who understands the equipment and the test. The test result is quite sensitive to the condition of the test equipment, methods of specimen preparation, and details of the test set up. Unless these details are carefully controlled, one should expect considerable variation in test results obtained by different laboratories.

## References

AASHTO 1993. Guide for Design of Pavement Structure. American Association of State Highway and Transportation Officials (AASHTO), Washington, D.C.

AASHTO 1997. Standard Test Method for Determining the Resilient Modulus of Soils and Aggregate Materials. Association of State Highway and Transportation Officials (AASHTO), Washington, D.C.

AASHTO 1997. Standard Test Method for Determining the Resilient Modulus of Soils and Aggregate Materials. Association of State Highway and Transportation Officials (AASHTO), Washington, D.C.

FHWA-RD-97-083. Design Pamphlet for the Determination of Design Subgrade in Support of the 1993 AASHTO Guide of Pavement Structures. U.S. Department of Transportation. Federal Highway Administration. Research and Development. Turner-Faribank Highway Research Center, 6300 Georgetown Pike. McLean, VA 22101-2296.

Soheil Nazarian,[1] Deren Yuan,[2] and Robert R. Williams[3]

# A Simple Method for Determining Modulus of Base and Subgrade Materials

**Reference:** Nazarian, S., Yuan, D., and Williams, R. R., **"A Simple Method for Determining Modulus of Base and Subgrade Materials,"** *Resilient Modulus Testing for Pavement Components, ASTM STP 1437,* G. N. Durham, W. A. Marr, and W. L. De Groff, Eds., ASTM International, West Conshohocken, PA, 2003.

**Abstract:** The resilient modulus test is commonly used to determine the modulus of base or subgrade materials as well as to establish their nonlinear behavior. Since the resilient modulus test is time consuming, the number of tests performed for a given project is limited. For day-to-day operation of highway agencies, a more rapid test method is needed. The stress wave (or seismic) method is being considered in Texas for this purpose. Seismic methods of testing can rapidly and nondestructively provide fundamentally correct moduli at known states of stress. Unlike the resilient modulus test, comparative field testing methods are available for seismic methods that can provide similar results under similar conditions. This paper describes the seismic test procedure and its relationship to the resilient modulus test results. Also discussed are the repeatability and reproducibility of the results as a function of operator experience, type of soil, and preparation method.

**Keywords:** seismic modulus, resilient modulus, laboratory testing, base, subgrade, quality control, quality assurance

Aside from traffic and environmental loading, the primary parameters that affect the performance of pavements are the moduli of its different layers. Current mechanistic-empirical design procedures for structural design of flexible pavements typically call for these parameters. The proposed 2002 AASHTO design guide seems to heavily rely on these parameters as well. Unfortunately, construction specifications are not based on these engineering properties. To successfully implement any mechanistic pavement design procedure and to move toward performance-based specifications, it is essential to develop tools that can measure the modulus of each layer in a rapid manner. For a comprehensive quality management of pavement layers, from the design stage to the completion of the project, laboratory and field tests should preferably be carried out on a daily basis to ensure a consistent and durable highway. We have studied a method based

[1]Professor, [2]Research Engineer, and [3]Graduate Research Assistant, Center for Highway Materials Research, The University of Texas at El Paso, 500 W. University, El Paso, TX 79968.

on stress wave propagation that is quite suitable for this purpose. The results of over four years of effort in developing a user-friendly surrogate to the resilient modulus tests are summarized here.

A review of the fundamentals of resilient modulus testing and the state-of-practice in performing these tests can be found in Barksdale et al. (1997) as well as a number of papers in this publication. The step-by-step procedure used to determine the resilient moduli of different materials in this study can be found in Nazarian et al. (1999). Either 100 mm by 200 mm (4 in. by 8 in., for subgrade) or 150 mm by 300 mm (6 in. by 12 in., for base) specimens were compacted in cylindrical molds to the modified proctor energy. The resilient modulus tests consisted of applying various deviatoric stresses at different confining pressures. Table 1 contains the sequence for base materials. The loading sequence used was a modified form of the sequence found in AASTHO TP46-94. Three tests at zero confinement were added.

Table 1 – *Loading Sequence for Resilient Modulus Test*

| Confining Pressure (kPa) | Deviatoric Stress (kPa) |
|---|---|
| 15 | 15 (conditioning cycle) |
| 0 | 7 |
| 0 | 14 |
| 0 | 21 |
| 21 | 21 |
| 21 | 41 |
| 21 | 62 |
| 34 | 34 |
| 34 | 69 |
| 34 | 103 |
| 69 | 69 |
| 69 | 138 |
| 69 | 207 |
| 103 | 69 |
| 103 | 103 |
| 103 | 207 |
| 138 | 103 |
| 138 | 138 |
| 138 | 276 |

The axial deformations were measured along the middle one-third of the specimen with six non-contact proximitor sensors as shown in Figure 1. Twenty-five cycles of loading are applied at every stage to optimize testing time, and to minimize the degradation of the specimen. From the measured axial displacements at a particular deviatoric stress and confining pressure, the resilient modulus of the specimen was determined.

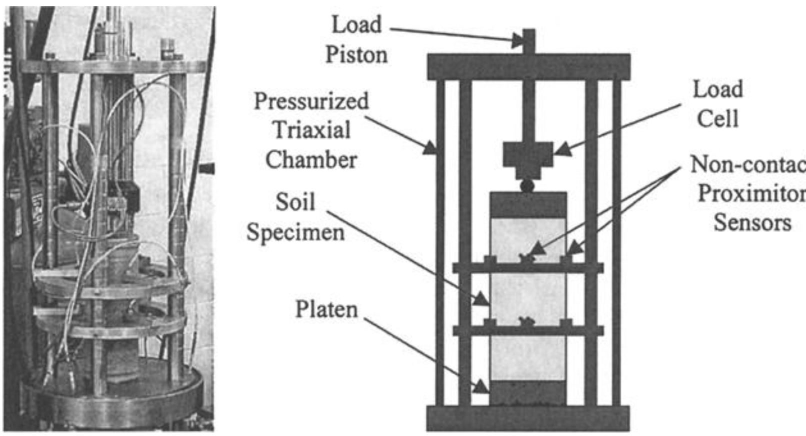


Figure 1 – *Photograph and schematic of resilient modulus test setup*

The constitutive model used to describe the results of the resilient modulus tests is

$$M_R = k_1\,\sigma_d^{\,k_2}\,\sigma_c^{\,k_3} \tag{1}$$

where $\sigma_d$ and $\sigma_c$ are the deviatoric stress and confining pressure, respectively. Parameters $k_1$, $k_2$, and $k_3$ are statistically-determined coefficients. Typical results from one test are shown in Figure 2. Since seismic tests are performed at a confining pressure of zero, a set of three resilient modulus tests was performed at zero confining pressure to facilitate the establishment of relationships.

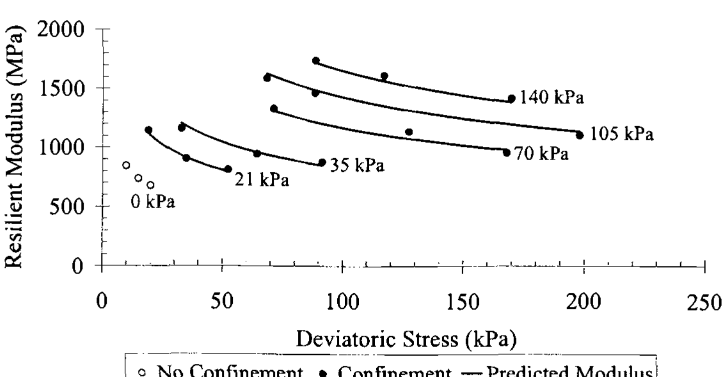


Figure 2 – *Typical resilient modulus test results*

The disadvantage of the seismic methods is that they provide moduli at small strains and thus require adjustment for design purposes. Seismic moduli are low-strain, high-strain-rate values; whereas the design moduli are based on high-strain, low-strain-rate values. Numerous investigators in the field of geotechnical engineering have addressed this matter in the past 25 years. Horhota (1996) and Ke et al. (2000) have shown two approaches to this problem in pavement design. For the sake of brevity, this subject has not been pursued any further. The readers are encouraged to review the publications mentioned above. Briefly under the Ke et al. (2000) approach, the seismic modulus and nonlinear parameters of each layer are input to a structural model. The structural model can be based on either nonlinear, layered solutions or finite element algorithms. The nonlinear material model for base and subgrade, which is adopted from Barksdale et al. (1994), is in the form of:

$$E_{design} = E_{seis} \left(\frac{\sigma_{c\_ult}}{\sigma_{c\_init}}\right)^{k_2} \left(\frac{\sigma_{d\_ult}}{\sigma_{d\_init}}\right)^{k_3} \qquad (2)$$

where $E_{design}$ and $E_{seis}$ are the design modulus and seismic modulus, respectively. Subscripts "ult" and "init" correspond to the condition when the maximum truckload is applied to the pavement and the free-field condition, respectively. The derivation of Equation 2 can be found in Ke et al. Parameters $k_2$ and $k_3$ are regression parameters that are preferably determined from resilient modulus laboratory tests on the specimen. A relationship can be determined by conducting seismic tests on specimens to be tested with the traditional resilient modulus setup.

In this paper, the experimental and theoretical background of the seismic modulus test is described first. The typical results and trends as well as the repeatability of the test methods are demonstrated. Finally, the correlation between the seismic and resilient modulus test results is provided.

*Seismic Modulus Test*

The free-free resonant column test is a simple laboratory test for determining the modulus of pavement materials. The modulus measured with this method is the low-strain seismic modulus. The method was originally developed for testing Portland cement concrete specimens; however, with appropriate modifications in hardware and software, it is also applicable to specimens of base and subgrade materials. Since the seismic tests are nondestructive, a membrane can be placed around the specimen so that it can be tested later for stiffness (resilient modulus). Performing both tests simultaneously will allow highway agencies to develop a database that can be used to smoothly unify the design parameters and construction quality control as described in Nazarian et al. (2002).

When a cylindrical specimen is subjected to an impulse load at one end, seismic energy over a large range of frequencies will propagate within the specimen. Depending on the dimensions and the stiffness of the specimen, energy associated with one or more frequencies are trapped and magnified (resonate) as they propagate within the specimen. The goal with this test is to determine these resonant frequencies. Since the dimensions of the specimen are known, if one can determine the frequency(ies) that are resonating (i.e. the resonant frequencies), one can readily determine the modulus of the specimen using principles of wave propagation in a solid rod (see Richart et al., 1970 for the theoretical background).

The procedure used in the seismic test is to find the Young's modulus by measuring the velocity that a wave propagates through a cylindrical specimen and combining those results with other measurable properties. The schematic of the test set up is shown in Figure 3. To perform the test an accelerometer is placed securely at one end of a specimen, and the other end is tapped with a hammer that has a load cell attached to it. The two sensors are connected to a data acquisition system placed in a laptop computer. Software has been developed to acquire and manipulate the time records from the accelerometer and the load cell. Typical time records are shown in Figure 4. The load consists of a short-duration half-sine pulse. The response measured with the accelerometer contains an oscillation that corresponds to the standing wave energy trapped within the specimen.

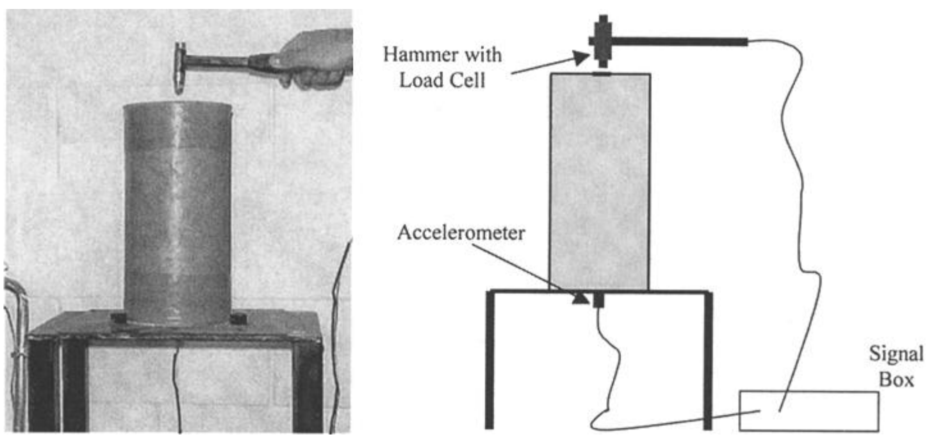


Figure 3 – *Photograph and schematic of free-free resonant column test setup*

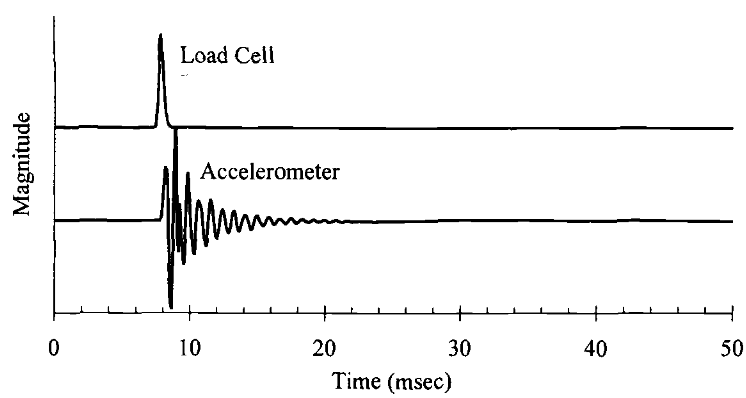


Figure 4 – *Typical load cell and accelerometer responses from free-free test*

A more convenient way of determining the frequency of oscillation consists of transforming the two signals into the frequency-domain using a fast-Fourier transform and then normalizing the acceleration amplitude with the load amplitude. The variation of normalized amplitude as a function of frequency, which is called a transfer function, contains peaks that correspond to the oscillation of the standing waves. A typical transfer function is shown in Figure 5 with the peak frequency clearly marked. Knowing the resonant frequency, $f_P$, mass density, $\rho$, and the length of the specimen, L, Young's modulus, E, can be found using:

$$E = \rho\,(2\,f_P\,L)^2 = \rho\,(V_P)^2 \tag{3}$$

where $V_P$ is the compression wave velocity.

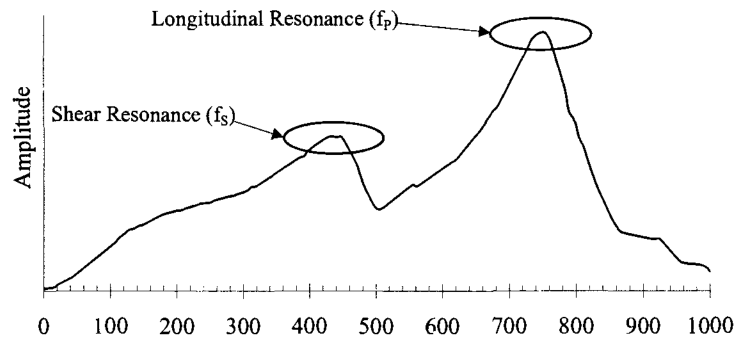


Figure 5 – *Typical free-free test transfer function*

The sample preparation described for the resilient modulus test is also applicable here. Similar to the resilient modulus tests, a height-to-diameter ratio of 2 is recommended for specimens. However, if necessary, this can be relaxed to 1.5. Another important practical issue is securing the accelerometer to the specimen. We have found that a roofing nail embedded in the specimen during compaction provides a convenient pedestal for securing the accelerometer with a magnet. We have also found that a nail placed on the opposite side will provide a nice anvil for the hammer.

**Presentation of Results**

Major concerns with any test procedure are the robustness, repeatability of the measurements. These matters are reported here first. Three materials (a typical base, a sand, and a clay) were used for this purpose. The base specimens were nominally 150 mm (6 in.) in diameter by 300 mm (12 in.) in length while the sand and clay specimens were nominally 100 mm (4 in.) by 200 mm (8 in.). The clay material is a highly-plastic clay from Dallas area, and mainly consisted of materials passing No. 200 sieve. The liquid and plastic limits of that material were 65% and 24%, respectively. The sand is primarily fine and medium sand with some small amount of silt also from the Dallas area. The optimum moisture contents of the two materials were about 18% and 8% for the fine-grained and coarse-grained materials, respectively.

*Best Test Configuration*

Alexander et al. (1996) estimate that the repeatability of the method on concrete specimens is better than 1%. But because of the attenuation of signals in softer granular materials and the sensitivity of the modulus to change in moisture and uniformity of compaction, such a level of repeatability cannot be achieved in base and subgrade materials. Even though the resonant frequencies in the seismic tests are not sensitive to the locations of the accelerometer and impact on the specimen ends, the amplitude associated with each resonance varies with these two parameters. Fortunately, the amplitudes are not important at all and only the frequencies at which the peak amplitudes (resonant frequencies) occur are significant. However, it is desirable to propose locations where the results are more robust.

A series of tests were conducted on about eight-dozen specimens to study this phenomenon. As reflected in Figure 6, thirty-five possible combinations of impact (load cell) and receiver (accelerometer) locations that would produce a primary wave were tried on each specimen. For convenience, the specimens were impacted on top. Thumbtacks were placed in a sideways "T" shape to distinguish the different locations and to provide a place to hit the specimen. The bottom of the specimen, where the receiver is placed consists of an "L" shape with location A being across from 1, B from 2, and so on.

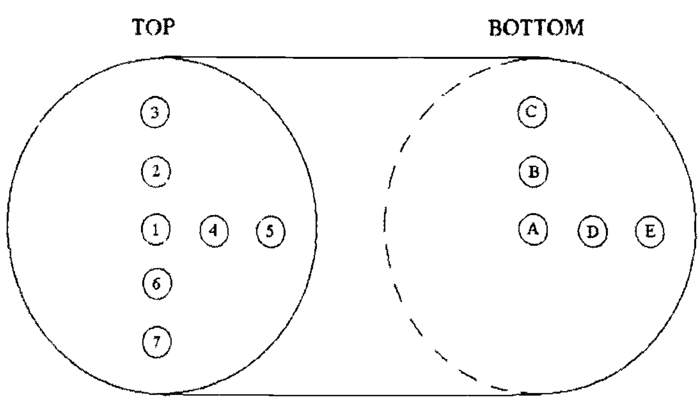


Figure 6 – *Source and receiver locations*

Statistically, the majority of the tests configurations yielded repeatable results. The best test setups seem to be when the source is placed near the center of the specimen (within one-third of the radius). The location of the receiver worked best when it was placed on the same half of the specimen as the source but not beyond two-thirds radius out from the center. Locations A1, C1, and E1 proved to provide results that were highly repeatable. If only the A1 (center-to-center) test combination is used, there is less of a chance to generate detectable shear energy. Thus, it is recommended to test with the C1 or E1 configuration in addition to A1.

*Repeatability of Tests*

The variation in modulus with moisture for the clay, sand and base materials are shown in Figure 7. From Figure 7a, the clay exhibits a peak seismic modulus at water content of about 13%. A relatively large number of specimens were prepared to demonstrate the repeatability and reproducibility of the test method. The goal was to prepare the specimens at six discrete water contents. Some variability between the target and actual moisture contents are observed. Nevertheless, the results follow a reasonably tight trend, demonstrating the reproducibility of the results.

The sandy material demonstrates a different trend as reflected in Figure 7b. The modulus increases with a decrease in moisture content until a point (say 3%). Below that moisture content, the specimens are so fragile that they could not stand alone without cracking. As such, their measured moduli are quite low. Ignoring the moduli from specimens with moisture contents below 3%, the results are again reasonably repeatable and follow a tight trend.

The base material, as shown in Figure 7c, exhibited large variability in our experiment. Since the test method is repeatable on other materials, the variability was attributed to the specimen preparation method. A visual observation of the specimen demonstrated segregation of materials during specimen preparation. Several steps were taken to address this issue. The sample preparation method was modified to incorporate a thorough mixing of the materials before and during the specimen preparation. The materials used for each lift was ensured to visually contain a balanced distribution of all aggregates. Aggregate larger than 25.4 mm (1 in.) was also removed from the sample. Each lift was deeply scarified to ensure intimate and seamless contact between each layer.

The other parameter that was studied was the method of compaction – manual (hand) or mechanical (machine). We determined that the two methods provide consistent results as long as the compaction device is routinely and carefully maintained and its cables were stretched properly. After these modifications, another repeatability study was carried out. The specimens prepared using the machine yield similar results with a much smaller coefficient of variation. As is evident in Figure 8, "identical" specimens prepared with precaution yield repeatable results with only one outlier. The coefficient of variation drops from 18% to 9% when the outlier is removed. In summary, these corrective measures not only have significantly improved the repeatability of the seismic tests on base materials, they have also improved the repeatability of the resilient modulus and triaxial tests conducted. Machine compaction is recommended because there is less variation from specimen-to-specimen and operator-to-operator than arises with hand compaction.

The other parameter that should be controlled in this and other tests is the time between the preparation of the specimen and testing. On one hand, the specimen "cures" with time; that is its strength and modulus increases. On the other hand, the specimen "dries out" with time. To minimize the loss of moisture with time, it is essential to cover the specimen as soon as it is prepared. Figure 9 demonstrates the impact of time from specimen preparation on the measured modulus for a sandy material when proper precautions are not taken to minimize moisture loss. As a note, these tests were conducted in El Paso where the relative humidity is normally extremely low (less than

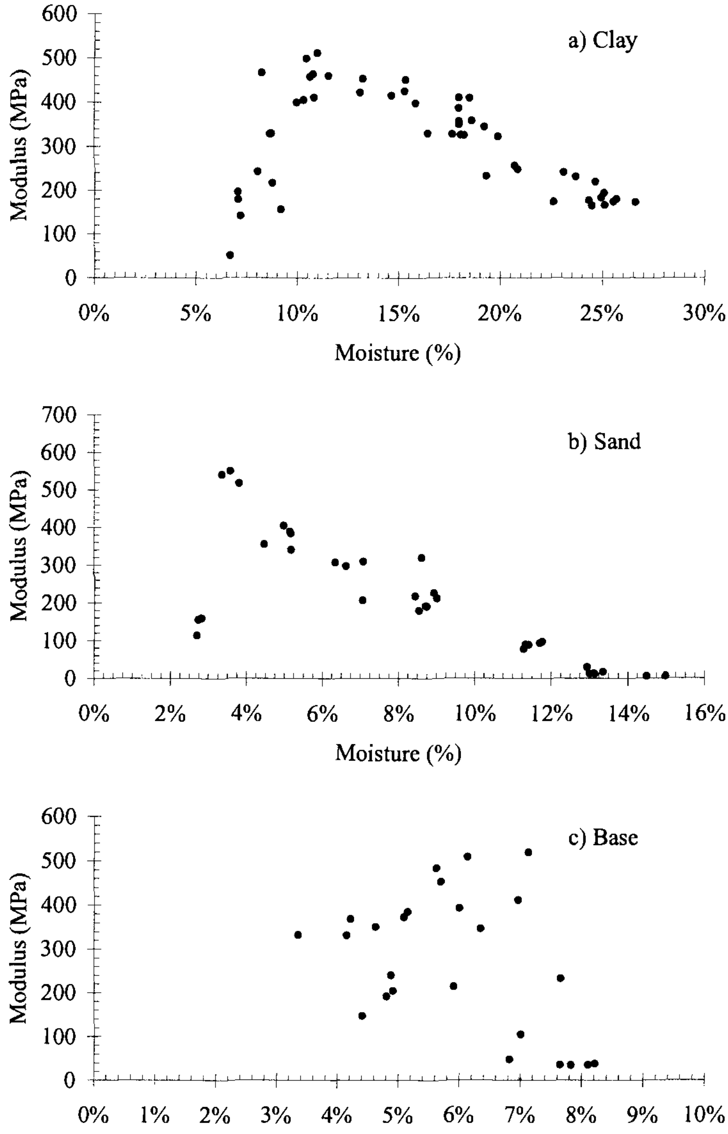


Figure 7 – *Moisture-modulus plots for a) clay, b) sand, and c) base*

15%). The modulus changed from day-to-day in magnitude. Specimens dry of and near the peak on the modulus-moisture curve tended to have moduli that increased slightly as the days progressed. Specimens wet of the peak generally had moduli that decreased slightly or stayed the same with time. With the increase in time between specimen

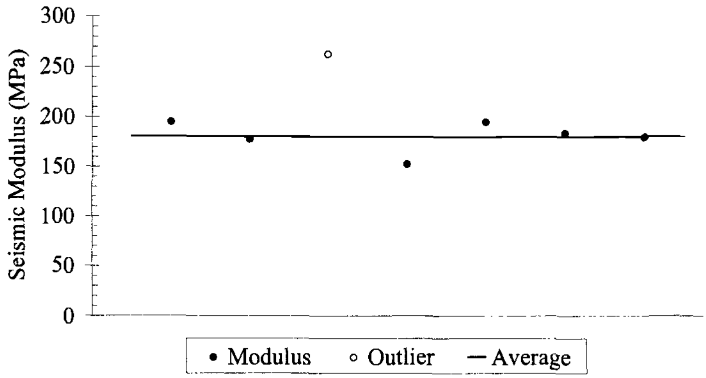


Figure 8 – *Seismic modulus of samples prepared with precautionary measures*

preparation and testing the data became increasingly scattered. For the first 24 hours, similar specimens yield similar moduli. A careful observation of Figure 9 demonstrates that different specimens prepared at similar water content lose moisture at different rates, hence more scatter in the test results. Based on this study, we recommend that either sand specimens be tested about 24 hours after preparation or the specimens be maintained in a manner that the moisture loss is minimal.

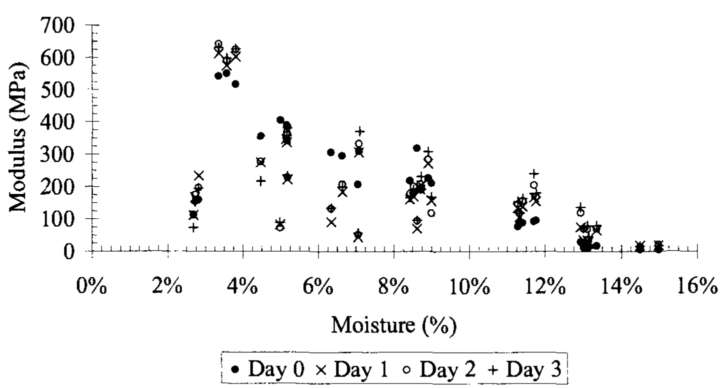


Figure 9 – *Overall modulus-moisture plot for sand material*

A similar experiment was carried out for the clay. Even though not shown here, the clay material can be tested on any day with virtually no difficulties and with relatively small changes in the modulus from day to day as long as it is protected from moisture loss. Over the four days of testing, the modulus changed very little and the data did not scatter for individual specimens.

Under the new specimen preparation protocol, the base became easier to test as the days progressed since the specimen was maturing. The optimum time to test the base material was the first 48 hours after the preparation of the specimen with appropriate attention to minimizing the loss of moisture.

## Relating Seismic Modulus to Other Strength and Stiffness Parameters

One important quality indicator of the materials is the triaxial strength of a material. Nazarian et al. (2002) describe an attempt by a highway agency to relate seismic modulus to the strength of a base material. The variation in compression wave velocity, $V_P$, with the angle of internal friction, $\phi$, is shown in Figure 10.

As Equation 3 indicates, the compression wave velocity and seismic modulus are related through density. Since the compression wave velocity is an independent variable whereas the modulus is related to two independent variables (compression wave velocity and density), it is more desirable to develop correlations based on this parameter. This will eliminate the effects of density when comparing the compression wave velocity to the angle of internal friction. The correlation between these two parameters ($V_P$ and $\phi$) is quite reasonable, especially for stronger bases. Correlations such as the one shown could permit an evolutionary transition from the standard quality control based on moisture-density to a more mechanistic-based approach that takes into account other parameters such as modulus and internal friction.

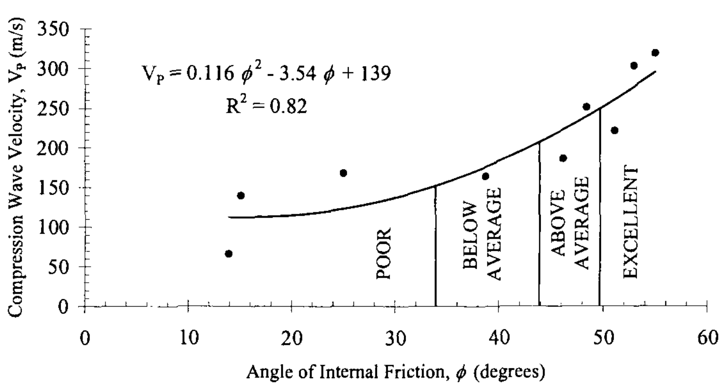


Figure 10 – *Correlation between strength parameter and compression wave velocity of a base from one district*

The resilient and seismic moduli were also compared to develop a model that relates these two tests. A detailed description of process can be found in Williams et al. (2002). For the sake of brevity, we have demonstrated an example. Since the specimens are not subjected to confinement when the seismic test is performed, resilient modulus values for the unconfined test were used in this analysis even though the resilient modulus test was performed at several different confining pressures. The results from tests on about two-dozen soils are shown in Figure 11. The relationship between the two moduli is more or less linear. As indicated before, the unconfined $M_R$ tests were added to the test protocol for this purpose. This does not impact the generality of the resilient modulus data since the constitutive model described in Equation 1, can be used to determine the modulus at any other state of stress. The ratio of seismic modulus to resilient modulus is approximately two to one with an $R^2$ value of about 0.8. Figure 11 contains data from tests on several different materials and material types. The correlation can be improved

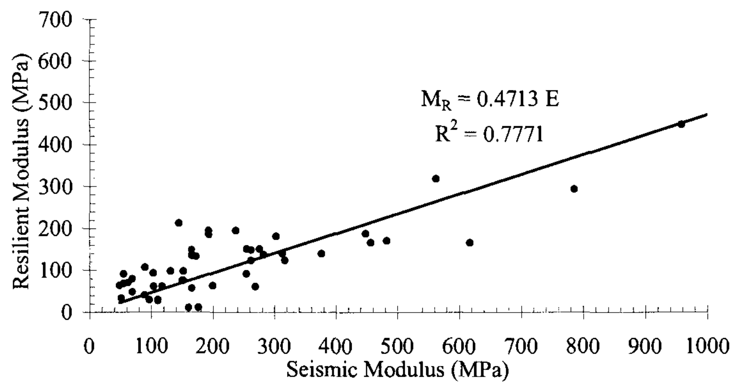


Figure 11 – *Unconfined resilient modulus average vs. seismic modulus*

by developing relationships for individual material types. These methods and other methods can be used to further explore the relationship between the resilient modulus and the seismic modulus, and explored thoroughly in Williams et al. (2002).

## Summary and Conclusions

The seismic modulus test is a rapid and accurate way to determine the modulus of base and subgrade materials. This method will aid in the implementation of a mechanistic pavement design procedure and to move toward performance-based specifications.

In this paper, the seismic modulus test was analyzed under several different conditions and compared with several parameters. The practicality of the test in relation to moisture content, time, and preparation method was examined to determine the best way to perform seismic tests on base and subgrade materials. Furthermore, seismic modulus test data were compared with data from other tests in an attempt to develop correlations among them. The resilient modulus and the angle of internal friction were compared with the seismic test results to show the applications of the seismic test in relation to those tests.

The best test configuration consists of the source within one-third radius of the center. The receiver can be placed anywhere within two-thirds radius of the center if the source is in the center. From testing experience, it is recommended to place the source on the center and one receiver at the center and one at two-thirds radius out for regular testing. In general, it is best to perform seismic tests within 24 hours of preparation, or the specimens should be protected from moisture loss.

The relationship between compression wave velocity from seismic tests and angle of internal friction from triaxial tests is quite reasonable.

A comparison of resilient modulus and seismic modulus shows that the resilient modulus is approximately half of the seismic modulus when data for a number of materials and material types are used. Better relationships can be developed for individual material types.

*Acknowledgments*

The work being reported herein is part of Project 0-1735 funded by the Texas Department of Transportation at the University of Texas at El Paso. The authors would like to offer their sincere appreciation to the Advisory Committee of that Project, especially Steve Smith, Mike Arellano, and Mark McDaniel for their support. We would also like to thank Eddy Rodriguez, Thomas Driscoll, and Pradeep Ghuge for their assistance in data collection and reduction.

**References**

Alexander, D. R., 1996, "In Situ Strength Measurements with Seismic Methods," Report from U. S. Army Engineer Waterways Experiment Station, Vicksburg, Mississippi for the U. S. Air Force Civil Engineering Support Agency, Tyndall AFB, Florida.

Barksdale, R. D., Alba, J., Khosla, P. N., Kim, R., Lambe, P. C., and Rahman, M. S., 1997, "Laboratory Determination of Resilient Modulus for Flexible Pavement Design," Interim Report Project 1-28, Federal Highway Administration, Washington, DC.

Horhota, D. J., 1996, "Evaluation of SASW Test Method for Florida Department of Transportation Applications," Ph.D. Thesis, University of Florida, Gainesville, FL, 444 p.

Ke, L., Nazarian, S., Abdallah, I., and Yuan, D., 2000, "A Sensitivity Study of Parameters Involved in Design with Seismic Moduli," Research Report 1780-2, Center for Highway Materials Research, The University of Texas at El Paso.

Kramer, S. L., 1996, Geotechnical Earthquake Engineering, Prentice Hall, Inc., Upper Saddle River, California.

Nazarian, S., Yuan, D., and Tandon, V., 1999, "Structural Field Testing of Flexible Pavement Layers with Seismic Methods for Quality Control," Transportation Research Record 1654, Washington, DC, pp. 50-60.

Nazarian, S., Yuan, D., and Arellano, M., 2002, "Quality Management of Base and Subgrade Materials with Seismic Methods," Journal of Transportation Research Board Washington, DC, 2002.

Richart Jr., F. E., Woods, R. D., Hall Jr., J. R., 1970, Vibrations of Soils and Foundations, Prentice-Hall, Inc., Englewood Cliffs, New Jersey.

Williams, R. R., Nazarian, S., Yuan, D., 2002, "Methods of Data Analysis for Correlating Resilient Modulus and Seismic Modulus Test Results," submitted to Journal of Materials in Civil Engineering, American Society of Civil Engineers, New York, NY.

Jean-Marie Konrad [1] and Claude Robert[2]

**Resilient Modulus Testing Using Conventional Geotechnical Triaxial Equipment**

---

**Reference:** Konrad, J.-M. and Robert, C., "**Resilient Modulus Testing Using Conventional Geotechnical Triaxial Equipment,**" *Resilient Modulus Testing for Pavement Components, ASTM STP 1437,* G. N. Durham, W. A. Marr, and W. L. De Groff, Eds., ASTM International, West Conshohocken, PA, 2003.

**Abstract:** This paper presents the results of a comprehensive laboratory investigation program on the mechanical properties of an unbound aggregate used in pavement base courses. Repeated load triaxial tests were used to assess the influence of test conditions (specimen size, degree of saturation, pulse loading and loading sequence) on resilient modulus. A conventional triaxial setup, used by most geotechnical laboratories, was adapted for the testing of 100-mm-diameter and 200-mm-high specimens. The material response under a sinusoidal variation of load was compared with the AASHTO procedure on larger samples and different pulse loading. The test program showed that the resilient modulus obtained from the different loading sequences agreed well for given density and moisture content conditions. Conventional triaxial equipment can be used to determine the resilient modulus of unbound aggregates provided accurate displacement gauges are used in the middle-third of the specimen.

**Keywords:** aggregate, base course, triaxial test, repeated loading, resilient modulus

---

[1] Professor, Dept. Civil Engineering, Université Laval, Quebec City, QC, Canada, G1K 7P4.

[2] Project manager and research scientist, Ministry of Transportation of Québec, 2700 Einstein Street, Ste-Foy, QC, Canada, G1P 3W8.

## Introduction

Pavement design requires a knowledge of the material properties of each layer. For the base course material, which is usually a well-graded crushed stone with maximum particle size of about 20 mm, elastic properties may be obtained from repeated load triaxial tests. Several equipment and test procedures have been developed by different countries and there is no standard test or standard procedure to date. In 1989, SHRP introduced a testing procedure for the determination of resilient modulus of base course materials, and a comprehensive comparison and performance of repeated triaxial test equipment for unbound granular material was done by Paute et al. (1996).

A common feature of all these highway-oriented triaxial equipments is the size of the specimen used: 150 mm x 300 mm at the University of Nottingham (UK), 300 mm x 600 mm at the LNEC (Portugal), 160 mm x 320 mm at the LCPC (France), 400 mm x 800 mm at Delft University of Technology and generally 150 mm x 300 mm for the SHRP equipment. Furthermore, most of the laboratories use hydraulic actuators to apply axial loads at frequencies up to 10 Hz.

In view of this brief review of repeated triaxial testing in highway engineering, it became evident that most geotechnical laboratories in Quebec would not be able to purchase equipment capable of using large unbound granular specimens. However, most of these laboratories are well equiped with conventional triaxial systems able to test 100 mm x 200 mm samples. Since the AASHTO triaxial test method recommends a minimum diameter of sample 5 times the maximum aggregate size, 100 mm diameter appears to be sufficiently large to test granular material up to 20 mm maximum aggregate size.

The purpose of this paper is to report the results of a comparative study of triaxial testing on a typical crushed stone used in base courses using a modified conventional triaxial testing equipment developed by the University Laval NSERC research chair (CREIG) and a SHRP equipment available at the ministry of Transportion of Quebec (MTQ).

## Material Tested

A crushed granitic aggregate from the Quebec region , approved for granular material base course, was selected for this study. The aggregate sampled on the quarry stockpile was cut at 20 mm and fractionated in 20/14, 14/10, 10/5, 5/2.5, 2.5/1.25, 1.25/0.63, 0.63/0.315, 0.315/0.16, 0.16/0.08 and passing 0.08 mm. Samples were prepared by recombining the aggregate fractions to meet the average curve of the MG-20 (base course material) specifications of the ministry of Transportation of Quebec (Figure 1).

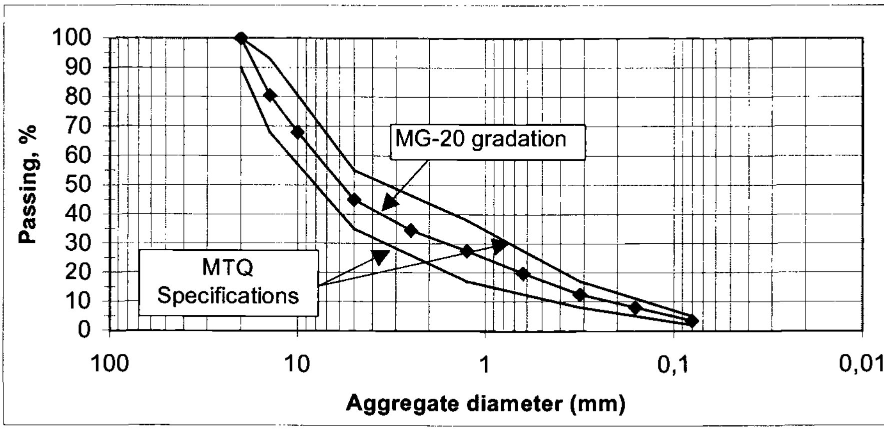


Figure 1 – *Grain size distribution of material tested.*

## Testing Equipment and Experimental Procedure

The testing apparatus used at CREIG is composed of a standard geotechnical triaxial cell and loading frame by Wykeham & Farrance. The cell is designed for cylindrical samples 100 mm in diameter by 200 mm in height.

The apparatus used at MTQ was manufactured by the American firm Structural Behavior Engineering Laboratories, Inc., and is composed of an adapted triaxial cell designed to receive 150-mm-diameter by 300-mm-height sample.

### *Sample Preparation*

Dried aggregates were first recombined from the 10 fractions to meet precisely the gradation of this study. For the conventional triaxial cell, samples were prepared in a cylindrical PVC mould composed of two half cylinders bolted together. The mould is internally lined with a latex membrane which purpose is to facilitate unmoulding and provide protection for a second latex membrane used during triaxial testing.

Samples were compacted in 6 layers using 25 blows of Proctor hammer followed by a vibratory pneumatic hammer. Each layer batch is carefully weighted and the corresponding layer thickness recorded during compaction. Number of blows and time of vibration have been adjusted to reach maximum density as defined by a modified Proctor test. The height of the sample was monitored during compaction. For the SHRP cell, samples were prepared in a metal split mould without latex membrane; the membrane was put on the sample after the extraction from the mould.

## Repeated Loading Tests

For the conventional triaxial equipment, the mechanical loading system of the triaxial frame was locked and vertical cyclic loads were applied to the sample using a pneumatic Bellofram piston. The following configuration was used:

- A 7 cm diameter Bellofram attached to the top of the loading frame. The loading was sinusoidal with a frequency of 0.2 Hz.
- Load measured by a load cell installed inside the triaxial cell.
- Vertical displacements of the sample recorded by 2 LVDTs attached on the sample at mid-height with a recording distance of 100 mm, i.e. about 5 times the maximum grain size. Each LVDT has a stroke of ± 0.5 mm with an accuracy of 0.7 μm as specified by the manufacturer. Actual measurements on calibration dummies indicate a precision of ± 0.5 μm.
- Stress path selected for this study was composed of three levels of axial loading (q = 100, 200 and 280 kPa) and three levels of cell pressure ($\sigma_c'$ = 50, 70 and 120 kPa). For each combination of axial load and confining pressure, deformations were recorded for the last three cycles after 97 load repetitions. All samples were subjected to 1000 initial cycles for conditioning under a cell pressure of 150 kPa and an axial repeated loading of 55 kPa.
- Tests were carried out in the drained mode (bottom and top valves open).

For the SHRP equipment used at the MTQ, the axial stress is applied by a hydraulic servo-system with a function generator capable of applying a Haversine-type pulse in which the signal crest corresponds to the load application time (0.1 seconds), followed by a relaxation period of 0.9 seconds. Vertical displacements were measured by 2 LVDTs attached on either side of the sample to the top platen and the bottom platen. Each LVDT has a stroke of ±2.54 mm with an accuracy of 6.35 μm.

The tests were done in accordance with the AASHTO T 307-99 "Determining the Resilient Modulus of Soils and Aggregate Materials" test method for specimen of Type 1. For each of the five predefined confinement stresses, representing the minor principal stress $\sigma_3$, three different deviator stresses $\sigma_d$ are successively applied to the sample (Table 1). The sum of the principal stresses, refers to as θ in the model K-θ, varied from about 84 kPa to 690 kPa.

Table 1 – *Stresses applied to the sample in the AASHTO T 307-99 test method*

| Confinement stress, $\sigma_3$ (kPa) | Deviator stress, $\sigma_d$ (kPa) | | |
|---|---|---|---|
| 21 | 21 | 41 | 62 |
| 35 | 35 | 69 | 103 |
| 69 | 69 | 138 | 207 |
| 103 | 69 | 103 | 207 |
| 138 | 103 | 138 | 276 |

The sample was subjected to pre-loading of at least 200 cycles under confinement and deviator stresses of 103.4 kPa. For each confinement stress, the axial load is applied for 100 cycles. It is assumed that, beyond the 95th cycle, the soil behavior is practically elastic. Consequently, only the results of the last five cycles are taken into consideration in calculating the resilient modulus. An average value for these last five cycles is used. The lateral deformation of the sample was not measured.

Table 2 summarizes the main differences between both equipments used herein.

Table 2 – *Characteristics of testing equipment used*

| | Equipment SHRP | Equipment CREIG |
|---|---|---|
| Sample diameter | 150 mm | 100 mm |
| Sample height | 300 mm | 200 mm |
| Type of loading | haversine pulse (0.1 second) | sinusoidal wave (5 seconds) |
| Displacement measurement | 2 LVDTs between platens | 2 LVDTs at sample's mid height |

## Test Results

### *Typical Data Using the Conventional Triaxial Cell (CREIG)*

Typical recording from the internal LVDTs presents the axial load versus strain for the last 3 cycles after the 97th load repetition under a maximum deviator stress q = 75 kPa and a constant confining pressure of 50 kPa. The modulus value for these stress conditions was determined from the slope of this q/strain relationship and was 312 MPa and 391 MPa using data from LVDT1 (Figure 2) and LVDT2 (Figure 3), respectively. The modulus of sample 171.1 was thus defined by the average modulus determined from the two LVDT recordings as 351.5 MPa for a mean principal effective stress of 91.6 kPa.

### *Typical Data Using the SHRP Equipment (MTQ)*

With the SHRP equipment, the graph of the axial load versus strain is presented for the last cycle of 100 cycles under a maximum deviator stress q = 85 kPa and a confining pressure $\sigma_3$ = 64 kPa. The modulus values for these stress conditions was 272 Mpa and 454 Mpa using data from LVDT1 (Figure 4) and LVDT2 (Figure 5), respectively. The results obtained with the LVDT2 are explained by a problem of parallelism of the platens. The displacement measured by the LVDT1 reaches 0.085 mm, a higher value than the one measured at mid-height of the sample by CREIG. The average modulus measured by

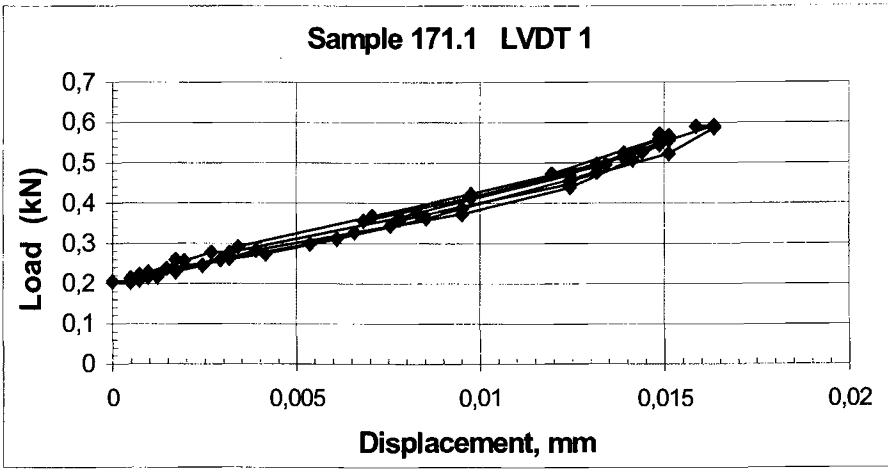


Figure 2 – *Typical data obtained from LVDT 1, for sample 171.1 with a confining pressure of 50 kPa and dry density of 2250 kg/m*$^3$.

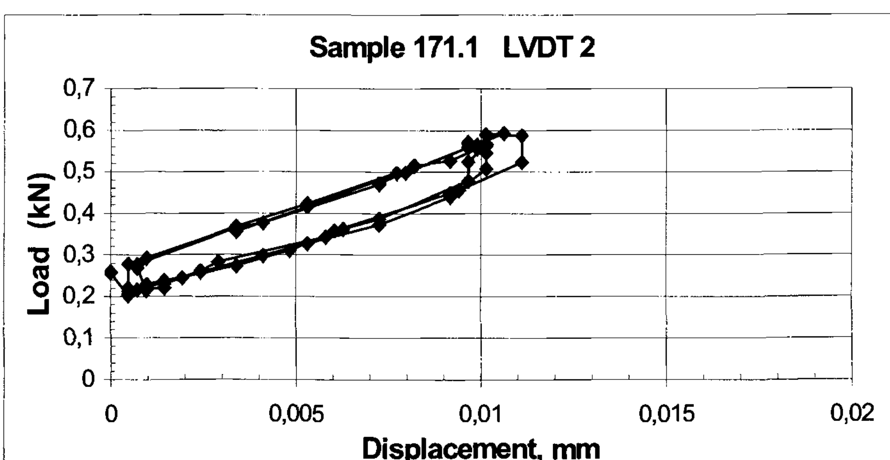


Figure 3 – *Typical data obtained from LVDT 2, for sample 171.1 with a confining pressure of 50 kPa and a dry density of 2250 kg/m*$^3$.

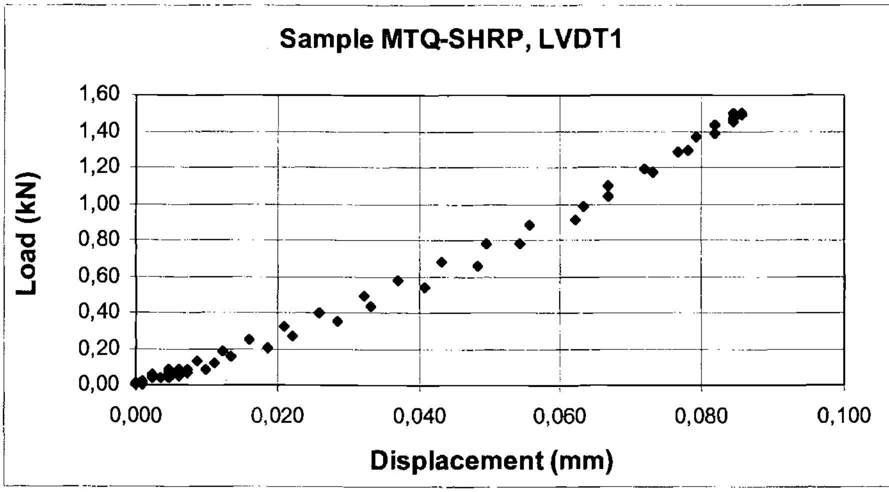


Figure 4 – *Measurement of the axial deformation obtained from LVDT 1, for the sample MTQ-SHRP with a confining pressure of 64 kPa and a dry density of 2260 kg/m³.*

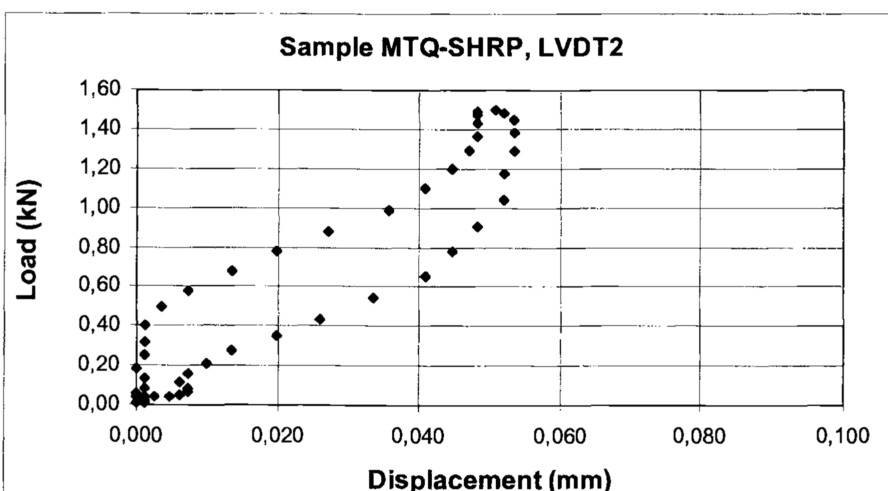


Figure 5 – *Measurement of the axial deformation obtained from LVDT 2, for the sample MTQ-SHRP with a confining pressure of 64 kPa and a dry density of 2260 kg/m³.*

MTQ is 363 Mpa, a value higher than the modulus of CREIG, for a slightly higher stress level.

The values of the resilient modulus are presented versus the sum of principal stresses, and fitted based on the K-θ model (Figure 6). This graph allows to see that the results obtained for low stress levels must be excluded because the values of the modulus are not in accordance with the other values obtained at higher stress levels. At low stress levels, the LVDTs are maybe not enough accurate to measure small strains. The values obtained by the LVDTs are not realistic values, and lead to an overestimation of the resilient modulus.

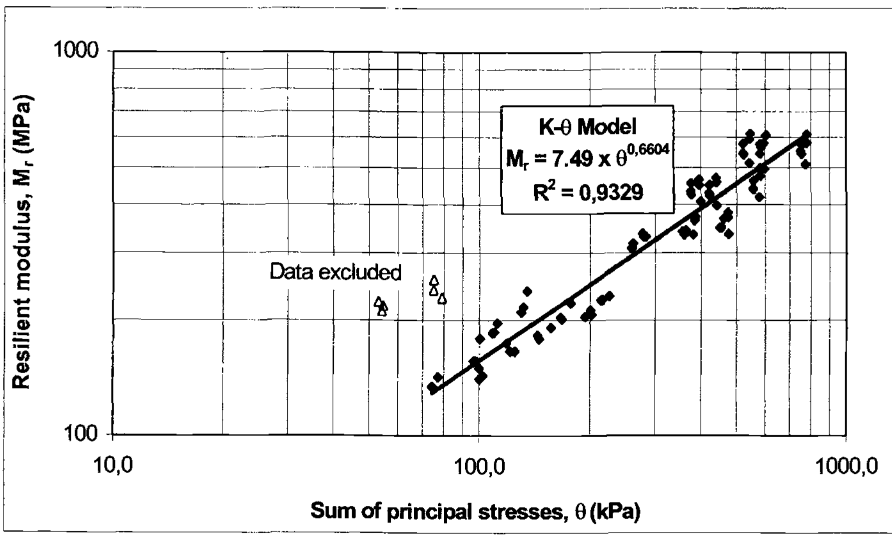


Figure 6 – *Resilient modulus values of MG-20 aggregate material, obtained with SHRP equipment according to the AASHTO T 307-99 test method.*

**Comparison of Results**

The resilient modulus values obtained from the data with the conventional CREIG triaxial equipment are compared with those obtained from the MTQ SHRP equipment (Figure 7). The resilient modulus data were plotted against the mean effective stress $p' = (\sigma'_1+2\sigma'_3)/3$ for samples compacted at different densities. In the CREIG cell, Mr values were obtained for three different dry density values of 2160, 2210 and 2250 kg/m$^3$ respectively, while the samples prepared for the SHRP equipment had a dry density of 2260 kg/m$^3$. As anticipated, resilient moduli of base course materials increase with increasing density and mean stress. Close examination of the data for samples at about the same density (2250 kg/m$^3$ for CREIG and 2260 kg/m$^3$ for MTQ-SHRP) reveals that the resilient moduli obtained with the convential triaxial equipment used by CREIG are about 1.2 to 1.5 times higher than those obtained on the same soil using the MTQ-SHRP equipment. However, in both cases, Mr increases with increasing stress level at about the same rate. Mohammed et al. (1994) observed that the values of resilient modulus measured at mid-third of the sample are 1.1 to 1.2 times higher than the values obtained with the measures of the displacements between the end platens.

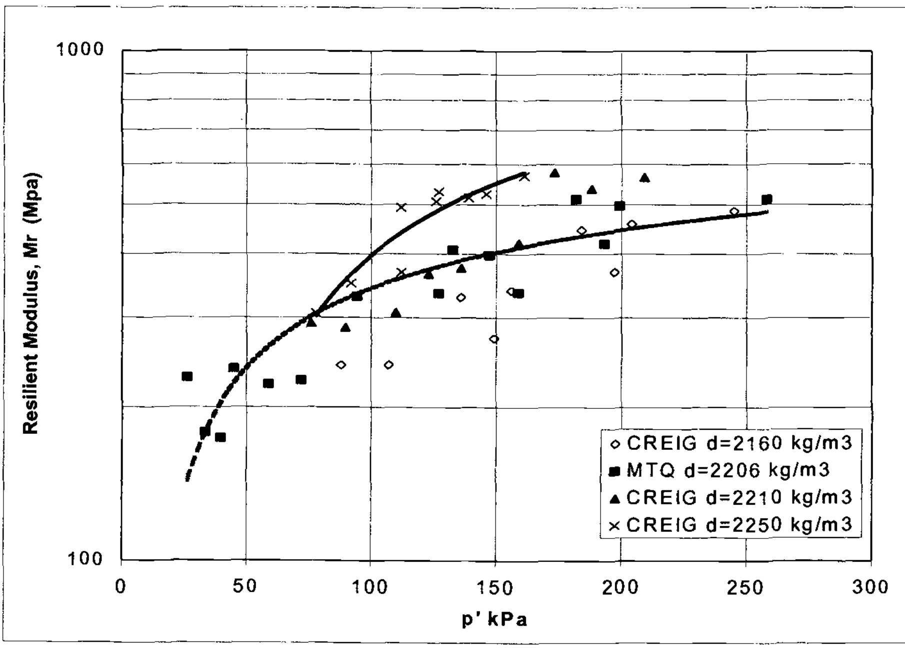


Figure 7 – *Resilient modulus values for MG-20 at different dry densities.*

## Discussion

This section provides some valuable insight into why there is a lot of scatter on the low strain results for stiff samples. It is well known that the stiffness parameters measured in the laboratory depend on many factors including : the fabric of the sample, the loading path and rate of testing, as well as location and performance of instruments. Major sources of error in the measurement of stiffness in triaxial tests can be associated with seating errors and misalignments of the loading ram with the top platen (Baldi et al. 1988). These errors can be minimised by using local gauges attached to the sample (Jardine et al. 1984). The use of displacement transducers between the platens as presently done by the MTQ procedure leads to an overestimation of the soil strain, hence an underestimation of the resilient modulus for a given stress condition. Furthermore, it must be emphasized that the actual AASHTO loading procedure may also result in strains too low to be accurately measured by LVDTs which have a stroke that is too large in order to accomodate the displacements between platens distant of 300 mm. For instance, consider a base course material with a resilient modulus value of 250 MPa subjected to a vertical stress of 25 kPa, the resulting axial strain would be 0.01% and the actual displacement 0.03000 mm. Considering that the stroke of the LVDT in the SHRP equipment is ±2.5 mm with a linearity of ± 0.25%, the precision of the LVDT of ± 0.00625 mm may not provide sufficient accuracy for the determination of resilient modulus at low stress levels. For the same granular material in the CREIG set-up, the actual displacement between the rings attached to the sample would be 0.01 mm which can be accurately measured using the 0.5 mm stroke LVDT since its precision is ± 0.5 μm.

## Conclusion

A comparative study of repeated triaxial loading using two different equipments and procedures was undertaken to validate the use of a conventional triaxial equipment using 100 mm x 200 mm samples for the determination of resilient modulus for unbound granular base course materials. The study led to the following conclusions:

- Axial strain must be measured with displacement gauges attached to the sample, usually over the middle third, at least over a diameter length.
- Displacement gauges need to be accurate enough to record the desired small strains for the lowest load level. Small samples require therefore relatively accurate displacement gauges.
- Reducing the frequency of loading permits to increase the accuracy of measurements, especially at low stress levels.
- Provided special attention is paid to these basic requirements, it was shown that conventional triaxial equipment with 100 mm x 200 mm samples are adequate to provide resilient modulus values for unbound granular materials.
- Modifications might be brought about the AASHTO T 307-99 test method to get accurate values of resilient modulus of granular materials, especially concerning the location of the LVDTs and to eliminate the lower stress levels.

*Acknowledgements*

This research work was funded through the NSERC industrial chair and its 22 partners, particularly the ministry of Transportation of Quebec. The authors want to express their appreciation to Mr. Nelson Dubé from the MTQ, and Mr. François Gilbert from University Laval for his assistance in instrumentation with both the repeated load and static triaxial tests.

**References**

Baldi, G., Hight, D. and Thomas, G. E., 1988, A Re-evaluation of Conventional Triaxial Test Methods, *In Advanced Triaxial Testing of Soil and Rock, ASTM STP 977*, pp 219-263.

Jardine, R. J., Symes, M. and Burland, J.B., 1984, The Measurement of Soil Stiffness in The Triaxial Apparatus, *Géotechnique* 34, No 3, pp 323-340.

Mohammed, L. N., Puppala, A. J. and Alavilli, P., 1994, Influence of Testing Procedure and LVDT Location on Resilient Modulus of Soils, *Transportation Research Record 1462*, Transportation Research Board, National Research Council, Washington, D.C., pp 91-101.

Paute, J.-L., Dawson, A. R., Galjaard, P. J., 1996, Recommendations for Repeated Load Triaxial Test Equipment and Procedure for Unbound Granular Materials, *Flexible Pavements*, Gomes Correia (ed.) Balkema, Rotterdam.

Richard L. Boudreau[1] and Jianren Wang[2]

# Resilient Modulus Test – Triaxial Cell Interaction

**REFERENCE:** Boudreau, R. L. and Wang, J., "**Resilient Modulus Test – Triaxial Cell Interaction,**" *Resilient Modulus Testing for Pavement Components, ASTM STP 1437*, G. N. Durham, W. A. Marr, and W. L. De Groff, Eds., ASTM International, West Conshohocken, PA, 2003.

**ABSTRACT:** During developmental work by the Strategic Highway Research Program (SHRP, 1987-1992) and the Federal Highway Administration (FHWA, 1993-present), it was recommended that knowledge and assessment of triaxial equipment and sample interaction be correctly applied to both test command and data reduction routines for the accurate measurement of resilient modulus properties of unbound materials using external instrumentation configuration. This concern is briefly addressed in the American Association of State Highway and Transportation Officials (AASHTO) test method T307-99, under paragraph 8.3.2.1. The paragraph refers only to calculations necessary to correct for the proper magnitudes of seating load based on known properties of the triaxial cell. The method does not contain information describing the methods and calculations needed to consider these parameters in the data reduction portion of the test. Further, the test method does not address other influences unique to a triaxial testing cell, namely frictional forces resulting from poorly manufactured or improperly designed seals, alignment issues and compliance.

This paper addresses the sensitivities of the results due to appropriate and inappropriate interpretation of the correction factors necessary, as well as influences of seal drag forces. The sensitivities have been calculated for two specific triaxial cells. Note that each triaxial cell and instrumentation configuration possesses unique values needed for the correction. Generally, the larger the triaxial cell (larger rod diameter, larger mass of rod), the greater the influences of the uplift and static weight components of load.

Users must be knowledgeable about their test equipment and the ability of the software to correctly apply proper loads and properly assess these loads for the correct calculation of resilient modulus. Further, physical tolerances must be developed for triaxial cells with respect to seal drag, alignment and compliance. These issues are extremely important when comparing results between laboratories, as the errors associated with miscalculation, misinterpretation or incorrect measurement of loads can result in variations outside the precision of the test itself.

**KEYWORDS:** resilient modulus, triaxial test, seal drag, compliance, subgrade

[1] President, Boudreau Engineering, Inc., 5392 Blue Iris Court, Norcross, GA 30092.
[2] Branch Manager, GeoTesting of GA, 2658 Holcomb Bridge Rd., Alpharetta, GA, 30022.

## Introduction

As the much-anticipated release of the 2002 Pavement Design Guideline draws near, many State Departments of Transportation have begun the implementation phase of laboratory resilient modulus testing. Results of the resilient modulus test will most certainly be utilized in the design methodologies contained in this new guideline. The use is anticipated in the form of stiffness characterization for unbound materials (i.e., subgrade soils and aggregate base/subbase materials).

The current and perhaps most accepted and widespread test method, AASHTO T-307, has been adopted by AASHTO following numerous years of modifications and production-level work as part of the Strategic Highway Research Program (SHRP) and Federal Highway Administration's (FHWA) Long Term Pavement Performance (LTPP) study. The primary objective in developing an accepted test method was to provide a relatively simple, useable, precise, repeatable, reproducible and productive test.

Although the test method provides for a uniform methodology in which to measure load and deformation (stress and resilient strain behavior), it is recognized as an extremely sensitive test, measuring relatively small strain magnitudes at low to moderate stress levels. To this end, the method falls short in recognizing certain influences of equipment variables that could lead to precision errors that will in turn lead to biased results. Some of the precision errors are small, while others could be significant.

## Historical Development

Since 1944, when the Federal-Aid Highway Act created a blueprint for a 40 000-mile "National System of Highways," significant developments have been achieved with respect to the structural design of pavements. The primary intent of this blueprint was and still remains the fundamental concept of providing and promoting a uniform means to design pavements. The first significant achievement included an empirical-based design methodology derived primarily from data obtained at the AASHO Road Test in the late 1950s.

As our industry has evolved, the process of pavement design has advanced. The 1986 AASHTO Pavement Design Guide provided a mechanistic-empirical basis for the design of pavement structures. This guide required the use of resilient modulus in place of soil support as the primary input for subgrade. Advances made in technology and knowledge gained primarily through research allowed this parameter to be directly measured in the laboratory; however, very few laboratories acquired the capability to conduct the test, relying on correlations to derive resilient modulus from other more common soil properties.

The first standardized test method to measure the resilient modulus properties of soil was AASHTO Test Method T-274. When SHRP began the 20-year LTPP effort in 1987, this method was used as the foundation that created SHRP Test Protocol P46. The primary objective of this protocol was to provide for a standardized method that could be performed easily, with a high degree of productivity and precision. The decision to measure load and deflection outside the chamber was made primarily to promote the productivity aspect of the objective.

During the work conducted by SHRP, numerous attempts were made to measure the quality of data being measured at the contracted laboratories. The first effort was to administer a round-robin proficiency test program. Numerous laboratories volunteered for this effort, which included laboratories from academia, DOT, industry and private test labs. Cylindrical test specimens comprised of materials ranging from extruded urethanes, teflons and nylons were sent to participating laboratories, and results were examined by the program administrator.

The data obtained from these early rounds of testing were widely scattered. Under close examination, numerous problems existed, both with the test procedure as well as with the specimens utilized. First, it was recognized that, by developing a static stiffness envelope for each material, a minimum stiffness threshold could be realized. Data provided by laboratories furnishing dynamic stiffness values less than these minimum threshold values could be eliminated. Still, the variability in data from labs that were not eliminated was still unacceptable. Many of the participating laboratories were utilizing antiquated equipment using "black-box" software, could not demonstrate waveform control, and even misinterpreted the intent of deviator stress. The misinterpretation of stress levels required to apply to the test specimen, and how to calculate the measured response load magnitude for resilient modulus resulted in an inherent 20 percent error of the result.

Following the evaluation of the synthetic round-robin testing, the LTPP Team included a graph in Protocol P46 illustrating seating loads, cyclic loads and haversine shape, in an effort to minimize errors associated with misinterpretation. In addition, the Team recognized certain influences that act on the rod of the triaxial cell. Because of the external mounting of the system load cell, knowledge and compensation is required for both the static weight of the load rod and deformation measurement assembly above the test specimen as well as the uplift forces caused by the confining pressure applied to the test specimen, which act on the cross-sectional area of the load rod. Neglected was the measurement or understanding of the influence of seal drag, alignment and triaxial cell compliance on the results.

## Objectives

This paper examines the influences of the parameters that may affect the resilient modulus results derived from actual test measurements made in various triaxial chambers. An understanding of these influences should be considered in any future modification of a standardized test method. These influences may better enable a potential user, test operator or even software designer a quick enlightenment and appreciation for variables that can be better specified or controlled in order to minimize or eliminate variations of results that are not considered material variations (i.e., mineralogy, density, moisture content).

The primary goal of this paper is to heighten awareness that a tightly controlled tolerance for triaxial test equipment is necessary. This necessity pertains to external instrumentation, which represents a secondary goal. With the development of the stated triaxial cell tolerances, the authors anticipate that the test standard will be capable of providing results with a high degree of precision and productivity, both essential for the ultimate acceptance of the standard. Recognizing that internal instrumentation may alleviate or minimize these influences, this mode of instrumentation is much more difficult than the external instrumentation configuration, thus a trade off for higher precision while sacrificing productivity (and cost) should be examined. Additionally, if backpressure saturation becomes important, internal instrumentation may not be an option. By eliminating variables that contribute to result variations, our industry should be capable of providing and promoting a more uniform and productive standardized test method with an acceptable precision and bias.

**Influencing Factors**

Many factors are known to influence the resilient behavior of soils. These factors can be broadly categorized as material variables and equipment variables. Material variables may include such items as the geological makeup, density level, moisture content and compaction methodology of the test specimen. These variables can be controlled to a predetermined value and tolerance. Equipment variables are less known as to their affects on resilient modulus values. These factors include load waveform shape, duration, frequency (each of which can be controlled), test operator and other specific equipment variables.

The specific equipment variables consist of the test system, the electronic transducers (load cell and linear variable deflection transducers or LVDTs), and the triaxial cell. In addition, proper quality management including equipment calibration and software verification and validation is important in the resilient modulus testing process.

If two laboratories remold a soil obtained by splitting a bulk sample, each lab would expect to get the same result, when testing in accordance with AASHTO T-307. Let us assume that both laboratories produced the remolded test specimens to yield the exact same density and moisture content, using the same compactive effort and methodology to achieve the density. First, how close should the answer be to consider both labs equal? Unfortunately, we do not know what the tolerance or anticipated difference should be. Secondly, if the labs produce values that are significantly different, which lab, if either, has produced the correct result? Unfortunately, this is the scenario that develops each time a round-robin program is initiated.

There is no simple, inexpensive answer to these questions. The short answer is that both laboratories should be fully evaluated for proper implementation of their respective resilient modulus test systems, its components, the proper application of the test method, and the correct processing of the acquired data resulting from the test.

The current test procedure, AASHTO T-307, contains provisions that provide control tolerances on material variables and some of the equipment variables (limited to accuracy and precision of the electronic transducers). In addition, a report (Alavi 1997) addresses the integrated function of the system and software. Neither of these references adequately address the variables associated with the triaxial chamber used to test the specimen. A provision included in T-307 (paragraph 8.3.2.1) recognizes certain influences acting on the triaxial chamber's load rod. This provision requires that adjustments be made to account for both the static weight of the rod and deformation measurement system as well as the uplift force on the load rod due to the confining pressure applied within the triaxial cell. This provision is not restated anywhere in the standard that would require that this adjustment be accounted for again during data reduction and reporting. Further, neither of the references addresses influences of seal drag forces, alignment of top and bottom platens, or system compliance.

The purpose of the triaxial chamber is two-fold: first to properly align the cylindrical sample under the axially applied load, and second to allow a constant application of confining pressure to be held during the repeated loading portions of the test. In order to meet both of these objectives, a load rod is extended from the outside of the chamber, though a collar housing linear Thompson ball bushings, to the sample loading cap or top platen. The Thompson ball bushing keeps the system properly aligned throughout the testing sequences. This bushing allows for very minute lateral or horizontal movement while allowing the rod to move freely in the vertical direction with negligible load. In order to provide for constant confining pressure, the load rod must be sealed inside the chamber so as to not allow leakage through the collar housing. This is typically achieved using a lip seal, o-ring seal or other type of seal.

That said, if two or more individual laboratories were fully evaluated for their respective systems, then tested splits of the same bulk soil as before, would we expect them to get the same result? Maybe not. Remember, none of the laboratories would have had their respective triaxial cell measured for the amount of seal friction, alignment of top and bottom platens or system compliance. There currently is no specification that would limit the seal drag force, the allowable eccentricity of the top and bottom platen or allowable system compliance of the triaxial cell, thus an examination of how these factors may affect the results is worthwhile.

**Sensitivity of Variables**

In order to understand and appreciate the potential sensitivities of these triaxial chamber influences, an attempt to illustrate and compare data for actual or theoretical tests has been performed. Breaking the resilient modulus down to its most basic form is necessary.

$$M_r = \sigma/\varepsilon_r, \quad \text{or} \quad (P/A)/(\Delta_r/L) \tag{1}$$

where:
$M_r$ = resilient modulus, psi
$\sigma$ = cyclic stress, psi
$\varepsilon_r$ = recoverable strain, in./in.
$P$ = applied cyclic load, lb
$A$ = specimen cross sectional area, in.$^2$
$\Delta_r$ = recoverable deformation, in.
$L$ = specimen height, in.

*Uplifting Force*

Failure to account for and adjust the static weight and uplift forces acting on the load rod would be expected to only affect the P term shown in Equation 1. These effects, however, only apply to the seating load prior to the application of cyclic load. Thus, they will never enter the equation to affect the resulting resilient modulus. If the influences are significant (i.e., a rod which weighs 12 to 15 lb, and is 1 to 1.5 inches in diameter), this could result in a specimen that has an excessive amount of seating load (or overburden pressure), which may in turn slightly 'stiffen' a sample prior to the repeated load portion of the test. Worse yet, in some instances the loading requirement may be such that the load rod looses contact with the top platen if the static weight of the rod and uplift force is not properly accounted for. This will most certainly result in erroneous deformation measurements. Future modifications to a standardized test method should emphasis this issue to ensure proper amounts of seating load are applied regardless of cell properties.

*Seal Drag*

In a similar manner, one can predict the effects or even accurately measure the effects of resilient modulus values tested in a triaxial cell that exhibit some magnitude of seal drag. An experiment was performed utilizing two different triaxial chambers, identified as Cell A and Cell B. First, each chamber was instrumented such that the amount of seal drag could be measured, as shown in Figure 1.

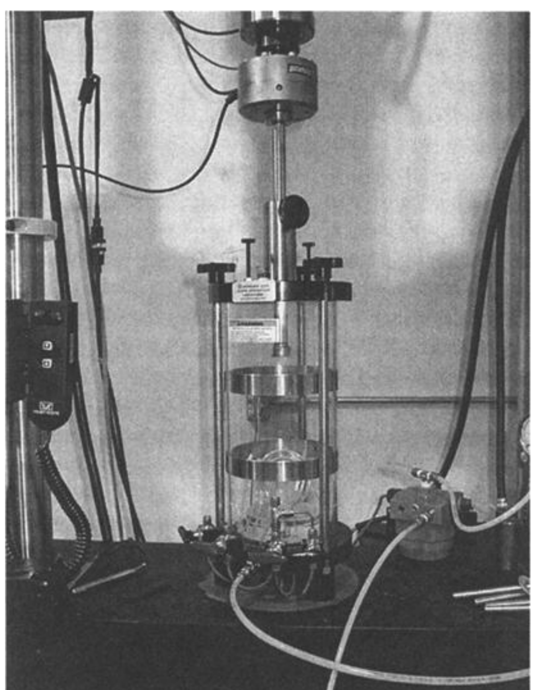

FIG. 1—*Configuration of seal drag test.*

The seal drag was measured by installing each triaxial cell without a specimen, with the load rod threaded tightly to the bottom of the actuator-mounted load cell. Testing was performed with each triaxial cell pressurized to 0, 2, 4 and 6 psi of compressed air using 1, 5 and 10 mils (1mil = 0.001 inch) of controlled movement at each level of air pressure.

Load readings were measured during pulse deformations (deformation amplitude waveform control, 0.1 sec loading followed by 0.9 sec rest period).

Recognizing the potential for inertia resulting from the load cell mass rapidly moving up and down when attached to the moving actuator, a preliminary effort was made to measure this force. This was accomplished by attaching the triaxial cell load rod to the load cell without the triaxial cell assembled. Although some amount of inertia force was measured, the system utilized – Instron 8502/8800 Series Controller – contains an internally-mounted accelerometer in the load cell, which is integrated in the system's feedback capability, thus the inertia affects are automatically compensated.

Cell A was measured to have approximately 0.5lb of friction while Cell B had slightly more than 2lb of friction.

Once the amount of frictional forces was determined for each triaxial chamber, an experiment was performed on an A-4 soil from Georgia. Nineteen test specimens were replicated to nearly the same remolded values of 95 percent of the material's maximum standard dry density at optimum moisture, and tested per AASHTO T-307 in Cell A. The triaxial cell configuration for the tests performed in Cell A is shown in Figure 2.

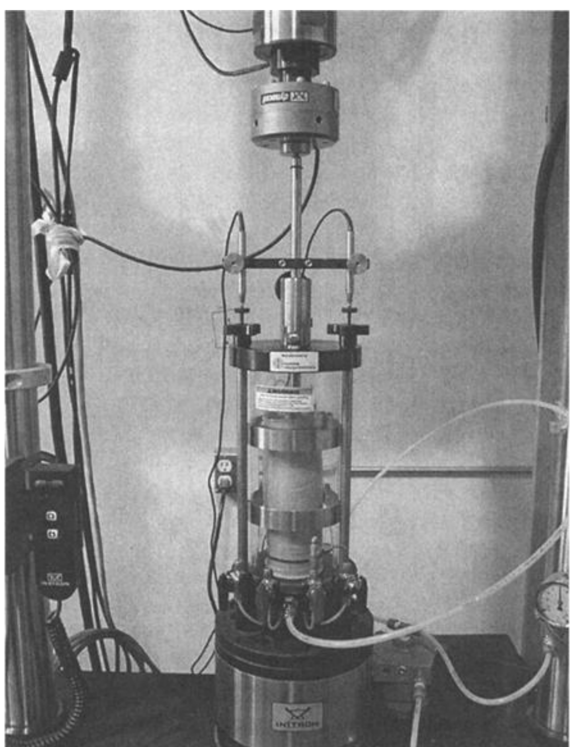

FIG. 2—*Triaxial cell configuration*

The stress level targets presented in Table 1 of AASHTO T307 are nominal levels suggested to achieve. This table consists of 15 different combinations of cyclic axial stress and confining pressure, each combination referred to as a sequence. It would be hard to believe that these targets could be exactly matched between command and feedback signals. Because of the difficulty in achieving precise feedback, a constitutive model is necessary in order to compare results of tests. The constitutive model used in this study is that which was first introduced by SHRP in the early 1990's:

$$M_r = K1 S_C^{K2} S_3^{K5} \tag{2}$$

where
$M_r$ = resilient modulus, psi
$S_C$ = cyclic stress, psi
$S_3$ = confining pressure, psi
K1, K2 and K5 = nonlinear elastic regression coefficient/exponents

Results of the testing following the regression of data from each specimen to fit the constitutive model are provided in Table 1. In order to compute the regression constant and coefficients, the dependent variable, $M_r$ and independent variables $S_C$ and $S_3$ must first be transformed to a $Log_{10}$ base. This allows a linear regression to be performed. Once completed, the y-intercept is used as a 10-base exponential to derive the K1 constant, while the K2 and K5 coefficients are used as exponentials in Equation 2.

TABLE 1—*Nonlinear elastic coefficient/exponents.*

| | Regression Coefficients | | | |
|---|---|---|---|---|
| Sample No. | K1 | K2 | K5 | $R^2$ |
| 1 | 7 515 | -0.17220 | 0.21615 | 0.98 |
| 2 | 7 922 | -0.18555 | 0.22319 | 0.98 |
| 3 | 7 762 | -0.18606 | 0.21680 | 0.98 |
| 4 | 7 898 | -0.19693 | 0.24964 | 0.99 |
| 5 | 7 859 | -0.18428 | 0.25522 | 0.99 |
| 6 | 8 321 | -0.19894 | 0.23261 | 0.99 |
| 7 | 7 905 | -0.20854 | 0.25953 | 0.99 |
| 8 | 7 872 | -0.22103 | 0.26367 | 0.98 |
| 9 | 8 178 | -0.19842 | 0.25590 | 0.99 |
| 10 | 7 938 | -0.21171 | 0.23770 | 0.99 |
| 11 | 6 956 | -0.21025 | 0.30340 | 0.99 |
| 12 | 7 775 | -0.20790 | 0.25843 | 0.99 |
| 13 | 8 484 | -0.21230 | 0.23373 | 0.99 |
| 14 | 8 118 | -0.20199 | 0.23251 | 0.98 |
| 15 | 7 592 | -0.20140 | 0.25691 | 0.98 |
| 16 | 7 911 | -0.22068 | 0.25496 | 0.99 |
| 17 | 7 904 | -0.20062 | 0.27061 | 0.99 |
| 18 | 7 597 | -0.21391 | 0.26113 | 0.99 |
| 19 | 7 468 | -0.21679 | 0.26751 | 0.99 |

The constitutive model selected provides an excellent fit for the data, as can be observed by the multiple-correlation coefficient, $R^2$. Although the regression constant, K1, and the coefficients, K2 and K5, seem to be quite variable for supposedly replicated specimens, there is no conclusive evidence of precision and bias that would indicate how much variability is acceptable.

Once satisfied that the constitutive model (Equation 1) was reasonable based on the good $R^2$, the results for each test specimen were calculated or predicted for resilient modulus at the exact stresses for each of the 15 sequences tested. This is done for the purpose of examining the differences in resilient modulus values from sample to sample or collectively as a group of replicated specimens.

As an illustration of importance, a test performed on a specimen targeted for a cyclic stress of 6 psi at a confining pressure of 4 psi (sequence number 8 of 15) may have achieved a cyclic stress of 5.75 psi, whereas another sample tested at the same targets may have achieved only a 5.4 psi value. If the material is sensitive to stress (stress dependent), comparing the raw resilient modulus values will not be ideal, or appropriate.

Table 2 presents the calculated resilient modulus values of each specimen tested at each of the 15 sequences. Summary information consisting of average, standard deviation, coefficient of variation and number of tests or observations are provided for each of the 15 sequences (table columns).

TABLE 2—*Estimated resilient modulus data.*

| Sample | Resilient Modulus (predicted by Constitutive Model at each test loading sequence), psi | | | | | | | | | | | | | | |
|---|---|---|---|---|---|---|---|---|---|---|---|---|---|---|---|
| No. | 1 | 2 | 3 | 4 | 5 | 6 | 7 | 8 | 9 | 10 | 11 | 12 | 13 | 14 | 15 |
| 1 | 9,824 | 8,719 | 8,131 | 7,738 | 7,446 | 9,000 | 7,987 | 7,448 | 7,088 | 6,821 | 7,747 | 6,876 | 6,412 | 6,102 | 5,872 |
| 2 | 10,391 | 9,137 | 8,475 | 8,034 | 7,708 | 9,492 | 8,346 | 7,741 | 7,339 | 7,041 | 8,131 | 7,150 | 6,632 | 6,287 | 6,032 |
| 3 | 10,062 | 8,844 | 8,202 | 7,774 | 7,458 | 9,215 | 8,100 | 7,511 | 7,120 | 6,830 | 7,929 | 6,970 | 6,463 | 6,126 | 5,877 |
| 4 | 10,777 | 9,402 | 8,680 | 8,202 | 7,850 | 9,739 | 8,497 | 7,845 | 7,413 | 7,094 | 8,192 | 7,147 | 6,598 | 6,235 | 5,967 |
| 5 | 10,927 | 9,617 | 8,924 | 8,463 | 8,122 | 9,853 | 8,671 | 8,047 | 7,631 | 7,324 | 8,255 | 7,265 | 6,742 | 6,394 | 6,136 |
| 6 | 10,998 | 9,581 | 8,838 | 8,347 | 7,984 | 10,008 | 8,719 | 8,043 | 7,596 | 7,266 | 8,517 | 7,420 | 6,845 | 6,465 | 6,184 |
| 7 | 10,891 | 9,425 | 8,661 | 8,157 | 7,786 | 9,803 | 8,484 | 7,796 | 7,342 | 7,008 | 8,189 | 7,087 | 6,513 | 6,133 | 5,854 |
| 8 | 10,832 | 9,294 | 8,497 | 7,974 | 7,590 | 9,734 | 8,351 | 7,635 | 7,165 | 6,820 | 8,108 | 6,956 | 6,360 | 5,968 | 5,681 |
| 9 | 11,273 | 9,825 | 9,065 | 8,562 | 8,191 | 10,162 | 8,856 | 8,172 | 7,718 | 7,384 | 8,510 | 7,417 | 6,844 | 6,464 | 6,184 |
| 10 | 10,494 | 9,062 | 8,316 | 7,825 | 7,464 | 9,530 | 8,229 | 7,552 | 7,106 | 6,778 | 8,082 | 6,979 | 6,405 | 6,027 | 5,749 |
| 11 | 10,355 | 8,951 | 8,219 | 7,737 | 7,382 | 9,157 | 7,915 | 7,268 | 6,841 | 6,528 | 7,420 | 6,414 | 5,890 | 5,544 | 5,290 |
| 12 | 10,696 | 9,260 | 8,512 | 8,018 | 7,654 | 9,632 | 8,339 | 7,665 | 7,220 | 6,893 | 8,052 | 6,972 | 6,408 | 6,036 | 5,762 |
| 13 | 11,132 | 9,609 | 8,816 | 8,294 | 7,910 | 10,125 | 8,740 | 8,019 | 7,544 | 7,195 | 8,611 | 7,433 | 6,820 | 6,416 | 6,119 |
| 14 | 10,705 | 9,306 | 8,574 | 8,090 | 7,734 | 9,742 | 8,469 | 7,803 | 7,362 | 7,038 | 8,292 | 7,208 | 6,641 | 6,267 | 5,990 |
| 15 | 10,463 | 9,099 | 8,386 | 7,914 | 7,566 | 9,428 | 8,199 | 7,556 | 7,131 | 6,818 | 7,890 | 6,862 | 6,324 | 5,968 | 5,706 |
| 16 | 10,720 | 9,200 | 8,412 | 7,895 | 7,515 | 9,667 | 8,296 | 7,586 | 7,119 | 6,777 | 8,101 | 6,952 | 6,357 | 5,966 | 5,679 |
| 17 | 11,169 | 9,719 | 8,960 | 8,458 | 8,087 | 10,009 | 8,709 | 8,029 | 7,579 | 7,247 | 8,297 | 7,220 | 6,656 | 6,282 | 6,007 |
| 18 | 10,458 | 9,017 | 8,268 | 7,774 | 7,412 | 9,407 | 8,111 | 7,437 | 6,993 | 6,667 | 7,850 | 6,768 | 6,206 | 5,835 | 5,563 |
| 19 | 10,378 | 8,930 | 8,178 | 7,684 | 7,321 | 9,311 | 8,012 | 7,338 | 6,894 | 6,569 | 7,735 | 6,656 | 6,096 | 5,727 | 5,457 |
| avg. | 10,660 | 9,263 | 8,532 | 8,049 | 7,694 | 9,632 | 8,370 | 7,710 | 7,274 | 6,953 | 8,101 | 7,040 | 6,485 | 6,118 | 5,848 |
| s.dev. | 376.8 | 311.4 | 287.3 | 275.4 | 268.5 | 328.8 | 280.7 | 264.3 | 256.7 | 252.5 | 296.2 | 266.5 | 256.6 | 251.8 | 249.1 |
| c.v. | 3.5% | 3.4% | 3.4% | 3.4% | 3.5% | 3.4% | 3.4% | 3.4% | 3.5% | 3.6% | 3.7% | 3.8% | 4.0% | 4.1% | 4.3% |
| obs. | 19 | 19 | 19 | 19 | 19 | 19 | 19 | 19 | 19 | 19 | 19 | 19 | 19 | 19 | 19 |

The coefficient of variance, c.v., is relatively small for each of the 15 sequences. This small variation provides a level of confidence that any of the 19 results are representative of the soil tested.

Next, a specimen was prepared to a similar level of wet density and moisture content and tested per AASHTO T-307 in Cell B. The results were regressed with the same Equation 2 model.

Finally, the results of the testing are summarized in Table 3. Included are results for Test A (tested in Cell A, Specimen No. 10), Test B (tested in Cell B), and Test $B_{adj}$ (same as Test B with 2 lb of load removed from the acquired load transducer readings, prior to input into Equation 2). Percent differences of Test B and Test $B_{adj}$ compared with Test A are also provided.

TABLE 3—*Summary of test results for seal drag sensitivity.*

| Parameter | Test A | Test B | %diff | Test $B_{adj}$ | %diff |
|---|---|---|---|---|---|
| K1 | 7938 | 10 365 | | 7973 | |
| K2 | -0.21171 | -0.26330 | | -0.15495 | |
| K3 | 0.23770 | 0.24074 | | 0.24064 | |
| Seq 1 | 10 494 | 13 294 | 27 | 11 021 | 5 |
| Seq 2 | 9062 | 11 076 | 22 | 9899 | 9 |
| Seq 3 | 8316 | 9954 | 20 | 9296 | 12 |
| Seq 4 | 7825 | 9228 | 18 | 8891 | 14 |
| Seq 5 | 7464 | 8702 | 17 | 8589 | 15 |
| Seq 6 | 9530 | 12 057 | 27 | 9997 | 5 |
| Seq 7 | 8229 | 10 046 | 22 | 8979 | 9 |
| Seq 8 | 7552 | 9029 | 20 | 8432 | 12 |
| Seq 9 | 7106 | 8370 | 18 | 8064 | 13 |
| Seq 10 | 6778 | 7892 | 16 | 7790 | 15 |
| Seq 11 | 8082 | 10 204 | 26 | 8461 | 5 |
| Seq 12 | 6979 | 8502 | 22 | 7599 | 9 |
| Seq 13 | 6405 | 7641 | 19 | 7137 | 11 |
| Seq 14 | 6027 | 7084 | 18 | 6825 | 13 |
| Seq 15 | 5749 | 6679 | 16 | 6593 | 15 |

It should be noted that both the triaxial chambers used for Test A and Test B trials possess a 0.5-inch diameter load rod

Although 2 lb seems like such a negligible amount of seal drag, its potential influence on results can approach 30 %. These errors are most pronounced at low load intervals that target only 8–10 lb of cyclic load at 2 psi cyclic stress levels on 2.8-inch diameter test specimen. Correcting for known amounts of seal drag is a dangerous proposition as well, as the amount of seal drag developed may be non-linear, thus could depend on the amount of rod movement as loads are pulsed on the specimen. Additionally, seal drag may change with time as the seal wears.

Experience has shown that seal drag increases as load rod diameter increases (more circumferential area in contact between the precision stainless steel rod and the seal) thus these potential errors are expected to increase in magnitude with larger cells.

*System Compliance*

System compliance can be a significant factor since the LVDTs are mounted outside the triaxial chamber. Not only will the LVDTs measure test specimen deformation, they may also measure system deformation that is not solely specimen deformation. System deformation could consist of load rod compression, load rod bending, compression of porous stones, contact points or interfaces such as top and bottom loading platens, and base bending. Current resilient modulus test procedures do not specify a tolerance for system compliance. ASTM Standard Test Method for the Determination of the Modulus and Damping Properties of Soils Using the Cyclic Triaxial Apparatus (ASTM D 3999) has a similar physical test configuration as the resilient modulus test and involves measurements of very small amounts of specimen deformation (on the order of 1 mil or less). Experience has shown that the system compliance could be more than 10% of the deformation measured. This could significantly affect the results. In fact, ASTM D 3999 requires that the system compliance be evaluated to ensure the compliance is less than 10 % of the deformation measured and reported. A similar tolerance for the system compliance should be established for the resilient modulus test.

No efforts were made to determine the system compliance for Triaxial Cell A or B in the experiment described in the previous section. An attempt was made to correct the results for seal drag, which did lead to a better match between Test A and Test B. It is quite possible that system compliance could explain more of the variation between the two tests.

Some may argue that if internally mounted LVDTs and load cell are used, system compliance will not be an issue. While this argument has valuable merit, a system with internally mounted transducers has inherent problems too, such as sensitivity of the transducers to pressure and difficulties of assembling these transducers inside the triaxial cell. Further, when saturation of a specimen is desired, the triaxial cell will be required to fill with water as the confining medium. This issue will make internal instrumentation extremely difficult, expensive and time consuming.

*Alignment of Load Rod and Top/Bottom Platens*

Alignment of the load rod and top/bottom loading platens is an important issue. Misalignment of the load rod and platens will result in eccentric loading that may in turn lead to erroneous deformation measurements. There is no specific requirement on the tolerance of alignment in the current AASHTO T-307 test standard. A tolerance for the alignment has been established as part of ASTM D 3999. Like system compliance, a tolerance pertaining to alignment may be warranted.

*Physical Dimension Measurements of Test Specimen*

Another point of potential sensitivity is the accurate measurement of diameter and height. The diameter measurement will affect the stress term while the height measurement will affect the strain term in Equation 1. By incorrectly measuring these dimensions, or neglecting to measure these dimensions and using nominal specimen dimensions or mold dimensions, can lead to final resilient modulus result errors of up to 5

%. Not only could this type of neglect lead to erroneous resilient modulus data, it will also compute erroneous volumetric data in the form of density.

**Conclusions and Recommendations**

This paper stresses the importance of influencing factors associated with the triaxial cell used to conduct resilient modulus testing based on years of experience in the area of dynamic testing of soils. These factors are not adequately addressed in the current resilient modulus test standard. Following careful review of the specification, analyzing the effects of various triaxial cell influences, and drawing upon experience spanning several years and numerous tests, the following conclusions are provided.

- The resilient modulus test is an extremely sensitive test, measuring small strains at low to moderate loads.
- In order to be as productive as possible, external instrumentation is allowable to measure load (stress) and deformation (strain).
- Care must be taken when implementing a resilient modulus test system. Assurances must be attained to provide accurate load and deformation measurements that will lead to the most accurate calculation of resilient modulus.
- Internal measurements for load (stress) and strain (deformation) can eliminate or reduce the inherent errors associated with equipment variation. This decision should recognize how difficult and time-consuming internal instrumentation is. Further, it should be recognized that the use of backsaturation techniques would make internal instrumentation extremely difficult.
- Laboratories that have not exercised caution towards these sensitivities, those that have not been evaluated for system conformance, and those that do not adhere to a satisfactory quality system program should not participate in round robin test programs. Without these controls, variation not attributed to material variation is possible, probable and uncontrollable.

It is recommended that a specification be developed that would provide tight tolerance control for manufacturers of triaxial testing equipment. The specification should, at a minimum, limit the amount of seal drag force while at the same time limit the amount of compressed air leakage. If these parameters are controlled, instrumentation can be made externally and these influences can be neglected. Some of these measures have been addressed in ASTM D 3999 and should be considered for this test method as well.

It is further recommended that a program be developed and administered to evaluate a precision and bias statement for a standardized test procedure that would include materials covering a wide range of expected resilient properties. These should include

A-4, A-5, A-6, and A-7 soils, as a minimum. Once selected, several laboratories that can demonstrate conformance (by on-sight evaluation) to the precise requirements of the test procedure should test a minimum of six replicates from each material combination to develop both within-laboratory and between-laboratory variation. It would be advantageous to evaluate the effects of compaction methodology during this recommended program as well as effects of moisture and density variations. This additional evaluation is recommended as a second phase, following the development of an accurate and acceptable precision and bias of the test procedure.

**References**

Alavi, S., Merport, T., Wilson, T., Groeger, J., and Lopez, A., 1997, "LTPP Materials Characterization Program: Resilient Modulus of Unbound Materials (LTPP Protocol P46) Laboratory Startup and Quality Control Procedures," *Federal Highway Administration Report No. FHWA-RD-96-176.*

# SESSION 5: MODELING DATA REDUCTION AND INTERPRETATION

B. F. Tanyu,[1] W. H. Kim,[2] T. B. Edil,[3] and C. H. Benson[3]

# Comparison of Laboratory Resilient Modulus with Back-Calculated Elastic Moduli from Large-Scale Model Experiments and FWD Tests on Granular Materials

---

**Reference**: Tanyu, B. F., Kim, W. H., Edil, T. B., and Benson, C. H., **"Comparison of Laboratory Resilient Modulus with Back-Calculated Elastic Moduli from Large-Scale Model Experiments and FWD Tests on Granular Materials,"** *Resilient Modulus Testing for Pavement Components, ASTM STP 1437*, G. N. Durham, W. A. Marr, and W. L. De Groff, Eds., ASTM International, West Conshohocken, PA, 2003.

**Abstract:** A comparison is made between resilient moduli obtained from (i) a conventional small-scale resilient modulus test, (ii) a large-scale model experiment (LSME), and (iii) a falling weight deflectometer (FWD) in the field. The LSME is a large prototype-scale test simulating a pavement section. The FWD tests were conducted on a highway test section. All tests were conducted on a typical base course material and two granular industrial by-products used as subbase. Relationships between elastic modulus and bulk stress were derived from the LSME data by modeling the set-up as a nonlinear elastic layered system using the computer program KENLAYER. Elastic moduli were back-calculated from the FWD data using the program MODULUS. Reasonable correspondence between the elastic moduli measured at different scales was obtained when empirical corrections were made for strain amplitude using a backbone curve for granular materials and by matching stress levels. However, even when corrections are applied, the low-strain (or maximum) elastic modulus for the industrial byproducts inferred from the laboratory resilient modulus test tends to be lower (by a factor of 1.5 to 4) than the operative elastic modulus inferred from the LSME and the FWD tests. In addition, the minimum bulk stress provided by the laboratory resilient modulus test can be higher than the bulk stress existing in the field. In such cases, the elastic modulus at the field bulk stress can be estimated by extrapolation using a power function.

**Keywords:** resilient modulus, elastic modulus, gravel, foundry slag, bottom ash, falling weight deflectometer test, large-scale model experiment, industrial byproducts, prototype test

[1]Grad. Res. Asst., Geological Engineering Program, University of Wisconsin-Madison, Madison, WI, 53706, USA, bftanyu@students.wisc.edu

[2]Grad. Res. Asst., Dept. of Civil & Environmental Engineering, University of Wisconsin-Madison, Madison, WI, 53706, USA, wkim@cae.wisc.edu

[3]Professor, Geological Engineering Program and Dept. of Civil & Environmental Engineering, University of Wisconsin-Madison, Madison, WI, 53706, USA, edil@engr.wisc.edu, benson@engr.wisc.edu

## Introduction

The resilient modulus is a material property used in pavement engineering that describes the deformation of materials comprising a pavement structure subjected to repetitive loads similar to those imposed by vehicles. The resilient modulus is typically measured in the laboratory on specimens of pavement materials compacted using laboratory compaction equipment. A loading protocol is followed where the confining pressure and the repetitive deviator stress are varied to simulate different states of stress. Changes in the loading protocol have been made periodically since the test method was initially developed. However, the general characteristics of the test method have remained the same.

Unlike many other mechanical properties of earthen materials, there is no direct way of verifying that the resilient modulus measured in the laboratory is representative of elastic moduli operative in the field under wheel loads. Therefore, there is uncertainty regarding how faithfully the resilient modulus measured in the laboratory corresponds to the operative elastic modulus in the field. Direct comparison of the resilient modulus with elastic moduli obtained from other methods is also difficult because of differences in stress and strain conditions, frequency of dynamic loading, and other factors. This paper presents a study focused on comparing the resilient modulus measured in the laboratory on test specimens of granular materials with elastic moduli back calculated from a large-scale model experiment (LSME) and falling weight deflectometer (FWD) tests conducted in the field. The laboratory tests were conducted using a conventional resilient modulus test procedure (AASHTO T294-94), whereas back-calculation methods were used to obtain elastic moduli from the LSME and FWD tests.

A typical granular base course and two granular industrial by-products were used for all three methods of evaluation. Properties of the materials are summarized in Table 1. Grade 2 gravel is a natural material commonly used as base course in Wisconsin. Bottom ash and foundry slag are granular industrial by-products that are used as subbase over soft subgrades to enable construction. Both of the industrial byproducts are well-graded coarse-grained sand-like materials. All of the materials are nearly insensitive to water content during compaction (Fig. 1).

Table 1 - *Properties of Industrial Byproducts and Grade 2 Gravel.*

| Material | Specific Gravity | $D_{10}$ (mm) | $D_{60}$ (mm) | $C_u$ | USCS Symbol | Maximum Dry Unit Weight ($kN/m^3$) | | Optimum Water Content per D 698 (%) | CBR |
|---|---|---|---|---|---|---|---|---|---|
| | | | | | | Compaction per ASTM D 698 | Vibratory per ASTM D 4253 | | |
| Grade 2 | 2.65 | 0.09 | 6.0 | 66.7 | GW | 22.6 | NM | 8.2 | NM |
| Bottom Ash | 2.65 | 0.06 | 1.9 | 31.7 | SW | 15.1 | 13.7 | -- | 21 |
| Foundry Slag | 2.29 | 0.13 | 2.0 | 15.4 | SP | 10.0 | 8.4 | -- | 17 |

Note: NM = not measured.

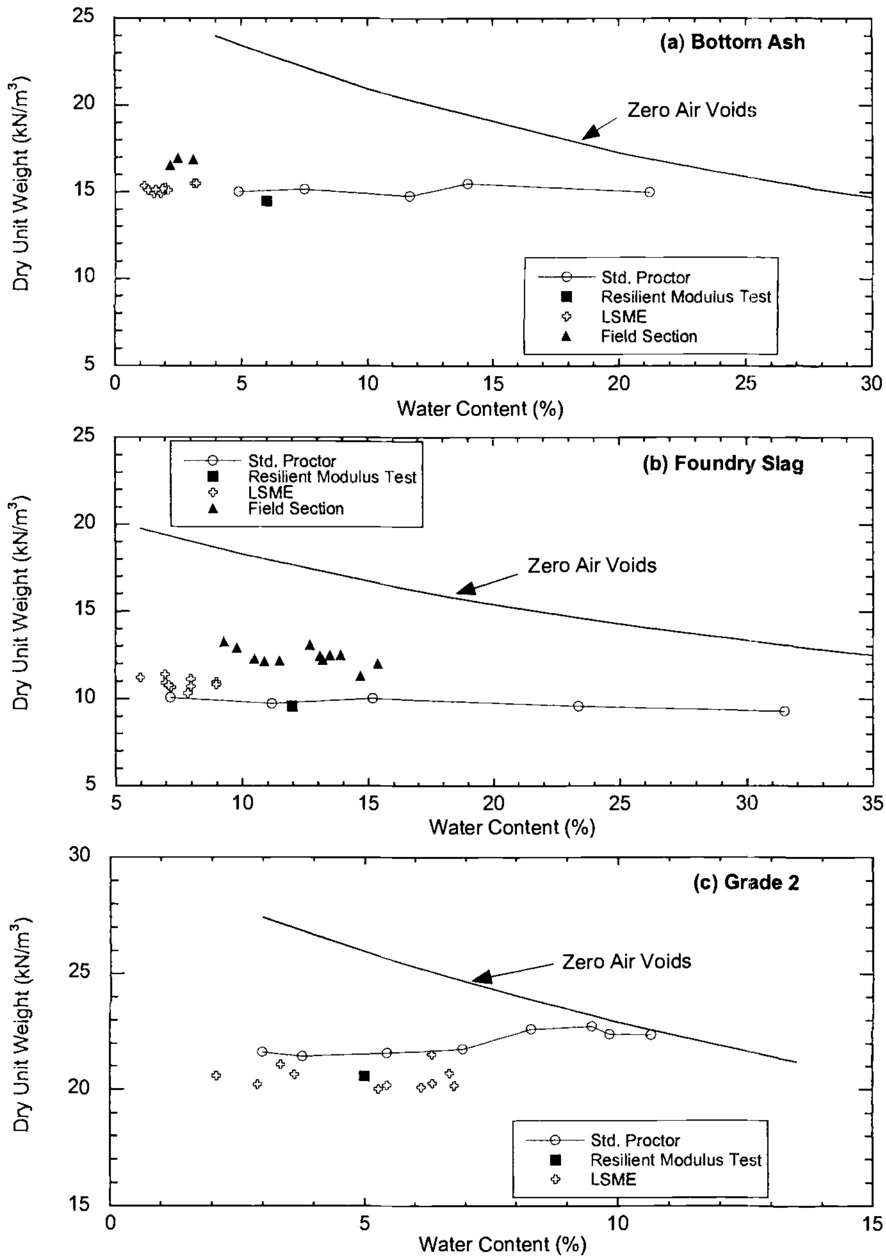


Fig. 1 – *Compaction Curves and Test Unit Weights for (a) Bottom Ash, (b) Foundry Slag, and (c) Grade 2 Gravel.*

## Laboratory Resilient Modulus Test (AASHTO T294)

Resilient moduli of the granular materials were evaluated using AASHTO T294-94 following the protocol for Type 1 materials (unbound granular base and subbase materials). The cell used for the resilient modulus test was identical to a triaxial cell used for shear strength testing, except air was used as the confining fluid instead of water as is required in AASHTO T294.

Dimensions of the test specimens were selected based on the particle size distribution of the materials being tested following the criteria in T294. Specimens of foundry slag and bottom ash samples had a height of 152 mm and a diameter of 76 mm, whereas specimens of Grade 2 gravel had a height of 305 mm and a diameter of 152 mm. All specimens were compacted to 95% of the maximum dry unit weight per standard Proctor. This dry unit weight is comparable to that achieved in the field and in the LSME (Fig. 1).

A loading system manufactured by Cox & Sons Inc. was used that included a temperature-controlled test chamber. Loads were applied using a hydraulic load actuator and were measured using a 22-kN load cell mounted externally. Deflections were measured using two LVDTs mounted externally. The loading sequence was applied using a haversine load pulse with a frequency of 1 Hz. The load was applied for 0.1 s at the beginning of each cycle, and was followed by a 0.9-s rest period. Resilient moduli were computed from the measured loads and deflections using the method in T294.

## Large-Scale Model Experiment (LSME)

The LSME is a method devised to model a pavement structure (or parts of it) at prototype scale in a manner that replicates field conditions as closely as practical. A photograph of the LSME is in Fig. 2 and a schematic is shown in Fig. 3.

A pavement profile is constructed in a 3 m x 3 m x 3 m test pit (Fig. 3) by placing three different layers of materials (from bottom to top): (i) a 2.5-m thick layer of dense uniform sand, (ii) a 0.45-m-thick simulated soft subgrade (expanded polystyrene foam), and (iii) a layer of coarse granular test material (0.22 to 0.90-m thick) simulating subbase. The surface of the soft subgrade is nearly at the top surface of the pit. The upper layer simulating subbase lies above the surface of the test pit. Wooden walls 1 m high confine the subbase material along the boundaries of the test pit.

A riding surface and a base course layer are not incorporated in the LSME, but their effect in transmitting wheel loads is considered, as described subsequently. Repetitive loads are applied to the surface of the profile with a steel plate using a 90-kN hydraulic actuator (Fig. 2).

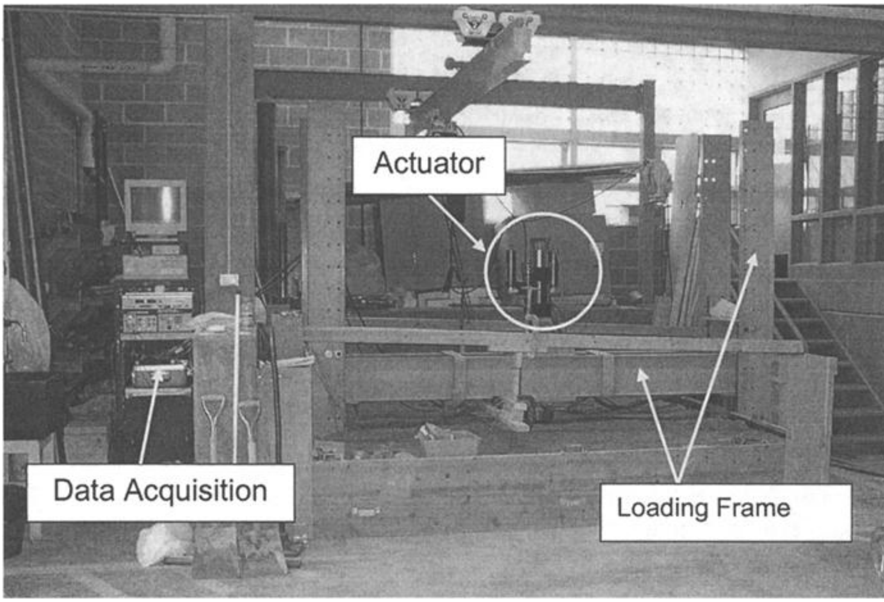


Fig. 2 – *Setup of LSME Showing Hydraulic Actuator, Load Frame, and Data Acquisition System.*

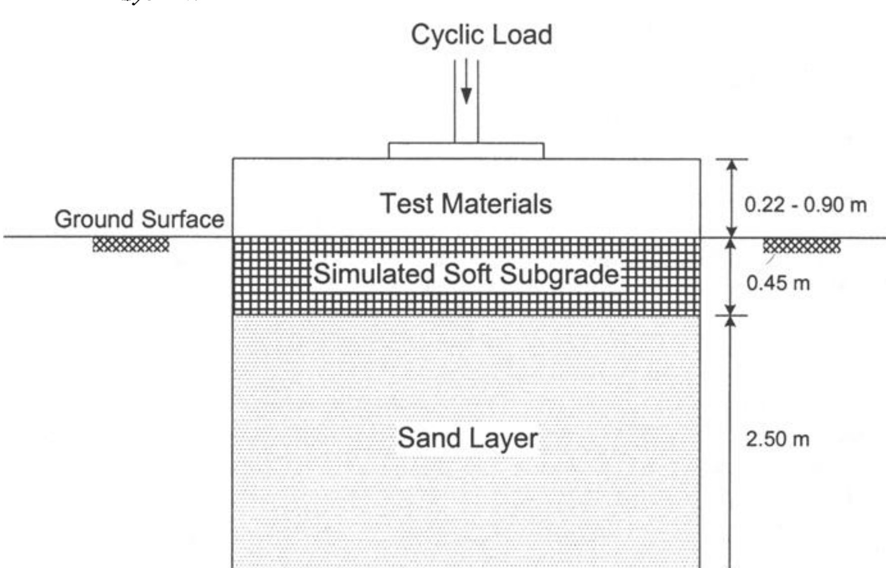


Fig. 3 – *Schematic Cross Section of Large-Scale Model Experiment (LSME).*

*Materials*

*Dense Uniform Sand* - The dense uniform sand layer at the base of the profile provides a firm foundation for the experiment, and simulates a deeper stiff layer. The sand has an effective grain size of 0.22 mm, a coefficient of uniformity of 1.8, a dry unit weight of 17.4 kN/m$^3$, and a void ratio of 0.49. This void ratio corresponds to a relatively density of 85%. The sand was originally placed using a loader, and has been in used in a variety of experimental programs over the last decade. To homogenize the sand, the pore water pressure is elevated until the sand is liquefied. Pumps located beneath the pit are used to apply the pore water pressure. After liquefaction, the sand is drained and compresses under its self-weight and the matric suction that develops during drainage. Before use in this test program, the upper 450 mm of the sand was compacted with a vibratory plate compactor.

*Simulated Soft Subgrade* - Expanded polystyrene (EPS) foam was used to simulate a soft subgrade similar to a silty clay. EPS was used in lieu of soil to ensure uniformity, and to reduce the time and effort required to prepare experiments. EPS is a geofoam, and has been used in a variety of geotechnical applications including pavement structures. For example, one-dimensional compression tests conducted by Negussey and Jahanandish (1993) show that the stress-strain behavior of low-density EPS (21.0 kg/m$^3$) is comparable to that of soft inorganic clay of moderate plasticity. In addition, Negussey and Jahanandish (1993) report that confinement and loading frequency have minimal effect on the compressibility of EPS.

An appropriate EPS material was selected for the LSME by identifying the density of EPS that has similar stress-strain behavior as a typical soft subgrade soil in Wisconsin (moist Antigo silt loam, the Wisconsin state soil). Unconfined cyclic loading tests were conducted on specimens of EPS (300 mm tall, 150 mm diameter) and resilient modulus tests were conducted on the Antigo silt loam. A comparison of the stress-behavior of the Antigo silt loam and that of the low-density EPS (17.1 kg/m$^3$) selected for use in the LSME is shown in Fig. 4. The EPS has similar stress-strain behavior as the Antigo silt loam, and has similar modulus.

The EPS does undergo significant plastic deformation at an axial stress of 100-120 kPa, whereas the Antigo silt loam does not. However, calculations indicated that the stress at the level of the EPS in the LSME would never exceed 100 kPa. Thus, the EPS in believed to remain within its elastic range in the LSME, with an elastic modulus similar to that of a soft clay.

The simulated soft subgrade in the LMSE was placed as three layers of EPS panels, each 0.15-m thick, to form a 0.45-m thick soft layer. This approach was used in lieu of a single block of EPS to simplify construction and reduce costs. Use of panels rather than a single block is not expected to affect deformation of the profile. Zou et al. (2000) show that block size and lateral restraint do not significantly affect deformation behavior of EPS.

*Granular Subbase Layer* - The coarse granular layer simulating subbase was placed in 0.11-m-thick lifts. Each lift was compacted with a vibratory plate compactor to obtain a dry unit weight in excess of 95% of maximum dry unit weight based on standard Proctor. A nuclear gauge was used to measure the density of each lift. The dry unit weights that were achieved are similar to those used for the laboratory resilient modulus tests and in the field (Fig. 1). Granular subbase layers were constructed with the Grade 2 gravel and both industrial byproducts. At least two thicknesses of each material were evaluated.

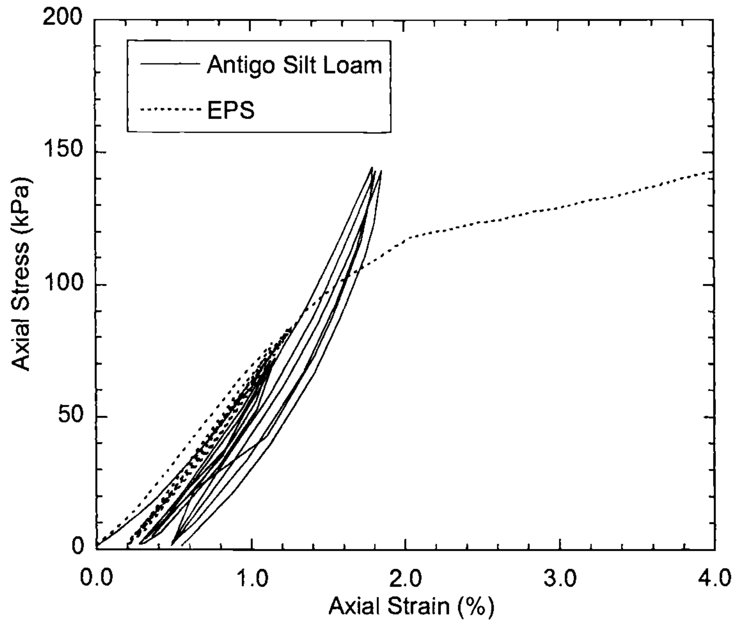


Fig. 4 - *Stress-Strain Behavior of 300-mm-Thick EPS and Antigo Silt Loam.*

*Loading*

Granular subbase materials are subjected to two loading levels: (i) higher intensity short duration loads during construction caused by heavy truck traffic directly on the subbase and (ii) lower intensity loads that persist for many years due to traffic on the finished pavement. These loading conditions were simulated for a typical rural highway (i.e., Wisconsin State Trunk Highway 60, referred to herein as STH 60, which is the site of the field tests) by applying different stresses to the surface of the compacted subbase layer in the LSME.

The construction loads were selected to simulate the load applied by 4-axle dump trucks applying a load of 70 kN per axle directly on the subbase. These trucks normally have a tire pressure of approximately 700 kPa, which results in a contact area of 0.05 $m^2$ under a 35 kN load. Therefore, a circular steel plate having a diameter of 250 mm (i.e., an area of 0.05 $m^2$) and a thickness of 25 mm was used to apply the wheel load. Loads applied by these trucks represent the heaviest repetitive loads applied to the subbase during construction.

Conventional traffic loads were estimated by conducting a multilayer elastic analysis of the pavement structure at STH 60 using the program KENLAYER (Huang 1993). The program was used to determine the loading on the subbase caused by an equivalent single axle load (ESAL) on the surface of the pavement structure. The asphalt was assumed have an elastic modulus of 3540 MPa, a Poisson's ratio of 0.30, and a thickness of 125 mm. The base course was assumed to be 255-mm thick and to have a Poisson ratio of 0.35 (corresponding to a at-rest earth pressure coefficient of 0.54). Moduli of the base and subbase and layers were assumed to follow the non-linear elastic power function model:

$$M = k_1 \sigma_b^{\,k_2} \tag{1}$$

where $k_1$ and $k_2$ are empirical constants and $\sigma_b$ is the bulk stress. The bulk stress equals $\sigma_d$ - $3\sigma_3$, where $\sigma_d$ is the deviator stress and $\sigma_3$ is the minor principal stress. For the base course, $k_1$ was assumed to be 15.3 MPa and $k_2$ was 0.50. For the subbase, $k_1$ was 3.3 MPa and $k_2$ was 0.62. The soft subgrade was assumed to be linearly elastic with a modulus of 69 MPa and a Poisson's ratio of 0.45.

The KENLAYER analysis indicated that stress applied to the subbase base layer is 140 kPa, or approximately 20% of that applied to the surface of the pavement. This stress was simulated by applying a force of 7 kN to the loading plate.

Loads were applied using a haversine load pulse consisting of a 0.1-s load period followed by a 0.9-s rest period, which is the same load pulse specified in the laboratory resilient modulus test. The dynamic motion of the actuator was provided by a 280-L/m MTS hydraulic pump. The 35-kN load was applied for the first 1000 cycles to simulate construction traffic. Then 10,000 cycles of the 7-kN load were applied to simulate post-construction traffic loads. A CR-9000 data logger manufactured by Campbell Scientific Inc. was used for recording vertical displacement of the loading plate and the applied load as a function of time. For each load cycle, 96 data points were recorded, including the minimum and maximum applied loads and corresponding deflections.

*Inversion of Elastic Modulus from the LSME*

KENLAYER was used to invert the elastic modulus of the subbase layer in the LSME from the measured loads and defections. The simulated soft subgrade was assumed to be linearly elastic, whereas the elastic modulus of the subbase was assumed to follow the elastic power function in Eq. 1. The subbase was divided into sublayers 50-mm thick in the analysis.

The parameter $k_2$ varies in a narrow range for a wide variety of granular materials. Thus, $k_2$ was fixed using the value obtained from the resilient modulus test conducted per T294. The parameter $k_1$, which varies over a broad range, was adjusted until the measured and predicted elastic deflections matched. The $k_1$ that provided matching deflections was assumed to be the operative $k_1$ of the subbase layer. The elastic deflections used as input to KENLAYER were derived from the total deflections (elastic and plastic) measured in the LSME by subtracting the accumulated plastic (non-recoverable) deflections from the total deflections.

## Field Experiment

### *Test Section*

A 654-m test segment containing several test sections was constructed during reconstruction of STH 60 between Lodi and Prairie du Sac, Wisconsin (Edil et al. 2002). This segment contained four test sections constructed with the granular materials used in the LSME. Plan and cross-sectional views of the test sections are shown in Fig. 5. Two of the test sections (at the ends) are controls. The controls were constructed using crushed rock for subbase, which is the same material used for the portion of STH 60 that was re-constructed. The other two test sections incorporated granular industrial by-products, i.e., foundry slag and bottom ash as subbase. All sections had a 125-mm-thick asphalt surface and a base course consisting of 115 mm of Grade 2 gravel and 140 mm of salvaged asphalt (total base course thickness = 255 mm).

Undisturbed samples of the subgrade were collected along the length of the test section at a depth of 1 m below ground surface using thin-wall sampling tubes having a diameter of 75-mm. The subgrade consisted of lean silt (ML) or lean clay (CL). Unconfined compression tests indicated that the subgrade was reasonably uniform, with unconfined compressive strengths ($q_u$) ranging between 100 and 160 kPa. Measurements made with a dynamic cone penetrometer (DCP) and a soil stiffness gauge (SSG) also indicated that the subgrade was uniform (Edil et al. 2002).

The two industrial by-products (bottom ash and foundry slag) were used as a subbase material, providing a stable working platform over the subgrade during pavement construction. Grade 2 gravel was used as base course along with a layer of salvaged asphalt, which has essentially the same properties as Grade 2 gravel. The bottom ash and foundry slag were used in bulk form (as a layer rather than being mixed with soil). Both were placed in 150-mm-thick lifts that were compacted with a tamping foot roller to achieve a dry unit weight exceeding 100% of maximum dry unit weight per standard Proctor (Fig. 1). The dry unit weight of each layer was measured periodically with a nuclear density gage. After placement and compaction of the last lift, the top of each subbase layer was compacted again with steel-drum and rubber-tire compactors to provide a smooth and uniform surface for the remaining pavement layers.

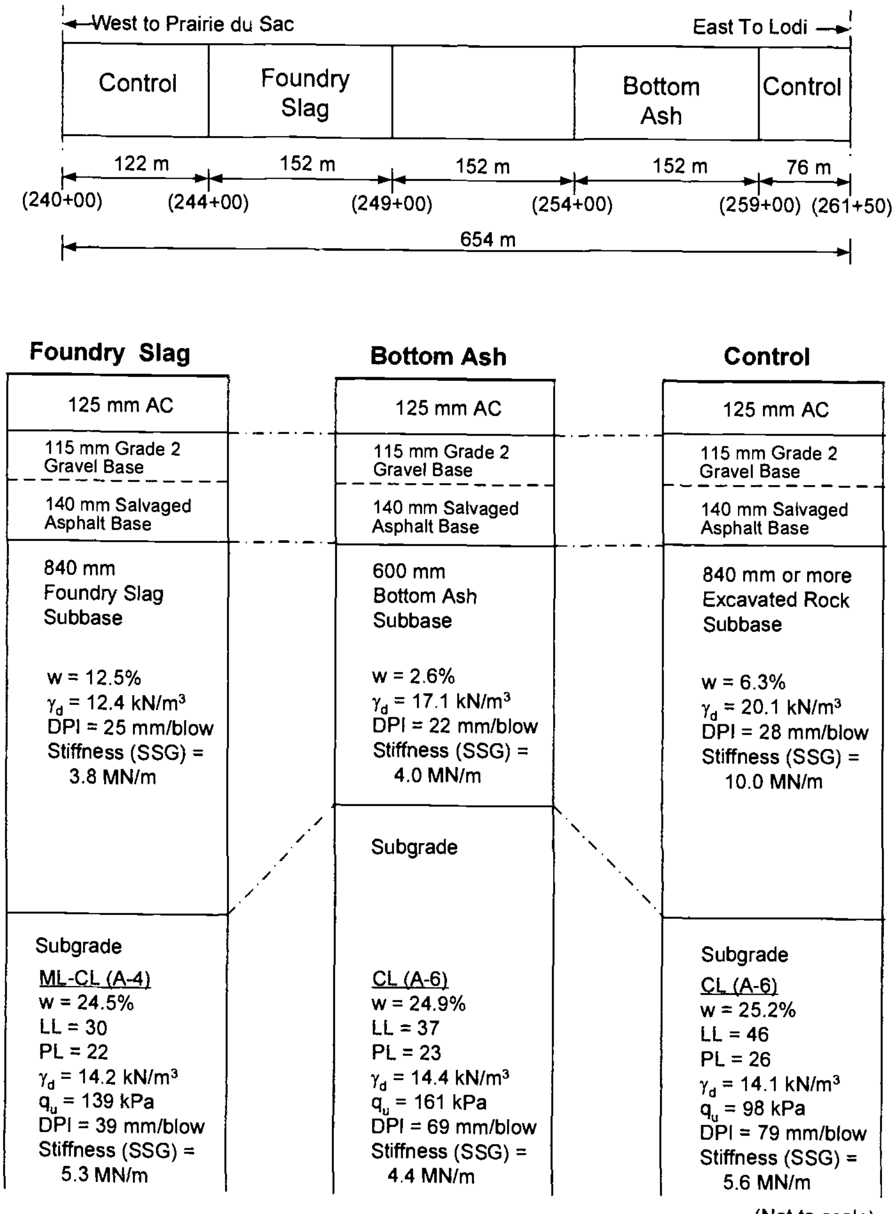


Fig. 5 – *Pavement Structure and Properties of Subgrade and Subbase at STH 60. DPI = Dynamic Penetration Index From Dynamic Cone Penetrometer. Stiffness Was Measured Using a Soil Stiffness Gage (SSG).*

*Falling Weight Deflectometer Tests*

Falling weight deflectometer (FWD) tests were performed at STH 60 to determine the operative elastic moduli of the Grade 2 subbase, bottom ash, and foundry slag. The FWD tests were conducted semi-annually for two years by the Wisconsin Department of Transportation (WisDOT) using a KUAB Model 2m-33 FWD. The KAUB 2m-33 FWD is trailer-mounted and is towed by a light truck. The FWD is automatically controlled by a computer in the towing vehicle. Loads and deflections are recorded and stored in the computer.

The FWD was used to drop a 49 kN weight onto a 300-mm-diameter plate in contact with the pavement surface. The drop applies a load with a rise time of 17 to 25 ms and duration of 34 to 50 ms. The peak load imposed on the pavement surface by the falling weight was measured using a load transducer. Surface deflections were measured with seven velocity transducers located at the center of the load and at distances of 0.30 (edge of load plate), 0.45, 0.60, 0.90, 1.20, and 1.52 m from the center of the load.

*Elastic Modulus from FWD Data*

Elastic moduli of the subbase and base layers were computed using the loads and deflections measured with the FWD. The layered elastic analysis program MODULUS (Texas Transportation Institute 1991) was used for the analysis because it provides routines for back-calculating elastic moduli from FWD data. Each pavement layer is assumed to be homogeneous, isotropic, and linearly elastic and to extend infinitely in the horizontal direction. The bottom layer is also assumed to extend downward infinitely. Elastic moduli assigned to each layer are adjusted iteratively until the measured and predicted deflections match within an accepted tolerance (Uzan et al. 1988).

A four-layer system (asphalt, base course, subbase course, and subgrade) was used for the back-calculation model. Each layer was assigned its average thickness (Fig. 5). The two base course layers (Grade 2 gravel and salvaged asphalt, Fig. 5) were treated as single layer with a combined thickness of 255 mm. A Poisson's ratio of 0.30 was used for the asphalt surface layer. The Poisson's ratio was set at 0.35 For the combined base course layer. Poisson's ratios of 0.33, 0.25, and 0.30 were used for the subbase layers constructed from foundry slag, bottom ash, and crushed rock. The Poisson's ratios for the base and subbase materials were estimated using elastic theory and the at-rest earth pressure coefficient computed using Jaky's equation. Depth to the "rigid layer" was fixed at 6 m to simulate the approximate depth of bedrock at the site. Bush and Alexander (1985) indicate that the rigid layer has little effect on the back-calculated elastic moduli when the depth is at least 6 m.

Once the field elastic moduli were back-calculated using MODULUS, an additional analysis was conducted with KENLAYER to determine the range of bulk stresses and vertical strains operative in the base and subbase layers in the field. A surface load equal to that applied by the FWD was included to simulate the stresses imposed during the FWD test. The elastic moduli back-calculated with MODULUS were

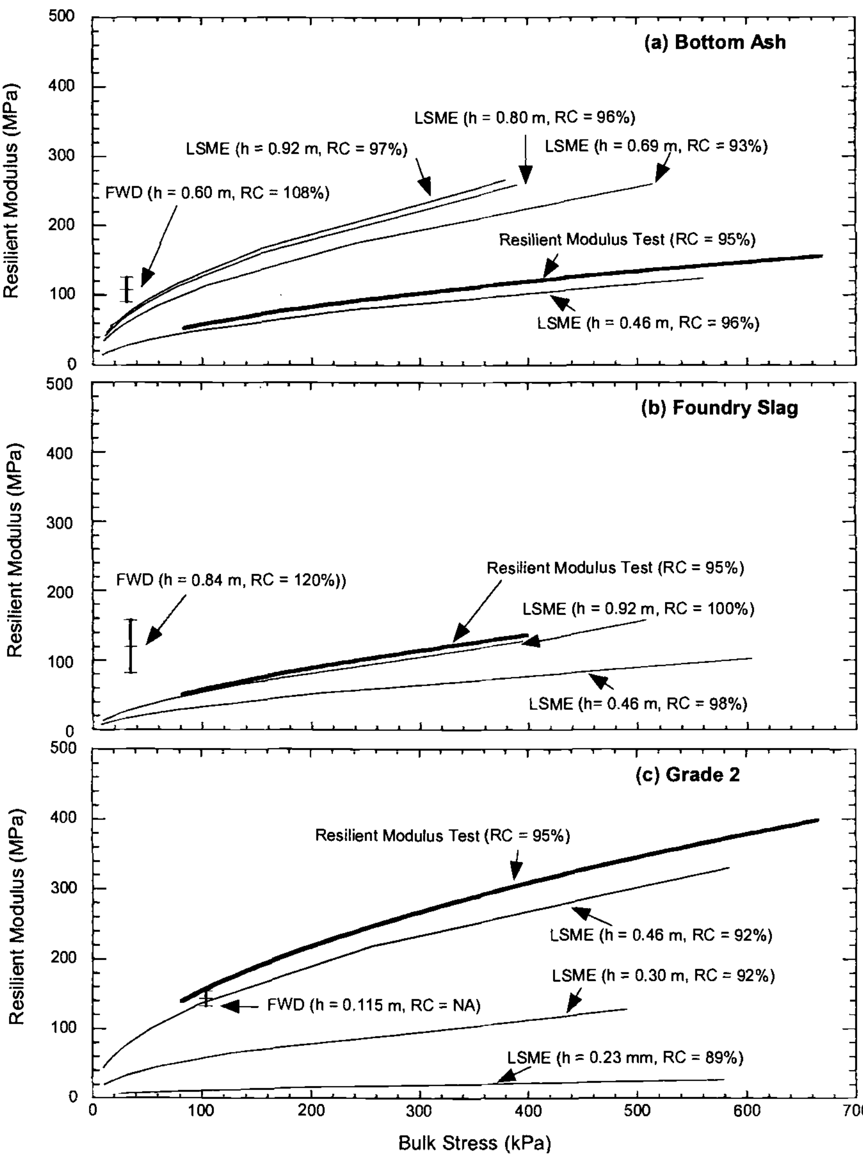


Fig. 6 – *Elastic Moduli for (a) Bottom Ash, (b) Foundry Slag, and (c) Grade 2 Gravel (h = Thickness, RC = Relative Compaction, NA = Data Not Available).*

used as input. The bulk stress and vertical strain at mid-depth of each layer were assumed to be representative of the operative conditions in the field.

## Results and Discussion

The elastic moduli measured in the laboratory, LSME, and the field are shown in Fig. 6. Elastic moduli determined from the laboratory resilient modulus test and the LSME are shown as functions of bulk stress. This relationship was determined directly from the laboratory resilient modulus test. For the LSME, the relationship was obtained from the KENLAYER analysis described previously. Only a single elastic modulus is presented for the FWD tests because only one loading condition was applied in the field. The error bars represent the range of moduli obtained from the four semi-annual FWD tests that have been conducted. The bulk stress operative during the FWD test was computed using KENLAYER, and represents the stress at mid-depth in the subbase layer.

Each of the evaluation methods provides a different modulus for a given bulk stress. For example, the elastic moduli measured in the laboratory using AASHTO T294 and in the field with the FWD differ by as much as a factor of four at the field bulk stress. This difference is consistent with other reports indicating that elastic moduli obtained using these methods may differ by as much as a factor of 10 (Newcomb 1986, Ali and Khosla 1987, Houston et al. 1990, Daleiden et al. 1994). The materials used in all three methods were prepared at comparable dry unit weight and water content (Fig. 1). Thus, differences in the elastic moduli for a given material are assumed to be due to differences in state of stress, strain level, number of loading cycles, and scale. The estimated bulk stress and number of loading cycles in each test method are summarized in Table 2.

For all materials, the elastic modulus increases appreciably with increasing bulk stress. For example, the elastic modulus of Grade 2 gravel measured in the laboratory resilient modulus test increases from 140 MPa to 400 MPa as the bulk stress increases from 70 kPa to 670 kPa. The sensitivity of elastic modulus to stress state illustrates the importance of maintaining a consistent stress state when comparing elastic moduli measured at different scales and with different methods.

The elastic modulus measured in the LSME is sensitive to the thickness of the subbase layer (h) being evaluated (i.e., thicker layers have a higher elastic modulus at a given bulk stress). The sensitivity to thickness in the LSME reflects the different levels of strain in layers having different thickness, which is known to affect the elastic modulus of granular materials (Seed and Idriss 1970, Hardin and Drnevich 1972, Edil and Luh 1978). Vertical strains determined from the KENLAYER analysis are summarized in Table 3. Lower vertical strains exist in the thicker layers due to greater stress distribution that occurs in a thicker layer under the same applied surface load.

Table 2 – *Stress and Loading Conditions in FWD, LSME, and Resilient Modulus Test.*

| Testing Method | Loading Cycles | Bulk Stress[b] (kPa) |
|---|---|---|
| Bottom Ash | | |
| FWD | 10,000[a] | 31 |
| LSME (0.46 m) | 10,000 | 28 |
| LSME (0.69 m) | 10,000 | 22 |
| LSME (0.80 m) | 10,000 | 18 |
| LSME (0.92 m) | 10,000 | 19 |
| AASHTO T294 | 1,500 | 84 – 718 |
| Foundry Slag | | |
| FWD | 10,000[a] | 35 |
| LSME (0.46 m) | 10,000 | 25 |
| LSME (0.92 m) | 10,000 | 13 |
| AASHTO T294 | 1,500 | 84 - 718 |
| Grade 2 Gravel | | |
| FWD | 10,000[a] | 104 |
| LSME (0.23 m) | 10,000 | 75 |
| LSME (0.30 m) | 10,000 | 59 |
| LSME (0.46 m) | 10,000 | 0 |
| AASHTO T294 | 1,500 | 84 - 718 |

Notes: [a]estimated traffic loading by the time of measurement; [b]mid-depth of the subbase and base layers for FWD and LSME.

Table 3 – *Resilient Modulus and Vertical Strain at Field Bulk Stress.*

| Method | Bulk Stress (kPa) | Elastic Modulus (MPa) | Vertical Strain (%) |
|---|---|---|---|
| Bottom Ash | | | |
| FWD | 31 | 108 | 0.030 |
| LSME (0.46 m) | 31 | 28 | 0.140 |
| LSME (0.69 m) | 31 | 60 | 0.050 |
| LSME (0.80 m) | 31 | 68 | 0.042 |
| LSME (0.92 m) | 31 | 72 | 0.036 |
| AASHTO T294 | 31 | 32 | 0.018 |
| Foundry Slag | | | |
| FWD | 35 | 119 | 0.022 |
| LSME (0.46 m) | 35 | 20 | 0.265 |
| LSME (0.92 m) | 35 | 29 | 0.130 |
| AASHTO T294 | 35 | 30 | 0.022 |
| Grade 2 Gravel | | | |
| FWD | 104 | 143 | 0.038 |
| LSME (0.23 m) | 104 | 28 | 0.770 |
| LSME (0.30 m) | 104 | 60 | 0.140 |
| LSME (0.46 m) | 104 | 68 | 0.058 |
| AASHTO T294 | 104 | 157 | 0.014 |

To compare the elastic moduli under similar levels of strain and stress, the small-strain modulus ($M_{max}$) of each material was estimated for the average stress condition existing in the field (the field bulk stresses are summarized in Table 2) using the backbone curves in Seed et al. (1986). The backbone curves describe the ratio of shear modulus at a given shear strain ($G_{\gamma'}$) to the maximum shear modulus ($G_{max}$) as a function of shear strain. The shear strain in each test was computed using:

$$\gamma' = (1+\upsilon)\varepsilon_v \tag{2}$$

where $\upsilon$ is the Poisson's ratio and $\varepsilon_v$ is the vertical elastic strain in the subbase layer (Kim and Stokoe 1992). The implicit assumption in this approach is that the ratio $M/M_{max}$ is comparable to ratio $G_{\gamma'}/G_{max}$. The backbone curve for sand in Seed et al. (1986) was used for the sand-like bottom ash and foundry slag, whereas the backbone curve for gravel was used for the Grade 2 gravel. For the bottom ash and foundry slag, the field bulk stress is lower than the lowest bulk stress applied in the laboratory resilient modulus test. Thus, for these materials, the elastic modulus at the field bulk stress was estimated by extrapolation using the power function in Eq. 1.

The $M_{max}$ obtained using this approach are tabulated in Table 4 for each material. For the LSME, the $M_{max}$ for a given material are similar regardless of the layer thickness, except for the thinnest layer of Grade 2 gravel (h = 0.46 m). This similarity supports the effectiveness of the correction method to account for strain effects. The $M_{max}$ from the FWD is slightly (approximately 1.6 times) higher than the $M_{max}$ obtained from the LSME for all materials, and is appreciably higher (approximately 4 times) than $M_{max}$ obtained from the laboratory test following AASHTO T294 for the bottom ash and foundry slag. For Grade 2 gravel, $M_{max}$ from the FWD is slightly (approximately 1.3 times) higher than $M_{max}$ obtained from the laboratory test following AASHTO T294. The similarity of the $M_{max}$ from the FWD and the LSME suggests that the LSME provides a realistic assessment of elastic moduli operative in the field.

The cause of the difference between the laboratory-measured resilient modulus and the elastic moduli back calculated from the LSME and field tests for the industrial byproducts is not known. Inaccuracy in the extrapolation to lower bulk stresses may be responsible. There may also be some aspect of the particle composition of the byproducts that is different from those characteristic of the predominantly silica-based sands that form the basis for the power function in Eq. 1 and the backbone curve for sands in Seed et al. (1986). Nevertheless, moduli for the byproducts obtained using the laboratory resilient modulus test tend to be lower than those operative at the prototype and field scales. Thus, pavement designs incorporating similar byproducts that have employed moduli from laboratory resilient modulus tests should be conservative.

## Conclusion

The data from this study indicate that the elastic modulus of granular materials used in pavement systems depends on the state of stress and the strain amplitude. Comparison of elastic moduli measured in a conventional laboratory test to those operative at the prototype and field scales requires that state of stress and strain amplitude be comparable. Differences in strain amplitude can be dealt with by applying an empirical correction using backbone curves for granular materials. The effects of stress are handled by limiting comparisons only to elastic moduli measured at a comparable state of stress. However, the laboratory resilient modulus test does not always provide elastic moduli for the range of bulk stresses encountered in the field. In such cases, an estimate of the elastic modulus at the field state of stress can be obtained by extrapolation using a power function.

Table 4 – *Low Strain Elastic Modulus Obtained at Field Bulk Stress*

| Method | Elastic Modulus (MPa) | Shear Strain, γ' (%) | Shear Modulus Ratio | Maximum Modulus, $M_{max}$ (MPa) |
|---|---|---|---|---|
| Bottom Ash, Bulk Stress = 31 kPa | | | | |
| FWD | 108 | 0.038 | 0.48 | 225 |
| LSME (0.46 m) | 28 | 0.175 | 0.18 | 156 |
| LSME (0.69 mm) | 60 | 0.063 | 0.39 | 154 |
| LSME (0.80 m) | 68 | 0.053 | 0.44 | 155 |
| LSME (0.92 m) | 72 | 0.045 | 0.46 | 157 |
| AASHTO T294 | 32 | 0.018 | 0.60 | 53 |
| Foundry Slag, Bulk Stress = 35 kPa | | | | |
| FWD | 119 | 0.029 | 0.57 | 209 |
| LSME (0.46 m) | 20 | 0.352 | 0.15 | 133 |
| LSME (0.92 m) | 29 | 0.173 | 0.23 | 130 |
| AASHTO T294 | 30 | 0.029 | 0.57 | 53 |
| Grade 2 Gravel, Bulk Stress = 104 kPa | | | | |
| FWD | 143 | 0.049 | 0.30 | 477 |
| LSME (0.23 m) | 28 | 1.001 | 0.07 | 400 |
| LSME (0.305 m) | 60 | 0.182 | 0.16 | 375 |
| LSME (0.46 m) | 68 | 0.075 | 0.23 | 296 |
| AASHTO T294 | 157 | 0.018 | 0.43 | 365 |

Even when corrections are applied, the elastic modulus obtained from a laboratory resilient modulus test tends to be lower than the operative elastic modulus obtained by back-calculation from prototype tests (e.g., the LSME) and field tests using the FWD. For conventional gravels used as subbase materials, the difference between the elastic moduli measured in the laboratory and field is small. However, for sand-like industrial byproducts, the field elastic moduli can be as much as four times higher than that measured in a laboratory resilient modulus test.

**Acknowledgment**

The Wisconsin Highway Research Program provided financial support for the study described in this paper. However, the conclusions and recommendations are those of the authors and do not reflect the opinions or policies of WisDOT. Alliant Energy Corporation supplied the bottom ash, Grede Foundries Inc. supplied the foundry slag, and Yahara Materials supplied the Grade 2 gravel. The assistance provided by Alliant Energy, Grede Foundries, and Yahara Materials is greatly appreciated. The LSME experiments described in this paper were conducted in the University of Wisconsin Structures and Materials Testing Laboratory (SMTL). Professor Steven Cramer (Director of SMTL) and Mr. William Lang (Manger of SMTL) provided valuable assistance during the study.

**References**

Ali, N. A., and Khosla, N. P., 1987, "Determination of Layer Moduli Using a Falling Weight Deflectometer," *Transportation Research Record,* 1117, Transportation Research Board, National Research Council, Washington, DC, pp. 1-10.

Bush, A. J. and Alexander, D. R., 1985, "Pavement Evaluation Using Deflection Basin Measurements and Layered Theory," *Transportation Research Record,* 1022, Transportation Research Board, National Research Council, Washington DC, pp. 16-29.

Daleiden, J. F., Killingsworth, B. M., Simpson, A. K., and Zamora, R. A., 1994, "Analysis of Procedures for Establishing In Situ Subgrade Moduli,' *Transportation Research Record*, 1462, Transportation Research Board, National Research Council, Washington, DC, pp. 102-107.

Edil, T., Benson, C., Bin-Shafique, M., Tanyu, B., Kim, W., and Senol, A. (2002), Field Evaluation of Construction Alternatives for Roadway Over Soft Subgrade, *Transportation Research Record*, 1786, Transportation Research Board, National Research Council, Washington, DC, pp. 36-48.

Edil, T. B. and Luh, G. F., 1978, "Dynamic Modulus and Damping Relationships for Sands," *Proceedings of the Specialty Conference on Earthquake Engineering and Soil Dynamics*, ASCE, Reston, VA, pp. 394-409.

Hardin, B. O. and Drnevich, V. P., 1972, "Shear Modulus and Damping in Soils: Design Equations and Curves," *Journal of the Soil Mechanics and Foundations Division*, ASCE, Vol. 98, No. 7, pp. 667-692.

Houston, W., Mamlouck, M., and Perera, R., 1990, "Laboratory versus Nondestructive Testing for Pavement Design," *Journal of Transportation Engineering*, ASCE, Vol. 118, No. 2, pp. 207-222.

Huang, Y. H., 1993, *Pavement Analysis and Design,* Prentice Hall, Inc., Englewood Cliffs, New Jersey.

Kim, D. S., and Stokoe II, K. H., 1992, "Characterization of Resilient Modulus of Compacted Subgrade Soils Using Resonant Column and Torsional Shear Tests," *Transportation Research Record,* 1369, Transportation Research Board, National Research Council, Washington, DC, pp. 83-91.

Negussey, D. and Jahanandish, M. 1993, "Comparison of Some Engineering Properties of Expanded Polystyrene with Those of Soils," *Transportation Research Record,* 1418, National Research Council, Washington, DC, pp. 43-50.

Newcomb, D. E., 1986, *Development and Evaluation of Regression Methods to Interpret Dynamic Pavement Deflections,* Ph.D. Dissertation, Department of Civil Engineering, University of Washington, Seattle, Washington, USA.

Seed, H. B. and Idriss, I. M., 1970, "Soil Moduli and Damping Factors for Dynamic Response Analyses," Report No. EERC 70-10, University of California, Earthquake Engineering Research Center, Berkeley, CA, USA.

Seed, H. B., Wong, R. T., Idriss, I. M. and Tokimatsu, K., 1986, "Moduli and Damping Factors for Dynamic Analyses of Cohesive Soils," *Journal of Geotechnical Engineering,* ASCE, Vol. 112, No. 11, pp. 1016-1032.

Texas Transportation Institute, 1991, *MODULUS 4.0, User's Manual,* Texas Transportation Institute, Texas A&M University, College Station, TX, USA.

Uzan, J., Scullion, T., Michalak, C. H., Paredes, M., Lytton, R. L., 1988, "A Microcomputer Based Procedure for Backcalculating Layer Moduli from FWD Data," Research Report No. 1123-1, Texas Transportation Institution, College Station, Texas, USA.

Zou, Y., Small, J. C. and Leo, C. J., 2000, "Behavior of EPS Geofoam as Flexible Pavement Subgrade Material in Model Tests," *Geosynthetics International,* Vol. 7, pp. 1-22.

Gonzalo R. Rada,[1] Jonathan L. Groeger,[2] Peter N. Schmalzer,[3] and Aramis Lopez[4]

# Resilient Modulus Testing of Unbound Materials: LTPP's Learning Experience

**Reference:** Rada, G. R., Groeger, J. L., Schmalzer, P. N., and Lopez, A., **"Resilient Modulus Testing of Unbound Materials: LTPP's Learning Experience,"** *Resilient Modulus Testing for Pavement Components, ASTM STP 1437*, G. N. Durham, W. A. Marr, and W. L. De Groff, Eds., ASTM International, West Conshohocken, PA, 2003.

**Abstract:** Resilient modulus is a key data element for characterizing unbound pavement materials within the LTPP program. Although the test has been around for nearly three decades, its implementation within the program has been a challenge. A suitable test protocol was not available when the program began in 1987. It was incorrectly assumed in the early years that equipment manufactured for the test would work as intended. It was also incorrectly assumed that properly operating equipment and knowledgeable personnel imply good data. This paper has been prepared to share LTPP's experience over the past 14 years in achieving repeatable, high-quality resilient modulus data. Specific issues addressed in the paper include the test protocol, laboratory startup and quality control procedures, quality control and quality assurance processes, and comprehensive guidelines contained in an easy-to-use, interactive CD-ROM.

**Keywords:** resilient modulus, laboratory testing, unbound materials, quality control and quality assurance, guidelines, LTPP

## Introduction

The Long-Term Pavement Performance (LTPP) program is a 20-year study of pavement performance and the factors that affect it. Its main goal is to provide the data necessary to explain how pavements perform and why they perform as they do. To meet this goal, the program has established nearly 2500 test sections on in-service highways throughout North America. The data collected at each of those test sections are intended to characterize pavement performance and the conditions associated with that

[1] Assistant Vice President, LAW PCS, 12104 Indian Creek Court, Suite A, Beltsville, MD 20705.

[2] Vice President, Axiom Decision Systems, Inc., 6420 Dobbin Road, Suite E, Columbia, MD 21045.

[3] Project Engineer, LAW PCS, 1575 Delucchi Lane, Suite 201, Reno, NV 89502.

[4] LTPP Team Leader, Federal Highway Administration, 6300 Georgetown Pike, McLean, VA 22101.

performance.

Data characterizing the pavement materials obtained via sampling and laboratory testing are of paramount importance to meeting the program's goal. In the case of unbound materials, one of the most important data elements is the resilient modulus ($M_r$). This value is a key input to the current AASHTO design procedures. It is also a basic material property that can be used in mechanistic analysis of multi-layered systems for predicting elastic deformations that ultimately correlate to pavement performance.

Although the test has been around for almost three decades, its implementation within the program was a challenge. For starters, there was no suitable test protocol when the program began in 1987, which meant a significant level of effort was spent in the preparation of such a protocol. It was also incorrectly assumed early in the program that equipment manufactured for $M_r$ testing would work as intended. The lesson learned from this mistake led to development of the LTPP laboratory startup and quality control (QC) procedure, which is designed to verify the operating accuracy of all essential system components in a logical manner and increase the user's confidence in the resulting data. Besides its routine use within the program, the procedure has also been implemented by a number of states as well as academia and private laboratories.

LTPP's efforts to ensure the highest quality $M_r$ data did not stop after the implementation of the startup and QC procedure. Indeed, another lesson learned shortly after its implementation was not to assume that properly operating equipment and knowledgeable personnel imply good data. More to the point, a thorough review of the data revealed, albeit infrequently, the presence of anomalies. This led to the development of detailed quality control and quality assurance (QC/QA) processes and software to check over 2000 data components to ensure accuracy and consistency.

Clearly, much has been learned within the LTPP program in the past 14 years with regards to the $M_r$ characterization of unbound materials. Many of the lessons learned have been shared with the pavement community, but certainly not all. To address that shortcoming, an effort to develop comprehensive guidelines on the $M_r$ test for unbound materials was recently completed. The guidelines are contained in an easy-to-use, interactive CD-ROM and they are being distributed to a wide audience – highway agencies, universities, industry, and consultants.

This paper expands on each of the topics addressed above – test protocol, laboratory startup and quality control procedure, quality control and assurance processes, and $M_r$ guidelines on CD-ROM. Its main objective is to share LTPP's learning experience in consistently achieving repeatable, high-quality $M_r$ data with the pavement community.

## Test Protocol

At the outset of LTPP, program planners designated $M_r$ testing as a key input for the project. This was determined because of the usefulness of the test results in empirical and mechanistic pavement design procedures. During this time, AASHTO T 274 was the predominant protocol used for $M_r$ testing of unbound pavement materials. After careful review of the procedure by a group of materials testing experts, it was determined that the Standard Method of Test for Resilient Modulus of Subgrade Soils, AASHTO Designation T 274 (discontinued in 1990) was not adequate for the LTPP program. The standard contained too great a risk of potential variability because of its wording. As such, it was decided that a new procedure was needed for the LTPP program.

In 1989, a group of materials testing experts again convened to produce what is now known as the Long-Term Pavement Performance Protocol P46: Resilient Modulus of Unbound Granular Base/Subbase Materials and Subgrade Soils. The first version attempted to make the procedure as standard as possible and eliminated many of the opportunities for deviation invited by T 274. After a lengthy review process, the first version of P46 was issued later that year. Four laboratories under contract to LTPP used the protocol for several months in a pilot study. From the results of this pilot study, many recommendations for improvement to the procedure were developed. Based upon these recommendations, the protocol was thoroughly revised and re-issued in 1992.

The 1992 protocol was used for several years in the LTPP program and many additional lessons were learned as a result. In 1996, another significant review and revision cycle was undertaken. Many improvements were made based upon the experience of four years of testing. Thereby, the final version of the protocol, as it exists today, was issued by LTPP. The protocol in its existing condition incorporates a vast amount of theoretical and practical knowledge gleaned from testing over 3000 samples.

The protocol contains many conditions and requirements that apply only to the LTPP program. For example, measurement of deformation outside of the test chamber is a requirement that is very specific to the goals and objectives of the LTPP program. Because of the large numbers of samples to be tested, the expert task group that reviewed the protocol decided that this was the most practical and efficient method. However, this method may not apply to all test conditions.

Subsequent to the publication of the final protocol, an AASHTO committee undertook the task of using the LTPP protocol to develop a new resilient modulus protocol for use in the AASHTO materials specifications document. This protocol was meant to replace the T 274 protocol. This new protocol, Standard Method of Test for Determining the Resilient Modulus of Soils and Aggregate Materials, AASHTO Designation T 307, was issued in 1999. While the standard contains many similarities to P46, the authors of T 307 took great care to incorporate other practical applications to the procedure to make it user-friendlier for a wide variety of users. An example is the allowance of the use of pneumatic systems in T 307, which are prohibited in P46.

P46 describes the laboratory preparation and testing procedures for $M_r$ determination of unbound granular base and subbase materials and subgrade soils under specified conditions representing stress states beneath pavements subjected to moving wheel loads. The methods described in the protocol are applicable to undisturbed samples of natural and compacted subgrade soils and to disturbed samples of unbound base and subbase and subgrade soils compacted in the laboratory. Stress levels used for testing specimens are based upon the location of the specimen within the pavement structure. Samples located within the base and subbase are subjected to different stress levels as compared to those specimens that are from the subgrade. Generally, specimen size for testing depends upon the type of material based upon the gradation and the plastic limit of the material.

Protocol P46 covers the following topics: scope, testing locations, definitions, applicable documents, unbound materials testing prerequisites, apparatus, preparation of test specimens, test procedures, calculations, reporting, and compaction of test specimens. It is suitable for use by organizations wishing to perform their tests exactly as they were conducted by LTPP for correlation or other purposes. However, its use as a general test method for use by all organizations should be considered very carefully.

As mentioned previously, T 307 was developed primarily by modifying LTPP Protocol P46. Many features of the standard are similar to P46 while some sections have been modified to facilitate use of the procedure by a broader range of organizations. At the time of the development of this tool, this is the only test standard adopted by AASHTO to determine resilient modulus values from pavement materials.

There are several other test procedures developed, or under development, throughout the world. Each procedure has its own strengths and weaknesses. For example, NCHRP 1-28 [Barksdale et al. 1998] has proposed new procedures for testing asphalt and unbound materials. Several other researchers have also put forth revised test procedures. For now, it seems that AASHTO T 307 is the state-of-the-practice within the United States. P46 can be downloaded from the Federal Highway Administration (FHWA) LTPP web site, while T 307 is available from AASHTO.

**Laboratory Startup and Quality Control Procedure**

Resilient modulus testing of unbound materials within the LTPP program began shortly after completion of the P46 test protocol. A significant level of effort had been spent on developing the protocol, thus high-quality test results were anticipated. Unfortunately, it was incorrectly assumed at the time that equipment manufactured for $M_r$ testing would work as intended. A review of the data obtained after testing commenced identified numerous problems, which in turn raised questions over the accuracy and reliability of the collected data.

A subsequent investigation revealed that most of the problems could be traced to incorrect settings in the equipment electronic filters. These incorrect settings resulted in problems such as non-symmetrical loading conditions, peak deformation occurring prior to peak loading, deformation response occurring for shorter time period than loading, deformation response fluctuations, and a deformation-clipping phenomenon. Figures 1 and 2 illustrate a couple of the problems identified during the investigation.

The lessons learned from this investigation led to the development of the laboratory startup and quality control procedure, which is intended to ensure the accuracy and reliability of the raw data produced while testing materials using closed-loop servo-hydraulic systems. The procedure is designed to verify the operating accuracy of all essential system components in a logical manner. Each part of the system is verified individually and then the entire system is checked to make sure all of the parts work together.

The procedure is divided into the three distinct components described below. A more detailed description of the procedure and its components is presented in [Alavi et al. 1997].

- Electronics System Performance Verification Procedure – This procedure characterizes the frequency response of the signal conditioners and data acquisition component of the test system. The procedure is generally used prior to the initiation of a $M_r$ testing program. As long as all of the electronics of the test system remain the same, this procedure does not need to be repeated on a continuing basis. However, the

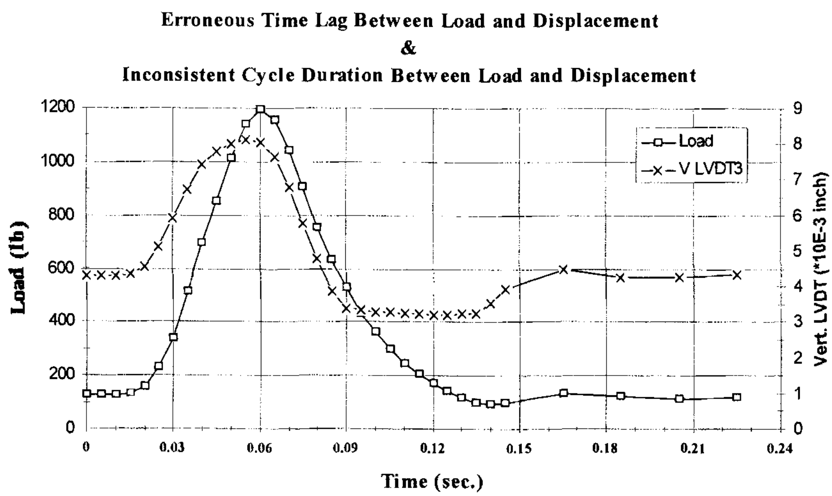


*Figure 1 – Example of Peak Deformation Occurring Prior to Peak Loading*

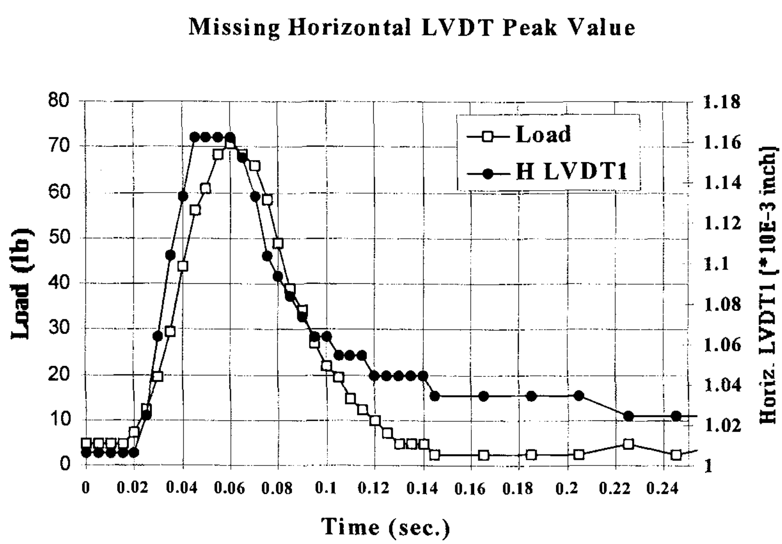


*Figure 2 – Example of Typical Deformation Clipping Phenomenon*

procedure should be conducted at least every year or when any part of the electronics is replaced or modified. Also, this procedure is performed when other circumstances suggest that the electronics may be suspect. An electronics technician well versed in data acquisition systems is needed to perform the procedure. The amount of time required to perform this procedure depends on the complexity of the test system and experience of the technician, but on average, it takes about 8 to 10 hours to complete.

- Calibration Check and Overall System Performance Verification Procedure – Dynamic testing procedures require a system made up of many different pieces of equipment: load frame, load cells, hydraulic system, deformation devices, triaxial pressure chamber, temperature chambers, computer, etc. For the calibration check and overall system performance verification procedure, individual elements of the test equipment are checked first followed by the overall test setup to verify that the system is producing the expected responses. The individual subcomponents addressed include: verification of displacement transducer calibration check, load cell zero check, load cell calibration check, verification of load cell calibration check (static), load versus deformation response check (dynamic), system dynamic response check, and triaxial pressure chamber check. By first checking the individual components of the test system, many problems that would be encountered during actual dynamic testing can be identified and eliminated prior to checking the overall system. This procedure is generally used prior to initiation of a testing program and subsequently on a continuing basis (i.e., monthly) to verify the system response. On average, the procedure requires approximately 16 hours to complete
- Proficiency Procedure – The ability of laboratory personnel to conduct dynamic testing is evaluated in this procedure, prior to initiation of a testing program and subsequently on a continuing basis to verify the operator's ability to conduct $M_r$ testing. The procedure requires approximately 2 days to complete. The primary goals of the procedure are (1) to ensure that the test system and technicians are capable of performing a test procedure, and (2) to develop a benchmark performance standard against which the laboratory can be evaluated on an on-going basis. This is a very important part of any QC/QA system.

As part of the electronics system verification procedure, the signal conditioning channels, data acquisition processes, and transducers are checked for proper operation. On completion, the calibration check and overall system performance verification procedure is performed. Load and displacement measuring devices; (i.e., load cells, linear variable deformation transducers or LVDTs) are checked for linearity and proper calibration. The ability of the software to control and acquire data is also assessed. When the process of verifying the individual system components is complete, the overall capability of the machine to conduct a specific experiment is assessed through specially designed static and dynamic experiments on materials with known properties. Once the system has been evaluated, the proficiency phase of the procedure addresses the competence of the laboratory personnel to prepare and test samples. Through the use of this procedure, all of the components necessary to obtain repeatable, accurate $M_r$ test results are verified.

The startup and QC procedure enables laboratories to verify their testing systems and procedures prior to the start of production testing by using a comprehensive and logical process. It can also be used to perform ongoing QC checks of the equipment and testing processes being used by the laboratory during the production testing process. From use of the procedure to date, many potential sources of error have been identified and rectified prior to starting a testing program, thus potentially saving a large amount of effort and resources. They include:

- Electronic errors – over-ranged load cells, inadequate filters (amplitude attenuation), and unmatched filters (excessive time delay between channels).
- Software errors – inadequate software control of load, inadequate sampling rates, raw data without units, lack of gain control adjustment during testing, and improper raw data format, command values were saved rather than feedback values.
- Mechanical errors – system not fast enough to apply proper haversine loads, oversized servo-valve, friction in servo-valve piston, friction in triaxial cell seals, misalignment caused by improperly designed triaxial cell, excessive deformation, up to 76% of deformation due to bending of triaxial cell base plate, excessive deformation due to unrestrained fixture, slippage of LVDT holders, lack of control of pressure transducer, and air pressure regulator malfunction.

In summary, there are several obvious benefits of using the startup and QC procedure. The first is that the procedure provides guidelines for standardization of an entire test process. It also provides a benchmark performance standard for equipment. If implemented correctly, it can minimize equipment and operator variability and thus provide greater confidence in the test results and their application in research or design.

**Quality Control and Assurance of Data Components**

The laboratory startup and QC procedure is intended to ensure the accuracy and reliability of the raw $M_r$ data. Its implementation, however, does not imply that $M_r$ data produced by properly operating equipment and knowledgeable personnel will be error free. Indeed, studies conducted shortly after implementation of the startup and QC procedure revealed, albeit infrequently, the presence of data anomalies.

Due to the inherent complexity of the $M_r$ test procedure and the associated equipment, quality control and quality assurance is paramount to producing reliable, repeatable $M_r$ test values. There are several types of QC/QA checks that should be addressed in this process. The following outlines some of the QC/QA processes implemented within the LTPP program based on lessons learned over the past 14 years. Implementation of these processes is recommended for every laboratory performing the $M_r$ test.

- General QC/QA – A laboratory performing $M_r$ testing should give consideration to participation in an intra and inter-laboratory testing program to verify the calibration of the equipment and procedures with respect to other laboratories. It may also be desirable to manufacture or procure a standard specimen to test on a continuing basis to detect gross changes in the performance of the system over time.
- Sample Preparation – It is highly recommended that a standard preparation worksheet be utilized to walk the technician through the process. It is best if the process can be automated through Excel or some other software. This allows the technician to

automatically perform standard mathematical computations, thus eliminating the possibility of calculation errors. After sample preparation and compaction, another technician or supervisor should check the entries for completeness and accuracy.

- Operator Checks – The $M_r$ test is not a "push the button and walk away" type of test procedure. There are many things that happen during the testing process that must be monitored on an ongoing basis. These include the following items:
  + Load Pulse Reasonableness – Many modern test systems allow the operator to fully automate the testing process. However, closed-loop servo-hydraulic systems also rely heavily on the appropriate setting and maintenance of the PID controls (also known as "gain" settings). The PID settings must be "tuned" for every sample and test configuration. One of the reasons for the number of conditioning load pulses necessary to conduct $M_r$ testing is to give the operator a chance to tune the system for a particular sample. This tuning is not static; as the test progresses, the PID values need to be adjusted to ensure an adequate haversine waveform. This adjustment is critical to obtain repeatable $M_r$ test values. During testing, the load pulse should be very close to a haversine shape; within 10 percent of the expected shape. In addition, the load pulse should be within 10 percent of the expected maximum load. Finally, the required contact load should be adhered to as close as possible but not further than 10 percent from the intended value. Many test systems today allow the operator to monitor load and displacement on the computer screen and some even provide error bands around the load to alert the user of out of tolerance loading. These "scopes," as they are sometimes referred to, should be closely monitored by the technician during conduct of the test. If the load pulse is not as prescribed the operator has a great deal of control using the PID settings to adjust the controls to produce a suitable waveform.
  + Deformation Response Reasonableness – Like the load pulse, the deformation response of the system should be monitored. Although the operator has no direct control over the deformation response, they should be monitored to detect LVDTs out of range, slippage of the LVDT holder, "sticking" of the LVDT, LVDTs out of balance, etc. If any abnormalities are detected with the deformation transducers, the operator should stop the test and correct the problem. Usually in these cases the test will have to be re-run.
  + Confining Pressure Conformity – The confining pressure should be monitored to ensure that the proper pressure is maintained, and that the system is reaching the targeted pressure in a timely manner. $M_r$ values are very susceptible to changes in confining pressure values and the achievement of accurate, consistent pressures is critical in modulus testing. The actual confining pressure should be within 5 percent of the targeted value. If the correct pressures are not achieved, or are not reached in a reasonable amount of time, the test should be stopped and the operator should fix the problem.
  + Sample Integrity – During the test procedure, the operator should monitor the sample to ensure that it has not failed. This is primarily accomplished by monitoring the total permanent deformation experienced by the specimen. If the specimen incurs greater than 5 percent strain, the specimen is considered failed and the test should be stopped. Usually specimen failure cannot be seen by the naked eye – rather it is determined by monitoring the average deformation values. In order

to perform the $M_r$ test accurately, the operator must be cognizant of the testing process and monitor the test as it progresses. This is critical to ensuring accurate, consistent $M_r$ testing values.

- Post Processing – Following completion of the test procedure, in the LTPP program the resultant data is analyzed using an automated QC/QA program. Most laboratories have not prepared such a program nor does one exist on the market today. An outline of checks that could be conducted by such a program follows:
  - Data Completeness – File should be read to ensure it is complete and is not corrupt.
  - Load Pulse Reasonableness – Verify that load pulse is within allowable tolerance range. To do this, plot actual load values versus time for a representative cycle(s) at each load. Next, construct a theoretical ideal loading pulse for each load sequences from the maximum load and the 0.1-second loading duration specified in the LTPP P46 protocol. The peak theoretical load is matched in time with the peak-recorded load of a given sequence. An acceptance tolerance band is then created around the theoretical load pulse that is used to flag suspect data falling outside of the band. Development of the minimum and maximum values of the acceptance band is based on the following considerations:
    - *Acceptance tolerance range:* ±10 percent variation from the theoretical load is judged to be acceptable.
    - *Servo valve response time:* ±0.006 second time shift in load from the theoretical load pulse is reasonable to allow for the physical limitations on the response time of the servo-hydraulic system.
    - *Resolution of the electronic load cell:* Resolution of electronic load cells used in $M_r$ testing of unbound materials is generally ± 4.4 N. Therefore, a range of twice the minimum load cell resolution (± 8.8 N) is considered acceptable.
    - *Logic:* Minimum load allowed is 0 N.

    For each time step in the load curve, the tolerance range from all of these components is computed. The maximum value of these three components is selected as the upper tolerance limit, while the minimum value is used for the lower limit at each time step. Over the entire range of loading, five points are allowed to be out of tolerance before the load cycle is considered failed. An example of this check is shown in Figure 3.
  - Deformation Response Reasonableness – Verify that deformation pulse is within allowable tolerance range. To do this, plot actual deformation values versus time for a representative cycle(s) at each load level. Next, using the equation for a haversine waveform, construct a theoretical ideal deformation pulse for each load sequences from the maximum load and the 0.1-second loading duration specified in the LTPP P46 protocol. The peak theoretical deformation is matched in time with the peak-recorded deformation of a given sequence. An acceptance tolerance band is then created around the theoretical deformation pulse that is used to flag suspect data falling outside of the band. Development of the minimum and maximum values of the acceptance band is based on the following considerations:
    - *Acceptable tolerance range:* ±10 percent variation from the theoretical deformation is judged to be acceptable.
    - *Logic:* Minimum deformation allowed is 0.

    For each step in the deformation curve, the tolerance range from these components

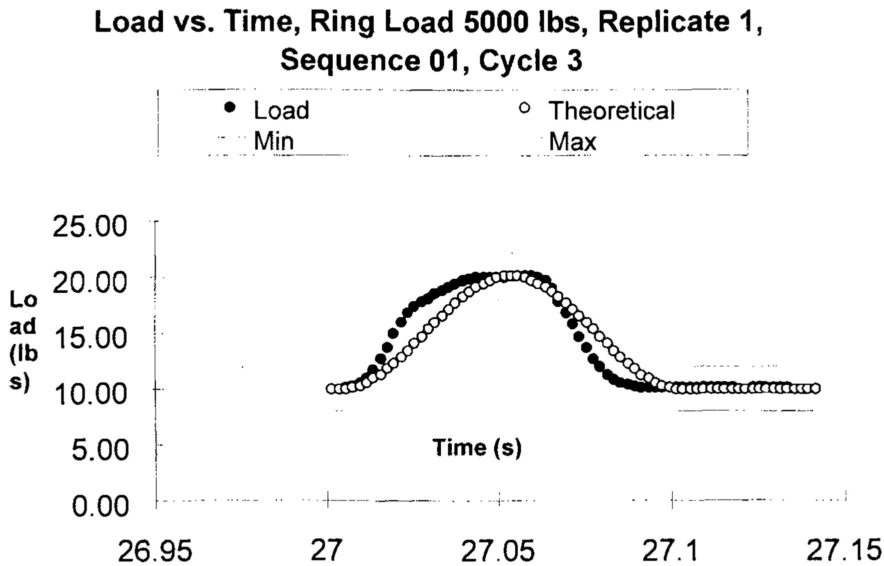


*Figure 3 – Example of Load Pulse Response Reasonableness Check*

is computed based upon the maximum deformation point for the cycle. The maximum value of these checks is selected as the upper tolerance and the minimum value of these checks is selected as the lower limit for each time step. The actual deformation is then compared with the tolerances at each time step to determine conformance. Over the entire range of loading, five points are allowed to be out of tolerance before the deformation cycle is considered failed. This test is performed for all deformation devices.

+ Load versus Deformation Time Lag – Determine the maximum load point for a given cycle and extract the corresponding time stamp. Determine the maximum deformation for the same cycle and extract the corresponding time stamp. Subtract the maximum deformation point time stamp from the maximum load point time stamp. This value should be positive and less than 0.008 s. If the time delay is greater than 0.008 s, most likely there is a problem with the system electronics or software. If the time delay is negative, it means that the maximum deformation is occurring prior to the maximum load, a practical impossibility, which again would lead to the suspicion that there is a problem with the system electronics or software. This analysis should be performed for each deformation device.
+ Review of Data Computation Process – In this analysis, the raw data are manually reduced and the results compared to the summary data developed by the computer software system. For $M_r$ testing, the following values should be analyzed as is practical: cyclic load, maximum load, contact (seating) load, deformation response (for all deformation devices), confining pressure (soils and aggregate testing), temperature (asphalt), deviator stress (soils and aggregate testing), strain (soils and

aggregate testing), and resilient modulus. These values should be derived from the raw data using procedures stated in the protocol.

+ Conformance to Test Parameters – After the summary data have been verified by hand, adherence to the protocol parameters should be analyzed. This analysis is undertaken to determine how close the laboratory is to the protocol test requirements. All test parameters should be within 5% of the test requirements. The following items should be checked as appropriate for a particular protocol: target deviator stress and target confining pressure.
+ Deformation Device Variation – The deformation devices should be stable within a given loading regime and test cycle. In this analysis, the coefficient of variation of the deformation devices is calculated at a given test sequence. To perform this analysis, select the deformation values for all collected cycles of data at a given test sequence. Determine the coefficient of variation of the values. Repeat for all test sequences and deformation devices. Vertical deformation readings from each of the sequences should be checked to ensure that the deformation devices are recording values with averages that have a coefficient of variation less than 2.5 percent.
+ Deformation Balance – This test is only conducted if more than one deformation device is mounted on the system. All deformation devices used for this comparison should be mounted in approximately the same location in the system, such as on top of triaxial chamber or on test specimen. In this analysis, the balance of the deformation devices is evaluated. If deformation devices are mounted in approximately the same location on the sample or in the system, it can be reasonably expected that they would experience similar deformation measurements. For a given deformation cycle, extract the cyclic deformation value from the summary (calculated) data. The collected deformation readings are checked to ensure that acceptable vertical deformation ratios are being measured. Acceptable vertical deformation ratios ($R_v$) are defined as $R_v = Y_{max}/Y_{min} < 1.30$, where $Y_{max}$ equals the larger of the two vertical deformations and $Y_{min}$ equals the smaller of the two vertical deformations. This analysis should be performed for each deformation device in order. If more than two deformation transducers are used, one should be selected as the reference and the others compared to this reference. All values should be within $\pm$ 30% of the reference.
+ Reasonableness of Test Results – The final results of the test procedure should be reviewed for reasonableness. This check can only be conducted by personnel who are familiar with the test procedure. For soils and aggregate testing, a basic check can be made of the $M_r$ versus confining pressure results. Generally, $M_r$ values at lower confining pressures should be lower than those at higher confining pressures (for a given deviator stress). In this experiment, the results should look reasonable to the user. Any anomalies should be investigated.

- Range Checks – In the LTPP program, a great deal of effort was used to define valid ranges for the data produced. Other $M_r$ testing agencies may find these range checks useful to perform their own quality control procedures. Table 1 contains a list of all test parameters along with their applicable range checks. These ranges apply primarily to LTPP Protocol P46 but can also be applied to AASHTO T307. The definitions of the terms in Table 1 are contained in Protocol P46.

*Table 1 – Range Checks for $M_r$ Test Parameters*

| Data Item | Units | Subgrade | | Base/Subbase | |
|---|---|---|---|---|---|
| | | Type 1[1] | Type 2[2] | Type 1[1] | Type 2[2] |
| Specimen Diameter | mm | 146.0 to 158.0 | 66.0 to 80.0 | 146.0 to 158.0 | 66.0 to 80.0 |
| Specimen Area | Sq. mm | 16742 to 19600 | 3420 to 5030 | 16742 to 19600 | 3420 to 5030 |
| Specimen Length | mm | 295.0 to 315.0 | 137.0 to 158.0 | 295.0 to 315.0 | 137.0 to 158.0 |
| Contact Load | N | 10.0 to 143.0 | 0.1 to 33.0 | 10 .0 to 568.0 | 0.1 to 122.0 |
| Contact Stress | KPa | 0.5 to 8.0 | 0.1 to 8.0 | 0.1 to 32.0 | 0.1 to 32.0 |
| Cyclic Load | N | 182.0 to 1287.0 | 32.4 to 297.0 | 263.0 to 5049.0 | 60.7 to 1099.0 |
| Cyclic Stress | KPa | 9.0 to 72.0 | 9.0 to 72.0 | 16.0 to 270.0 | 16.0 to 270.0 |
| Max. Axial Load | N | 202 to 1430 | 36.0 to 330.0 | 292.0 to 5610 | 67.5 to 1221.0 |
| Max. Axial Stress | KPa | 10.0 to 80.0 | 10.0 to 80.0 | 18.0 to 300.0 | 18.0 to 300.0 |
| Deformation | mm | 0.012700 to 0.63500 | 0.0080 to 0.63500 | 0.01270 to 0.63500 | 0.00800 to 0.63500 |
| Resilient Strain | mm/mm | 0.00004 to 0.00210 | 0.00005 to 0.00440 | 0.00004 to 0.00210 | 0.00005 to 0.00440 |
| Resilient Modulus | MPa | 7 to 415 | 7 to 415 | 7 to 415 | 7 to 415 |

[1]Type 1 = cohesionless subgrade, base and subbase material
[2]Type 2 = cohesive subgrade, base and subbase material

## $M_r$ Guidelines on CD-ROM

Many of the lessons learned within the LTPP program in the past 14 years regarding $M_r$ testing have been shared with the pavement community, but certainly not all. To address this shortcoming, comprehensive guidelines on the $M_r$ test for unbound granular materials were recently completed and are contained in an easy-to-use, interactive CD-ROM. The guidelines include details on the usefulness of test results in pavement design, background and usefulness of test procedure, and techniques that can be used to reduce the within- and between-laboratory variability.

The CD-ROM has been developed as seven educational modules that describe the salient features of the $M_r$ test. They are: (1) fundamentals of resilient modulus testing, (2) implementation of a resilient modulus testing program, (3) resilient modulus startup and quality control procedures, (4) repeated load triaxial testing , (5) quality control/quality assurance, (6) keys to a successful resilient modulus testing program, and (7) resilient modulus in pavement design. Each of these modules covers fundamental issues that should be addressed prior to and during $M_r$ testing. Most of the key issues covered in the modules have been addressed earlier in this paper, but not a summary of the keys to successful testing as contained in the LTPP $M_r$ CD-ROM. The following is a list of the top ten issues to address to help ensure a successful $M_r$ testing program.

- Implement Intensive Training – There are two primary types of training that should be addressed. First, the equipment manufacturer should provide ample training to laboratory personnel in the operation, maintenance, calibration, and safety precautions surrounding the equipment used for $M_r$ testing. This training should also be documented so that the laboratory can train other operators. Secondly, laboratory personnel should be trained in the conduct of the test, including sample preparation and compaction, and data analysis procedures. This training should be re-emphasized every so often as operators have a tendency to develop habits that may be detrimental to the acquisition of quality $M_r$ data over time. Internal training should be documented so as to create an institutional knowledge base for future use.
- Use the Right Equipment – $M_r$ test equipment should be tailored to do the job. One of the leading causes of problems with $M_r$ testing is the use of equipment that is not correctly configured. Usually this means that load cells, servo-valves or pressure transducers are not of the proper range and capacity. For example, there is little need to use a 5,000-lb load cell for a subgrade $M_r$ test in which the maximum load is around 60 lb. If configuration is not performed properly, this may lead to poor control of the system and possible instability of the test equipment. Using the right tool for the job will greatly ease problems associated with system control and data acquisition.
- Implement Startup and Quality Control Procedures – An important lesson learned from the LTPP $M_r$ testing experience was that it is imperative that electronics and mechanics of the test system are thoroughly verified prior to testing and proficiency of operators be evaluated through a proficiency program. This should be done even if the manufacturer assures the laboratory that the equipment meets specifications. The verification and evaluation is accomplished by performing the LTPP Startup and Quality Control Procedure. Many important characteristics of the test system are evaluated through the startup process. In fact, some problems would never be found by merely performing normal calibrations or selective portions of the startup procedures.
- Perform Equipment Calibration – This item goes hand-in-hand with the implementation of the startup procedure but is related more closely to frequent calibrations required by the equipment manufacturer and the test protocols. Load cells and transducers have the potential to be damaged and fatigued during normal testing operations. These items need to be calibrated on a regular basis to ensure that they are reading correctly and ensure the safe operation of the test machine. Regular calibration of sensitive components is sometimes overlooked, but it is a very important part of the equipment maintenance and operators should be very conscientious of this task.
- Organize System Documentation – Laboratory should keep all test system documentation in a safe place. This documentation is extremely handy should maintenance need to be performed or the system otherwise malfunctions. Without this documentation, training of new operators and trouble-shooting become very difficult.
- Verify the Data Analysis Software – Many equipment vendors supply data analysis software with their product. This software should be checked prior to implementation

to ensure that the calculations performed by the software are consistent with the test protocol. In addition, many programs use the "Max/Min" approach to data analysis. While this is a convenient approach for the software developer, it has the potential for problems when analyzing $M_r$ data. During testing, it is possible that the system may experience a significant overshoot of the load, and thus deformation. If this occurs and the max/min approach is used, the load and deformation values can be significantly affected. Therefore the method of data analysis presented in LTPP Protocol P46 and AASHTO T 307 is preferred and highly recommended to determine maximum, minimum, and cyclic stresses and strains. This method utilizes a "maximum and average" algorithm that takes care of any potential overshoot issues in data analysis.
- Involve Yourself in the Testing Process – Some consider $M_r$ a "push the button and walk away" procedure. It is highly recommended, however, that the operator monitor the test as it progresses in a careful manner. Many potential problems can occur during the conduct of the test that will not be readily apparent if the operator is not monitoring the results. In addition, for many test systems, it is required that the operator adjusts machine settings during the test. This is a very important part of the $M_r$ testing process.
- Pay Close Attention to Compaction Procedures – One of the greatest influences on $M_r$ values is the consistency of sample compaction. It cannot be overstated how important it is to have properly trained, conscientious individuals perform this crucial role. In addition, if the laboratory is participating in a round robin or similar testing exercise, it is extremely important that samples be compacted using similar equipment, procedures and compaction targets (density and moisture) as the other laboratories. While this may seem obvious, it is very difficult to implement in real life.
- Factor in the Resultant Force – When performing $M_r$ tests, it is easy to ignore the forces other than the axial load on a specimen. However, it is extremely important to factor in the resultant force when testing large samples. The test configuration and/or the data analysis program must take into account the forces resulting from the weight of the actuator rod and top cap as well as the influence of the confining pressure. A detailed description of the influence of these forces is contained in LTPP Protocol P46 and AASHTO T307. Attention to this detail is a must.
- Practice, Practice, Practice – Just like a good sports team, practice makes perfect. The $M_r$ testing procedure should be practiced many times prior to full-scale implementation within an organization. This practice will help work out bugs in the system, familiarize operators with test parameters, and lead to rapid acknowledgement of problems if they occur.

While this list is not meant to be an all-inclusive rundown of all the issues to keep an eye on when conducting $M_r$ testing, it is aimed at providing the reader with a summary of the most important issues that should be addressed. Successful $M_r$ testing is highly dependent on attention to detail. Acknowledging and confronting these issues prior to implementation of a $M_r$ program could save valuable time and resources.

Additional information about the LTPP Mr CD-ROM, titled *Guide for Determining Design Resilient Modulus Values for Unbound Materials* [LAW PCS 2002], can be obtained by contacting the Federal Highway Administration at ltppinfo@fhwa.dot.gov.

**Summary and Conclusions**

The purpose of this paper was to share LTPP's experience over the past 14 years with regards to the $M_r$ characterization of unbound pavement materials. Towards that end, the first part of the paper addressed the LTPP P46 test protocol, including its development through many years of experience a well as the various topics covered by the protocol. This protocol served as the primary basis for development of the AASHTO T 307 protocol, which is at present the state-of-the-practice in the United States.

The laboratory startup and quality control procedure developed by LTPP to ensure the accuracy and reliability of the raw $M_r$ data was also covered in the paper. Development of this procedure was triggered by findings early in the program that equipment manufactured for $M_r$ testing was not working as intended. The resulting procedure enables laboratories to verify their testing systems and methods prior to the start of production testing and, if necessary, to identify and correct electronic, software and/or mechanical errors.

Quality control and quality assurance processes developed and implemented within the LTPP program based on lessons learned since 1988 were outlined in the paper. These processes included general quality control and quality assurance, sample preparation, operator checks, data post-processing, and data range checks.

Finally, an easy-to-use, interactive CD-ROM containing comprehensive guidelines on the $M_r$ test for unbound granular materials was discussed. Particular emphasis was placed on a list of the top ten issues that need to be addressed to help ensure a successful $M_r$ testing program.

The information contained or referenced in this paper will help others achieve repeatable, high-quality $M_r$ data for unbound pavement materials. It is also the authors' opinion that such repeatable, high-quality data would not have been possible without the many experiences and lessons learned in the course of the LTPP program to date.

**References**

Alavi, S., Merport, T., Wilson, T., Groeger, J., Lopez, A., January 1997, "LTPP Materials Characterization Program: Resilient Modulus of Unbound Materials (LTPP Protocol P46) Laboratory Startup and Quality Control Procedure," Report No. FHWA-RD-96-176, U.S. Department of Transportation, Federal Highway Administration, McLean, Virginia.

Barksdale, R. D., Alba, J., Khosla, N. P., Kim, R. K., Lambe, P. C., and Rahman, M. S., 1988, "*NCHRP Web Document 14 Laboratory Determination of Resilient Modulus for Flexible Pavement Design*," Project 1-28 Final Report, National Cooperative Highway Research Program, Transportation Research Board, National Research Council, Washington, D.C.

LAW PCS, a Division of Law Engineering & Environmental Services, Inc., and Axiom Decision Systems, Inc., 2002, "*Guide for Determining Design Resilient Modulus Values for Unbound Materials*," LTPP CD-ROM Product, LTPP Team, Federal Highway Administration, McLean, Virginia.

Richard L. Boudreau[1]

**Resilient Modulus – Pavement Subgrade Design Value**

---

**Reference:** Boudreau, R. L., "**Resilient Modulus – Pavement Subgrade Design Value,**" *ASTM STP 1437, Resilient Modulus Testing for Pavement Components*, G. N. Durham, W. A. Marr, and W. L. De Groff, Eds., ASTM International, West Conshohocken, PA, 2003.

**Abstract:** Much resilient modulus research work has been completed recently, mostly as part of the Long Term Pavement Performance (LTPP) study. This work has led towards the adoption of the resilient modulus test procedure, T307-99, in the current release of the American Association of State Highway and Transportation Officials (AASHTO) Tests. Neither the test procedure nor the current design guideline addresses how to approach selecting a design resilient modulus value from the fifteen stress-dependent numbers generated by the laboratory test.

Cohesive and non-cohesive subgrade soils are generally nonlinear inelastic materials, thus their stiffness is dependent on the stress condition subjected to. Recognizing this, the project-specific case study discussed in this paper examines the stress-dependency of soils encountered through laboratory determination of resilient modulus.

This paper uses a recognized constitutive model and layered elastic methodology approach (iterative solution) to objectively interpret results from a laboratory test program and apply the results for input into the 1993 AASHTO Design Guide for Pavement Structures (or DarWIN).

Through the use of the stress-dependent constitutive model: $M_r = K1(S_c)^{K2}(S_3)^{K5}$ and simple 85th percentile statistics, the process created uses the predicted subgrade modulus values at an assumed stress state. The 85th percentile value is selected as input into the 1993 AASHTO structural number (SN) requirement. A conventional pavement system (layer type and thickness) is then developed using typical mechanistic properties of asphalt concrete and aggregate base, which satisfy the SN. The layered elastic model ELSYM5 is then used to approximate vertical and horizontal stresses at the top of the subgrade layer. These stresses are compared to those assumed values used in the initial iteration. Adjustments are made and iterations continue until the values used to predict subgrade modulus reasonably match the calculated stresses in the pavement system.

The final iterated value for resilient modulus is the design resilient modulus. It is recommended that this design value be used to calculate pavement thickness requirements for all pavement types under consideration for the project.

**Keywords:** subgrade, resilient modulus, pavement design

---

[1] President, Boudreau Engineering, Inc., 5392 Blue Iris Court, Norcross, GA 30092.

The American Association for State Highway and Transportation Officials (AASHTO) released a revolutionary design manual in 1986 that integrated mechanistic design principles with generally accepted empirical relationships. This manual, referred to as the *AASHTO 1986 Pavement Design Guide*, replaced the pure empirical-based interim design guide from 1972. Perhaps the most significant change in this new guide was the requirement for subgrade support, changing from a California Bearing Capacity (CBR) derived soil support number (SSN) to the resilient modulus.

Although the preferred method of determining the subgrade resilient modulus was through a direct laboratory test measurement (AASHTO T-274), a conversion factor of 1500xCBR was allowable. Laboratories that were unwilling to invest in the sophisticated equipment necessary to perform a resilient modulus test opted to continue to perform CBR testing and use the convenient correlation factor. Those laboratories that made the investment to directly measure the resilient modulus faced a new challenge. Interpretation of a CBR test was fairly simple, picking either the value at 0.1 or 0.2 inches of penetration. Recognizing that soil is generally a nonlinear inelastic material, a resilient modulus test is conducted over a range of 15 different states of stress (combinations of vertical and horizontal stresses representing possible in-situ conditions in a pavement system).

As the pavement design industry has evolved, the design guide has been updated (AASHTO 1993 Pavement Design Guide) and the laboratory test method to directly measure the resilient modulus has gone through changes (AASHTO T-307). Unfortunately, the test method still results in 15 values, and the guide still requires a singular value for input. The challenge becomes which of the 15 values should be selected for design input? To further complicate the situation, if a project consists of test results for numerous tests, say 10 different specimens, which of the 150 values should be selected? This decision has not been addressed in a technical document, thus practitioners have been left to choose their own value.

This paper is intended to bridge this longstanding gap. A practical approach to select a design subgrade resilient modulus value from a laboratory testing program is outlined.

## Development of a Model

In a scenario that has repeated itself numerous times over the past decade, a laboratory testing program is completed and test results are furnished to the design engineer. The most commonly asked question is:

Q: What value of resilient modulus should I use?
A: Depends.

Because soil is generally a nonlinear inelastic material, it is stress dependant. Thus, the answer "depends" deserves some attention. What does it depend on? Several factors. Let us assume that the laboratory test program was conducted on soil remolded to appropriate density and moisture conditions that are acceptable to the design engineer (i.e., within acceptable tolerance of intended targets). The design resilient modulus depends on the anticipated stress state in the subgrade layer. Thus, a proper assessment of in-situ stress is required. This stress must be calculated for the design traffic traversing over a constructed pavement cross section built on these stress dependant subgrade soils.

*Example*

For demonstration, let us assume that a laboratory sampling and test program has been conducted. The material sampled for this new alignment project has been tested and analyzed. Based on the length of the project, the boring log information recorded in the field, and the soil classification testing from the laboratory, eight soils were selected for stiffness characterization.

Each of the eight soils selected were remolded to approximately 95% of their standard Proctor maximum dry densities at optimum moisture content (targets established by the construction specifications) using procedures set forth in Annex A3 of test method AASHTO T-307. Resilient modulus tests were conducted on each of the eight remolded test specimens. The design assumes that each of these eight soils will be equally represented in the finished, prepared roadbed profile.

In order to properly handle the data, each test result must be converted or fit in a constitutive model. Using a constitutive model first introduced during the SHRP work (Equation 1), the data is transformed into a form in which modulus values can be computed for any level of stress desirable (Table 1).

$$M_r = K1(S_c)^{K2}(S_3)^{K5} \tag{1}$$

where

$M_r$ = resilient modulus, psi
$S_c$ = cyclic applied axial stress, psi
$S_3$ = chamber confining pressure, psi
K1, K2, K5 = nonlinear regression constant/coefficients

In order to compute the regression constant and coefficients, the dependent variable, $M_r$ and independent variables $S_C$ and $S_3$ (as measured from the 15-sequence loading regime required by the AASHTO T-307 test standard) must first be transformed to a $Log_{10}$ base. This allows a linear regression to be performed. Once completed, the y-intercept is used as a 10-base exponential to derive the K1 constant, while the K2 and K5 coefficients are used as exponentials in Equation 1.

Table 1 – *Summary of Test Results*

| Sample | Dry | Moisture | Regression Coefficients | | | |
|---|---|---|---|---|---|---|
| No. | Density (pcf) | Content, % | K1 | K2 | K5 | $R^2$ |
| 1 | 118.3 | 15.5 | 9838 | -0.13187 | 0.22194 | 0.99 |
| 2 | 120.3 | 17.2 | 6259 | -0.14293 | 0.21102 | 0.99 |
| 3 | 117.8 | 18.9 | 13 123 | -0.14105 | 0.21493 | 0.98 |
| 4 | 115.2 | 16.3 | 7502 | -0.12825 | 0.23100 | 0.99 |
| 5 | 113.6 | 12.2 | 10 387 | -0.15483 | 0.23229 | 0.98 |
| 6 | 119.7 | 17.8 | 9463 | -0.05394 | 0.29379 | 0.98 |
| 7 | 113.0 | 12.1 | 10 294 | -0.10049 | 0.17310 | 0.99 |
| 8 | 118.6 | 16.1 | 8670 | -0.23156 | 0.21455 | 0.98 |

The constitutive model selected provides an excellent fit for the data, as can be observed by the multiple-correlation coefficient, $R^2$. In order to make use of the data, the summary results are best served in a spreadsheet form with an additional column added that can readily compute the resilient modulus at any level of vertical ($S_c$) and horizontal ($S_3$) stress. The calculated or predicted resilient modulus will have very small errors associated with it, based on the good $R^2$ values.

Once the predicted resilient modulus values are computed for each soil modeled in the project-specific soil profile, a singular value is selected and used in the iterative sequence described below. This singular value could be the average, the average minus a couple of standard deviations, a median or 50th percentile value, or some other preferred value. This example uses the 85th percentile value. By selecting this value, the designer is willing to accept potential premature failures over 15% of the designed and constructed pavement area. These failures are anticipated only in that the thickness design will be insufficient for potentially 15% of the subgrade soils that could be encountered. Premature failures are anticipated to occur prior to the end of the analysis period, and could be repaired in the form of patches. More conservative designs could be implemented (by selecting the minimum value), but this selection may lead to a much greater pavement thickness that is excessive for the majority of the pavement profile. Designers should develop their own acceptable level of risk, and make their selection accordingly.

The selection of the design resilient modulus is an iterative solution. In order to find the proper solution, input parameters for design are required. The design policy utilized will be the AASHTO 1993 Guide for flexible pavements. These inputs can be determined through laboratory testing, experience or policy. The parameters and values used in this example are listed in Table 2.

Table 2 – *Design Assumptions*

| *Material/Layer*<br>Parameter | Value | Units |
|---|---|---|
| *Asphaltic Concrete* | | |
| Layer coefficient, a | 0.44 | |
| Modulus, E | 400 000 | psi |
| Poisson's ratio, $\nu$ | 0.35 | |
| Unit Weight, $\gamma$ | 145 | pcf |
| *Graded Aggregate Base* | | |
| Layer coefficient, a | 0.14 | |
| Modulus, E | 40 000 | psi |
| Poisson's ratio, $\nu$ | 0.40 | |
| Unit Weight, $\gamma$ | 138 | pcf |
| *Subgrade* | | |
| Poisson's ratio, $\nu$ | 0.45 | |
| *Traffic* | | |
| Volume | 1 000 000 | ESALs |
| Tire pressure, $\sigma_c$ | 80 | psi |
| *Serviceability, $\Delta PSI$* | 2.5 | |

The following steps have been created in order to illustrate the iterative process.

*Step 1 (Trial 1)* – Select a combination of vertical and horizontal stresses anticipated in the subgrade layer. For this example, a first trial iteration of 4 psi vertical and 4 psi horizontal stress is assumed (Table 3), resulting in an 85th percentile resilient modulus value of 8477 psi (use 8500 psi).

Table 3 – *Computed 85th Percentile Value (Trial 1)*

| Sample No. | Dry Density (pcf) | Moisture Content, % | Regression Coefficients K1 | K2 | K5 | Est. Resilient Modulus, psi [1] |
|---|---|---|---|---|---|---|
| 1 | 118.3 | 15.5 | 9838 | -0.13187 | 0.22194 | 11 146 |
| 2 | 120.3 | 17.2 | 6259 | -0.14293 | 0.21102 | 6879 |
| 3 | 117.8 | 18.9 | 13 123 | -0.14105 | 0.21493 | 14 538 |
| 4 | 115.2 | 16.3 | 7502 | -0.12825 | 0.23100 | 8650 |
| 5 | 113.6 | 12.2 | 10 387 | -0.15483 | 0.23229 | 11 564 |
| 6 | 119.7 | 17.8 | 9463 | -0.05394 | 0.29379 | 13 196 |
| 7 | 113.0 | 12.1 | 10 294 | -0.10049 | 0.17310 | 11 384 |
| 8 | 118.6 | 16.1 | 8670 | -0.23156 | 0.21455 | 8468 |
| | | | | | AVG | 10 728 |
| | | | | | StDev | 2568 |
| | | | | | 85th % | 8477 |

Note 1: Resilient modulus estimated at axial stress = 4 psi, confining stress = 4 psi.

*Step 2 (Trial 1)* – Using the design values provided in Table 2 and a subgrade resilient modulus of 8500 psi, determine the required structural number (SN) from either the equation or the nomograph that solves the equation. The SN required for this first iteration is 3.2.

*Step 3 (Trial 1)* – Provide a pavement cross section that satisfies the required SN. An asphaltic concrete (AC) thickness of 5.0 inches on a graded aggregate base (GAB) thickness of 8.0 inches provides an adequate SN just in excess of the required 3.2. Once completed, simulate the design load on the pavement surface and cross section, and perform computations based on layered elastic theory to determine the horizontal ($\Delta\sigma_{x,y}$) and vertical ($\Delta\sigma_z$) stress changes at the top of the subgrade that result from the loading. The computer program ELSYM5 (SRA Technologies 1985) can readily calculate these values.

*Step 4 (Trial 1)* – Using ELSYM5, the vertical and horizontal stress changes of 5.3 psi and 0.94 psi, respectively, are estimated. These values must be added to the static, in-situ pressures existing from the pavement system overburden. The static pavement overburden vertical ($\sigma_z$) and horizontal ($\sigma_{x,y}$) stresses can be estimated using traditional soil mechanics principles (Sowers 1979). The vertical pressure is simply the summation of each layer density multiplied by the layer thickness above the subgrade. The horizontal pressure can be calculated using the lateral at-rest earth pressure coefficient, $k_0$ (estimated by the subgrade soils Poisson's ratio, $\nu$, in the form $k_0 = \nu/1\text{-}\nu$) multiplied by the vertical overburden pressure at the top of the subgrade. The determination of stress resulting from Trial 1 data is summarized in Table 4.

Table 4 – *Determination of Stress (Trial 1)*

| Property | units | Layer AC | Layer GAB | Total |
|---|---|---|---|---|
| Thickness | inch | 5.0 | 8.0 | 13.0 |
| Density | lb/cu ft | 145.0 | 138.0 | |
| Vertical Overburden Pressure, $\sigma_v$ | psi | 0.42 | 0.64 | 1.06 |
| Poisson's ratio - Subgrade $\nu$ | | | | 0.45 |
| Subgrade $k_0 = (\nu/1-\nu)$ | | | | 0.818 |
| Horizontal Pressure $\sigma_{x,y} = (k_0 \times \sigma_z)$ | psi | | | 0.866 |
| Vertical Pressure change, $\Delta\sigma_v$ | psi | | | 5.31 |
| Horizontal Pressure change, $\Delta\sigma_{x,y}$ | psi | | | 0.94 |
| In-situ Vertical Stress ($\sigma_v + \Delta\sigma_v$) | psi | | | 6.37 |
| In-situ Horizontal Stress ($\sigma_{x,y} + \Delta\sigma_{x,y}$) | psi | | | 1.81 |

*Step 5 (Trial 1)* – Compare the results of the computation with the values used to estimate the trial resilient modulus. These values of 6.4 psi (4 psi used for trial) and 1.8 psi (4 psi used for trial) are not a particularly close match, thus a second iteration is required.

The 5-step process is repeated using an estimate of 6.4 psi vertical stress and 1.8 psi horizontal stress.

*Step 1 (Trial 2)* – A second trial iteration using 6.4 psi vertical and 1.8 psi horizontal stress is assumed (Table 4), resulting in an 85th percentile resilient modulus value of 6418 psi (use 6400 psi).

Table 5 – *Computed 85th Percentile Value (Trial 2)*

| Sample No. | Dry Density (pcf) | Moisture Content, % | Regression Coefficients K1 | K2 | K5 | Est. Resilient Modulus, psi [1] |
|---|---|---|---|---|---|---|
| 1 | 118.3 | 15.5 | 9838 | -0.13187 | 0.22194 | 8775 |
| 2 | 120.3 | 17.2 | 6259 | -0.14293 | 0.21102 | 5434 |
| 3 | 117.8 | 18.9 | 13 123 | -0.14105 | 0.21493 | 11 460 |
| 4 | 115.2 | 16.3 | 7502 | -0.12825 | 0.23100 | 6773 |
| 5 | 113.6 | 12.2 | 10 387 | -0.15483 | 0.23229 | 8932 |
| 6 | 119.7 | 17.8 | 9463 | -0.05394 | 0.29379 | 10 175 |
| 7 | 113.0 | 12.1 | 10 294 | -0.10049 | 0.17310 | 9457 |
| 8 | 118.6 | 16.1 | 8670 | -0.23156 | 0.21455 | 6399 |
| | | | | | AVG | 8426 |
| | | | | | StDev | 2053 |
| | | | | | 85th % | 6418 |

Note 1: Resilient modulus estimated at axial stress = 6.4 psi, confining stress = 1.8 psi.

*Step 2 (Trial 2)* – Using the design assumptions provided in Table 2 and a subgrade resilient modulus of 6400 psi, determine the required structural number (SN) from either the equation or the nomograph that solves the equation. The SN required for this second iteration is 3.5.

*Step 3 (Trial 2)* – Provide a pavement cross section that satisfies the required SN. An asphaltic concrete (AC) thickness of 5.5 inches on a graded aggregate base (GAB) thickness of 8.0 inches provides an adequate SN just in excess of the required 3.5. Once completed, simulate the design load on the pavement surface and cross section, and perform computations based on layered elastic theory to determine the horizontal and vertical stress changes at the top of the subgrade that result from the loading. The computer program ELSYM5 can readily calculate these values.

*Step 4 (Trial 2)* – Using ELSYM5, the vertical and horizontal stress changes of 4.2 psi and 0.73 psi, respectively, are estimated. Again, these values must be added to the static, in-situ pressures existing from the pavement system overburden, as shown in Table 6.

Table 6 – *Determination of Stress (Trial 2)*

| | | Layer | | |
|---|---|---|---|---|
| Property | units | AC | GAB | Total |
| Thickness | inch | 5.5 | 8.0 | 13.5 |
| Density | lb/cu ft | 145.0 | 138.0 | |
| Vertical Overburden Pressure, $\sigma_v$ | psi | 0.46 | 0.64 | 1.10 |
| Poisson's ratio - Subgrade $\nu$ | | | | 0.45 |
| Subgrade $k_0 = (\nu/1-\nu)$ | | | | 0.818 |
| Horizontal Pressure $\sigma_{x,y} = (k_0 \text{ x } \sigma_z)$ | psi | | | 0.900 |
| Vertical Pressure change, $\Delta\sigma_v$ | psi | | | 4.20 |
| Horizontal Pressure change, $\Delta\sigma_{x,y}$ | psi | | | 0.73 |
| In-situ Vertical Stress $(\sigma_v + \Delta\sigma_v)$ | psi | | | 5.30 |
| In-situ Horizontal Stress $(\sigma_{x,y} + \Delta\sigma_{x,y})$ | psi | | | 1.63 |

*Step 5 (Trial 2)* – Compare the results of the computation with the values used to estimate the trial resilient modulus. These values of 5.3 psi (6.4 psi used for trial) and 1.6 psi (1.8 psi used for trial) are still not a close enough match, but are greatly improved from the first trial. A third iteration is required.

The 5-step process is repeated using an estimate of 5.3 psi vertical stress and 1.6 psi horizontal stress.

*Step 1 (Trial 3)* – A third trial iteration of 5.3 psi vertical and 1.6 psi horizontal stress is assumed (Table 5), resulting in an 85th percentile resilient modulus value of 6529 psi (use 6500 psi).

Table 7 – *Computed 85th Percentile Value (Trial 3)*

| Sample | Dry | Moisture | Regression Coefficients | | | Est. Resilient |
|---|---|---|---|---|---|---|
| No. | Density (pcf) | Content, % | K1 | K2 | K5 | Modulus, psi [1] |
| 1 | 118.3 | 15.5 | 9838 | -0.13187 | 0.22194 | 8764 |
| 2 | 120.3 | 17.2 | 6259 | -0.14293 | 0.21102 | 5446 |
| 3 | 117.8 | 18.9 | 13 123 | -0.14105 | 0.21493 | 11 475 |
| 4 | 115.2 | 16.3 | 7502 | -0.12825 | 0.23100 | 6752 |

| | | | | | | |
|---|---|---|---|---|---|---|
| 5 | 113.6 | 12.2 | 10 387 | -0.15483 | 0.23229 | 8949 |
| 6 | 119.7 | 17.8 | 9463 | -0.05394 | 0.29379 | 9930 |
| 7 | 113.0 | 12.1 | 10 294 | -0.10049 | 0.17310 | 9444 |
| 8 | 118.6 | 16.1 | 8670 | -0.23156 | 0.21455 | 6518 |
| | | | | | AVG | 8410 |
| | | | | | StDev | 2011 |
| | | | | | 85th % | 6529 |

Note 1: Resilient modulus estimated at axial stress = 5.3 psi, confining stress = 1.6 psi.

*Step 2 (Trial 3)* – Using the design assumptions provided in Table 2 and a subgrade resilient modulus of 6500 psi, determine the required structural number (SN) from either the equation or the nomograph that solves the equation. The SN required for this third iteration is 3.5.

*Step 3 (Trial 3)* – Provide a pavement cross section that satisfies the required SN. An asphaltic concrete (AC) thickness of 5.5 inches on a graded aggregate base (GAB) thickness of 8.0 inches provides an adequate SN just in excess of the required 3.5. Once completed, simulate the design load on the pavement surface and cross section, and perform computations based on layered elastic theory to determine the horizontal and vertical stresses at the top of the subgrade. Using ELSYM5, the vertical and horizontal stresses of 4.2 psi and 0.73 psi, respectively, are determined.

*Step 4 (Trial 3)* – Using ELSYM5, the vertical and horizontal stress changes of 4.2 psi and 0.73 psi, respectively, are estimated. Again, these values must be added to the static, in-situ pressures existing from the pavement system overburden, as shown in Table 8.

Table 8 – *Determination of Stress (Trial 3)*

| | | Layer | | |
|---|---|---|---|---|
| Property | units | AC | GAB | Total |
| Thickness | inch | 5.5 | 8.0 | 13.5 |
| Density | lb/cu ft | 145.0 | 138.0 | |
| Vertical Overburden Pressure, $\sigma_v$ | psi | 0.46 | 0.64 | 1.10 |
| Poisson's ratio - Subgrade $\nu$ | | | | 0.45 |
| Subgrade $k_0 = (\nu/1-\nu)$ | | | | 0.818 |
| Horizontal Pressure $\sigma_{x,y} = (k_0 \times \sigma_z)$ | psi | | | 0.900 |
| Vertical Pressure change, $\Delta\sigma_v$ | psi | | | 4.20 |
| Horizontal Pressure change, $\Delta\sigma_{x,y}$ | psi | | | 0.73 |
| In-situ Vertical Stress ($\sigma_v + \Delta\sigma_v$) | psi | | | 5.30 |
| In-situ Horizontal Stress ($\sigma_{x,y} + \Delta\sigma_{x,y}$) | psi | | | 1.63 |

*Step 5 (Trial 3)* – Compare the results of the computation with the values used to estimate the trial resilient modulus. These values of 5.3 psi (5.3 psi used for trial) and 1.6 psi (1.6 psi used for trial) are a close enough match to consider the iterative solution closed. Another iteration will not close this solution any further.

Based on this final iteration, the design subgrade resilient modulus should be 6500 psi.

**Discussion**

This is a fairly simple approach that does not take a great deal of time. From the beginning of Trial 1 to the completion of Trial 3 requires approximately 20 minutes. This process considers and utilizes the stress-strain behavior of the project-specific soils encountered. It should be recognized that certain errors are inherent in this process. First, the estimate of resilient modulus at any given level of stress is an approximation. The errors associated with this approximation are attributed by how well the constitutive model fits the data ($R^2$ resulting from the Equation 1 regression). Obviously, the larger the $R^2$, the more accurate this approximation is. Secondly, the design assumes that each soil is represented equally. If this assumption is not valid (for example, if soil sample number 2 will not be utilized during construction, or soil sample number 5 will be used for an estimated 50% of the project) appropriate adjustments are required prior to the iterative process. A weighted average can be used, or a different percentile value. As stated earlier, designers should develop their own acceptable level of risk, and make their selection accordingly.

The values utilized in this design example do not consider seasonal affects. Efforts should be made to incorporate seasonal variation of subgrade stiffness.

**References**

Sowers, George F., 1979, *Introductory Soil Mechanics and Foundations: Geotechnical Engineering*, Fourth Edition, Macmillan Publishing, New York, pp 383-384.

SRA Technologies, 1985, ELSYM5 Computer Program, Version 1.0, "Pavement Design and Analysis Procedures on Microcomputers," Study Contracted by the Federal Highway Administration.

Louay N. Mohammad,[1] Ananda Herath,[2] and Hani H. Titi[3]

# The Use of Continuous Intrusion Miniature Cone Penetration Testing in Estimating the Resilient Modulus of Cohesive Soils

**Reference:** Mohammad, L. N., Herath, A., and Titi, H. H., "**The Use of Continuous Intrusion Miniature Cone Penetration Testing in Estimating the Resilient Modulus of Cohesive Soils**," *Resilient Modulus Testing for Pavement Components, ASTM STP 1437,* G. N. Durham, W. A. Marr, and W. L. De Groff, Eds., ASTM International, West Conshohocken, PA, 2003.

**Abstract**: This paper presents an application of the continuous intrusion miniature cone penetration testing in evaluating the resilient modulus of cohesive soils. Four cohesive soils were selected for the field and laboratory testing program. The field tests were performed on these soils using the continuous intrusion miniature cone penetration test system. The laboratory testing program included repeated load triaxial tests on undisturbed soil samples, and soil physical and strength properties testing. A statistical analysis was performed on the test results of two soils to develop a correlation among the resilient modulus, cone penetration test parameters, in-situ stresses, and soil properties. The model was used to predict the resilient modulus of other two soils. The predicted and measured values of the resilient modulus were in agreement.

**Keywords:** resilient modulus, cone penetration testing, cohesive soil

## Introduction

The American Association of State Highway and Transportation Officials (AASHTO) guide for design of pavement structures (AASHTO 1993) recommends the use of the resilient modulus ($M_r$) for characterization of base and subgrade soil and for design of flexible pavements. The subgrade soil characterization, based on the resilient modulus, is a realistic way to analyze the moving vehicle loads on a pavement. The resilient modulus represents the dynamic stiffness of pavement materials under the repeated loads of vehicles.

[1] Associate Professor, Department of Civil & Environmental Engineering and Louisiana Transportation Research Center, Louisiana State University, 4101 Gourrier Ave., Baton Rogue, LA 70808.
[2] Postdoctoral Researcher, Louisiana Transportation Research Center, 4101 Gourrier Ave., Baton Rogue, LA 70808.
[3] Assistant Professor, Department of Civil Engineering and Mechanics, University of Wisconsin – Milwaukee, P.O. Box 784, Milwaukee, WI 53201.

The resilient modulus can be estimated from the empirical correlations, in-situ nondestructive test methods (NDT), and laboratory testing on soil samples. The laboratory procedures are considered laborious, time consuming, and highly expensive. The field nondestructive test procedures have certain limitations with respect to repeatability of test results. The shortcomings of these test methods signify the need for an in-situ technology for determining the resilient characteristics of subgrade and base soils underneath a pavement.

The cone penetration testing (CPT) is popular in the geotechnical field for soil characterization. This is because the CPT is economical, fast, and provides repeatable and reliable results. The CPT is conducted by advancing a cylindrical rod with a cone tip into the soil and measuring the tip resistance and sleeve friction due to this intrusion. The cone resistance parameters, tip resistance and sleeve friction, are used to classify soil strata and to estimate strength and deformation characteristics of soils.

This paper presents the results of a study performed to investigate the applicability of the intrusion technology in evaluating the resilient modulus of subgrade soils. Laboratory and field-testing programs were conducted at three sites comprising four cohesive soils in Louisiana. The field tests consisted of continuous intrusion miniature cone penetration tests. These tests were conducted using a continuous intrusion miniature cone penetration test (CIMCPT) system. The laboratory tests consisted of repeated load triaxial test on undisturbed soil samples to evaluate the resilient characteristics of these soils. Other soil tests were conducted to characterize the soils such as physical properties, compaction characteristics, and strength parameters.

Statistical analyses were performed to correlate the cone penetration test parameters, and the resilient characteristics and physical properties of the investigated soils. A model was proposed in which the resilient modulus of subgrade soil is predicted from the cone tip resistance, sleeve friction, moisture content, unit weight, and the in-situ stresses. The model was developed using the test results of two soils and used to predict the resilient modulus of the other two investigated soils.

## Objective and Scope

The objective of this study was to develop and validate a correlation among the continuous intrusion miniature cone penetration test parameters, resilient characteristics of subgrade soils, in-situ stresses, and soil properties.

The miniature cone penetration tests were performed using the 2-cm$^2$ miniature friction cone penetrometer. The laboratory repeated load triaxial tests were performed on the undisturbed soil samples.

## Background

The resilient modulus of soils is influenced by many factors including the soil type, the variation of moisture content, unit weight, and the in-situ stresses. Investigators have attempted a variety of methods to evaluate the dynamic resilient properties of subgrade soil and to investigate the different factors affecting the resilient modulus. The test methods included laboratory as well as in-situ test methods. The laboratory methods are mainly conducted using triaxial systems, simple shear, resonant column, gyratory, and the hollow cylinder test device. Mohammad et al. (1994) presented a summary of the research results conducted using these devices. Because of its simplicity, repeatability, and accuracy, the triaxial cell is the most popular resilient modulus laboratory-testing device. The resilient modulus ($M_r$) in a repeated load test is defined as the ratio of the maximum deviator stress ($\Phi_d$) and the recoverable elastic strain ($\gamma_r$) as follows:

$$M_r = \frac{\sigma_d}{\varepsilon_r} \tag{1}$$

Figure 1 illustrates the definition of the resilient modulus in a repeated load triaxial test. Generally, the resilient modulus determined from the laboratory tests is influenced by many factors including moisture content, dry unit weight, confining and deviator stresses, size of the specimen, stress pulse shape, duration, frequency and sequence of stress levels, testing equipment and specimen preparation as well as conditioning methods (Fredlund et al. 1977, Nataatmadja and Parkin1989, Monismith 1989, McGee 1989, Allen 1989, Kamal et al. 1993, Mohammad et al. 1994, Mohammad and Puppala 1995, Drumm et al. 1997 ).

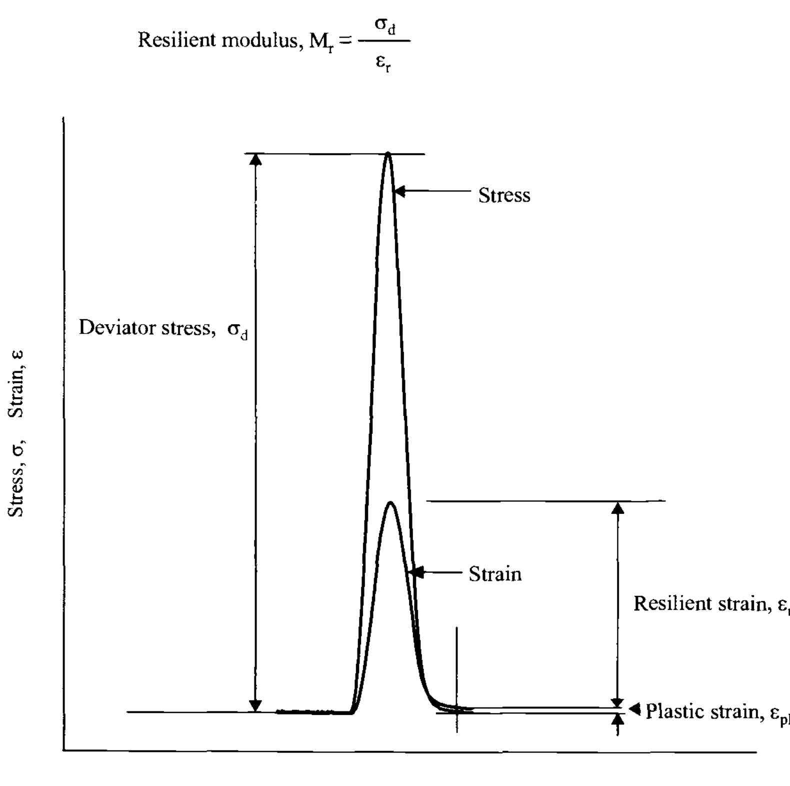


Figure 1 – *Definition of Resilient Modulus*

Several in-situ methods have been developed to determine the resilient modulus. Nondestructive test methods such as the Dynaflect and Falling Weight Deflectometer (FWD) have also been subjected to a lot of scrutiny. Deflections of pavement materials are measured in the field by such equipment, and these deflections are used with backcalculation subroutines for estimating the resilient properties. Several types of backcalculation software are already available and reported in the literature. Results obtained from this software are not repeatable and appear to be affected by factors such as the testing load, the relative stiffness between layers and environmental conditions.

Both laboratory and in-situ methods are improving with developments in hardware technologies, particularly in areas such as data acquisition systems and computer technology. However, the laboratory methods are rather laborious, time consuming, and expensive and they require a highly sophisticated testing system. Moreover, these methods are still being modified to make them more accurate and reliable. These limitations in laboratory and in-situ NDT methods signify the need to develop a more realistic, reliable and economical in-situ method for determining the resilient properties of subgrade soils. The in-situ method should be able to save a significant amount of time and money, which would have been spent on sampling and laboratory testing.

Several types of in-situ testing equipment have been used in geotechnical investigations for the past two decades. The cone penetration test has been recognized as one of the most widely used in-situ tests. In the U.S., cone penetration testing has gained rapid popularity in the last decade and is currently replacing the traditional standard penetration test (Tumay et al. 1998). Cone penetration testing is an in-situ method used for classification and interpretation of engineering properties of soils in the field of geotechnical engineering. The cone penetration test consists of advancing a cylindrical rod with a conical tip into the soil and measuring the forces required to push this rod. There are two forces measured during the CPT: the cone tip resistance ($q_c$) is the soil resistance to advance the cone tip and the sleeve friction ($f_s$) is the friction developed between the soil and the sleeve of the penetrometer because of the penetration. The friction ratio ($R_f$) is defined as the ratio of the sleeve friction and tip resistance and is expressed in percent. These cone-measured parameters are used to identify the soils and determine their properties.

Applications of CPT in the field of pavement engineering, particularly related to subsoils, have also been attempted. Badu-Tweneboah et al. (1989) conducted cone penetration tests on various highway pavements in Florida. They correlated the cone test results with $M_r$ results from NDT methods. Inaccuracies and uncertainties involving NDT backcalculation subroutines may affect the reliability of these correlations. In spite of this limitation, this study revealed the potential of CPT in determining resilient properties.

The concern regarding the use of the cone penetration test method to determine the resilient modulus of subsoils is with respect to the differences in the modes of testing used. The tip resistance and sleeve friction are obtained from the cone penetration test, which is considered a quasi-static test method, whereas the resilient modulus is a property obtained from a dynamic repeated load test. It is often assumed that test parameters obtained from different test backgrounds may not provide reasonable correlations with one another. However, this is not always the case. Earlier studies (Tumay 1985, Puppala et al. 1995) showed the potential of the quasi-static CPT method in determining the low strain dynamic shear modulus and liquefaction of soil. The dynamic shear moduli and

CPT parameters are less influenced by stress and strain history. In fact, these parameters are controlled by the same soil variables, which may have led to the development of better correlations between them. The resilient modulus is considered analogous and also related to the shear modulus. Therefore, the influence of stress and strain behavior on resilient modulus will be similar to that of shear modulus. Previous studies Mohammad et al. (1994) also indicated that the resilient property of subgrade soil is less dependent on stress and strain history. The strain history influence is also expected to be insignificant in a nondestructive repeated load triaxial test. Furthermore, the cone penetration tests and repeated load resilient modulus tests were conducted on soil under identical environmental conditions. This implies that both test parameters were subjected to similar environmental variables such as density, moisture content, and geomaterial fabric. In such conditions, the cone penetration test and resilient moduli parameters depend on the same soil variables. Therefore, it is reasonable to assume that a correlation is possible between cone penetration test parameters and resilient modulus.

## Methodology

Field and laboratory testing programs were conducted on cohesive soils from three different sites comprising four cohesive soils in Louisiana. The location of the test sites is shown on Louisiana map in Figure 2. The field tests carried out at the investigated sites consisted of continuous intrusion miniature cone penetration tests. Undisturbed and disturbed soil samples were obtained from these sites using a conventional drilling rig. Figure 3 depicts a typical plan for the field tests conducted at the investigated sites. The laboratory-testing program was conducted on the undisturbed and disturbed soil samples to determine their resilient modulus, physical properties, strength parameters, and compaction characteristics. The laboratory tests conducted are: Resilient Modulus of Unbound Granular Base/Subbase Materials and Subgrade Soils-SHRP Protocol P46 (AASHTO 1995), Determining the Atterberg Limits of Soils, Determination of Moisture Content, Moisture Density Relationships, Mechanical Analysis of Soils, Organic Material in Soil, Test Method for Specific Gravity of Soils, Test Method for Consolidated Undrained Triaxial Compression Test on Cohesive Soil, Test Method for Classification of Soil For Engineering Purposes (Unified Soil Classification System ), and Classification of Soil and Soil Aggregate Mixtures for Highway Construction Purposes. These tests were performed in accordance with the corresponding test protocols of ASTM and/or Louisiana Department of Transportation and Development (LA DOTD).

## Characterization of the Investigated Soils

### *Pavement Research Facility Site, Port Allen*

The first site selected was the Pavement Research Facility (PRF) in Port Allen, Louisiana. This site is located on six acres of mainly a natural soil deposit of heavy clay with 1.52 m thick embankment constructed of silty clay constructed on part of the site. These two soils were selected for this study. The silty clay consists of 23 percent clay and 70 percent silt and 4.7 percent organic content. The clay is classified as CL-ML (silty clay) according to the USCS and A-4 (silty soil) according to the AASHTO classification system. Standard Proctor test on the silty clay showed that the optimum moisture content of the soil ($w_{opt}$) is 18.0 percent and the corresponding maximum dry unit weight ($(_{dmax}$) is 16.7 kN/m$^3$.

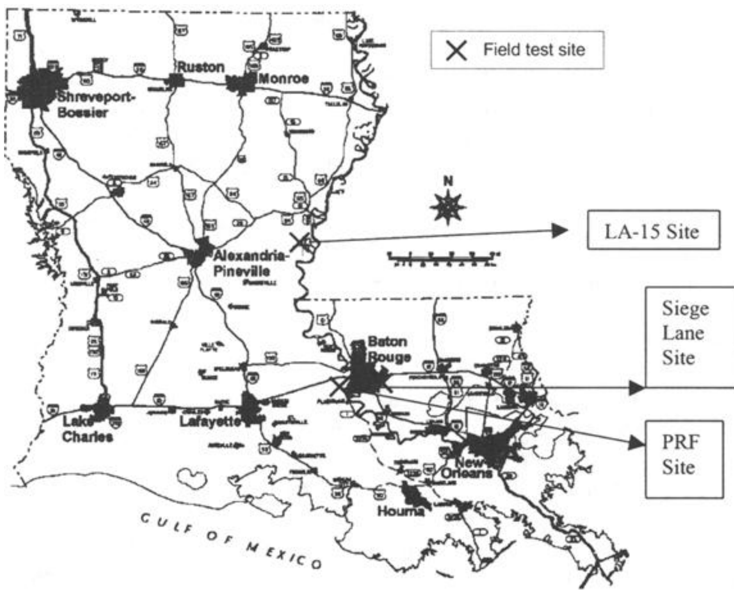


Figure 2 – *Location of the Investigated Soil Sites*

The heavy clay consists of medium gray soft normally consolidated clay with traces of organic materials and iron oxide. The topsoil layer with an average depth of 0.5 m is mainly soft clay mixed with organic materials and traces of roots. Approximately a 6.0 m deep soft normally consolidated clay layer underlies this layer. The heavy clay consists of 2 percent sand, 14 percent silt, 84 percent clay and colloids. The soil possesses high moisture content with an average of 51 percent (average LL=93 and average PL= 27). The average unit weight of the soil is 17.2 kN/m$^3$. The heavy clay is classified as CH (fat clay) using the USCS and A-7-6 (clay) according to the AASHTO classification system. Standard Proctor test on the heavy clay showed that the optimum moisture content of the soil ($w_{opt}$) is 31.4 percent and the corresponding maximum dry unit weight ($(_{dmax}$) is 13.6 kN/m$^3$. Unconsolidated undrained triaxial (UU) test was conducted to evaluate the undrained shear strength of the heavy clay. Test results showed that the average undrained shear strength is 51.5 kPa. The properties of the silty clay and heavy clay are summarized in Table 1.

Table 1 – *Properties of the Investigated Cohesive Soils*

| | PRF-Silty clay | PRF-Heavy clay | LA-15 clay | Siegen Lane clay |
|---|---|---|---|---|
| Passing sieve #200 (%) | 93 | 98 | 98 | 98 |
| Clay (%) | 23 | 84 | 44 | 33 |
| Silt (%) | 70 | 14 | 54 | 65 |
| Organic content (%) | 4.7 | 9.2 | NA | NA |
| Liquid limit, *LL* (%) | 28 | 93 | 52 | 35 |
| Plastic limit, *PL* (%) | 22 | 27 | 25 | 23 |
| Plasticity index, *PI* | 6 | 66 | 27 | 12 |
| Specific gravity, $G_S$ | 2.67 | 2.68 | 2.70 | 2.69 |
| Angle of friction, $\phi$ (°) | 22.0 | 14.0 | 14.0 | 19.2 |
| Optimum water content, $w_{opt}$ (%) | 18.0 | 31.4 | 28.1 | 17.5 |
| Max. dry unit weight ($kN/m^3$) | 16.7 | 13.6 | 15.1 | 17.0 |
| Soil classification, *USCS* | CL-ML (Silty clay) | CH (Fat clay) | CH (Fat clay) | CL (Lean clay) |
| Soil classification, *AASHTO* | A-4 (Silty soil) | A-7-6 (Clayey soil) | A-7-6 (Clayey soil) | A-6 (Silty clay) |

*State Route LA-15, Deer Park*

The embankment of State Route LA-15 in Concordia Parish is located approximately 15 miles south of Vidalia. The embankment at this location is part of the Mississippi River Levee. The soil considered in this study is located at the up slope of the roadway on the Levee. The soil consists of 44 percent clay and 54 percent silt. The average Liquid Limit (*LL*) is 52 percent and the average Plasticity Index (*PI*) is 27. The soil is classified as CH (fat clay) using the Unified Soil Classification System and A-7-6 (clayey soil) using the AASHTO classification system. The optimum moisture content of the soil is 28.1 percent and the corresponding maximum dry unit weight 15.1 kN/m$^3$. Properties of LA-15 clay are summarized in Table 1.

*Siegen Lane, Baton Rouge*

The test site is located at the intersection of Siegen Lane and the Industriplex in Baton Rouge. The soil at this site consists of 33 percent clay and 65 percent silt. The soil is classified as lean clay (CL) according to the USCS and silty clay (A-6) according to the AASHTO classification. The average Liquid Limit of the soil is 35 percent and the average Plasticity Index is 12. Compaction characteristics of the soil showed that the optimum moisture content is 17.5 percent and the corresponding maximum dry unit weight is 17.0 kN/m$^3$.

**Continuous Intrusion Miniature Cone Penetration Test**

The cone penetration test systems used to execute the field-testing program is the continuous intrusion miniature cone penetration test system, which was developed at the Louisiana Transportation Research Center (LTRC) by Tumay and co-workers (Tumay et al. 1998, Tumay and Titi 2000, Titi et al. 2000) for shallow site characterization. The system, shown in Figure 3, consists of continuous push device, hydraulic motor, miniature cone penetrometer, and data acquisition system. The cone is attached to a coiled push rod, which allows a continuous penetration, and is mechanically straightened as the cone is pushed into the soil. The miniature cone penetrometer has a cross sectional area of 2 cm$^2$, the friction sleeve area is 40 cm$^2$, and the cone apex angle is 60 degrees. Researchers at LTRC (Tumay et al. 1998, Tumay and Titi 2000, Titi et al. 2000) conducted field and laboratory tests to calibrate and evaluate the results of the CIMCPT with respect to the results of the 10 and 15 cm$^2$ cone penetrometers in different soil types. Results showed that the CIMCPT results are consistent with those obtained by the 10 and 15 cm$^2$ cone penetrometers. Generally, the CIMCPT system tends to record higher tip resistance and lower sleeve friction in the amount of 10 percent compared to the 10 and 15 cm$^2$ cone penetrometers.

The CIMCPT procedure described herein was used at all sites. During CIMCPT, the cone was advanced into the ground at a rate of 2 cm/sec with continuous measurements of the tip resistance ($q_c$) and sleeve friction ($f_s$). The CIMCPTs were conducted around the borehole from which the laboratory samples were obtained for resilient modulus determination. This is to ensure that the CIMCPT soundings represent the soil tested in the laboratory. A typical cone penetration test plan at the investigated sites is presented in Figure 4.

Figure 5 depicts the results of CIMCPT on the silty clay for field test set 1. As shown in the figure, the tip resistance and sleeve friction (of the silty clay layer) measured by the CIMCPT system are consistent and reflect similar patterns. Results of CIMCPTs conducted on the heavy clay are presented in Figure 6. The CIMCPT soundings of the heavy clay are also consistent. The cone penetration test parameters ($q_s$ and $f_s$) were used to develop a model for predicting the resilient modulus of cohesive soils from the cone parameters. Therefore, it is important to evaluate the variability of the CIMCPT profiles at same site using statistical analysis. The soil profile was divided into thin 20-mm soil layers and the CIMCPT parameters ($q_c$ and $f_s$) of each test were averaged along the 20-mm layers. For each 20-mm soil layer (at each test set), there are four values for $q_c$ and four values for $f_s$. The average of these four values, the standard deviation, and the coefficient of variation are calculated. The average values of the coefficient of variation of $q_c$ and $f_s$ are presented in Table 2. The average coefficient of variation for $q_c$ ranges from 17 to 20 for test set #1 at the PRF site. Generally, the results presented in Table 2 quantify the natural variability of the soil at the same test site. In addition, these results indicate that the CIMCPT repeatability is function of the soil variability and is site specific.

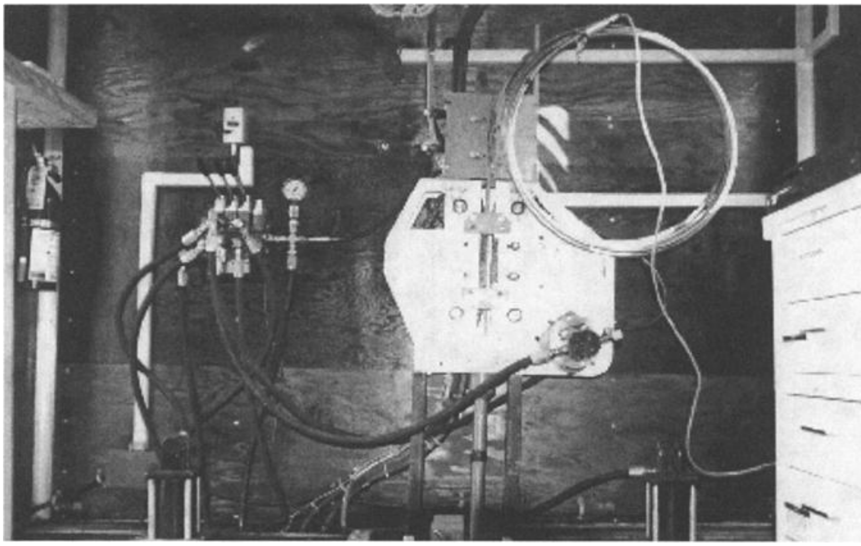

Figure 3 – *The Cone Penetration Test Systems Used in the Study*

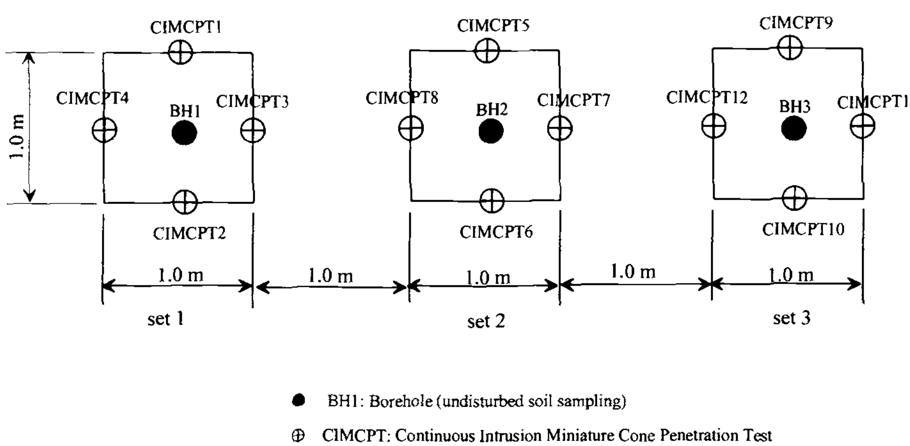


Figure 4 – *A Typical Layout for the Field Testing*

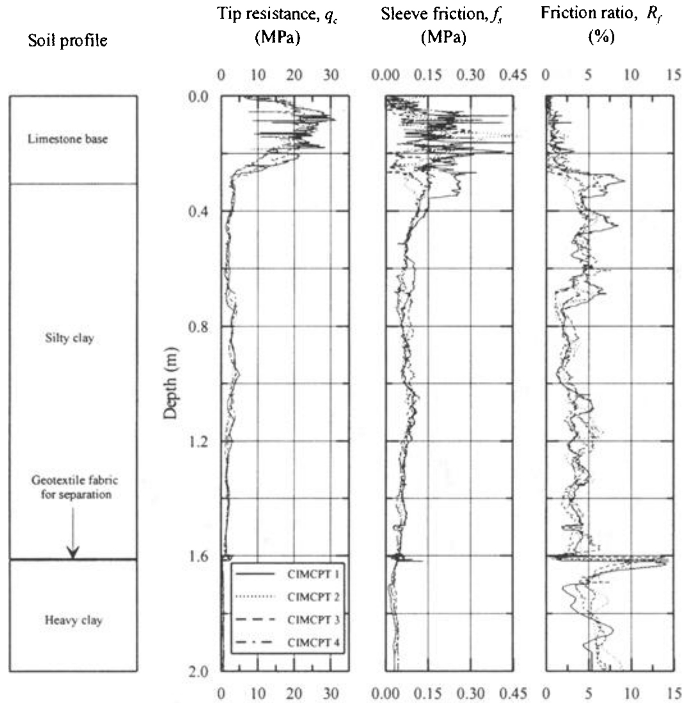


Figure 5 – *Cone Penetration Test Results of Silty Clay*

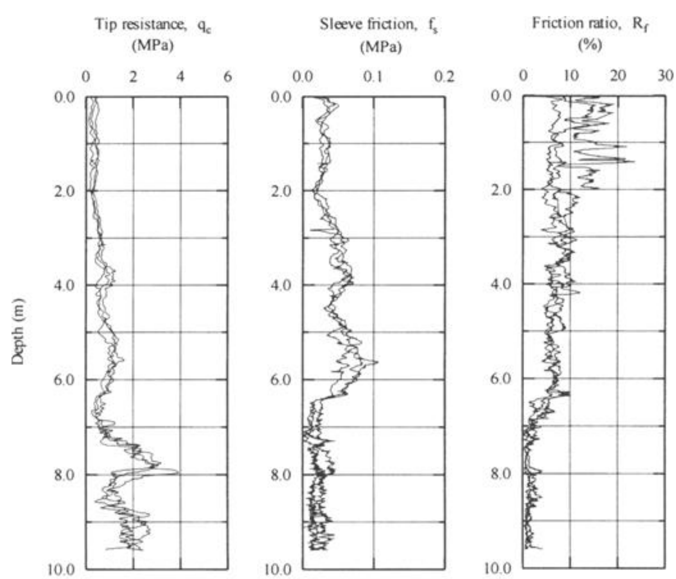


Figure 6 – *Cone Penetration Test Results of Heavy Clay*

Table 2 – *Statistical Analysis Conducted on the Penetration Test Results*

| Test Site | Test Set | Depth (m) | Cone resistance, $q_c$ COV average (%) | Sleeve friction, $f_s$ COV average (%) |
|---|---|---|---|---|
| PRF-Silty clay | Set 1 | 0.8 | 20 | 22 |
| | | 1.0 | 17 | 15 |
| | Set 2 | 0.8 | 22 | 25 |
| | | 1.0 | 19 | 16 |
| | Set 3 | 0.8 | 26 | 16 |
| | | 1.0 | 27 | 25 |
| PRF-Heavy clay | Set 1 | 0.8 | 30 | 14 |
| | | 1.0 | 33 | 5 |
| | Set 2 | 0.8 | 31 | 11 |
| | | 1.0 | 11 | 28 |
| | Set 3 | 0.8 | 14 | 39 |
| | | 1.0 | 23 | 22 |
| LA-15 clay | Set 1 | 0.8 | 21 | 34 |
| | | 1.0 | 26 | 36 |
| | Set 2 | 0.8 | 21 | 23 |
| | | 1.0 | 23 | 19 |
| | Set 3 | 0.8 | 27 | 38 |
| | | 1.0 | 18 | 26 |
| Siegen Lane clay | Set 1 | 0.8 | 44 | 43 |
| | | 1.0 | 39 | 42 |
| | Set 2 | 0.8 | 18 | 38 |
| | | 1.0 | 27 | 39 |
| | Set 3 | 0.8 | 10 | 9 |
| | | 1.0 | 13 | 11 |

## Resilient Modulus

The resilient modulus of the investigated soils was determined using the repeated load triaxial test. The test was conducted using an MTS model 810-closed loop servo-hydraulic material-testing system as shown in Figure 7. The major components of this system are the loading system, digital controller, and load unit control panel.

The undisturbed soil samples were trimmed and prepared for the laboratory resilient modulus test. The repeated loading triaxial tests were conducted according to the AASHTO procedure T 294-94 "Resilient modulus of Unbound Granular Base/Subbase Materials and Subgrade Soils - SHRP Protocol P46." The soil samples were conditioned by applying one thousand repetitions of a specified deviator stress at a certain confining pressure. Conditioning eliminates the effects of specimen disturbances from sampling, and specimen preparation procedures and minimizes the imperfect contacts between end platens and the specimen. The specimen is then subjected to different stress sequences. The stress sequence is selected to cover the expected in-service range that a pavement or subgrade material experiences under traffic loading. Some of the investigated soils are very soft and possesses low unconfined compressive strength. These soil specimens could not be tested at high stress levels, therefore, the maximum deviator stress was limited to less than half of the unconfined compressive strength of the specimen as specified by AASHTO T 294-94.

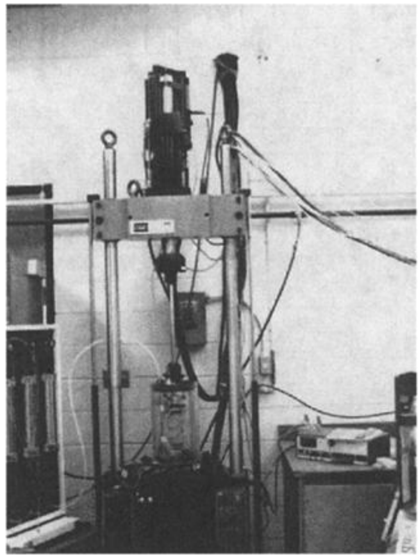

Figure 7 – *The MTS Test System*

The results of the repeated load triaxial test on the soil samples from the PRF test site are shown in Table 3. Inspection of Table 3 shows that the coefficient of variation of the calculated resilient modulus ranges from 0 to 2.0. This indicates that the repeated load triaxial test on the investigated soil samples was repeatable. The variations of the resilient modulus ($M_r$) with deviator stress at different confining pressures for the samples are shown in Figure 8. The resilient modulus at a constant confining pressure decreases as the deviator stress increases, whereas, the resilient modulus at a constant deviator stress increases as the confining pressure increases. This reflects a typical behavior of the effect of stresses on the resilient modulus. Inspection of Figure 8a indicates that the silty clay exhibited high resilient modulus values. The in-situ moisture content of silty clay ranges from 20.8 to 25.4 percent and the unit weight varies between 19.9 and 20.8 kN/m$^3$. These values are close to the optimum moisture content ($w$=16.5%) and the corresponding unit weight ((=19.8 kN/m$^3$) obtained from the laboratory compaction test. However, the resilient modulus of the heavy clay is low compared to the silty clay, Figure 8b. The heavy clay is a soft soil with a range of in-situ moisture content between 59 and 65.1 percent and the unit weight ranges from 16 to 16.4 kN/m$^3$. The optimum moisture content of the heavy clay obtained in the laboratory is 31.4 percent and the corresponding unit weight is 17.8 kN/m3. The high amount of moisture in the heavy clay is the main reason for the lower resilient modulus of this soil.

The resilient modulus of the investigated fine-grained soils reflects a typical behavior where the values of the resilient modulus at constant confining pressure decrease with the increase of the deviator stress. In addition, the resilient modulus values at a constant deviator stress increase with the increase of the confining pressure.

Table 3 – *Results of the Repeated Load Triaxial Test*

| Soil type | Depth (m) | $\sigma_c$ (kPa) | $\sigma_d$ (kPa) | $M_r$ (MPa) | COV (%) |
|---|---|---|---|---|---|
| PRF-silty clay | 0.8 | 41.8 | 26.4 | 37.8 | 0.4 |
| | | 41.4 | 13.1 | 45.0 | 0.1 |
| | | 41.5 | 26.3 | 38.5 | 0.3 |
| | | 41.5 | 38.4 | 33.6 | 0.2 |
| | | 41.5 | 51.0 | 29.9 | 0.1 |
| | | 41.5 | 63.9 | 27.9 | 0.1 |
| | | 20.7 | 13.1 | 40.5 | 0.3 |
| | | 20.7 | 25.8 | 32.1 | 0.2 |
| | | 20.7 | 37.9 | 28.3 | 0.1 |
| | | 20.7 | 50.8 | 26.7 | 0.1 |
| | | 20.7 | 63.9 | 26.1 | 0.1 |
| | | 0.4 | 12.8 | 33.8 | 0.2 |
| | | 0.4 | 25.2 | 26.7 | 0.2 |
| | | 0.4 | 37.4 | 24.2 | 0.0 |
| | | 0.4 | 50.6 | 23.5 | 0.2 |
| | | 0.4 | 63.7 | 23.7 | 0.2 |
| | 1.0 | 41.3 | 26.1 | 43.7 | 0.5 |
| | | 41.3 | 13.0 | 50.4 | 0.4 |
| | | 41.3 | 26.2 | 44.1 | 0.3 |
| | | 41.4 | 38.2 | 37.7 | 0.3 |
| | | 41.3 | 50.8 | 32.5 | 0.2 |
| | | 41.3 | 63.5 | 30.1 | 0.1 |
| | | 20.6 | 12.9 | 42.9 | 0.4 |
| | | 20.6 | 25.6 | 34.1 | 0.2 |
| | | 20.7 | 37.7 | 30.0 | 0.1 |
| | | 20.6 | 50.7 | 28.4 | 0.2 |
| | | 20.6 | 63.7 | 27.9 | 0.2 |
| | | 0.3 | 12.7 | 35.1 | 0.1 |
| | | 0.3 | 25.1 | 28.4 | 0.1 |
| | | 0.3 | 37.3 | 25.6 | 0.1 |
| | | 0.3 | 50.5 | 24.9 | 0.0 |
| | | 0.3 | 63.5 | 25.1 | 0.0 |
| PRF-heavy clay | 0.8 | 41.6 | 12.0 | 6.2 | 1.0 |
| | | 41.7 | 5.8 | 8.3 | 0.2 |
| | | 41.7 | 11.8 | 6.3 | 0.4 |
| | | 41.7 | 17.4 | 5.5 | 0.3 |
| | | 20.9 | 5.8 | 8.2 | 0.2 |
| | | 20.9 | 11.7 | 6.2 | 0.4 |
| | | 21.0 | 17.4 | 5.4 | 0.1 |
| | | 0.6 | 5.7 | 7.9 | 2.0 |
| | | 0.5 | 11.6 | 6.1 | 1.0 |
| | | 0.6 | 17.2 | 5.3 | 0.3 |
| | 1.0 | 41.4 | 12.1 | 7.0 | 2.0 |
| | | 41.5 | 5.9 | 8.6 | 2.0 |
| | | 41.5 | 12.3 | 7.1 | 1.0 |
| | | 41.4 | 17.3 | 5.8 | 0.3 |
| | | 20.9 | 5.9 | 8.8 | 1.0 |
| | | 20.9 | 12.1 | 6.8 | 1.0 |
| | | 20.9 | 17.3 | 5.8 | 0.2 |
| | | 0.6 | 5.8 | 8.2 | 0.4 |
| | | 0.6 | 11.9 | 6.5 | 0.4 |
| | | 0.6 | 17.2 | 11.7 | 0.2 |

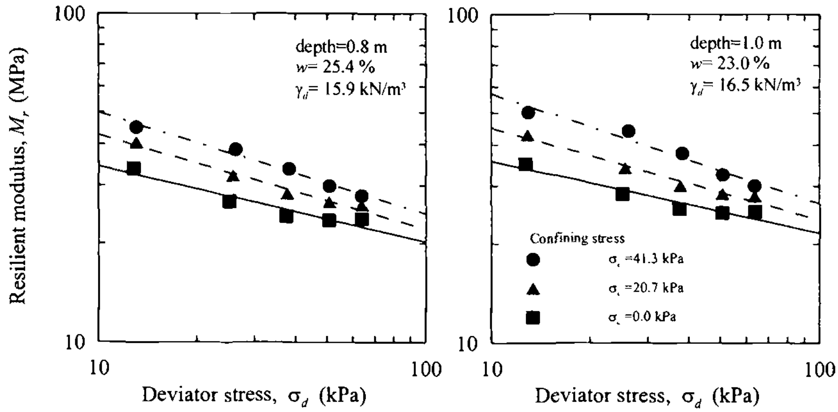


(a) Results of the repeated load triaxial test on the silty clay.

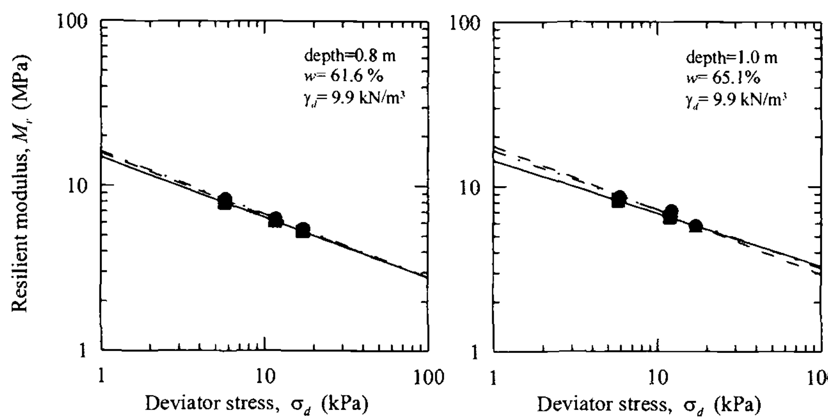


(b) Results of the repeated load triaxial test on the heavy clay.

Figure 8 – *Resilient Modulus*

## Development of the Resilient Modulus Model

This study aimed to establish a correlation between the cone penetration test parameters ($q_c$ and $f_s$) and the resilient modulus of cohesive soil and to validate the proposed correlation. Therefore, an experimental program was carried out in which cone penetration tests were conducted near boreholes from which undisturbed soil samples were tested to determine their resilient modulus.

In order to establish a correlation between the cone penetration test parameters and the resilient modulus, the variables affect both tests are identified. The cone tip resistance

($q_c$), sleeve friction ($f_s$) and resilient modulus ($M_r$) are affected by the soil type, unit weight ($\gamma$), moisture content of the soil ($w$), and state of stress ($\Phi$). Therefore, an attempt was made in this study to account for the effects of the cone resistance, sleeve friction, soil properties and stresses on the prediction of resilient modulus.

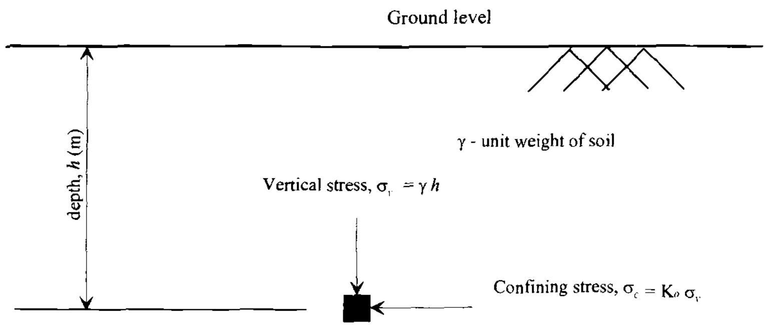


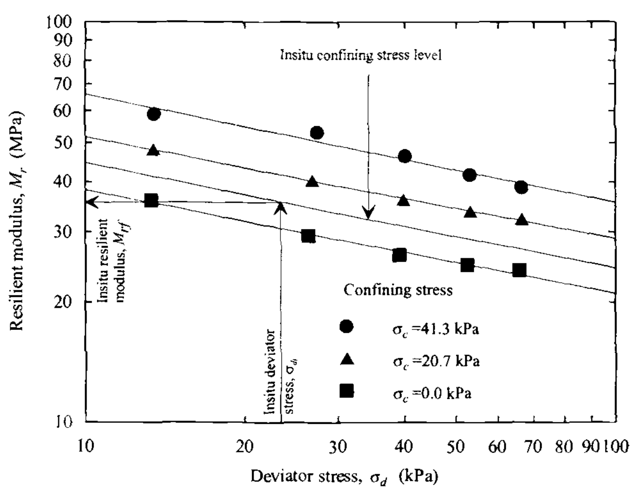


Figure 9 – *Estimation of the Field Resilient Modulus*

The resilient modulus obtained from the laboratory repeated loading triaxial test vary with deviator stress. Therefore, it is necessary to identify a single value of the resilient modulus from the laboratory test that corresponds to the in-situ stress conditions. This value of the resilient modulus is determined from the repeated load triaxial test and is referred to as the field resilient modulus ($M_{rf}$). A procedure was developed to determine the field resilient modulus for the investigated soils and is illustrated in Figure 9. The average depths of the undisturbed soil samples were 0.8 and 1.0 m. At these depths, the stresses acting on a soil element were computed. Then, the resilient modulus values were interpolated from the laboratory test results based on the stresses of each soil sample as illustrated in Figure 9. The soil is considered under in-situ ($K_o$) condition, where the in-situ stresses are calculated from the soil unit weight and the depth of the soil element under consideration. A summary of the field and laboratory test results and the analysis for the investigated soils is presented in Table 4. These results represent the resilient modulus values corresponding to the in-situ stress conditions ($M_{rf}$).

The variables presented in Table 4 are considered in the analysis to develop a model for predicting the resilient modulus using the CIMCPT output. Statistical analysis was performed using the Statistical Analysis System (SAS) program. The model is developed for the fine-gained soils under in-situ conditions. The variables for the PRF-silty clay and PRF-heavy clay were used to develop the model since they represent the stiff and the soft soil types, respectively. Based on the results of the statistical analysis, the following model was proposed to predict the resilient modulus of fine-grained soils using the cone penetration test:

$$\frac{M_r}{\sigma_c^{0.55}} = \frac{1}{\sigma_v}\left(31.79q_c + 74.81\frac{f_s}{w}\right) + 4.08\frac{\gamma_d}{\gamma_w}$$

where, $M_r$ is the resilient modulus (MPa), $q_c$ is the cone tip resistance (MPa), $f_s$ is the sleeve friction (MPa), $\sigma_c$ is the confining stress (kPa), $\sigma_v$ is the vertical stress (kPa), $w$ is the water content (decimal), $\gamma_d$ is the dry unit weight (kN/m$^3$), and $\gamma_w$ is the unit weight of the water (kN/m$^3$). The root mean squared error for this model is $RMSE$=1.37 and the coefficient of determination is $R^2$ = 0.99.

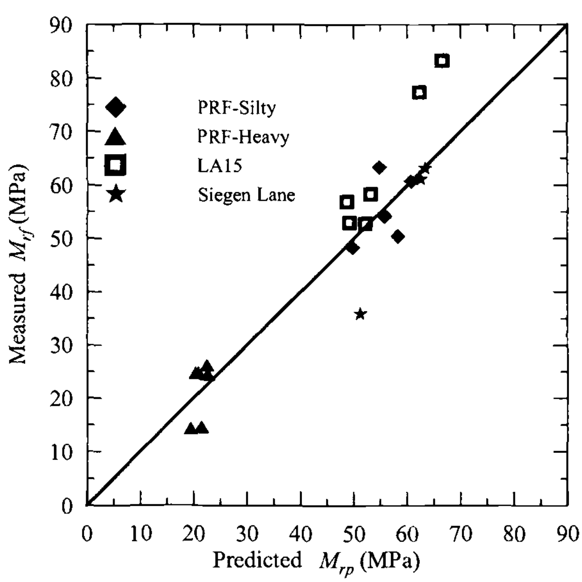


Figure 10 –*Measured versus Predicted Resilient Modulus*

Table 4 – *Summary of the Laboratory and Field Tests*

| Test site | Soil sample | Depth (m) | $q_c$ (MPa) | $f_s$ (MPa) | $w$ (%) | $\gamma_d$ (kN/m$^3$) | $\sigma_{cf}$ (kPa) | $\sigma_{df}$ (kPa) | $M_{rf}$ (MPa) |
|---|---|---|---|---|---|---|---|---|---|
| PRF-silty clay | BH1 | 0.8 | 2.50 | 0.066 | 25.4 | 15.9 | 12.4 | 4.5 | 48.4 |
| | BH1 | 1.0 | 3.20 | 0.071 | 23.0 | 16.5 | 15.7 | 5.3 | 50.4 |
| | BH2 | 0.8 | 2.69 | 0.091 | 20.8 | 16.8 | 12.4 | 4.5 | 54.1 |
| | BH3 | 0.8 | 2.82 | 0.073 | 23.2 | 16.9 | 12.4 | 4.5 | 63.4 |
| | BH3 | 1.0 | 3.15 | 0.092 | 21.5 | 17.0 | 15.7 | 5.3 | 60.7 |
| PRF-heavy clay | BH1 | 0.8 | 0.28 | 0.019 | 61.6 | 9.9 | 11.9 | 1.3 | 14.3 |
| | BH1 | 1.0 | 0.31 | 0.020 | 65.1 | 9.9 | 14.9 | 1.6 | 14.6 |
| | BH2 | 0.8 | 0.32 | 0.023 | 60.4 | 10.2 | 11.9 | 1.3 | 24.7 |
| | BH2 | 1.0 | 0.40 | 0.023 | 62.5 | 10.0 | 14.9 | 1.6 | 26.2 |
| | BH3 | 0.8 | 0.39 | 0.019 | 59.0 | 10.2 | 11.9 | 1.3 | 24.8 |
| | BH3 | 1.0 | 0.38 | 0.018 | 59.5 | 10.3 | 14.9 | 1.6 | 24.5 |
| LA-15 clay | BH1 | 0.8 | 2.85 | 0.151 | 24.1 | 17.3 | 13.0 | 4.1 | 77.4 |
| | BH1 | 1.0 | 2.08 | 0.114 | 23.0 | 16.2 | 15.1 | 4.8 | 58.3 |
| | BH2 | 0.8 | 2.07 | 0.123 | 28.4 | 16.8 | 13.1 | 4.1 | 52.8 |
| | BH2 | 1.0 | 2.14 | 0.097 | 27.3 | 15.3 | 14.8 | 4.7 | 53.0 |
| | BH3 | 0.8 | 3.07 | 0.135 | 18.8 | 17.8 | 12.9 | 4.1 | 83.3 |
| | BH3 | 1.0 | 2.05 | 0.110 | 31.4 | 15.2 | 15.2 | 4.8 | 56.9 |
| Siegen Lane clay | BH1 | 0.6 | 3.10 | 0.124 | 9.5 | 18.3 | 8.1 | 4.0 | 54.6 |
| | BH1 | 1.2 | 1.32 | 0.156 | 22.5 | 17.1 | 16.8 | 8.3 | 35.9 |
| | BH2 | 0.8 | 3.36 | 0.113 | 16.7 | 17.1 | 10.7 | 5.3 | 61.1 |
| | BH3 | 1.3 | 1.61 | 0.105 | 23.1 | 15.4 | 16.3 | 8.0 | 33.2 |

Legend: $q_c$ - tip resistance, $f_s$ - sleeve friction, $w$ - moisture content, $\gamma_d$ - dry unit weight, $\sigma_{cf}$ – computed confining stress, $\sigma_{df}$ – computed deviator stress, $M_{rf}$ - field resilient modulus, BH – borehole.

## Verification of the Resilient Modulus Model

The model for predicting the resilient modulus of cohesive soils by the cone penetration test was developed based on the field and laboratory test results on the PRF-silty clay and heavy clay. The model was then verified by predicting the resilient modulus of the other cohesive soils and comparing the model predictions and laboratory and field test results. The results of the predicted versus measured resilient modulus are shown in Figure 10. The predicted and measured values of resilient modulus are in good agreement.

## Conclusions

This paper presented a pilot investigation to assess the applicability of the intrusion technology for estimating the resilient modulus of subgrade soils. Field and laboratory testing programs were conducted on four cohesive soils in Louisiana. Cone penetration tests were conducted using the continuous intrusion miniature cone penetration test with measurements of the cone tip resistance and sleeve friction. Undisturbed and disturbed soil samples were obtained from different depths next to the cone penetration tests. Repeated load triaxial tests were conducted on the undisturbed soil samples to determine the resilient modulus. Other laboratory tests were conducted also to determine the strength parameters, physical properties, and compaction characteristics. Results of both field and laboratory testing programs were analyzed and critically evaluated.

Statistical analysis was conducted on the cone penetration test profiles and the repeated load triaxial test results to evaluate the quality of the field and laboratory tests. A statistical model for predicting the resilient modulus was developed based on the field and laboratory test results of two soils, which comprise stiff and soft cohesive soils. The model correlates the resilient modulus to the cone penetration test parameters, basic soil properties, and in-situ stress conditions of the soil. Predicting the resilient modulus of the other two soils and comparing the results with laboratory and field measurements validated the model.

## Acknowledgments

This research project is financially supported by the U.S. Department of Transportation, Federal Highway Administration/Priority Technology Program (USDOT FHWA/PTP) Contract No. DTFH71-97-PTP-LA-14, the Louisiana Department of Transportation and Development (LADOTD) State Project No. 736-99-0773, and the Louisiana Transportation Research Center Project No. 98-8GT.

The effort of William T. Tierney, Research Specialist/LTRC, in conducting the cone penetration tests and soil sampling is appreciated. The assistance of Amar Raghavendra, Research Associate/ LTRC, in getting the MTS system operational for the resilient modulus tests is acknowledged. Mark Morvant, Geotechnical Manager/LTRC, efforts and cooperation during the field and laboratory testing programs is gratefully appreciated. Paul Brady, Melba Bounds, and Kenneth Johnson, LTRC Geotechnical Laboratory helped in conducting various soil tests.

## References

AASHTO, 1993, Guide for Design of Pavement Structures, American Association of State Highway and Transportation Officials, Washington D.C.

AASHTO, 1995, "Resilient Modulus of Unbound Granular Base/Subbase Materials and Subgrade Soils," SHRP Protocol P-46, American Association of State Highway and Transportation Officials, Washington D.C., pp. 794-807.

Allen, D. L., 1989, "$M_r$ Testing in Kentucky," Workshop on Resilient Modulus Testing, Oregon State University, Corvallis, Oregon.

Badu-Tweneboah, K., Manzione, C.W., Ruth, B.E., and Miley, W.G. 1989, "Prediction of Flexible Pavement Layer Moduli from Dynaflect and FWD Deflections." American Society for Testing and Materials: *Non-destructive Testing of Pavements and Backcalculation of Moduli.* A.J. Bush III and G.Y. Baldi, Eds., *ASTM 1026*, Philadelphia, pp. 245-277.

Drumm, E. C., Reeves, J. S., Madgett, M. R., and Trolinger, W. D., 1997, "Subgrade Resilient Modulus Correction for Saturation Effects," *Journal of Geotechnical and Geoenvironmental Engineering*, Vol. 123, No.7, pp. 663-670.

Fredlund, D. G., Bergan, A. T., and Wong, P. K., 1977, "Relation Between Resilient Modulus and Stress Conditions for Cohesive Subgrade Soils", *Transportation Research Record*, No. 642, pp. 73-81.

Kamal, M. A., Dawson, A. R., Farouki, O. T., Hughes, D. A. B., and Sha'at, A. A., 1993 "Field and Laboratory Evaluation of the Mechanical Behavior of Unbound Granular Materials in Pavements," *Transportation Research Record*, No. 1406, pp. 88-97.

McGee, N., 1989, "Cold Region Facility - Subgrade Soils," Workshop on Resilient Modulus Testing, Oregon State University, Corvallis, Oregon.

Mohammad, L. N., Puppala, A. J., and Alavilli, P., 1994, "Influence of Testing Procedure and LVDT Location on Resilient Modulus of Soils", *Transportation Research Record*, No. 1462, pp. 91-101.

Mohammad, L. N., Puppala, A., and Alavilli, P., 1994, "Effect of Strain Measurements on Resilient Modulus of Granular Soils," *Dynamic Geotechnical Testing*: Second Volume, *ASTM STP 1213*, ASTM, pp.202-221.

Mohammad, L. N. and Puppala, A., 1995, "Resilient Properties of Laboratory Compacted Subgrade Soils," *Transportation Research Record*, No. 1504, pp. 87-102.

Monismith, C. L., 1989, "$M_r$ testing- Interpretation of Laboratory Results for Design Purposes," Workshop on Resilient Modulus Testing, Oregon State University, Corvallis, Oregon.

Nataatmadja, A. and Parkin, A., 1989, "Characterization of Granular Materials for Pavements," *Canadian Geotechnical Journal*, Vol.26, No.4, pp. 725-730.

Puppala, A. J., Acar Y. B., and Tumay, M. T. 1995, "Cone Penetration in Very Weakly Cemented Sands." *Journal of Geotechnical Engineering*, ASCE, Vol. 121, No. 8, pp. 589-600.

Rada, G. and Witczak, M. W., 1981, " Comprehensive Evaluation of Laboratory Resilient Moduli Results for Granular Material," *Transportation Research Record*, No. 810, pp. 23-33.

Titi, H. H., Mohammad, L. N., and Tumay, M. T., 2000, "Miniature Cone Penetration Tests in Soft and Stiff Clays," *Geotechnical Testing Journal*, ASTM, Vol. 23, No. 4, pp.432-443.

Tumay, M. T., and Titi, H. H., 2000, "Research Pays Off: Louisiana's Continuous Intrusion Miniature Cone Penetration Test System," *TR News*, Transportation Research Board, Issue 207, pp. 26-27.

Tumay, M. T., and Kurupp, P. U., and Boggess, R. L., 1998, "A Continuous Intrusion Electronic Miniature Cone Penetration Test System for Site Characterization," Geotechnical Site Characterization, Proc. 1st International Conf. On site characterization-ISC'98, Atlanta, Vol. 1, pp. 1183-1188.

Tumay, M. T. 1985, Field Calibration of Electric Cone Penetrometer in Soft Soil - Executive Summary, Report FHWA/LA-LSU-GE 85/02, Louisiana Transportation Research Center, Baton Rouge, Louisiana.

Hani H. Titi[1], Louay N. Mohammad[2], and Ananda Herath[3]

# Characterization of Resilient Modulus of Coarse-Grained Materials Using the Intrusion Technology

**Reference**: Titi, H. H., Mohammad, L. N., and Herath, A., "**Characterization of Resilient Modulus of Coarse-Grained Materials Using the Intrusion Technology,**" *Resilient Modulus Testing for Pavement Components, ASTM STP 1437,* G. N. Durham, W A. Marr, and W. L. De Groff, Eds., ASTM International, West Conshohocken, PA, 2003.

**Abstract:** The objective of this study was to investigate the applicability of the cone penetration test to determine the resilient modulus of coarse-grained materials. Field and laboratory investigations were conducted at the sites of two pavement projects in Louisiana. Field tests consisted of continuous intrusion miniature cone penetration tests and soil sampling. Laboratory tests included the repeated load triaxial test and other tests for materials characterization. The test results were used to develop a correlation for predicting the resilient modulus of coarse-grained materials using the cone penetration test parameters and basic soil properties. Another laboratory investigation was conducted to investigate the effect of moisture content and unit weight on the cone penetration test parameters and resilient modulus. Test results were used to validate the model developed for predicting the resilient modulus. The resilient modulus values predicted were consistent with those obtained using the repeated load triaxial test.

**Keywords:** resilient modulus, coarse-grained materials, cone penetration test

## Introduction

The methods of determining the resilient modulus of subgrade soils and pavement-unbound materials are based on laboratory and field tests. Laboratory test methods include the repeated load triaxial test, simple shear, resonant column, gyratory, and the

[1] Assistant Professor, Department of Civil Engineering & Mechanics, University of Wisconsin – Milwaukee, P.O. Box 784, Milwaukee, WI 53201.
[2] Associate Professor, Department of Civil & Environmental Engineering and Louisiana Transportation Research Center, Louisiana State University, 4101 Gourrier Ave., Baton Rouge, LA 70808.
[3] Postdoctoral Researcher, Louisiana Transportation Research Center, 4101 Gourrier Ave., Baton Rouge, LA 70808.

hollow-cylinder testing device. These laboratory tests require advanced testing equipment and skilled personnel, and are considered expensive, laborious, and time consuming. Field tests include the nondestructive testing (NDT) using devices such as the dynamic deflection determination system (DYNAFLECT) and the falling weight deflectometer (FWD). Nondestructive testing of pavements is quick and easy to perform; however, there is a concern regarding reliability of using these methods to evaluate pavement layers moduli. The NDT methods use backcalculation procedures to determine the pavement layers moduli. Analysis using these procedures does not result in a unique solution; moreover, the many provided solutions depend on the input parameters. Therefore, there is a need for a reliable, fast, and economical in-situ test method to estimate the resilient modulus of subgrade soils and pavement unbound materials.

The cone penetration test (CPT), an integrated methodology for site characterization, has been used for a wide range of applications in geotechnical and pavement engineering. The CPT technology is fast, cost effective, and can effectively be used during the different design and construction phases of a pavement project.

This paper presents the results of a study conducted to determine the resilient characteristics of coarse-grained materials (cohesionless subgrade soils and unbound granular pavement materials) using the cone penetration test. Field and laboratory testing programs were conducted at two pavement project sites in Louisiana. Field tests consisted of cone penetration tests and soil sampling, while laboratory tests consisted of the repeated load triaxial test and other laboratory tests for materials characterization. The field tests were conducted on the pavement materials under their natural conditions of moisture content and unit weight. Test results were analyzed and used to propose a correlation between the resilient modulus and the cone penetration test parameters. A laboratory investigation was also conducted to investigate the effect of the moisture content and unit weight of these materials on the resilient modulus determined using the cone penetration test.

## Background

Among the different laboratory methods, the repeated load triaxial test is the most popular for determination of the resilient modulus. The resilient modulus ($M_r$) in a repeated load triaxial test is defined as the ratio of the maximum deviator stress ($\sigma_d$) and the recoverable elastic strain ($\varepsilon_r$) as follows:

$$M_r = \frac{\sigma_d}{\varepsilon_r} \qquad (1)$$

Figure 1 illustrates the definition of the resilient modulus in a repeated load triaxial test. The resilient modulus determined from the laboratory tests is influenced by many factors including the material type (coarse-grained, fine-grained), moisture content, unit weight, size of the specimen, stress pulse shape, duration, frequency and sequence of stress levels, testing equipment, and specimen preparation, as well as conditioning methods (Fredlund et al. 1977, Rada and Witczak 1981, Allen 1989, McGee 1989, Monismith 1989, Nataatmadja and Parkin 1989, Kamal et al. 1993, Mohammad et al. 1994, Drumm et al. 1997).

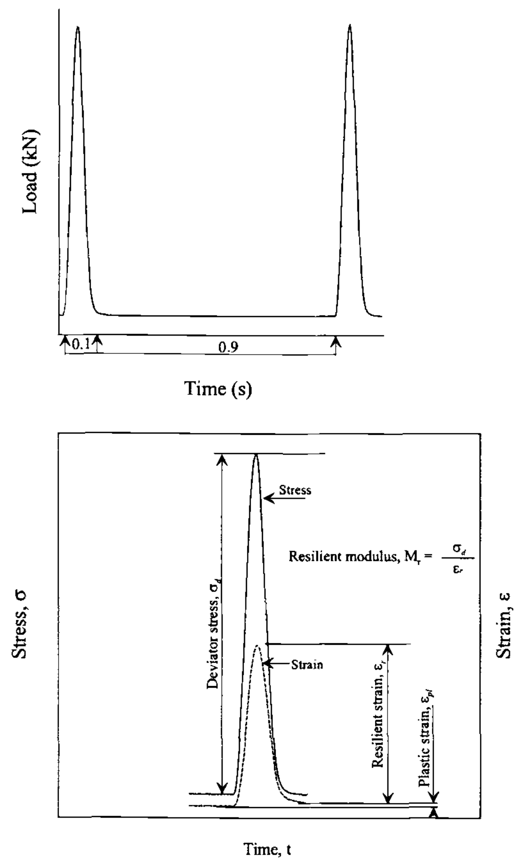


Figure 1 – *The definition of the resilient modulus in a repeated loading triaxial test*

The importance of reliable determination of the resilient modulus is illustrated in Figure 2. The AASTHO 1993 procedure for flexible pavement design requires the resilient modulus of subgrade soil as an input parameter. As shown in Figure 2, for the given design parameters, the variation of the overlay design thickness is influenced by the value of the resilient modulus. Underestimating the resilient modulus of subgrade soil by 10 MPa will result in an additional 37 mm increase of thickness of the overlay. Therefore, determination of a proper resilient modulus is desired in pavement design.

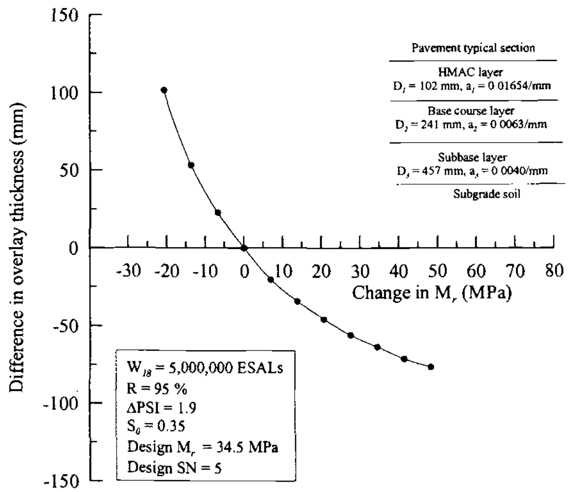


Legend
$W_{18}$ = predicted number of equivalent single axle load (ESAL)
R = reliability
ΔPSI = difference between the initial design serviceability index and the design terminal serviceability index
$S_0$ = combined standard error of the traffic prediction and performance prediction
$M_r$ = resilient modulus of subgrade soil
SN = structural number

Figure 2 – *The effect of varying the resilient modulus of subgrade soil on the overlay design thickness*

The cone penetration test has been successfully used for characterization of geomaterials. The cone penetration test consists of pushing a cylindrical rod with a conical tip into the soil and measuring the resisting forces. There are two forces measured during the penetration: the cone tip resistance ($q_c$), which is the soil resistance to advance the cone tip, and the sleeve friction ($f_s$), which is the friction developed between the soil and the sleeve of the penetrometer. The friction ratio ($R_f$) is the ratio of the sleeve friction and tip resistance and is expressed in percent. These measured parameters are used to classify the soils and determine their properties.

Applications of the CPT in the field of pavement engineering, particularly related to subsoils, have also been attempted. Badu-Tweneboah et al. (1989) conducted CPT tests on various highway pavements in Florida. They correlated the cone test results with the resilient modulus determined from NDT methods. Inaccuracies and uncertainties involving NDT backcalculation subroutines may have affected the reliability of these correlations. In spite of this limitation, this study revealed the potential of CPT in determining the resilient properties of subgrade soils and unbound pavement materials.

There is a concern regarding the use of the cone penetration test to determine the resilient modulus of geomaterials. The tip resistance and sleeve friction are obtained from the cone penetration test, which is considered a quasi-static test method, whereas the resilient modulus is a property obtained from a dynamic repeated load test. It is often assumed that test parameters obtained from different test backgrounds may not provide reasonable correlations with one another. However, this is not always the case. Earlier studies (Tumay 1985, Puppala et al. 1995) showed the potential of the quasi-static CPT method in determining the low strain dynamic shear modulus and liquefaction of soil. The dynamic shear moduli and CPT parameters are less influenced by stress and strain history. In fact, these parameters are controlled by the same soil variables, which may have led to the development of better correlations between them. The resilient modulus is considered analogous to the shear modulus. Therefore, the influence of stress and strain behavior on the resilient modulus will be similar to that of the shear modulus.

Previous studies also indicated that the resilient property of subgrade soil is less dependent on stress and strain history (Mohammad et al. 1994). The strain history influence is also expected to be insignificant in a nondestructive repeated load triaxial test. Furthermore, the cone penetration tests and repeated load resilient modulus tests were conducted on soil under identical environmental conditions. This implies that both test parameters were subjected to similar environmental variables such as density, moisture content, and geomaterial fabric. In such conditions, the cone penetration test and resilient moduli parameters depend on the same soil variables. Therefore, it is reasonable to assume that a correlation is possible between the cone penetration test and resilient moduli parameters.

## Objective of Research

The objective of this study was to evaluate the applicability of the cone penetration test in determining the resilient modulus of coarse-grained materials such as granular base course layers and embankments, and cohesionless subgrade soils. Moreover, this study attempted to develop and validate a model to determine the resilient modulus of these materials from the cone penetration test results and basic soil properties.

## Field and Laboratory Testing Programs

The research approach adopted is divided into two parts:

(1) Conducting field and laboratory testing programs at the sites of pavement projects to assess the applicability of the cone penetration test in determining the resilient modulus of coarse-grained materials. The field tests of this phase consisted of cone penetration tests and material sampling. The laboratory tests consisted of repeated load triaxial test in addition to other laboratory tests for material characterization.

(2) Conducting a detailed laboratory investigation to evaluate the effect of the unit weight and moisture content on the resilient modulus determined by the cone penetration test. This phase was completed in the laboratory and included miniature cone penetration tests conducted on materials prepared under different conditions of moisture content and unit weight. Repeated load triaixial tests were conducted on samples under the specified

moisture content and unit weight. Other laboratory tests were also conducted to determine the physical properties and compaction characteristics of these materials.

### *Equipment for Field and Laboratory Testing*

*Continuous Intrusion Miniature Cone Penetration Test (CIMCPT) System* – The system was developed, calibrated, and implemented (Tumay et al. 1998, Tumay and Titi 2000, Titi et al. 2000, Titi and Morvant 2001) for shallow depth site characterization. The system consists of a continuous push device, coiling/uncoiling mechanism, hydraulic motor, and data acquisition system. The cone is attached to a coiled push rod, which allows a continuous penetration of the cone. The coil is mechanically straightened as the cone is pushed into the soil. The continuous push device of the CIMCPT system is shown in Figure 3a. The system pushes a miniature cone penetrometer (Figure 3b) with a cross sectional area of 2 $cm^2$, a friction sleeve area of 40 $cm^2$, and a cone apex angle of 60 degrees.

*Miniature Cone Penetration Test (MCPT) System* – This system was fabricated to conduct the miniature cone penetration tests on the pavement materials under controlled unit weight and moisture content. The MCPT system, shown in Figure 3c, consists of a hydraulic push system, a depth encoder, a reaction frame, a miniature cone penetrometer, and a data acquisition system.

*Material Testing System (MTS)* – a model MTS-810 closed loop servo-hydraulic material testing system was used to perform the repeated load triaxial test. The major components of this system are the loading frame, digital controller, hydraulic actuator, load cell, triaxial cell, LVDTs, and pressure control panel.

### *Field and Laboratory Investigation*

The field-testing program was conducted at two pavement project sites in Louisiana. Description of the test sites is given below.

*State Route LA-28, Simpson* – This site is located near the intersection of the State Route LA-28 and Highway 465 near Simpson, Vernon Parish. The site is used by the Louisiana Department of Transportation and Development as a borrow pit for construction of roadway embankments. The soil at the site consists of 60 percent sand, 18 percent silt, and 12 percent clay. The soil is classified silty sand (SM) according to the USCS and silty sand (A-2-4) according to the AASHTO soil classification system. Standard Proctor test using this soil showed that the optimum moisture content of the soil is 11.4 percent and the corresponding maximum dry unit weight is 18.3 $kN/m^3$.

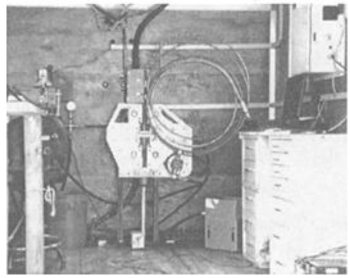

(a) The continuous intrusion miniature cone penetration test (CIMCPT) system used for field and laboratory investigation

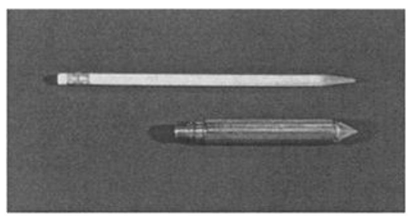

(b) The miniature cone penetrometer

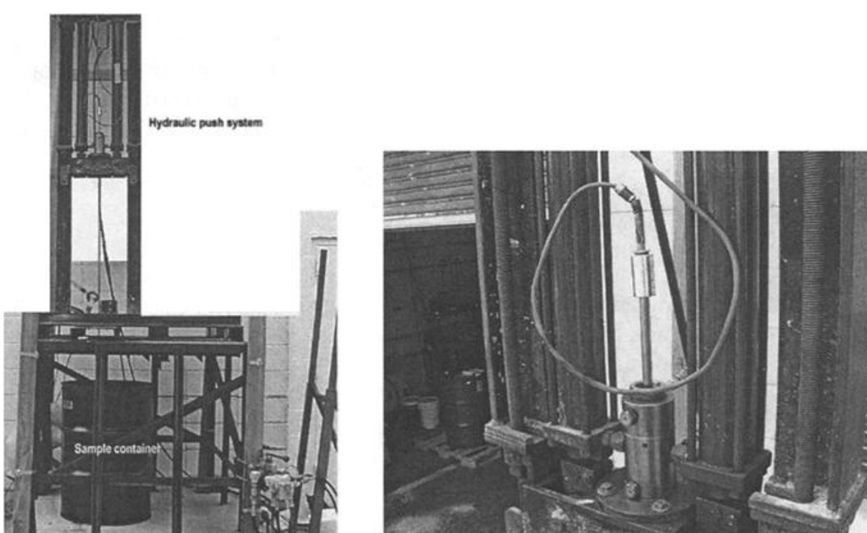


(c) The miniature cone penetration test (MCPT) system and the test setup used for laboratory investigation

Figure 3 – *Field and laboratory test equipment used in the investigation*

*State Route LA-89, New Iberia* – The test site is an embankment located on State Route LA-89, New Iberia. The embankment consists of recycled soil-cement base (granular material), which exhibited a behavior similar to that of granular materials under repeated load triaxial test. The soil is classified silty gravel (GM) according to the USCS and gravel and sand (A-1-b) according to the AASHTO soil classification system.

The CIMCPT system was used to conduct the cone penetration tests at each site. Cone penetration tests were conducted by continuously advancing the cone into the ground at a rate of 2 cm/sec. Continuous measurements of cone tip resistance ($q_c$) and sleeve friction ($f_s$) were obtained. As shown in Figure 4a, cone penetration tests were conducted at a certain pattern close to the borehole location from which the material samples were obtained for laboratory testing. This was to ensure that the cone penetration tests represent the material tested in the laboratory.

Material samples were obtained from boreholes at each test site down to a depth of 2.0 m. Samples were extracted, sealed, and kept in a humidity room. Material sampling and cone penetration tests were carried out at the same day in order to ensure similar in-situ conditions. Soil samples, under their natural moisture content and unit weight, were subjected to laboratory tests to determine the resilient modulus, physical properties, and compaction characteristics. The resilient modulus test was conducted according to AASHTO T 294-94: Resilient Modulus of Unbound Granular Base/Subbase Materials and Subgrade Soils-SHRP Protocol P46. Other laboratory tests included determining the Atterberg limits of soils, moisture content, moisture content-unit weight relationships, grain size distribution, and specific gravity.

### *Laboratory Investigation*

Two coarse-grained materials (silty sand and sand), which are commonly used in pavement layers, were selected for laboratory investigation under controlled conditions of moisture content and unit weight. These materials were collected and subjected to variety of tests to determine their properties and to establish their moisture content-unit weight relationships. In order to perform cone penetration tests on these materials under controlled moisture content and unit weight, a test setup was assembled as shown in Figure 3c. Each material was compacted in a 55-gallon rigid-wall metal container under three different values of moisture content and unit weight. These values are (1) the dry side (below the point of optimum moisture content), (2) the point of optimum moisture content, and (3) the wet side (above the point of optimum moisture content).

Each material was subjected to five miniature cone penetration tests under each moisture content and unit weight. The miniature cone penetrometer was advanced into the container at a rate of 20 mm/sec in three strokes. Continuous measurements of cone tip resistance ($q_c$) and sleeve friction ($f_s$) were obtained. The miniature cone penetration tests were conducted according to the layout shown in Figure 4b. The test layout was selected to avoid the container boundary effects on the results of the miniature cone penetration test.

After the miniature cone penetration tests were conducted, soil samples were collected at different depths for the laboratory resilient modulus and soil property tests.

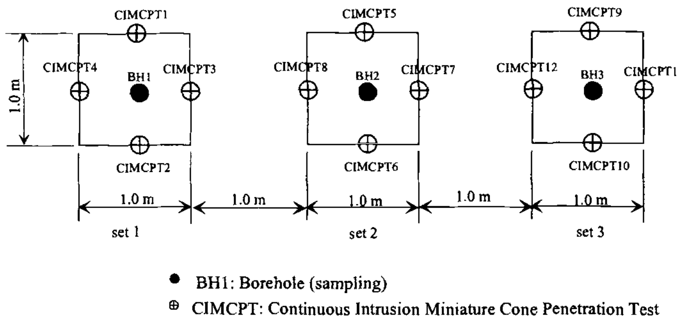


(a): Field testing and material sampling for the field and laboratory investigation

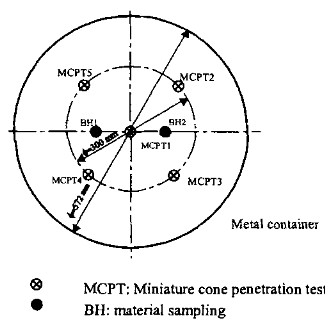


(b): Laboratory testing and material sampling for the laboratory investigation

Figure 4 – *Typical configuration for field and laboratory cone penetration tests and material sampling*

## Analysis of Field and Laboratory Test Results

### *Field and Laboratory Investigation*

The results of the laboratory tests conducted to evaluate the physical properties of the investigated materials are summarized in Table 1. All materials considered are coarse-grained, which were used in highway embankments or base course pavement layers.

The continuous intrusion miniature cone penetration test results (set #1) on the silty sand, LA-28 site are shown in Figure 5a. Inspection of the figure shows that the tip resistance and sleeve friction profiles are consistent among the four tests in set #1 and reflect similar pattern. Statistical analysis was conducted to quantitatively evaluate the repeatability of the miniature cone penetration tests. Each profile was divided into thin 20-mm soil layers in which the cone penetration test parameters ($q_c$ and $f_s$) were averaged along the 20-mm layers. For each 20-mm divided layer, there are four values for $q_c$ and four values for $f_s$. The average of these four values, the standard deviation, and the coefficient of variation were determined. The average values of the coefficient of variation for $q_c$ and $f_s$ are shown in Figure 5b. The variation of $q_c$ reflects the variability of each material at the same test site. It is not expected to have identical materials at two different locations at the same site. Generally, the cone penetration test results showed good compliance and are consistent within the same group and reflected similar patterns.

Table 1 – *Properties of the investigated materials*

| Property | LA-28, Simpson | LA-89, New Iberia | Material Type (Laboratory testing) | |
|---|---|---|---|---|
| | | | Silty Sand | Sand |
| Description | Base course | Base course | Embankment | Base course |
| Passing sieve #200 (%) | 30 | 24 | 39 | 2 |
| Clay (%) | 12 | 16 | 9 | 0 |
| Silt (%) | 18 | 8 | 30 | 2 |
| Specific gravity, $G_s$ | 2.68 | - | 2.69 | 2.67 |
| Optimum water content ($w_{opt}$) (%) | 11.4 | - | 15.2 | 8.1 |
| Maximum dry unit weight, $\gamma_{dmax}$ (kN/m$^3$) | 18.3 | - | 17.2 | 16.4 |
| Unified Soil Classification System - (USCS) | SM Silty sand | GM Silty gravel with sand | SM Silty sand | SP Poorly graded sand |
| AASHTO Soil Classification | A-2-4 Silty sand | A-1-b Gravel and sand | A-4 Sandy loam | A-3 Fine sand |

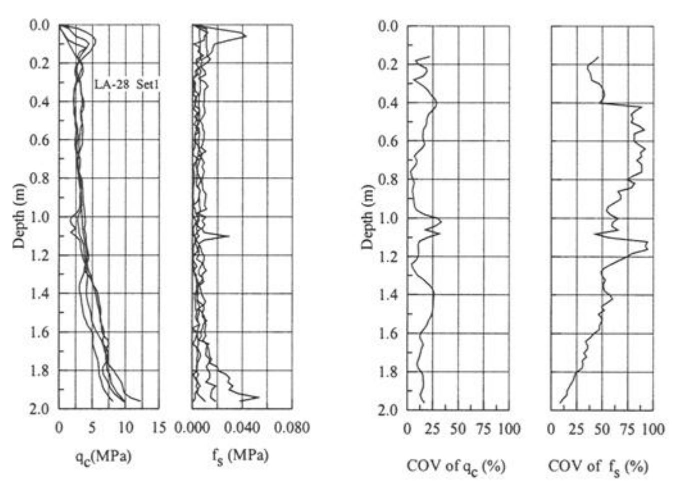


(a) Results of continuous intrusion miniature cone penetration tests

(b) Results of statistical analysis on continuous intrusion miniature cone penetration tests

Figure 5 – *Results of cone penetration testing at LA-28 pavement project site*

The results of the repeated load triaxial test on the silty sand at LA-28, Simpson, are shown in Figure 6. The figure shows a typical variation of the resilient modulus with the bulk stress for coarse-grained materials where the resilient modulus increases with the increase of bulk stress. The resilient modulus varies between 48 and 202 MPa, depending on the stress levels. When the bulk stress increases, the material particles become closer to each other, which result in better interlocking and frictional characteristics.

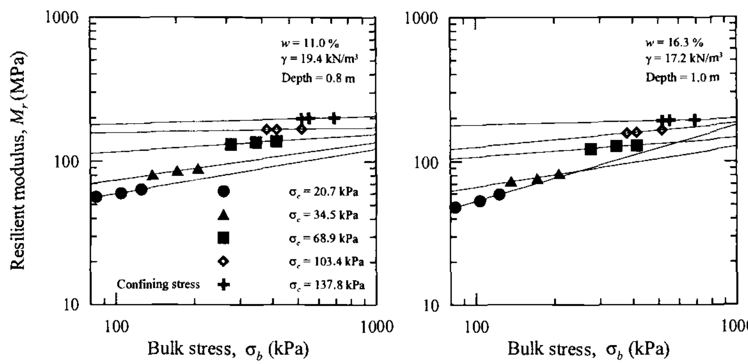


Figure 6 – *Results of the repeated load triaxial test on silty sand base course layer at the State Route LA-28 project, Simpson*

*Resilient Modulus- CPT Correlation*

The resilient modulus obtained from the laboratory repeated load triaxial test varies with the bulk stress. Therefore, it is necessary to determine a single value of the resilient modulus from the laboratory test that corresponds to the pavement stress conditions in the field. This resilient modulus values is identified as the field resilient modulus ($M_{rf}$). A procedure was developed to determine the field resilient modulus from laboratory test results as illustrated in Figure 7. The in-situ stresses acting on an element located at a depth $D$ under the pavement surface were determined from the unit weight of the material and the depth of the element. A traffic loading corresponding to 20-kN standard single wheel loading was applied on the pavement surface. The stresses induced on the material element due to the applied traffic loading were determined using a computer program for analysis of linear-elastic pavement systems called ELSYM5 (1985). The configuration of the different pavement layers considered in the elastic analysis is presented in Figure 7. Typical values of the modulus of elasticity and Poisson's ratio were used in the analysis. The stresses acting on the material element due to in-situ stresses and traffic loading were added. These stresses are considered the highest stress levels that the pavement system will experience. The levels of the bulk and confining stresses were determined and located on the graph shown in Figure 7. Finally, the resilient modulus corresponding to the stress levels of the in-situ and traffic loadings was determined as illustrated in the

Figure 7. A summary of the field and laboratory test results for the coarse-grained materials is presented in Table 2. These results represent the resilient modulus values corresponding to the in-situ and traffic stresses.

Table 2 – *Summary of the laboratory and field test results on the investigated coarse-grained materials (in-situ and traffic)*

| Test site | Soil sample | Depth (m) | $q_c$ (MPa) | $f_s$ (MPa) | $w$ (%) | $\gamma_d$ (kN/m$^3$) | $\sigma_c$ (kPa) | $\sigma_d$ (kPa) | $M_{rf}$ (MPa) |
|---|---|---|---|---|---|---|---|---|---|
| LA-89 | BH1 | 0.4 | 6.5 | 0.324 | 18.8 | 15.8 | 1.02 | 9.69 | 52.2 |
| | BH3 | 0.4 | 8.1 | 0.369 | 17.9 | 17.9 | 10.6 | 9.85 | 75.0 |
| LA-28 | BH1 | 0.8 | 2.30 | 0.015 | 11.0 | 17.2 | 13.4 | 13.7 | 43.3 |
| | BH1 | 1.0 | 2.10 | 0.025 | 16.3 | 17.2 | 14.9 | 15.0 | 34.8 |
| | BH2 | 0.8 | 2.30 | 0.0217 | 11.1 | 17.7 | 13.5 | 13.8 | 44.4 |
| | BH3 | 0.8 | 2.40 | 0.0238 | 10.3 | 17.5 | 12.5 | 12.8 | 38.9 |

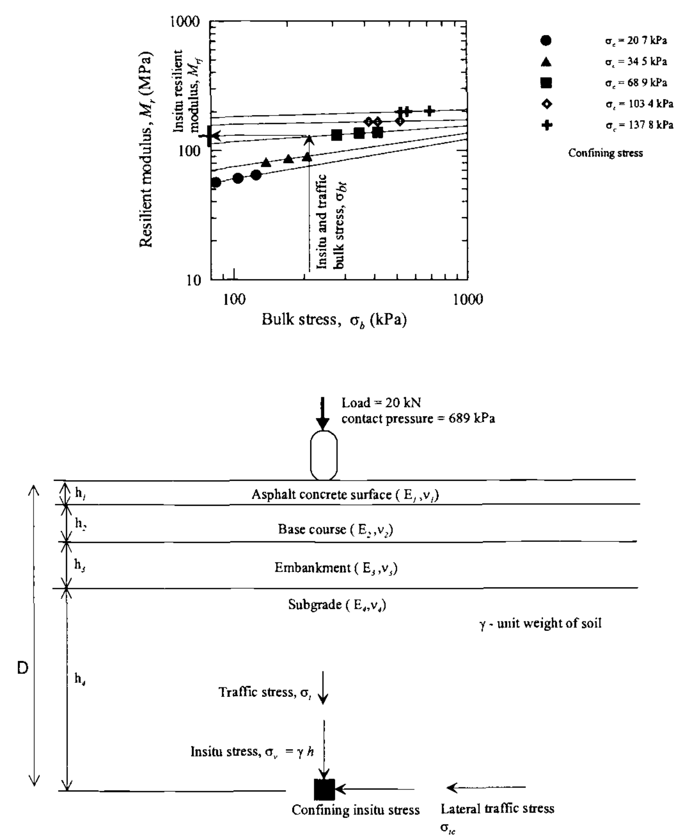


Figure 7 – *Determination of the field resilient modulus value under in-situ and traffic stresses*

In order to establish a correlation between the cone penetration test parameters and the resilient modulus, the variables that affect the results of both the cone penetration test and resilient modulus were identified. The tip resistance ($q_c$), sleeve friction ($f_s$), and resilient modulus ($M_r$) are affected by the material type (fine-grained, coarse-grained), unit weight ($\gamma$), moisture content ($w$), and the stress level ($\sigma$). Therefore, any proposed model should consider the effects of these variables on the resilient modulus. The variables presented in Table 2 were used in the analysis to correlate the resilient modulus and the cone penetration test parameters. Statistical analyses (multiple regression) were performed using the Statistical Analysis System (SAS) program. Forward selection, backward elimination, all possible regression, and stepwise procedures were used to select the variables in these correlations. The following relationship was developed based on the statistical analysis:

$$M_r = 18.95 q_c \frac{\sigma_3^{0.55} \sigma_b}{\sigma_1^2} + 0.41 \sigma_3^{0.55} \frac{\gamma_d}{w \gamma_w} \tag{2}$$

where $M_r$ is the resilient modulus (MPa), $\sigma_3$ is the confining stress (kPa), $\sigma_1$ is the vertical stress (kPa), $q_c$ is the tip resistance (MPa), $w$ is the water content, $\gamma_d$ is the dry unit weight (kN/m$^3$), $\gamma_w$ is the unit weight of water (kN/m$^3$), and $\sigma_b$ is the bulk stress (kPa). For this model, the coefficient of multiple determination, $R^2 = 0.99$ and root mean squared error, RMSE=1.25. The model presented in Equation 2 does not include the sleeve friction ($f_s$). Models that include $f_s$ were attempted and disregarded due to their low value of $R^2$ and high RMSE.

*Laboratory Investigation*

The results of the field and laboratory investigation were used to develop a correlation for predicting the resilient modulus of coarse-grained materials from the cone penetration test parameters and basic soil properties. The laboratory investigation intended to investigate the effects of the unit weight and moisture content of the material on the predicted resilient modulus. In addition, it will provide data required to validate the proposed model.

Analysis was conducted on the results of the laboratory miniature cone penetration tests on the investigated materials under controlled conditions of moisture content and unit weight. Figure 8 shows the cone penetration test profiles for the sand under three different conditions of moisture content and unit weight. The coarse-grained materials showed higher $q_c$ values for the samples prepared at the optimum moisture content and maximum dry unit weight. This is expected since the material possesses a higher strength under these conditions and therefore higher resistance to penetration. The samples on the wet side of the moisture content-unit weight curve showed the lowest $q_c$ values. The strength of these materials decreases with the increase of the moisture content and the decrease of the unit weight. It is evident that the tip resistance was influenced by the moisture content and the unit weight. Statistical analysis (described earlier) was also conducted to evaluate the repeatability of the miniature cone penetration tests. The average coefficient of variation for $q_c$ ranges from 7 to 16 for coarse-grained materials. The cone penetration test profiles showed good compliance and are consistent within the same group and reflected similar patterns.

The results of the repeated load triaxial test on the materials under controlled conditions of moisture content and unit weight are presented in Table 3. Inspection of Table 3 indicates that the materials with optimum moisture content and maximum dry unit weight exhibited the highest values of the resilient modulus. The results of the repeated load triaxial tests on the sand under controlled conditions of moisture content and unit weight are shown in Figure 9. The variation of the moisture content of the sand (from 5 to 11 percent) slightly affected the resilient modulus. This is due to effect of other factors on the resilient modulus of coarse-grained materials such as stress levels (confinement), particle shape, and particle size.

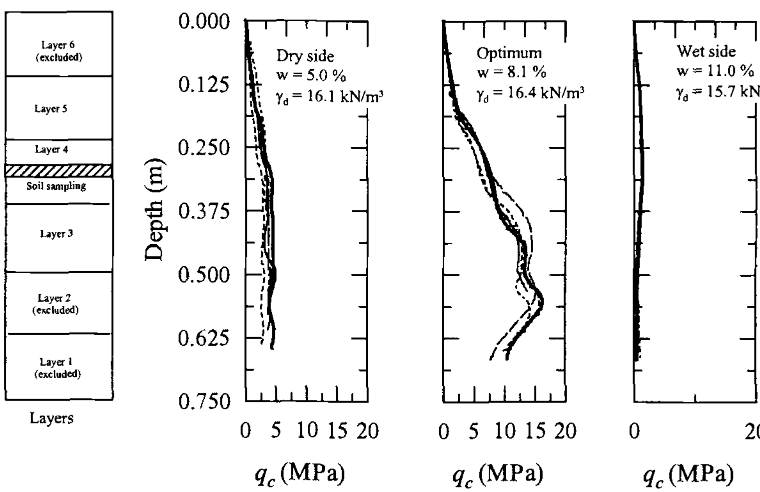


Figure 8 – *Results of the miniature cone penetration tests conducted on sand under controlled conditions of moisture content and unit weight*

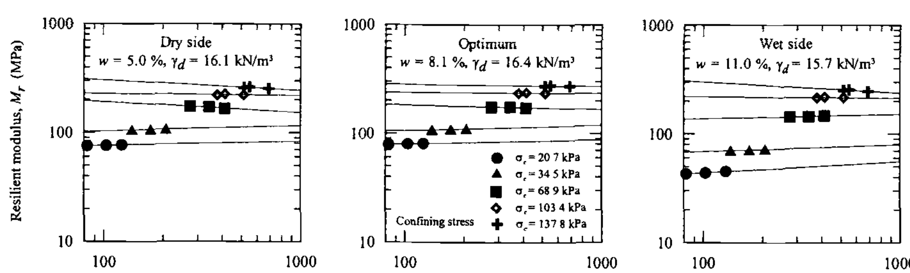


Figure 9 – *Results of the repeated load triaxial test on sand under controlled conditions of moisture content and unit weight*

Table 3 – *Resilient modulus test results for coarse-grained materials under controlled moisture content and unit weight*

| | $\sigma_c$ (kPa) | $\sigma_d$ (kPa) | $M_r$ (MPa) dry side | COV (%) | $M_r$ (MPa) optimum | COV (%) | $M_r$ (MPa) wet side | COV (%) |
|---|---|---|---|---|---|---|---|---|
| Silty sand | 21 | 21 | 58.94 | 4.1 | 56.25 | 5.3 | 33.94 | 9.5 |
| | 21 | 41 | 60.51 | 3.2 | 56.82 | 5.6 | 34.80 | 7.2 |
| | 21 | 62 | 64.27 | 4.6 | 57.39 | 9.0 | 35.42 | 4.7 |
| | 34 | 34 | 78.03 | 2.9 | 76.98 | 4.3 | 60.82 | 4.2 |
| | 34 | 69 | 80.81 | 3.0 | 77.62 | 3.6 | 61.92 | 4.2 |
| | 34 | 103 | 82.37 | 4.6 | 78.39 | 4.6 | 63.27 | 5.0 |
| | 69 | 69 | 121.33 | 3.3 | 110.21 | 2.8 | 103.52 | 2.5 |
| | 69 | 138 | 126.62 | 4.3 | 111.23 | 3.6 | 104.70 | 2.8 |
| | 69 | 207 | 126.45 | 3.0 | 113.71 | 3.2 | 105.12 | 3.1 |
| | 103 | 69 | 155.98 | 3.1 | 135.29 | 2.4 | 146.27 | 1.7 |
| | 103 | 103 | 157.93 | 2.0 | 136.35 | 2.5 | 148.48 | 2.3 |
| | 103 | 207 | 164.00 | 1.6 | 137.40 | 3.4 | 151.41 | 1.7 |
| | 138 | 103 | 187.01 | 1.5 | 165.13 | 2.0 | 180.67 | 1.7 |
| | 138 | 138 | 189.94 | 1.8 | 167.21 | 1.7 | 182.84 | 2.3 |
| | 138 | 276 | 191.98 | 1.8 | 167.90 | 2.8 | 184.16 | 1.9 |
| Sand | 21 | 21 | 75.51 | 2.2 | 79.17 | 3.1 | 42.92 | 7.6 |
| | 21 | 41 | 75.97 | 2.1 | 79.79 | 4.2 | 43.74 | 3.0 |
| | 21 | 62 | 76.71 | 2.3 | 80.49 | 3.8 | 45.04 | 3.3 |
| | 34 | 34 | 105.00 | 2.0 | 107.68 | 3.0 | 70.20 | 3.7 |
| | 34 | 69 | 106.00 | 2.1 | 108.39 | 3.2 | 70.75 | 5.5 |
| | 34 | 103 | 107.15 | 1.9 | 110.00 | 2.3 | 72.06 | 4.6 |
| | 69 | 69 | 172.58 | 1.3 | 174.07 | 1.4 | 143.99 | 2.7 |
| | 69 | 138 | 171.05 | 1.4 | 174.76 | 1.8 | 144.17 | 2.7 |
| | 69 | 207 | 165.74 | 1.5 | 171.34 | 1.3 | 146.58 | 1.5 |
| | 103 | 69 | 220.66 | 1.0 | 234.07 | 1.9 | 213.99 | 1.6 |
| | 103 | 103 | 225.22 | 0.9 | 237.06 | 1.1 | 217.50 | 1.6 |
| | 103 | 207 | 220.71 | 0.8 | 234.30 | 1.3 | 214.19 | 1.5 |
| | 138 | 103 | 257.80 | 0.9 | 271.46 | 1.4 | 251.97 | 1.8 |
| | 138 | 138 | 262.22 | 0.8 | 276.17 | 1.5 | 255.39 | 1.2 |
| | 138 | 276 | 252.64 | 1.1 | 271.56 | 0.9 | 246.28 | 1.0 |

### *Verification of the Proposed Model*

Equation 2 presented a model proposed for predicting the resilient modulus of coarse-grained materials using the cone penetration test parameters and basic soil properties. This model was developed using statistical analysis on field and laboratory test results of materials under its natural conditions. It is necessary to validate the model by predicting the resilient modulus of materials that were not used to develop the model. Therefore, the model was used to predict the resilient modulus of the coarse-grained materials used in the laboratory investigation. Comparison of predicted and measured resilient modulus values are depicted in Figure 10a. Inspection of Figure 10a shows the agreement of the predicted and measured resilient modulus values. In order to quantify the deviation of the predicted resilient modulus from the measured values, the absolute relative error was determined and depicted in Figure 10b. The model presented in Equation 2 predicted the resilient modulus of coarse-grained materials and is considered a step forward in the direction of in-situ characterization of pavement materials.

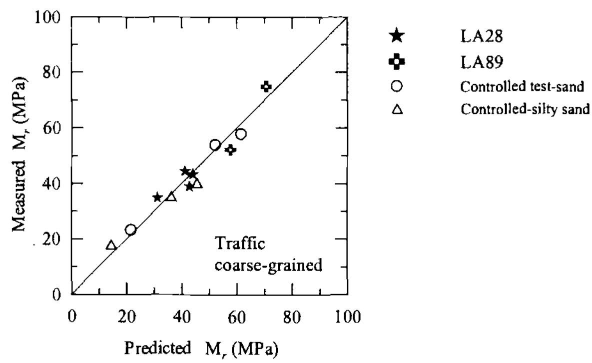


(a) Comparison of predicted and measured $M_r$

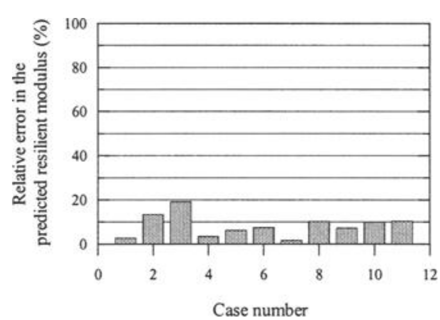


(b) Absolute relative error in predicting the measured resilient modulus.

Figure 10 – *Validation of the proposed model*

## Conclusions

This paper investigated the applicability of the cone penetration test in determining the resilient modulus of coarse-grained materials. Cone penetration tests were conducted at two pavement project sites in Louisiana. Materials samples were obtained and subjected to laboratory tests including the repeated load triaxial test and other tests for material characterization. Analysis was conducted on the test results, which were used to develop a model for predicting the resilient modulus of coarse-grained materials using the cone penetration test parameters and basic soil properties.

An additional laboratory investigation was conducted on coarse-gained materials prepared under controlled conditions of moisture content and unit weight. The results of the laboratory tests were utilized to investigate the effect of moisture content and unit weight on the cone penetration test parameters and resilient modulus. The results were also used to verify the model developed for predicting the resilient modulus. The predicted resilient modulus values were consistent with those obtained using the repeated load triaxial test. This study demonstrated the applicability of cone penetration test in predicting the resilient modulus of coarse-grained materials.

## Acknowledgments

This research project is financially supported by the U.S. Department of Transportation, Federal Highway Administration/Priority Technology Program (USDOT FHWA/PTP) Contract No. DTFH71-97-PTP-LA-14, the Louisiana Department of Transportation and Development (LADOTD) State Project No. 736-99-0773, and the Louisiana Transportation Research Center Project No. 98-8GT.

The effort of William T. Tierney, Research Specialist and Amar Raghavendra, Research Associate/ LTRC is acknowledged. Mark Morvant, Geotechnical and Pavement Administrator/LTRC, efforts and cooperation during the field and laboratory testing programs is gratefully appreciated. Paul Brady, Melba Bounds, and Kenneth Johnson, LTRC Geotechnical Laboratory helped in conducting various soil tests.

## References

AASHTO, 1993, *Guide for Design of Pavement Structures*, American Association of State Highway and Transportation Officials, Washington D.C.

Allen, D. L., 1989, "Mr Testing in Kentucky," Workshop on Resilient Modulus Testing, Oregon State University, Corvallis, OR.

Badu-Tweneboah, K., Manzione, C. W., Ruth, B. E.; and Miley, W.G., 1989, "Prediction of Flexible Pavement Layer Moduli from Dynaflect and FWD Deflections." *Non-destructive Testing of Pavements and Backcalculation of Moduli, ASTM STP 1026*, A. J. Bush III and G.Y. Baldi, Eds., ASTM, Philadelphia, PA.

Drumm, E. C., Reeves, J. S., Madgett, M. R., and Trolinger, W. D., 1997, "Subgrade Resilient Modulus Correction for Saturation Effects," *Journal of Geotechnical and Geoenvironmental Engineering*, Vol. 123, No.7, pp. 663-670.

ELSYM5,1985, Software Developed by SRA Technologies, Inc., Under Contract to FHWA.

Fredlund, D. G., Bergan, A. T., and Wong, P. K., 1977, "Relation Between Resilient Modulus and Stress Conditions for Cohesive Subgrade Soils", *Transportation Research Record*, No. 642, pp. 73-81.

Kamal, M. A., Dawson, A. R., Farouki, O. T., Hughes, D. A. B., and Sha'at, A. A., 1993, "Field and Laboratory Evaluation of the Mechanical Behavior of Unbound Granular Materials in Pavements," *Transportation Research Record*, No. 1406, pp. 88-97.

McGee, N., 1989, "Cold Region Facility - Subgrade Soils," Workshop on Resilient Modulus Testing, Oregon State University, Corvallis, OR.

Mohammad, L. N., Puppala, A. J., and Alavilli, P., 1994 "Influence of Testing Procedure and LVDT Location on Resilient Modulus of Soils", *Transportation Research Record*, No. 1462, pp. 91-101.

Mohammad, L. N., Puppala, A., and Alavilli, P., 1994, "Effect of Strain Measurements on Resilient Modulus of Granular Soils," *Dynamic Geotechnical Testing II, ASTM STP 1213*, Ebelhar, Drnevich, abd Kutter, Eds., ASTM, pp.202-221.

Mohammad, L. N. and Puppala, A., 1995, "Resilient Properties of Laboratory Compacted Subgrade Soils," *Transportation Research Record*, No. 1504, pp. 87-102.

Monismith, C. L., 1989, "Mr testing- Interpretation of Laboratory Results for Design Purposes," Workshop on Resilient Modulus Testing, Oregon State University, Corvallis, OR.

Puppala, A. J., Acar Y. B., and Tumay, M. T., 1995, "Cone Penetration in Very Weakly Cemented Sands." *Journal of Geotechnical Engineering*, ASCE, Vol. 121, No. 8, pp. 589-600.

Nataatmadja, A., and Parkin, A., 1989, "Characterization of Granular Materials for Pavements," Canadian *Geotechnical Journal*, Vol.26, No.4, pp. 725-730.

Rada, G. and Witczak, M. W., 1981, " Comprehensive Evaluation of Laboratory Resilient Moduli Results for Granular Material," *Transportation Research Record*, No. 810, pp. 23-33.

Titi, H. H., Mohammad, L. N., and Tumay, M. T., 2000, "Miniature Cone Penetration Tests in soft and Stiff Clays," *Geotechnical Testing Journal*, ASTM, Vol. 3, No.4, pp.432-443.

Titi, H. H. , and Morvant, M., 2001. "Implementation of Miniature Cone Penetrometer in Roadway Design and Construction," *Journal of the Transportation Research Board*, TRR 1755, pp 60-68.

Tumay, M. T., and Titi, H. H., 2000, "Louisiana Continuous Intrusion Miniature Cone Penetration Test (CIMCPT) System," Research Pays Off, *TR News*, No. 207, TRB, Washington, D.C., pp. 26-27.

Tumay, M. T., Boggess, R. L., and Acar, Y, 1981, "Subsurface Investigation with Piezocone penetrometer," *Proceedings*, ASCE National Convention, St. Louis, pp. 325-342.

Tumay, M. T., and Kurupp, P. U., and Boggess, R. L., 1998, "A Continuous Intrusion Electronic Miniature Cone Penetration Test System for Site Characterization," Proc. 1st International Conf. On site characterization-ISC'98, Atlanta, Vol. 1, pp. 1183-1188.

Tumay, M. T., 1985, "Field Calibration of Electric Cone Penetrometer in Soft Soil - Executive Summary," Report FHWA/LA-LSU-GE 85/02, Louisiana Transportation Research Center, Baton Rouge, LA.

# Author Index

# Subject Index

**S**



**T**



**U**



**W**



**Y**